Functional analysis of CBFA2T3: a breast cancer tumour suppressor from chromosome band 16q24.3

by

Zarqa Saif

M. Sc. (Zoology), The University of Punjab, Lahore, Pakistan

A thesis submitted for the degree of
Doctor of Philosophy

in

The Faculty of Medicine
The University of Adelaide,

in collaboration with

Hanson Institute, IMVS

Adelaide, July, 2009

To my lovely Son, Daughter

And my beloved Husband

Table of contents

Abstract

Loss of heterozygosity (LOH) of 16q is an early event occurring in 36-60% of primary sporadic breast cancers. *CBFA2T3* (*MTG16*) is a putative breast cancer tumour suppressor gene, localized at chromosome band 16q24.3. CBFA2T3 (MTG16) belongs to the CBFA2T protein family and shares a high homology with other two members, CBFA2T1 (MTG8) and CBFA2T2 (MTGR1). CBFA2T1 and CBFA2T3 proteins form transcriptional repressor complexes with the DNA binding zinc finger proteins like BCL6, PLZF, Gfi1 and ZNF652. CBFA2T3 protein exists as isoform "a" and "b" that arise from alternate start sites. These isoform differ in their N-terminal sequences. Previous studies determined that CBFA2T3a localized to the nucleolus, while CBFA2T3b has a putative role as tumour suppressor protein.

The present study confirms that the database entries of CBFA2T3a are incomplete and an extended N-terminus region is present to CBFA2T3a (NCBI NM_005187) isoform by RT-PCR and DNA sequencing. Two rabbit polyclonal anti CBFA2T3 antibodies were raised against the region unique to CBFA2T3. These antibodies specifically detect the endogenous CBFA2T3 proteins and not CBFA2T1 and CBFA2T2. Cell fractionation studies show that endogenous CBFA2T3a localized to the cytoplasm, while CBFA2T3b targeted to the nucleus. The N-terminus region specific to "a" isoform determined the cytoplasmic localization. The detailed studies show that CBFA2T3a localized to centrosome and this was confirmed by co–localization with known centrosomal proteins γ-tubulin. This was further confirmed by immunoprecipitation of γ-tubulin with N-terminus regions of CBFA2T3a protein. Further investigation showed that CBFA2T3a localizes to

the centrosome through out the centrosomal duplication. Presence of CBFA2T3a on procentriole was further confirmed by co-localization with known proteins having a crucial role in centrosome duplication like HsSAS6 and polyglutamilated tubulin.

Experiments were conducted to determined if the different subcellular localization of “a” and “b” isoforms resulted into functional differences between two isoforms. Immunoprecipitation experiments with known DNA binding proteins like BCL6 and PLZF showed that CBFA2T3b interacts with BCL6, while no interaction was found with PLZF. Consistent with the known transcriptional co-repressor function, real time RT-PCR showed that CBFA2T3b has an additive effect on BCL6 mediated repression of its target cyclin D2, while no effect was observed with CBFA2T3a. Real time RT-PCR data also showed that BCL6 not only recruits CBFA2T3b to repress its target but also have repressive effects on CBFA2T3 transcription. CBFA2T3b transcription regulation by BCL6 was found to be mediated through one or two BCL6 putative binding sites in CBFA2T3b promoter.

Immuno histochemical studies were carried out to analyse CBFA2T3b function as a breast cancer tumour suppressor. CBFA2T3 proteins are highly expressed in epithelial cell lineage of normal breast ducts, while its expression is lost in some tumours. CBFA2T3 expression was further analysed in a cohort of commercially available breast tumour sections. Data from these studies showed the loss of CBFA2T3 nuclear expression in some tumours, which was significantly correlated with tumours positive for HER2 expression, molecular subtypes and histological staging of the tumours. CBFA2T3 cytoplasmic expression was also down regulated in tumour sections. A significant association of CBFA2T3 cytoplasmic expression was observed with the TNM grading for tumour invasion and centrosomal abnormalities in BR701 TMA.

Knock down studies using shRNA were conducted to investigate the role of CBFA2T3a. Following CBFA2T3 knock down in cells with minimal CBFA2T3b expression, an increase in centrosomal abnormalities was observed. These abnormalities were associated with a significant increase in metaphase anomalies. Since the "a" isoform is localized to cytoplasm and particularly centrosome, it was considered that this isoform is determining centrosome integrity.

This work has provided a new insight into the localization pattern of CBFA2T3 isoforms, as CBFA2T3a and b isoforms were localized to different cellular compartments and were involved in distinct functions. CBFA2T3b function as a transcriptional co repressor, CBFA2T3b expression was lost in a group of breast tumours sections. Given that CBFA2T3a has a critical centrosomal function, the expression of this isoform would be expected to be maintained, even in the absence of the CBFA2T3b isoform in tumours. CBFA2T3a specific knock down studies may give a full insight on direct targets of CBFA2T3a, having a controlling role in normal centrosome duplication cycle.

Declaration

This work contains no material that has been accepted for the award of any other degree or diploma in any university or other tertiary institution and, to the best of my knowledge and belief, contains no material previously published or written by another person, except where due reference has been made in the text.

I give consent to this copy of my thesis, when deposited in the University Library, being available for loan and photocopying.

I also give permission for the digital version of my thesis to be made available on the web, via the University's digital research repository, the Library catalogue, the Australasian Digital Theses Program (ADTP) and also through web search engines, unless permission has been granted by the University to restrict access for a period of time.

Zarqa Saif

December 2009

Acknowledgements

I would like to thank my principal supervisor, David F Callen, for his support to my application of International Postgraduate Research Scholarship (IPRS) and providing me a chance to work in his group at IMVS. I also thank to David Millband, my co-supervisor, for his assistance and encouragement in my project and his valuable expertise of molecular biology. Thanks to Carmela Ricciardelli, my co-supervisor, for her help and guidance in immunohistochemistry and statistical analysis. In addition to her excellent guidance, I have respected her friendship and caring attitude. I am indebted to Raman Sharma for his assistance in molecular biology techniques. Raman I am greatly thankful to you for your help and guidance in designing some of the experiments during my studies. I am greatly thankful for your moral support and advices. I am grateful to the University of Adelaide for awarding me an IPRS scholarship to complete my studies in the University of Adelaide and IMVS for providing me the facilities to carry out my project.

I am grateful to Javed Qureshi (Head, Health Biotechnology Division, NIBGE) and Yusuf Zafar (Ex-Director, NIBGE) for their support of my leave application to accomplish my studies in Australia. I am thankful to all my colleagues and friends at NIBGE for their support and cooperation during my stay at NIBGE.

I would like to extend my thanks to all of the members of the Breast Cancer Genetics group at Hanson Institute, IMVS. In particular, I greatly appreciate the friendship of Jacky, Ross and Julee. Their friendship has provided me some fresh moments during exhaustive scientific work. I am also grateful to Paul M Nelson for his support in the lab

and useful suggestions to improve some of the experiments. Thanks to (late) Maggie Yard for her assistance in the lab and her friendship. Maggie managed to keep the laboratory consumables available whenever needed. More broadly, I would like to thank all the staff at Hanson Institute, IMVS for being very generous with their time and resources. Specifically I would like to mention Chris Hahn and Jantina Manning who were always happy to spare time for scientific discussions. Also, thanks to Jane Copeland, International Student Centre, for her administrative and moral support.

I am grateful to Dr Carston Janke (France), Dr Pierre Gonczy (Switzerland) and Dr Roncador, G (Spain) for providing me antibodies, Ghafar Sarvestani for help and assistance with the confocal scanning laser microscope.

I thank my family, particularly my Mum and Dad, and my two lovely sisters and a brother for their support and love. *Abbu Jee, Mian Yasin* the source of learning, I really appreciate your encouragement that has enabled me to achieve this goal. My heartiest thanks to my *Amee Jan,* from whom I learnt continuous and persistent struggle to achieve goals. Many thanks to my father-in-law, *Abdul Rashaid,* and mother-in-law, *Parveen Akhtar,* for their support and encouragement. Thanks to friends around Adelaide especially Saima, Nayla and Bhabhi Uzma and friends back in Pakistan, for their sincere company, happy distractions and life beyond the science.

Most importantly to my lovely Son, *Muhammad Afnan* and pretty daughter *Irha Fateema Saif* who really suffered by my PhD. Irha was born during last year of my candidature and because of my studies she has to start child care at the age of two months. I was unable to give her the support which she deserves at such a young age. My kids, the asset of my life, I love you both *Jan*. Finally I am thankful to my husband *Saif*, who owe a lot. Thanks for

your patience as you are the only one standing next to me in my sorrows and happiness throughout my candidature. Thank you *Saif*.

Abbreviations

AD – Activator domain

ADH – Atypical ductal hyperplasia

AML – Acute myeloid leukaemia

BAC – Bacterial artificial chromosome

B6BS – BCL6 binding sites

CBFA2T3 – Core-binding factor, runt domain α subunit 2; translocated to 3

CBFA2T1 – Core-binding factor, runt domain α subunit 2; translocated to 1

cDNA – complementary DNA

ChIP – Chromatin Immunoprecipitation

DAPI - 4',6-diamidino-2-phenylindole

DCIS – Ductal carcinoma *in situ*

DNA – deoxyribonucleic acid

DSB – double-strand breaks

DTT - Ditheothiol

E2 - Estradiol

ER – Estrogen receptor

ERE – Estrogen response element

EGF – epidermal growth factor

EGFP – enhanced green fluorescent protein

EGFR – Epidermal growth factor receptors

FCS – Fetal calf serum

GFP – Green fluorescent protein

HA - hemagglutinin

HDAC – Histone deacetyltransferase

HMEC – Human mammary epithelial cell

IDC – Invasive ductal carcinoma

IF – Immunofluorescence

IHC - Immunohistochemistry

ILC – Invasive lobular carcinoma

IP - Immunoprecipitation

LCIS – Lobular carcinoma *in situ*

LOH – Loss of heterozygozity

mRNA – messenger RNA

MTG16 – Myeloid transforming gene from chromosome 16 protein

MTG8 – Myeloid transforming gene from chromosome 8

MTGR – Myeloid transforming gene related protein-1

NCBI - National Center for Biotechnology Information

NES – Nuclear export sequences

NR – Nuclear receptor

NLS – Nuclear localisation signal

ONC – Oncogene

PCR – Polymerase chain reaction

PEST sequence – Proline, glutamic acid, serine and threonine rich sequence

PR – Progesterone receptor

Real-time RT-PCR – Reverse transcription real time-PCR

RD – Repressor domain

RNA – ribonucleic acid

SDS – Sodium dodecylsulphate

SDS-PAGE – SDS Polyacrylamide gel electrophoresis

SEM – Standard error of the mean

shRNA – Short hairpin RNA

siRNA – Small interfering RNA

SNP – Single nucleotide polymorphism

SRO – Smallest region of overlap

TSG – Tumour suppressor gene

WB – western blot

Y2H – yeast-2-hybrid

α-FLAG - anti-FLAG

α-Myc – Anti-myc antibody

Publications

In preparation:

1 **Saif Z**, Millband D, Ricciardelli C, Kumar R and Callen DF (2009). CBFA2T3a isoform is functionally distinct from CBFA2T3b (Manuscript in internal review)

2 **Saif Z**, Millband D, Ricciardelli C, Kumar R and Callen DF (2009). Evaluating CBFA2T3 as a novel prognostic marker for breast cancer. (Manuscript in preparation)

Conference presentations:

1 **Z Saif** , D Millband, C Ricciardelli, R Kumar and D F Callen. A discrete role for CBFA2T3a isoform in centrosome function, in contrast to CBFA2T3b: a breast tumour suppressor protein. July 22, 2008 Post graduate research Expo, Faculty of Health Sciences, The Adelaide University, Adelaide.

2 **Z Saif** , D Millband, C Ricciardelli, R Kumar and D F Callen. Evaluating CBFA2T3, a putative tumour suppressor from chromosome band 16q24.3, as a novel prognostic marker for breast cancer. April1-4 2006, 97th annual AACR meeting, Washington DC, USA.

3 **Z Saif**, J Forsyth, D Millband, P M Neilsen, J Lee, R Kumar and D F Callen. Functional studies of CBFA2T3, a putative breast tumour suppressor from chromosome band 16q24.3. Feb 2005, Lorn cancer meeting, Philip island,

Chapter 1 – Introduction

1.1 Introduction

Cancer is a complex disorder characterised by uncontrolled growth of cells. Such growth characteristics result in the disruption of tissue morphology and physiology. Multiple alterations at both genetic and cellular levels result in the conversion of normal cells to cancer cells. However, this is a rare phenomenon because normal cell growth is highly regulated and is under the control of a web of feedback pathways. Normally cells grow and form layers. The cell stops growing when it became surrounded by adjacent cells from all sides. This process is termed “contact inhibition of growth”. Because cancer cells lack this phenomenon they keep growing, resulting in the formation of tumour masses.

There are two classes of genes whose protein products are required to regulate the activities of normal cells:

1) Oncogenes: These are the mutated version of a proto-oncogene whose inappropriate activation results in uncontrolled proliferation. Proteins encoded by oncogenes act as positive regulators of cell growth and are usually active components of the signal transduction pathways.
2) Tumour suppressor genes (TSG): Inactivation of these genes contributes toward the transformation of normal cell into a cancer cell. The protein products of tumour suppressor genes are involved in inhibition of proteins directed by oncogenes, thus these proteins are negative regulators of the oncogene.

Genetic changes, resulting in a shift in balance between these genes, are the major cause of cancer development (Fearon & Vogelstein, 1990).

1.2 Breast cancer

Breast cancer is the most common non-cutaneous cancer in the Western world and is the second major cause of death among all malignancies. Breast cancer is found as a major cancer in females. In 2005 12,170 cases in Australia (incidence rate) accounted for over 27% of all diagnosed female cases of cancer. During 2006-2010 breast cancer was expected to be increasing with a rate of 0.1% per year which makes a total of 12,773 in 2006 to 14,017 till 2010, almost with a rise of 311 new cases per year (Cancer in Australia: an overview, 2008 by Australian Institute of Health and Welfare: AIHW, Statistics and Information agency based on AACR data). Breast cancer was the most common cause of cancer related deaths (2707 deaths in Australia) in female till 2005. Although the number of cases of breast cancer is increasing by 38 cases per year, the death rate is decreasing by the rate of 0.3%, due to the improvements in cancer treatments and development of better prognostic methods. All these facts have still made breast cancer the most common type of cancer among Australian women.

Several factors can enhance the risk of breast cancer development. Among these factors, increasing age is the most significant. In addition, factors like menstrual age, reproductive age and a family history of breast cancer are also important. Women with a history of breast and ovarian cancer in their first degree relatives are at higher risk for breast cancer development then the women without family history. Additional risk factors such as radiological dense breast and behavioural or environmental factors like usage of hormones for different medical treatments and alcohol intake may also affect breast cancer risk (Goodwin & Boyd, 1988; Ma et al., 1992) and Muller and Young, 1998, American Cancer Society, 2004).

Breast cancer development is a multistep phenomenon and involves gradual transformation of normal cells into a cancerous mass (Cornelis et al., 1994). Breast cancer originates from the epithelial cells of the terminal ducts and lobules (Russo et al., 1991). It forms localised tumorous masses, which later metastasize to other tissues.

Breast cancer is divided into four major types based on the origin and invasiveness of the cancer. The first type is called ductal carcinoma *in situ* (DCIS). It is a preinvasive lesion found in normal breast tissues. It is usually confined to its site of origin but this kind of lesion has the capacity to progress and change into more aggressive forms like invasive carcinoma of the breast (Bieche & Lidereau, 1995). The second type, infiltrating ductal carcinoma (IDC), is the most invasive kind of cancer. It starts in ducts, breaks through the walls of the duct, and invades the fatty tissue of the breast. IDC accounts for 80-90% of all breast cancers. The third type is lobular *in situ* carcinoma (LICS). It originates in the lobules, which are the glandular cells of the breast. It does not represent a true form of cancer but it increases the risk factor for the future development of cancer. For DCIS and LICS it has been suggested that these localized lesions can evolve to infiltrating form of cancers (Bieche & Lidereau, 1995). The fourth is known as infiltrating lobular carcinoma (ILC). It starts in the lobule or gland of the breast and constitutes only 10-15% of invasive breast cancers. Breast cancer can be divided into five stages, stage 0-4, on the basis of tumour type, tumour size and lymph node positivity. Furthermore, on the basis of hereditary origin breast cancer can also be classified as familial breast cancer or sporadic breast cancer.

1.2.1 Familial breast cancer

Familial breast cancer account for 20-30% of the all breast cancer cases (Olopade et al., 2008) illustrated in Fig 1.1A. Familial breast cancer is usually characterised by multiple cases in a family and by early age of onset. Genetic linkage studies have identified two breast cancer susceptibility genes, subsequently cloned as *BRCA1* (Hall et al., 1990) and *BRCA2* (Wooster et al., 1994). Mutations in these two high penetrance genes (*BRCA1* and *BRCA2*) are associated with increased risk for breast and ovarian cancer development. Changes in these genes account for less then 10% of total breast cancer cases (Olopade et al., 2008). These genes have a diverse role in transcription activation (Ouchi et al., 1998) and double strand break repairs which may be crucial for breast carcinogenesis. BRCA1 has a well characterized role in centrosome duplication regulation through its ubiquitination activities (Sankaran et al., 2006). Inhibition of BRCA1 results into centrosomal amplification between late S and G2/M phases of the cell cycle (Ko et al., 2006). BRCA1 has an indirect role in controlling genomic stability through its tight regulation of centrosome numbers, as increased centrosome number imparts default cell polarity leading to chromosomal aberrations which are the hallmark of aggressive tumours.

In addition, inherited rare mutations in *CHEK2*, *PTEN*, *TP53, RB, MYC* and the *ATM* genes are reported to impart increased susceptibility to breast cancer development (Fig 1.1A). The p53, RB and c-MYC proteins are involved in positive and negative regulation of a number of genes involved in apoptosis and cell cycle progression (Kinzler & Vogelstein, 1997; Ryan & Birnie, 1996).

1.2.2 Sporadic breast cancer

Sporadic breast cancer accounts for 70-80% of total breast cancer cases. The development of sporadic breast cancer does not involve genetic mutation in the familial cancer susceptibility genes, *BRCA1* and *BRCA2*, although these genes can be down-regulated by methylation of the promoter (Chen et al., 2003; Mueller & Roskelley, 2003). Changes like gains and losses at the chromosome level are frequently present. These changes may involve amplification of chromosomal regions containing oncogenes, deletions of regions having tumour suppressor genes, and translocation at a single gene locus or at multiple loci. One of the most frequently observed changes is loss of heterozygosity (LOH) (Bieche & Lidereau, 1995) which will be discussed in later sections. Other changes involved are silencing of tumour suppressor genes through methylation of CpG islands present in promoter regions as in, retinoblastoma 1 (*RB1*) which is involved with cancer of the retina (Feinberg et al., 2006). A recent report has also shown the loss of RB1 function associated with the development of a basal type breast cancers (Herschkowitz et al., 2008); *CBFA2T3* promoter methylation (a breast cancer tumour suppressor from chromosome band 16q24.3) has also been shown in breast cancer (Bais et al., 2004). Hypermethylation of the *BRCA1* promoter region has been found in 15%-31% of sporadic breast tumours (Wei et al., 2005). Histone modifications both hypoacetylation and hypermethylation have been reported for genes like *p16* (*CDKN2A*), MutL protein homologue 1 (*MLH1*) (Feinberg & Tycko, 2004; Jones & Baylin, 2002; Sakai et al., 1991). These epigenetic changes will be discussed in details in the next section.

1.2.3 Epigenetic changes in sporadic breast cancer

Extensive research in the past few decades had been focused on the analysis and characterization of genetic changes associated with breast cancer origin and development. These studies were able to define epigenetic changes, as the changes at gene expression level which are somatically inheritable and are reversible (Feinberg & Tycko, 2004). Epigenetic changes are not accompanied by changes of DNA sequence. Aberrant CpG island methylation of the promoter region of tumour suppressor genes, together with alteration of histone modification (deacetylation and methylation), are two mechanisms that causes aberrant gene expression. An epigenetic progenitor model of cancer origin has been proposed stating that cancer arise in three steps (1) epigenetic disruption of stem cell or progenitor cell or tumour progenitor genes (tumour progenitor genes TPG, mediate the expansion of progenitor cells by increasing their cancer proneness, stemness or pluripotency) (2) initiating mutation involving oncogene activation and silencing of tumour suppressor genes (3) genetic and epigenetic plasticity, an enhanced ability to stably evolve its cancer phenotype (Feinberg et al., 2006) (Fig 1.1B). Several studies have shown that cancer cells exhibit hypermethylation of promoter CpG islands related to tumour suppressor genes (Bais et al., 2004; Herman & Baylin, 2003; Sakai et al., 1991) and aberrant deacetylation (Oyer et al., 2009).

Olpade (Olopade et al., 2008) have proposed a model for the role of *BRCA1* in sporadic breast cancer saying that aberrant methylation of *BRCA1* promoter in sporadic breast cancer is the “second hit” according to Knudson’s “two hit” model, while the inactivation of the normal allele acts as the first hit which was followed by aberrant methylation of *BRCA1* promoter. Hypermethylation of the *BRCA1* promoter is observed

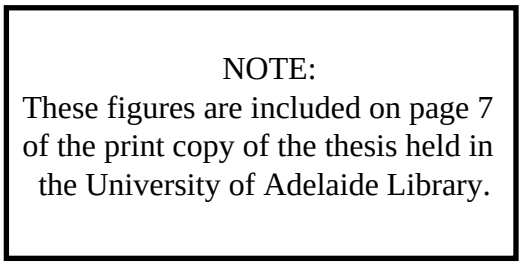

Figure 1.1. A. Genetic susceptibility to breast cancer.
A model presenting major penetrance genes associated with Familial breast cance r. Redrawn from Olopade et.al. (2008) Adopted from Wolters Kluwer /Lippincott, William & Wilkins; 2008; p1595-1605.
B. The epigenetic progenitor model for cancer development. Illustration of main steps involved with cancer devlopment and progression. Adapted from Feinberg et.al. (2006)

in 15-30% of sporadic breast tumours. A previous report by Wei et al (2005), suggests that the inactivation of one of the *BRCA1* allele by hypermethylation is followed by the loss of wild type *BRCA1* (Wei et al., 2005) resulting in progression to a tumour phenotype.

In inherited breast cancers cases, *BRCA1* promoter methylation was postulated to serve as a "first hit" like germline mutations, while the "second hit" results in reduced copy number of *BRCA1* or chromosome 17 aneusomy. *BRCA1* deficient cells must acquire additional changes such as mutations in the *Tp53* tumour suppressor (TSG) and amplification of *cMYC* oncogene (ONC) which otherwise force down the uncontrolled growth of cells or tumour progression under the same molecular pathways as seen in hereditary breast cancer. *BRCA1* was recognised as a stem cell regulator involved with differentiation of glandular epithelial cells. Further its inactivation restricts the epithelial cells to a basal cell subtype (Olopade et al., 2008).

Estrogen receptor α is also an epigenetically regulated gene. ERα promoter methylation is reported in 60.1% of breast cancers (Zhao et al., 2008) and is found associated with *BRCA1* promoter methylation (Wei et al., 2008). The restoration of ERα expression has been reported by treatment with histone deacetylase inhibitor LBH589 (LBH) in human breast cancer cell lines MDA-MB-231 and MDA-MB-435 (Zhou et al., 2007) indicating the possibility for treatment of breast cancers. This involves the removal of DNMT1, HDAC1, H3 lysine 9 methyltransferases from the ER promoter which results in reorganization of heterochromatin associated proteins and active transcription of ERα without altering methylation status (Zhou et al., 2007). DNA methylation of various genes has also been reported in premalignant lesions, indicating that these changes are

early events in breast tumourigenesis and they may have prognostic impact (Olopade et al., 2008; Visvanathan et al., 2006).

1.2.4 Molecular subtypes of breast cancer

Human mammary glands are comprised of two distinct subtypes of epithelial cells. The first are luminal cells, which compose the most upper and more differentiated layer of columnar epithelial cells with cytokeratin 8/18 expression. The second type is basal cells which lie close to the basement membrane and are positive for cytokeratin 5/6 expression. The majority of breast cancers originate from the luminal epithelial cell lining, while 3-15% of breast tumours have a basal cell lineage (Olopade et al., 2008). With genetic profiling of breast tumours by expression microarrays, breast cancer can be subdivided into different subtypes depending on their molecular signatures. On the basis of expression signatures breast cancer is classified into four different sub-groups. Current sub-grouping is based on expression of estrogen receptor (ER), progesterone receptors (PR) and human epidermal growth factor receptor-2 (HER-2). These subgroups are Luminal subtype A which is positive for ER and PR but negative for HER-2. Luminal subtype B is classified as subgroup positive for ER, PR and HER-2. Third sub-group is HER-2 types including ER and PR negative tumours which are positive for HER-2 expression. Fourth group is basal type tumours, also known as triple negative as are negative for the presence of all three receptors. It is worth to mention here that BRCA1-associated tumours falls only in triple negative or basal type category indicating the role of genetics changes in determining the tumour subtype (van der Groep et al., 2004). Work from several groups has shown the impact of different molecular subtypes on disease prognosis which is related to the disease free survival (Hu et al., 2006). Luminal A and luminal B subtypes are associated with the best

prognosis, while HER-2 type and basal type tumours have poor prognosis (Carey et al., 2006; Nielsen et al., 2004). As the changes in the expression profiles are related to clinical outcomes, the analysis and characterization of these profiles are essential. A brief description of these hormonal receptors is given in next section.

1.2.4.1 Estrogen and progesterone receptors (ER and PR)

Estrogen receptors (ER) and progesterone receptors (PR) are transcriptional factors which belong to the nuclear hormone family of receptors. Hormone E2 (17-β oestradiol), through binding with the ER receptors, stimulates different proliferation and differentiation pathways. There are two isomeric forms of ER receptors, ERα and ERβ, which are encoded by two different genes. Structurally ER consists of a DNA binding domain flanked on both sides by transcriptional activation domains, while binding to ligand is mediated through the ligand binding domain. ERα and ERβ are both expressed in the epithelial lining of normal mammary ducts, while the expression of ERα is increased in hyper-proliferative premalignant lesions (Allred et al., 2001). PR is one of the ER regulated genes. PR receptors mediate the effect of progesterone on breast mammary duct development and differentiation. It also exists in two isoforms PR-A and PR-B, but both isoforms originate from a single gene. Structurally PR is similar to the ER in reference to the presence of different domains as mentioned earlier. PR is also overexpressed in breast tumours and its expression is associated with resistance to tamoxifen (Hopp et al., 2004). ER not only mediates it's action by transcriptional activation of the target genes, but also interacts with several other proteins having crucial roles in breast cancer development like BRCA1 (Fan et al., 1999) and Cyclin D1 (Zwijsen et al., 1997) reviewed by Cui et.al (2005) (Cui et al., 2005).

ER was discovered initially as a predictor for response to hormone ablation treatment given to breast cancer patients. Estrogen receptors are overexpressed in about 75% cases of breast cancer patients. 65% of these are also found positive for progesterone receptors. While 25% of the total breast cancer cases are negative for both ER and PR. Expression of ER and PR is a strong prognostic factor, confirming a 70% chance of response to SERM (selective estrogen receptor modulators) or ablative endocrine therapies. If the patient is only positive for ER and negative for PR, or vice versa, there is 33% chance of responding to hormonal therapy. On the other hand, there is an overall 10% chance of response in patients negative for both ER and PR (reported by Australian Institute of Health and Welfare/ Australian Association of Cancer Registries 2008). ER is the most effective target for the treatment for breast cancer. Different drugs like Tamoxifen and Raloxifene have been developed, which block the site of interaction between the hormones E2 and ER. Other approaches, like the development of aromatase inhibitors for example anastrazole, block the conversion of testosterone to oestradiol (Bonneterre et al., 2000; Mouridsen et al., 2001). Rapid development in the field of tumour biology and molecular endocrinology has helped to improve cancer treatment. However, knowledge of the molecular pathways involved with the loss of PR expression in ER positive/ PR negative tumours, which leads to resistance against tamoxifen, will help to develop new therapeutic strategies for these advance staged cancers.

1.2.4.2 ErbB receptors or HER family receptors

ErbB receptor family members play a crucial role in pathogenesis of breast cancer. This receptor family is comprised of four proteins named ErbB1 (EGFR), ErbB2 (HER-2), ErbB3 (HER-3) and ErbB4 (HER-4). All members are transmembrane receptors known

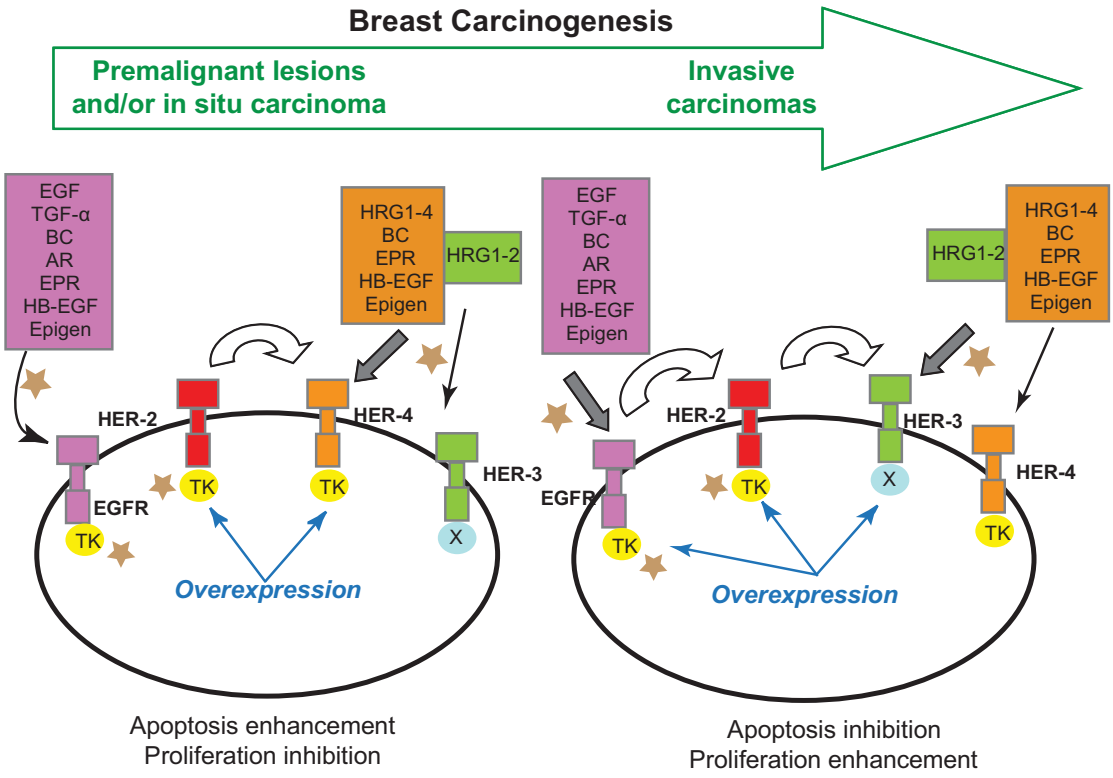

Figure 1.2. Proposed model for the implication of HER-3 and HER-4 in breast cancer evolution and possible intervention stratigies.
Redrawn from Karamouzis et.al. (2007)

for their tyrosine kinase activity. These receptors are phosphorylated upon binding of a ligand such as heregulins (HRGs) and EGF related proteins and form homodimers or heterodimers. As a consequence of these dimer formation various signalling pathways are initiated (Mosesson & Yarden, 2004) (Fig 1.2). Existence of these receptors as homo and heterodimers is predicted to be related to tumour progression. Tumours expressing HER-2 heterodimers with HER-3 and HER-4 are aggressive in nature and are more mitogenic as compared to the tumours expressing homodimers (Citri et al., 2003). Although overexpression of HER-2 is well known, overexpression of other members like HER-3 and HER-4 is also observed in breast cancer (Badra et al., 2006; Barnes et al., 2005). Expression of HER-2 is generally associated with resistance to hormone therapy and aggressiveness of tumours, while tumours expressing HER-4 respond well to hormone therapy. In addition overexpression of HER-4 in HER-2 expressing cells results in reduction of proliferation and induction of apoptotic pathways which infact is the reverse of HER-2 signalling pathways (Barnes et al., 2005). Some reports suggest that HER-3 and HER-4 over-expressing tumours may belong to different sub-types of breast tumours, as in invasive tumours a positive association of HER-3 and an inverse association of HER-4 with other HER members was described (Abd El-Rehim et al., 2004). All these studies indicate a crucial role for these family members during breast tumourigenesis as indicated in Figure 1.2 (Karamouzis et al., 2007).

1.3 Loss of heterozygosity

Loss of heterozygosity (LOH) in a tumour is defined as the loss of an allele at a heterozygous locus in tumour resulting in homozygosity or hemizygosity for the second allele. LOH is the most common somatic change observed among breast tumours.

Several studies have shown increased LOH of a number of different chromosome arms 1, 3p, 6q, 7q, 8p, 11p, 13q, 16q, 17, 18q and 22q in primary breast tumours (Callahan & Campbell, 1989; Callahan et al., 1993; Cleton-Jansen et al., 1994).

Loss of heterozygosity of 16q is one of the most frequent events found in breast cancer as well as other cancers like hepatocellular carcinoma, lung cancer (Sato et al., 1998), ovarian and prostate cancer (Godfrey et al., 1997). The frequent loss of 16q suggests the presence of one or two tumour suppressor genes at this region of the chromosome. For example, frequent loss of 17q resulted in the identification of the p53 tumour suppressor gene (Eccles et al., 1992) .

LOH at 16q is reported in about 36-67% of primary sporadic breast cancer cases (Caligo et al., 1998; Cleton-Jansen et al., 1994; Tsuda et al., 1994). Ductal carcinoma *in situ* (DCIS) is considered a preinvasive type of breast cancer and accounts for 70% of total breast carcinomas. Since LOH of 16q is present mostly in DCIS, it is suggested that 16q LOH is an early event in breast carcinogenesis (Hulten et al., 1993). Moreover, the LOH, defined by analysis of polymorphic genetic markers, at 16q is reported in 29-55% of *in-situ* breast tumours (Vos et al., 1999). Tirkkonen et al. (1998) reported loss of 16q21-qter in 38% of analysed breast tumours in a comparative genomic hybridization (CGH) study (Tirkkonen et al., 1998). Another study of 90 invasive ductal breast carcinomas, comprising grade I and grade III breast tumours has revealed the loss of 16q in 65% of the grade I tumours compared to 16% of grade III tumours. The grade I tumours are recognized as more differentiated as compared to the grade III tumours which are poorly differentiated. Grading of the tumour in this study was done on a histological basis (Roylance et al., 1999).

A recent report has successfully correlated the gene expression array profiles of different sub classes of invasive breast cancers with their LOH pattern. Wang et al. have clustered the breast cancers in two groups, cluster I and cluster II, based on ER, HER-2 and p53 status (each cluster is further divided into class A and B, on the basis of invasiveness of the tumours). Cluster I is comprised of high-grade tumours with ER negative, HER-2 and p53 positive status, while cluster II consists of low-grade tumours which are positive for ER and negative for both HER-2 and p53. LOH at 16q24.3 was found in 88% of low grade tumours in cluster II B compared to 50% of tumours in IIA, while 16q loss was seen in 33% of tumours in cluster I (Fig 1.3) (Wang et al., 2004b). All these findings lead to the conclusion that LOH at 16q is an early event in breast carcinogenesis and is associated with good prognosis.

Another report has shown that allelic loss (LOH) in ER positive breast tumours has a differential pattern in the two histological subtypes of infiltrating lobular and ductal breast cancer (Loo et al., 2008). Molecular changes for the whole genome were assessed using Affymetrix Genechip arrays for ER positive tumours. Single nucleotide polymorphisms (SNPs) showed a high frequency of LOH (>50%) for 11q, 16q and 17p in both ER positive infiltrating lobular or ductal carcinomas. Hierarchical clustering of SNPs resulted into four tumour groups based on the pattern of LOH. IDC tumours having LOH in chromosome arm 8p and 5q is grouped as group 1. Group 2 comprised primarily of IDC of intermediate to high grade tumours having LOH in 3p, 8p, 13q and 16q. Group 3 predominantly consisted of IDC with several ILC tumours having 3p, 6q, 13q and 16p LOH. Group 4 consist of ILC and low grade IDC having overall lower rate of LOH but predominantly all have 16q loss in common. Thus the loss of 16q is commonly found in both low grade infiltrating ductal and lobular carcinomas.

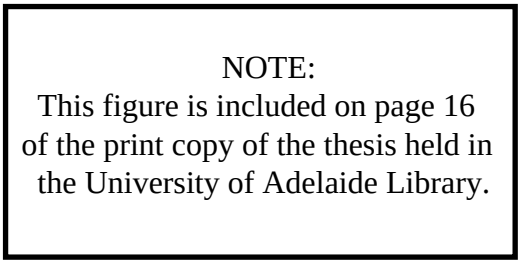

Figure 1.3. Loss of heterozygosity (LOH) frequency of common LOH sites in cluster I and II tumours identified by gene expression profiles
Wang et al. (2004b)

These previous studies consistently found LOH at 16q is associated with low grade invasive ductal and lobular carcinomas. A recent study used microdisection of breast tumour sections and highly sensitive 32K BAC re-array collection (CHORI) platform that uses CGH to measure gains and losses over whole genome, shows that 16q loss is

These previous studies consistently found LOH at 16q is associated with low grade invasive ductal and lobular carcinomas. A recent study used microdisection of breast

also associated with high grade ER positive tumours (Natrajan et al., 2009). Genomic profile of GIII-IDC-NST (grade-III invasive ductal carcinoma of no special type) showed the presence of 16qWL (16q whole arm loss) in 36.5% cases, which was found significantly associated with ER expression and genetic instability as compared to the tumours negative for ER without 16qWL. The most commonly deleted region on 16qWL ER+ tumours was 16q24.2 (58.0 %), harbouring various genes including FBXO31 (was identified as a candidate tumour suppressor (Kumar et al., 2005)). Further the 16qWL is found associated with the luminal subtype with the prevalence of *BRCA2* locus deletion while 16qPL (partial loss) or 16qNL (no loss) showed a significant association with basal like tumours (Natrajan et al., 2009). Contrary to the previous reports, this study has shown the loss of 16q is prevalent in high grade tumours. This may be due to the use of microdisection and highly sensitive BAC arrays. Note that in the current study pericentromeric and peritelomeric BACs (region covering 16q24.3) are ignored due to inaccurate read outs.

1.3.1 LOH of 16q24.3

Several studies have attempted to narrow down the region of LOH on the chromosome arm 16q by using a panel of RFLP and microsatellite markers. Different groups have

identified three common regions of frequent loss on 16q. These regions are named SROs for the "smallest region of overlap" (Driouch et al., 1997).

In a study comprising 712 breast tumours, Cleton et al (2001) have further defined these SROs to the following regions of 16q: one at 16q22.1 (SRO A) and two at 16q24.3 (SRO B and C). They further refined the SRO C region to the interval between polymorphic marker D16S498 and the telomere (16q24.3-telomere). However, no significant differences in LOH patterns among different grades of breast tumours were found (Cleton-Jansen et al., 2001).

Extensive research work has resulted in construction of the physical map and sequencing of 16q24.3 with detailed *in silico* and *in vitro* analysis identifying 104 genes from the 2.4Mb region of 16q24.3 (Powell et al., 2002). An expression analysis of these genes has identified three putative tumour suppressor genes. These three putative tumour suppressor genes, *CBFA2T3, CYBA* and *FBX031, (*also termed *Hs 7970)* (Powell et al., 2002), possessed ten times more variability of expression in a panel of breast cancer cell lines with known 16q24.3 LOH than various house keeping genes (Powell et al., 2002). Highly variable expression of these genes in breast cancer cell lines led to the hypothesis that these genes may have a tumour suppressor role in breast carcinogenesis. The present proposal is based on further studies of *CBFA2T3* as a tumour suppressor gene.

1.4 CBFA2T3 as a putative breast tumour suppressor

Kochetkova et al (2002) have shown reduced levels of *CBFA2T3* expression, a previously identified partner of AML1 protein from rare (16;21) translocation in

leukaemia, in a number of breast cancer cell lines as compared to the non transformed mammary epithelial cell lines. RNA *in situ* hybridization was used to determine the expression of *CBFA2T3* in breast tissue sections. *CBFA2T3* expression was found in normal breast ductal epithelial cells while loss of *CBFA2T3* message was seen in the primary breast carcinomas previously known to harbour LOH of 16q region. Furthermore, a reduction in growth or colony formation on plastic and soft agar was observed when CBFA2T3 was reintroduced in the breast cancer cell lines having low expression of CBFA2T3. Above data suggested CBFA2T3 as a candidate breast tumour suppressor gene known to function as a transcriptional co-repressor (Kochetkova et al., 2002).

1.5 The *CBFA2T* gene family

The *CBFA2T* gene family (also known as the *ETO* family) consists of three members. The first member, *CBFA2T1* (eight twenty one, *ETO*), is also known as the myeloid transforming gene, *MTG8*, from the chromosome translocation t(8;21) found in patients with acute myeloid leukaemia (Miyoshi et al., 1993). The second member, *CBFA2T2* is the myeloid transforming gene related protein-1 (*MTGR-1*) (Kitabayashi et al., 1998a). The third member, *CBFA2T3*, is the myeloid transforming gene chromosome 16 protein, also named *MTG16* (Gamou et al., 1998).

CBFA2T1 was first identified and cloned as the AML1-MTG8 fusion transcript by (Miyoshi et al., 1993). Subsequently cDNA clones representing fused transcripts from chromosome 8 and chromosome 21 were isolated by Erickson et al. They named the gene on chromosome 8 *CBFA2T1* (Erickson et al., 1992). The *CBFA2T1* gene consists of 13 exons and is expressed in two isoforms, CBFA2T1a (Miyoshi et al., 1993) and

CBFA2T1b (Wolford & Prochazka, 1998). It is widely expressed in many organs of the mouse embryo, whereas reduction in expression level is observed with the progression of age (Davis et al., 1999).

CBFA2T2 has been characterised as the myeloid transforming gene related protein-1. *CBFA2T2* was originally isolated from the L-G murine myeloid cell line as a AML-1/ETO interacting 85 KDa phosphoprotein, immunologically related to ETO (Kitabayashi et al., 1998a). It consists of 14 exons and encodes two splice variants *CBFA2T2a* and *CBFA2T2b*. Although the structure of *CBFA2T2* is greatly similar to *CBFA2T1* and *CBFA2T3* (Morohoshi et al., 2000) this gene is not associated with any disease. *CBFA2T2* is well expressed in the adult skeletal muscles, heart and brain, but less in the kidney, pancreas, spleen and thymus (Calabi & Cilli, 1998). Expression of the two isoforms is not the same in all tissues (Fracchiolla et al., 1998).

Characterisation of a translocation t(16;21), associated with therapy-related acute myeloid leukaemia (AML), resulted in the identification of the third member of the family named *CBFA2T3* (Gamou et al., 1998). In this translocation the *AML1 (RUNX1)* gene was fused to a novel gene on chromosome 16, *CBFA2T3*. Gamou et al (1998) have shown that *CBFA2T3* transcript is about 4261 base pair and 4021 base pair comprising of 13 exons (Gamou et al., 1998). CBFA2T3 is present in the form of two alternative splice variants, CBFA2T3a and CBFA2T3b. CBFA2T3a codes for a 653 amino acid protein while CBFA2T3b codes for a 567 amino acid protein. The two isoforms differ from each other in sequences in the N-terminus region. Recently it has been reported that overexpressed CBFA2T3a is targeted to the nucleolus, whereas the AML-CBFA2T3 fusion is targeted to the nucleoplasm (Hoogeveen et al., 2002). The amino

acid sequences present at the N-terminal region of the CBFA2T3a protein are responsible for targeting it to the nucleolus. Later studies have shown that CBFA2T3 protein has a strong homology with CBFA2T1 (Davis et al., 2003). Further details regarding the structure and the interaction of CBFA2T family with other proteins are given in Chapter 6.

1.5.1 Structure of human CBFA2T proteins

Most of the information on this protein family is developed from studies carried out on one member. All the members of the family show homology. CBFA2T3a and CBFA2T3b are 67% and 75% identical to CBFA2T1. On the other hand, the homology of CBFA2T2 to CBFA2T1 is 54% and 61% (Gamou et al., 1998). (Davis et al., 2003) have shown that CBFA2T3 has a high homology with CBFA2T1 (MTG8) while it has less homology with CBFA2T2 (MTGR1) and nervy, a putative homologue of CBFA2T1 from *Drosophila*. Fig 1.4 shows the structure as well as homology among the members of the CBFA2T proteins family (Davis et al., 2003). On the basis of the high homology among members the following comments are generalised to all three family members.

CBFA2T proteins have four conserved domains. These domains are termed nervy homology regions 1-4 (NHR1-4) after a common gene nervy from *D. melanogaster*. All four domains have high similarity to the Drosophila nervy protein, ranging from 50 % to 70% among different members of the family (Davis et al., 2003; Feinstein et al., 1995).

The NHR1 region is homologous to various TATA binding protein associated factors

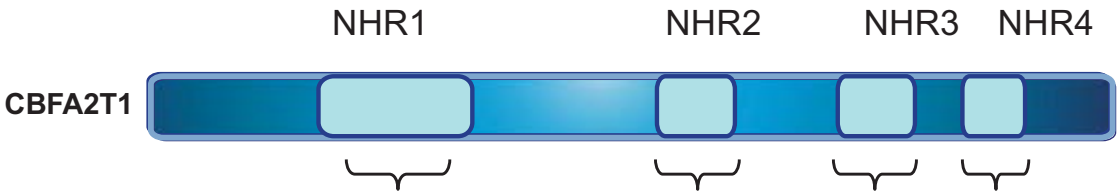

CBFA2T3	**98%**		**88%**		**84%**		**90%**	
CBFA2T2	**95%**		**79%**		**66%**		**87%**	
Nervy	**50%**		**51%**		**46%**		**70%**	

NHR1 has homology with hTAT100

NHR2 is a homodimerization domain

NHR4 is MYND class of zinc fingers

Figure 1.4. Structure and homology among CBFA2T family proteins
Adapted from Davis et al. (2003)

TAF105 and TAF130 from humans, and TAF110 from *D. melanogaster* (Erickson et al., 1994; Kitabayashi et al., 1998a). This domain imparts the nuclear localization to the CBFA2T proteins as it contains nuclear localization signals (Odaka et al., 2000).The second region, NHR2, has a role in dimerisation of the CBFA2T with itself or with other members of the family. The alpha helical sequences of the domain form hydrophobic heptad repeat regions (HHR). These HHR regions are important for the hetero-dimerisation and homo-dimerisation of the proteins (Lutterbach et al., 1998a). It has been reported that dimerisation is also required for oncogenic activities of AML1-ETO (Minucci et al., 2000).

The third region, NHR3, has a coiled-coil structure (Minucci et al., 2000). NHR3 does not share any informative characteristics with any other described domains. Studies of CBFA2T1 have suggested that it may be involved in recruiting certain co-repressors (Hildebrand et al., 2001).

The fourth domain, the C terminal region (NHR4), is also known as MYND [myeloid nervy deformed epidermal auto regulatory factor (DEAF)]. The NHR4 region contains two zinc finger regions, one of CxxC7xCxxC consensus sequence, while the second motif has CxxC7xHxxC consensus sequence (Erickson et al., 1994; Gross & McGinnis, 1996). These zinc finger regions mediate binding to other zinc finger proteins.

1.6 Transcriptional co-repressors

Transcription regulation (gene expression) is an essential process, required to control many cellular events for example cellular proliferation and development. Large numbers of proteins are involved in the regulation of transcription. Recent studies have

shown that the regulation of transcription provides control for both activation and down regulation of genes. Silencing of a gene is also termed gene transcriptional repression. Thus transcriptional repression plays a major role in the regulation of gene expression. Transcriptional repression is controlled by factors called co-repressors, while co-activators are the factors which activate gene transcription.

The interactions of co-repressors with transcription factors (repressors or silencers like BCL6, PLZF, Gfi-1 and ZNF652) results in recruitment of other co-repressors complexes like HDACs, NCoR and Sin3A for transcription repression. Co-repressors actively regulate gene silencing but they do not bind to DNA directly. In fact they recruit other transcription factors, which can bind to the regulatory regions of target genes and with the help of these transcription repressors mediate gene silencing.

These interactions have made transcriptional silencing a complex phenomenon. Different studies have shown that transcription repression involves the interaction of different HDAC (histone deacetylases) which in fact are recruited by different complexes like Sin3A (David et al., 1998; Lutterbach et al., 1998b; Nan et al., 1998). Another transcription repressor N-CoR also interacts with DNA bound nuclear receptors to repress target genes by recruiting HDAC complexes (Horlein et al., 1995). The following sections will give some insight into the transcriptional repression activities of CBFA2T family proteins.

1.6.1 CBFA2T1 (MTG8) as co-repressor

Studies have shown that CBFA2T1 protein functions as a co-repressor (Gelmetti et al., 1998; Hiebert et al., 2001; Hildebrand et al., 2001). These studies have been successful

in identifying the partners (the interacting proteins) with CBFA2T1. Specific regions of CBFA2T1 mediate these interactions, thus multiple domains of CBFA2T1 recruit various transcriptional repressors to form repressor complexes.

Lenny was the first to demonstrate that the NHR2 and NHR4 regions are required to mediate transcription repression of AML-CBFA2T1 targets (Lenny et al., 1995). Wang et al., 1998 first proposed the co-repressor model and isolated the human nuclear co-repressor receptor (N-CoR) in the yeast two hybrid system by using CBFA2T1 as bait. They also reported that even in the absence of the zinc finger motif, NHR4 CBFA2T1 was still able to interact with N-CoR (Lutterbach et al., 1998b; Wang et al., 1998; Wang et al., 2004a). A brief illustration of the locations of all interacting proteins with CBFA2T1/CBFA2T3 is listed in Fig 1.5 (Peterson & Zhang, 2004). The silencing mediator of retinoic acid and thyroid hormone receptor (SMRT) has also been identified as a CBFA2T1 interacting protein (Gelmetti et al., 1998). Both these complexes SMRT and N-CoR work by recruiting histone deacetylase enzymes, and therefore mediate the indirect interaction of CBFA2T1 with HDACs. In one study Wang et al. (1998) provided evidence for indirect interaction of CBFA2T1 with HDACs. They co-expressed FLAG tagged N-CoR and HDAC1 and CBFA2T1 in 293T cells. Immunoprecipitation was done using anti-FLAG antibody, and immunoblotted with anti-CBFA2T1 and anti-HDACs antibodies. They successfully demonstrated the interaction between N-CoR, HDAC1 and CBFA2T1.

Recent data from Zhang et al (2001) have demonstrated that NHR4 zinc finger region imparts interactions with N-CoR and SMART. In addition, NHR2 also interacts with N-

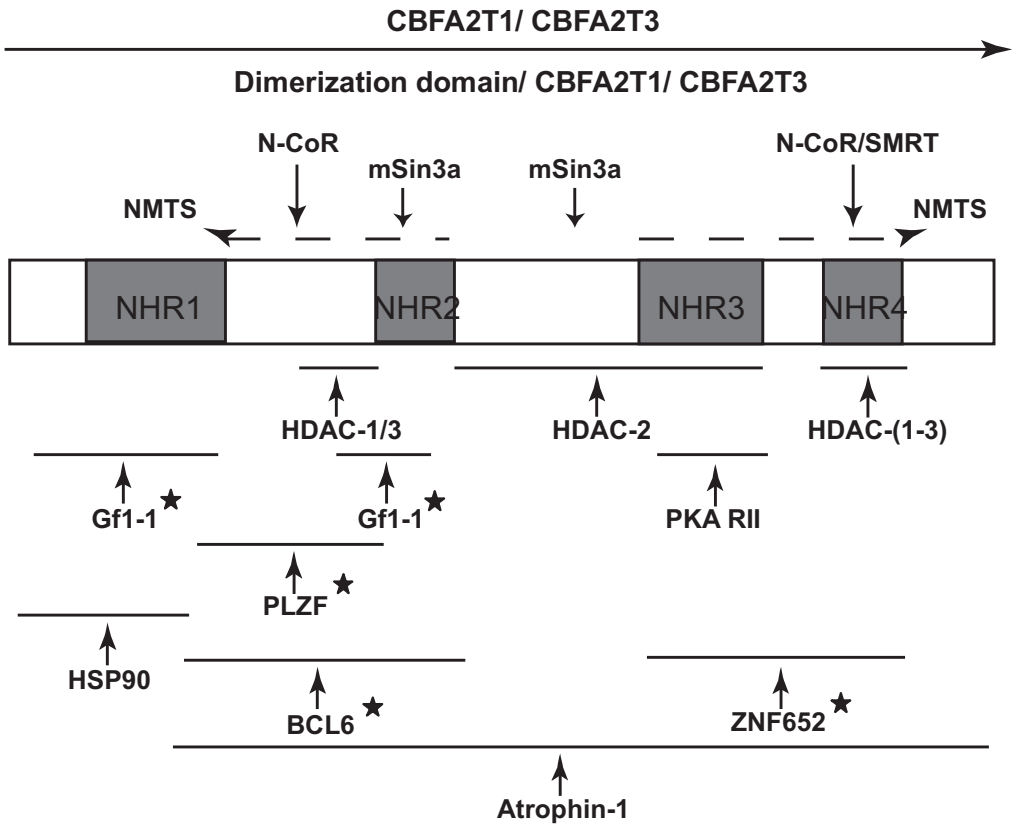

Figure 1.5. Summary of CBFA2T1 and CBFA2T3 interacting proteins. ★ indicates zinc finger containing proteins. Human CBFA2T3 has shown no interaction with PLZF, while murine ETO2 interacts with PLZF. No interaction of mSin3a with murine cbfa2t3 was seen. Instead endogenous mSin3a was shown to interact with CBFA2T3 proteins immunoprecipitated from a breast cancer cell line MCF7 (Fig 6.7 Chapter 6). Atrophin-1 has been found in a yeast two hybrid screen for CBFA2T3 interacting proteins (Callen unpublished data). Current figure was adapted from Peterson and Zhang 2004 and modified for Atrophin-1 and ZNF652 interaction.

CoR, as deletion of NHR2 region results in the reduction of binding activity of CBFA2T1 to N-CoR (Hildebrand et al., 2001; Zhang et al., 2001). Moreover the deletion of NHR2 region reduces the repression activity to 20% but does not eliminate the repression activity. Amann et al (2001) has shown that an NHR2 and NHR4 region mediates the interaction of CBFA2T1 with HDACs (Amann et al., 2001). Sin3A, another transcription repressor, also interacts with CBFA2T1. Interaction between CBFA2T1 and Sin3A is mediated by the NHR2 region but the sequences upstream and downstream of this region also contribute to their interaction (Lutterbach et al., 1998b). Amann et al. 2001, found the deletion of the NHR2 and NHR3 regions abolished the contact of Sin3A with CBFA2T1 (Amann et al., 2001). Wang et al (1999) have shown that the transcription repression activity of CBFA2T1 is related to the recruitment of transcription repressors. The repressive effect of CBFA2T1 was removed with the addition of trichostatin A (TSA) which directly interferes with HDACs (Wang et al., 1999).

1.6.2 CBFA2T3 (MTG16) is a co-repressor

CBFA2T3 also functions as a co-repressor. Kochetkova et al (2002) have performed Gal4 DNA binding domain assays to demonstrate the function of CBFA2T3 as a transcriptional repressor. In this study the repression domain was mapped using constructs with various deletions of the full length CBFA2T3 open reading frame fused to the Gal4 DNA binding domain (DBD). The results showed that the region coding for the central 254 amino acids is responsible for repression activity (Kochetkova et al., 2002), similar to CBFA2T1 (Wang et al., 2004a) corresponding to the NHR2 region of the CBFA2T proteins family.

The repression activity of the CBFA2T family is mediated through its interaction with various additional transcriptional repressors like N-CoR / SMRT and mSin3A. These interactions in turn recruit HDAC enzymes that mediate conformational changes of chromatin material called histone modifications. The human CBFA2T1 binds to Sin3A (Amann et al., 2001), the murine homologue of CBFA2T3, does not interact with Sin3A, although the regions involved in interaction with Sin3A are more then 67% similar between cbfa2t1 and cbfa2t3 (murine homologue). Therefore it is possible that human CBFA2T3 also does not bind to Sin3A suggesting that CBFA2T1 and CBFA2T3 complexes are functionally distinct from each other. Murine cbfa2t3 interaction with HDAC1, HDAC2 and HDAC3, as well as HDAC6 and HDAC8 were reported (Amann et al., 2001). Contrary to the above data another study has shown that HDAC6 does not interact with the transfected human CBFA2T3a (Hoogeveen et al., 2002). The equivalent data relating to binding of different HDACs, including HDAC6 and HDAC8, with the endogenous human CBFA2T3 have not been established. Since the interaction of Sin3A, HDACs and CBFA2T3 are unknown, these will be investigated in this thesis.

A recent study has shown that CBFA2T1 HHR (NHR2) domain imparts cell type specificity, which mediates CBFA2T1 association with other protein complexes in a particular cell environment (Hug et al., 2004). Although the previous data have suggested CBFA2T1 and CBFA2T3 role in haematopoiesis, there is likelihood that the CBFA2T3 transcription repression complexes have a possible role in breast tumourigenesis.

1.7 CBFA2T interacting transcription factors

CBFA2T family proteins do not bind to DNA directly but they bind to transcription factors (DNA binding proteins), which bind to specific DNA sequences of target genes. These DNA binding proteins are part of the co-repressor complexes. To date four zinc fingers transcription factors have been found which bind with CBFA2T1. Gfi-1 a transcriptional repressor, involved in haematopoiesis, has been identified as a CBFA2T1 interacting protein. Furthermore Gfi-1 interaction with CBFA2T3 has also been reported (McGhee et al., 2003). Details about the transcription factors BCL6, PLZF and ZNF652 are given in the following sections.

1.7.1 Promyelocytic leukaemia zinc finger protein (PLZF)

PLZF is a zinc finger protein involved in t(11;17) myeloid leukaemia. This translocation generates a fusion protein derived from the two fused genes. First is the retinoic acid receptor gene *RARα* located on 17q12. The second gene, promyelocytic leukaemia zinc finger gene (*PLZF*) is located on chromosome 11(Chen et al., 1993; Mistry et al., 2003). PLZF and PLZF-RARα both function as transcription factors and result in the block of cell growth and differentiation, while at the same time promote apoptosis (Shaknovich et al., 1998). This aberrant transcription factor affects genes, regulated by RARα, in a dominant negative mechanism (Melnick & Licht, 1999).

Structure of the PLZF protein is shown in Fig 1.6 (Mistry et al., 2003). PLZF is a zinc finger transcription factor comprising nine kruppel like Cys_2 His_2 zinc finger motifs. It is a sequence specific transcriptional repressor and recruits the co-repressors molecules, N-CoR, SMRT and HDAC1, for its repression activity (Hong et al., 1997; Lin et al., 1998). These interactions with co-repressors are mediated through a *N-terminal*

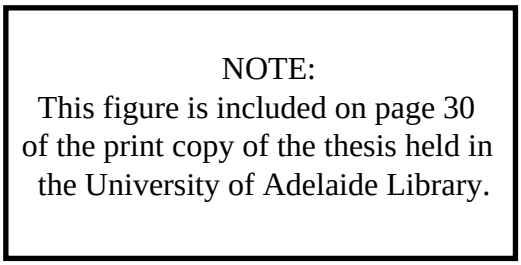

Figure 1.6. Structure of Promyelocytic Leukaemia Zinc Finger protein (PLZF).
Redrawn from Petrie. K et al. (2008).

conserved region called the BTB/POZ domain of PLZF. This region also mediates homo- and hetero-dimerization. However, the repression domains are more complex. since (Melnick et al., 2000a) has shown that the central domain also has a role in the repression activity.

PLZF is expressed in early haematopoietic cells (Reid et al., 1995) but during the later stages of haematopoietic differentiation its expression is down regulated. PLZF has been shown to regulate the genes involved in the cell cycle such as *cyclin A2, c-myc and the hox* gene complex. Melnick et al., (2000b) have demonstrated that the CBFA2T1 (ETO) protein physically and functionally interacts with PLZF. They assayed transcription repression in the 293T cell line using reporter plasmids having four copies of the PLZF DNA binding sites linked to the gene coding for firefly luciferase. The results showed that CBFA2T1 enhances the repression caused by PLZF, and this repression is abrogated when the cells were treated with HDAC inhibitors. The POZ/BTB domain of PLZF is important for stabilising the multi-protein complex, and the second repression domain NHR2 of CBFA2T1 is required for this interaction. Moreover PLZF has multiple sites for interaction with co-repressors.

CBFA2T1 and PLZF interact to form the functional repression complex in myeloid leukaemia but whether CBFA2T3 interacts with PLZF is unknown. Studies suggest that the major function of PLZF is in hematopoietic differentiation. If an interaction between PLZF and CBFA2T3 does occur than PLZF-CBFA2T3 target genes may also have a role in breast cancer (see section for role of CBFA2T3 in breast cancer, Chapter 5 and Chapter 6).

1.7.2 B-cell lymphoma gene 6 protein (BCL6)

BCL6 is an oncoprotein, most frequently involved in B-cell lymphomas, a common haematological malignancy among patients between 20-40 years of age. Almost 40% of the B-cell lymphoma patients are reported to have alteration in the *BCL6* gene (Ye, 2000).

The *BCL6* gene is located at chromosome band 3q27. The *BCL6* gene is frequently translocated to different chromosomal loci, particularly the immunoglobulin light and heavy chain gene loci. These translocations result in alterations in the promoter region rather then any changes to the structure and function of the protein (Ye et al., 1995). These translocations do not appear to cause the over-expression of BCL6 but rather they inhibit down regulation of the gene as this gene after translocation is under the control of immunoglobulin promoter. Somatic hypermutations of the *BCL6* locus are also reported (Pasqualucci et al., 1998).

BCL6 is the member of BTB/POZ (***b****ric-a-brack****, t****ramtrack, **b****road complex/**po**xi virus **z**inc finger*) family of transcription factors. The protein has a POZ domain and several kruppel C2-H2 zinc finger binding domains. The structure for these two regions is 80-90% conserved among all the homologues from different species.

The zinc finger domains of the BCL6 protein bind to DNA in a sequence specific manner. Several groups have identified the 9 base pair consensus DNA binding sequence, TTCCT (A/C) GAA (Chang et al., 1996). The consensus binding sequences of the BCL6 protein have perfect homology with the binding sites of the STAT protein. This indicates the possibility that BCL6 represses transcription through the STAT factor binding sites (Dent et al., 1997; Harris et al., 1999). However, the BCL6 protein has less

affinity to STAT consensus DNA binding sequences so the number of genes repressed through the consensus STAT sequences is limited. It is still not clear whether the target genes are regulated by BCL6, the STAT factor or both.

The BCL6 protein has multiple potential phosphorylation sites and is known to be phosphorylated (Moriyama et al., 1997). However the role of phosphorylation in the regulation of BCL6 transcriptional function is still unclear. Rapidly proliferating germinal centre B cells have high levels of BCL6 protein expression, suggesting that BCL6 acts as a positive regulator of B cell proliferation or in other words it acts as transcriptional regulator.

The BCL6 protein contains two non-contiguous domains termed as "repression domains" that confer further repression activity. The first domain is POZ domain responsible for mediating protein-protein interaction. The *N-terminal* BTB/POZ domain of BCL6 protein has a major role in transcriptional repression. It interacts with co-repressors N-CoR, SMRT (Huynh & Bardwell, 1998) and BCoR (Huynh et al., 2000). These co-repressors recruit histone deacetylases protein complexes to repress the transcription of target genes. The second domain is located between 240-395 amino acid sequences. This domain is characterized by the presence of charged amino acids and proline rich regions. The mechanism of action of the second domain is still unclear (Chang et al., 1996).

A recent study carried out by Chevallier et al (2004). reported that BCL6 interacts with the CBFA2T1 protein. CBFA2T1 binds to the fourth zinc finger of BCL6 and the zinc fingers of BCL6 fold in such a way that they both bind to CBFA2T1 and also make

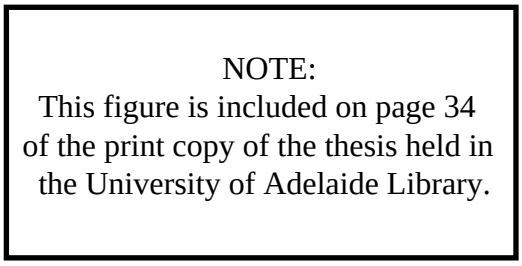

Figure 1.7. A model of BCL6 transcription repressor complexes showing its interaction with CBFA2T1, SMRT, N-CoR and HDACs.
Adopted from Chevallier et al. (2004).

contact with DNA. A proposed model for these interactions is shown in Fig 1.7 (Chevallier et al., 2004). The interaction between CBFA2T1 and BCL6 is further supported by the co-localization of endogenous BCL6 and CBFA2T1 to nuclear speckles. CBFA2T1 also enhances the BCL6 repression of its endogenous target genes. EMSA super shift experiments have also shown that CBFA2T1 is present in BCL6 DNA complexes.

BCL6 represses the transcription of many genes involved in cell cycle control, for example *BLIMP1* (B cell activation and terminal differentiation*)*, *PDCD2* (Programmed cell death–2) and *CCND2* (Cyclin D2) (Shaffer et al., 2000). It also act as an immortalising oncogene, as it imparts resistance against the *p53* and *p19* ^{ARF} pathways (Shvarts et al., 2002) which are important check points for the progression of cellular proliferation.

Cyclin D1 and D2 are also targets of the BCL6 protein (Schmidt et al., 2002). Cyclin D1 is frequently expressed in invasive breast cancers (van Diest et al., 1997). BCL6 is expressed at low levels in normal breast ducts, while its overexpression is reported in 16% of invasive breast cancers (Bos et al., 2003). A study on invasive breast cancer has shown the overexpression of BCL6 is likely to be related to the overexpression of cyclin D1, p53 and HIF-1α positivity (Bos et al., 2003). BCL6 is reported to be a potent inhibitor of senescence response. It mediates its function by induction of cyclin D1 expression downstream of $p19^{ARF}$-p53 pathways (Shvarts et al., 2002). All these studies suggest a possible role of BCL6 protein in cell cycle regulation.

BCL6 interacts with CBFA2T1 and BCL6 is shown to be overexpressed in malignancies other then leukaemia, like breast cancer (Bos et al., 2003). CBFA2T3 is a known putative breast tumour suppressor protein (Kochetkova et al., 2002), which also functions as a transcriptional co-repressor. Based on these findings, there is the likelihood that BCL6 interacts with CBFA2T3 protein and plays a role in normal mammary ducts development or in pathways related to breast tumour development and progression.

1.7.3 ZNF652: a novel zinc finger protein interacts with CBFA2T3

ZNF652 was identified as a novel protein in a yeast two-hybrid screen using a segment of the CBFA2T3 protein as bait (Kumar et al., 2006). In a general survey of cDNA profiling array, a decreased expression of ZNF652 was found in tumours as compared to their matched normal tissues. Down regulation of ZNF652 level was also reported in breast cancer cells lines negative for ER expression, but not in cell lines positive for ER expression. In addition, reduced ZNF652 protein expression was seen in 25% of VIN II, 100% of VINIII (vulvar intraepithelial neoplasia) and 50% of vulvar squamous cell carcinomas (Holm et al., 2008).

In silico analysis has shown that ZNF652 contains seven classical zinc finger motifs with two conserved cystine and histidine residues (C2H2) (Kumar et al., 2006). Three of these zinc fingers are joined by classical linker sequences known to be associated with DNA binding properties (Matthews & Sunde, 2002; Wolfe et al., 2000). It is of interest that ZNF652 does not posses an identifiable repression domain, as does the other CBFA2T interacting zinc finger proteins BCL6 and PLZF. It is suggested that the transcriptional repression effects mediated by ZNF652-CBFA2T3 repressor complexes

are mediated by the other proteins, in particular CBFA2T3, recruiting co-repressors to the complex.

Coimmunoprecipitation experiments have shown a strong interaction of ZNF652 with CBFA2T3 while on the other hand a week interaction with CBFA2T1 and CBFA2T2 was observed (Kumar et al., 2008). Interaction of CBFA2T3 with ZNF652 is through the NH3 and NH4 domains of CBFA2T3 and is mediated through the proline-rich region present in the C-terminus of ZNF652. Kumar *et.al* have identified the E box containing gene *HEB* as a direct target of the CBFA2T3-ZNF652 repressor complexes (Kumar et al., 2008). ZNF652 RE (response elements) have been found in the HEB promoter region. Promoter binding assays have successfully shown the binding of CBFA2T3- ZNF652 complexes to the HEB promoter leading to the HEB transcriptional repression. Another report has demonstrated the role of CBFA2T3 (ETO2) in regulation of haematopoiesis and myogenesis (Goardon et al., 2006). The TAL-1 transcription factor recruits CBFA2T3 through interaction with E2A/HEB. CBFA2T3 represses erytheroid related TAL-1 target genes required for erytheroid progenitor's expansion, while a change in CBFA2T3 levels to TAL-1 complexes is reported with commencement of erytheroid differentiation. Stoichiometric changes in CBFA2T3 levels relative to E2A/HEB activators determine the activation or repression of the TAL-1/SCL target genes. This eventually leads to switching of proliferation pathways to differentiation pathways or vice versa.

The CBFA2T3 is a breast tumour suppressor and specifically interacts with ZNF652, a novel zinc finger protein. One of the aims of this study is to determine the expression of these two proteins in paraffin embedded normal and breast tumour sections. This will

provide data regarding any association among these proteins and the known breast tumour markers.

1.8 Role of cell cycle proteins in breast cancer

Cellular proliferation is regulated through number of different kinases, with the cyclin-dependent kinases (CDKs) being the most important (Reed et al., 1994; Sherr, 1994). CDKs belong to a family of serine-threonine kinases. CDKs levels remain constant during normal cellular proliferation. The constant levels of CDKs are due to a net balance between its positive and negative regulators. CDKs are positively regulated by phosphorylation. On the other hand the CDKs inhibitors (CKIs) mediate the negative regulation of cyclin dependant kinases (Reed et al., 1994). The levels of CKIs vary during different stages of the cell cycle (Koepp et al., 1999).

Several studies have identified the important role of cyclin D1, cyclin E and cyclin dependent kinase inhibitors p21 and p27 in the control of cell cycle in breast cancer (Fig 1.8) (Caldon et al., 2006; Keyomarsi et al., 2002). These proteins act as potential oncogenes or tumour suppressor genes. Through mitogenic stimuli or steroid hormone receptors these proteins are activated in breast cancer cells. These three proteins regulate the cell's progression through the different phases of the cell cycle. Cyclin D1, involved into the G1 to S phase progression of the cell, function through the phosphorylation of retinoblastoma protein (Rb). Cyclin-E and cyclin-A promote S phase entry and progression through S phase of the cell cycle through activation of CDK2.

Cyclin D1 overexpression in mice, results in development of mammary cancers but of long latency. It is suggested that cyclin D1 may cooperate with other oncogenes. Studies

have shown the crucial role of cyclin D1 in HER-2 (erbB2) mediated mammary tumours (Fu et al., 2004). Another report has shown upregulation of the cyclin D1 levels in invasive breast tumours which was found related to the upregulation BCL6 (Bos et al., 2003). Recent studies have indicated the potential involvement of BCL6 in breast carcinogenesis. Albagli et al (1999) have shown that overexpression of BCL6 in U2OS cells mediate growth suppression, which is found, associated with impaired S phase progression. The overexpressed BCL6 colocalize to the sites of DNA synthesis, which directly interfere with the S phase transition (Albagli et al., 1999).

Cyclin D over-expression is reported in 30-50% of breast cancers (Musgrove et al., 1994; Wang et al., 1994). In general, ER positive cancers showed frequent amplification of cyclin D1 as compare to the ER negative breast cancers (Sutherland & Musgrove, 2004).

Overexpression of cyclin E is also frequently observed among breast cancers, particularly ER negative breast tumours (Sutherland & Musgrove, 2004). Cyclin E overexpression is associated with its low molecular weight isoform having greater binding capacity towards Cdk2. The resulting complexes due to these low molecular cyclin E isoforms are resistant to p21 and p27 mediated inhibition (Wingate et al., 2005). Cyclin E is commonly used as a prognostic marker in breast cancer but its use is of significance only when restricted to the tumours with low levels of p27 expression.

p27 is an important inhibitor of CDKs. A high level of p27 has been found in quiescent cells, which indicates its role in the control of cell cycle (Sherr & Roberts, 1999) and

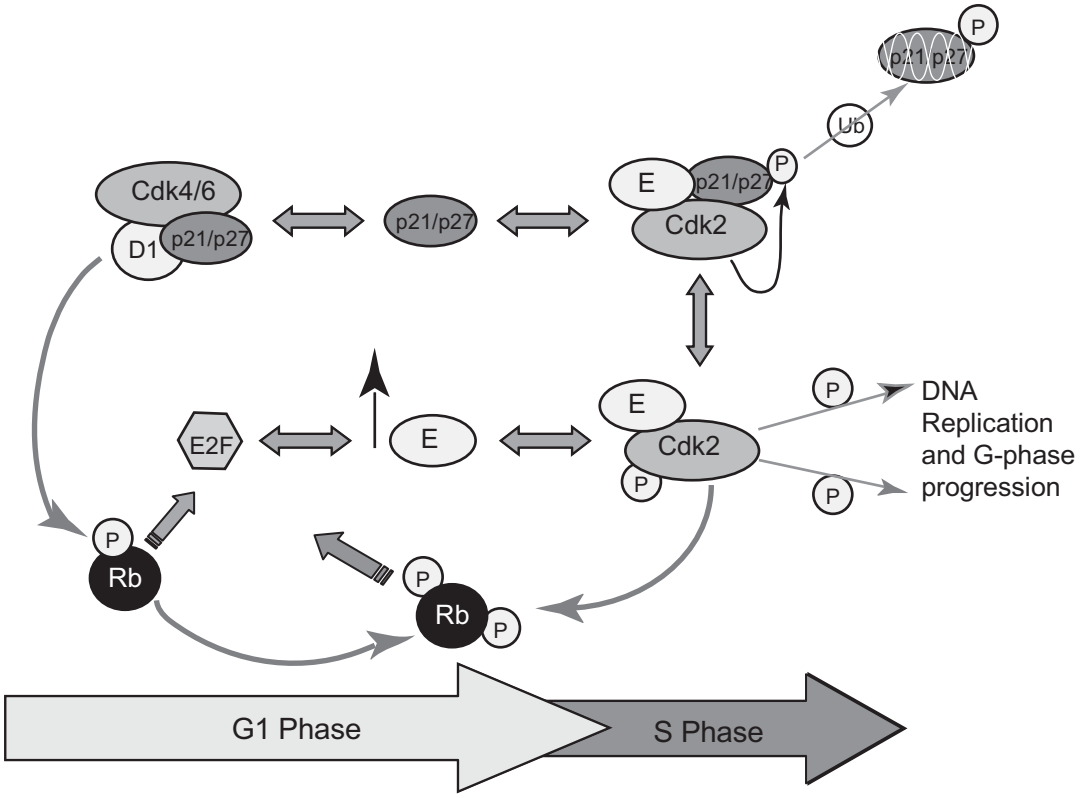

Figure 1.8. Control of cell cycle progression from G1 into S phase.
The model illustrating the role of cyclin D1 (D1) and cyclin E (E1) in G1-S phase progression. Sequential phosphorylation of Rb by cyclin D1 and cyclin E-Cdk2 allows E2F mediated transcription of target genes and consequent progression of S phase. Encircled P marks for phosphorylation. Adapted from (Caldon et.al. (2006).

induction of senescence in preinvasive lesion of prostate cancer (Majumder et al., 2008). p27 also has a role in cell to cell adhesion and in inhibition of cellular growth. Increased levels of p27 resulted into the disruption of cell to cell adhesion. Different studies have shown the decreased level of p27 in breast tumours compared to normal breast tissue (De Paola et al., 2002). These observed p27 deregulation were found in very early breast cancer lesion.

Another recent report has shown the role of AML-CBFA2T1 in leukaemia cell proliferation. The authors have shown that the AML-CBFA2T1 siRNA resulted in inhibited proliferation of the leukaemia positive cell line. Additionally, it inhibits the G1_S transition during the cell cycle. They also suggested that the change in cell cycle is associated with p27 as they found a two-fold increase in the level of p27 after the introduction of AML-CBFA2T1 siRNA into leukaemia cells (Martinez et al., 2004).

As reviewed in this section various published studies have shown the up and down regulation of different cell cycle regulatory proteins in breast cancer. Interaction of CBFA2T family proteins with these cell cycle regulators or modulation of these cell cycle regulators by CBFA2T family proteins suggest a possible role for CBFA2T in cell cycle regulation through interaction with various transcription factors such as BCL6 and PLZF. In this thesis a possible role of the CBFA2T3 protein in cellular proliferation will be investigated.

1.9 Summary

Breast cancer is the most common cancer in women and is the second major cause of death among cancer. In breast tumours, the most commonly observed somatic

chromosomal change is LOH. LOH at 16q is found in pre-malignant types of breast cancers such as ADH and DCIS indicating that loss of 16q is an early event (Wang et al., 2004b). Three putative tumour suppressor genes, *CBFA2T3*, *CYBA* and *FBX031* have been identified from this region of the chromosome (Powell et al., 2002). This thesis investigates the role of CBFA2T3 in breast tumourigenesis.

CBFA2T protein family functions as transcriptional co-repressors by recruiting a number of transcription factors (DNA binding proteins like ZNF652 and Gfi1) and other co-repressors as HDACs. The interaction and roles of these complexes (DNA binding proteins) with CBFA2T3 are yet to be elucidated. Additionally, the functional pathways of these complexes are also not clear.

1.9.1 Aims and significance of the project

The present study aims to determine the protein expression profile of the CBFA2T3 isoforms in different breast cancer cell lines and breast tumour tissues. Localization studies on exogenously expressed tagged forms of CBFA2T3 “a” and “b” proteins as well as endogenous CBFA2T3 proteins will give an insight into the role of these proteins in various cellular processes.

In order to evaluate CBFA2T3 as a prognostic marker, expression analysis of CBFA2T3 in normal breast tissue and breast tumour sections will be carried out. Analysis of CBFA2T3 expression with known breast tumour markers will be determined in a cohort of breast tumours to evaluate CBFA2T3 as a prognostic marker.

Tumour suppressor genes are not good drug targets, but the genes that are transcriptionally repressed by the tumour suppressor genes are oncogenic and thus more likely to be possible drug targets. As CBFA2T3 does not directly bind DNA, this study aims to investigate the interaction of CBFA2T3 with various DNA binding proteins and to further characterize the transcriptional repressor complexes. Knowledge of these will eventually help to determine the target genes which are silenced by the CBFA2T3 transcriptional repressor complexes, and these will be potential targets for breast cancer drug development.

Chapter 2 - General Material and Methods

2.1 - Cell lines

The majority of the human cell lines like MCF-7, BT-20, T47-D, MDA-MB-231, MDA-MB-468, SKBR-3 (human breast cancer), HEK293T (human embryonic kidney), HeLa (human cervical cancer), U2OS (human osteosarcoma cell line) and CHO (chinese hamster ovary) cell lines were purchased from the American Type Culture Collection (ATCC) and were grown in the recommended media. Cells were grown at 37°C in 5% CO_2. Two finite life span human mammary epithelial cell lines 184V and 48RS (HMEC) and 184A1, a non-malignant immortally transformed cell line derived from normal breast epithelium, were kindly supplied by Dr Martha Stampfer and were grown in MCDB-170 medium (Life Technologies) (Stampfer & Yaswen, 2003).

2.2 - Transient transfection of cell lines

Transient transfection of DNA constructs were performed in a 6-well plate format. Cells were seeded at 60-80% confluency in antibiotic-free medium overnight. Media was changed to Opti MEM with 5% fetal calf serum before transfection and incubated at 37°C. Transfections were performed in Opti-MEM media without fetal bovine sera using Lipofectamine 2000 transfection reagent (Invitrogen, Carlsbad, CA) in accordance with the manufacturer's protocol. 1 to 4µg DNA was mixed well with 250 µl Opti-MEM while 2.5 to10 µl of Lipofectamine 2000 was mixed with 250 µl Opti-MEM in a second tube. Both tubes were left for 5 minutes at room temperature. DNA and Lipofectamine complexes were mixed and incubated for a further 20 mins at room

temperature. DNA-Lipofectamine complexes were added to the cells (with caution to avoid cell disturbance as HEK293T cells easily detach from the plastic surface) drop-wise and incubated at 37°C for a further 24 hours before analysis. If cells were required to be left for a longer period, the media was replaced with DMEM containing 10% FCS.

2.3 - Transient transfection for immunolocalization studies

Immunolocalization studies were carried out either in 4 well or 8 well format chambered slides (Nalge Nunc, Naperville, IL). The number of cells seeded in chambered slides was modified depending upon the cell line used, for example HEK293T due to its more rapid growth, was plated at less than 60-80% confluence as compared to HeLa cell line. For 4 well chambered slides 800ng-1µg of DNA was transfected using 2-2.5 µl amount of Lipofectamine 2000. The remaining procedure was same as described in section 2.2.

2.4 - Oligonucleotide primers and DNA constructs

Different primers were designed for the generation and validation of sequences of various clones throughout this research work. The details of primers and construct generated and used during the current study are given in Table 2.1 and Table 2.2 respectively. Note that sometimes CBFA2T family members were termed according to previously used nomenclature as CBFA2T1/MTG8, CBFA2T2/MTGR1 and CBFA2T3/MTG16.

2.5 –Buffers and solutions used

Recipes for various buffers used during the current study are detailed in Table 2.4.

Table 2.1 Oligo primers.

#	Primer name	Direction	Sequence 5-3'	Description
1	LNCX2-2637	Forward	CCTACTTGGCAGTACATCTACGTA	Sequencing of insert
2	MTG16a-BglIIIR	Reverse	CACACAGATCTCGGAGCAGCCGGCAGATGCCA	*CBFA2T3a ORF* amplification
3	MTG16a-EcoR1F	Forward	CACACGAATTCCTGCAGGAGGTCGGGAAAGGCAG	*CBFA2T3a ORF* amplification
4	MTG16EX4F2	Forward	ACCACACTGCAGCAGTTTGGCAGC	Real time RT-PCR *CBFA2T3*
5	MTG16EX6R1	Reverse	AGTAGCAGCTCTGAGGAGTCGAT	
6	MTG16-F1754	Forward	CGTGCCAAGATGGAGCGGGCCCTG	Real time RT-PCR *CBFA2T3*
7	MTG16-R1935	Reverse	TCCAGGCACCGGGTCGGCCACCAC	
8	MTG8-F1837	Forward	GGCAGGCGGCGGAGGACGCACTGG	Real time RT-PCR *CBFA2T1*
9	MTG8-2035	Reverse	GGCTCCCAGCCCCGCTGTTGGGCG	
10	MTGR-F1943	Forward	AGAGCACGAATGGAGCAAACCATA	Real time RT-PCR *CBFA2T2*
11	MTGR-R2177	Reverse	AGCAGCGGCCGGCCCTGGCCGTGG	
12	Cyc-D2-F4961	Forward	TGGGTCATCCTTGGTCTATGTGCTC	Real time RT-PCR *CCND2*
13	Cyc-D2-R5049	Reverse	AGGGTTGTCTTCTCCTCTGGCTTTG	
14	BCL6-BH1-F	Forward	CACACACACAGGATCCCCATGGCCTC GCCGGCTGACAGCTG	*BCL6* cloning in pCMV-HA

15	BCL6-BH1-R	Reverse	CACACACACACAGGATCCTCAGCAGG CTTTGGGGAGCTCCG	
16	PLZF-ER1-F	Forward	CACACACACAGAATTCGGATGGATCTG ACAAAAATGGGCATG	*PLZF* cloning in pCMV-HA
17	PLZF-BH1-R	Reverse	CACACACACAGGATCCTCACACATAGCAC AGGTAGAGGTAC	
18	BCL6-F-540	Forward	CAGCCTGTACAGTGGCCTGTCC	Sequencing *BCL6 ORF*
19	BCL6-F-1023	Forward	AACTCGCCCACAGAGTCCTGC	
20	BCL6-F-1572	Forward	CTGCCGCTTCTCTGAGGAGGC	
21	PLZF-F-359	Forward	GATGCTGGAGACCATCCAGGC	Sequencing *PLZF ORF*
22	PLZF-F-778	Forward	GCCGAGTCCAGCATCTCAGGAGG	
23	PLZF-F-1420	Forward	AGGATGCCCTGGAGACACACAGG	
24	MTG16b-Xba1-F	Forward	CACACATCTAGAATGCCGGACTCCCCAGCGGAGGTG	*CBFA2T3b* cloning
25	MTG16b-ER1-R	Reverse	CACACAGAATTCTAGCGGGGCACGGTGTCCAGTGG	
26	CYC/F1	Forward	GGCAAATGCTGGACCCAACACAAA	Real time PCR *Cyclophilin-A*
27	CYC/R1	Reverse	CTAGGCATGGGAGGGAACAAGGAA	
28	MTG16a ZF1	Forward	AGATACCCCAGGCTGAAGGAAG	*CBFA2T3a* Start site

29	MTG16a ZF2	Forward	AGGATGGAGCTGCCCTCAGGC	*CBFA2T3a* Start site
30	MTG16a ZR1	Reverse	TGTCCCTCAGTCTTGAAGCCG	*CBFA2T3a* Start site
31	MTG16a 5'ext F1	Forward	AGGTACTTTGAGGACAGGTCAGGT	
32	MTG16a 5'125F2	Forward	AAGGCAGTCCTGGTAGAGGCCTGT	
33	MTG16-Cla1-R	Reverse	CACACACACACACAATCGATGCGGGGC ACGGTGTCCAGTGGGCCA	Used in cloning (as mentioned)
34	Z16a F-Bgl II	Forward	CACACACACAGATCTCCACCATGCCGGC TTCAAGACTGAGGGA	*CBFA2T3a* cloning pEGFP-N1
35	Z16a R-ER1	Reverse	CACACAGAATTCGGCGGGGCACGGTGTC CAGTGGGCCA	
36	Z16aT-BglII-myc-F	Forward	CACACACACAGATCTCGAGATGGAGCAGAAG CTGATCAGCGAGGAGGACCTGATGCCGGCTTCAA GACTGAGGGACAG	*CBFA2T3aT* cloning pEGFP-N1
37	Z16b-BglII-myc-F	Forward	CACACACACAGATCTCGAGATGGAGCAGAAGCT GATCAGCGAGGAGGACCTGATGCCGGACTCCCCA GCGGAGGTGAAG	*CBFA2T3b* cloning in pEGFP-N1
38	shM16-EMBO-F	Forward	GATCCCCGAAGTGATCGACCACAAGCTTCAAG AGA GCTTGTGGTCGATCACTTCTTTTTGGAAA	*CBFA2T3* short hairpin primers *EMBO* (Goardon et al., 2006)
39	shM16-EMBO-R	Reverse	AGCTTTTCCAAAAAGAAGTGATCGACCACAAGC TCTCTTGAAGCTTGTGGTCGATCACTTCGGG	

40	BCL6-Kpn-F	Forward	CACACACACAGGTACCCCATGGCCTCGCCGGCT GACAGCTG	*BCL6* reverse cloning in pCMV-HA
41	BCL6-BH1-R	Reverse	CACACACACACAGGATCCTCAGCAGGCTTTGG GGAGCTCCG	
42	MTG16-RNAi-I	Forward	GATCCCGTCCACAGCCTCCTTGTCCTTCAAGAGAG GACATAGGAGGCTGTGGACTTTTTGGAAAA	*CBFA2T3* short hairpin I (*MTG16 hp I*)
43	MTG16-RNAi-I	Reverse	CGCGTTTTCCAAAAAGTCCACAGCCTCCTTGTCCTC TCTTTGAAGGACAAGGAGGCTGTGGACGG	
44	MTG16-RNAi-II	Forward	GATCCCGCAACGCGGCACGCTACTGCTTCAAGAGA GCAGTTAGCGTGCCGCGTTGCTTTTTGGAAAA	*CBFA2T3* short hairpin II (*MTG16 hp II)*
45	MTG16-RNAi-II	Reverse	CGCGTTTTCCAAAAAGCAACGCGGCACGCTACTGCT CTCTTTGAAGCAGTAGCGTGCCGCGTTGCGG	
46	R378	Forward	CACACACACAGAATTCGGAGACAGACCATAGACCA TTTTAAG	*CBFA2T3a* Start site
47	R183	Reverse	CACACACACAGAATTCGCGCTGAGGCCTTAGCTTTC CTGT	*CBFA2T3a* Start site

Table 2.2 List of different constructs generated or used (generated by other persons) during this study.

	Clone name	Glycerol stock #	Details of various *ORF* and Vectors
1	pCMVmyc-MTG16b	356	MTG16b BclI-Not1 fragment from MTG16-pQCXIN GS#208 cloned at BglII site in pCMV-myc.
2	pEGFP-C1-MTG16b	380	MTG16b PCR-ed from myc-MTG16b-pLNCX2 with myc-EcoRI-F and pLNCX2-3075-EcoRI-R and cloned at EcoRI site of pEGFP-C1 vector.
3	3n4 (BCL6-HA)	378	BCL6-orf PCR-ed with BCL6-BHI-F and -R primers and cloned at BglII site of pCMV-HA (generated by *Ross McKirdy*).
4	3n1 (BCL6-HA)	473	BCL6-orf PCR-ed with BCL6-BHI-F and -R primers and cloned at BglII site of pCMV-HA Contain mutation at 1652 bp position changing Cystine to Tyrosine.
5	MTG16b promoter-into DM50602A1	503	MTG16b promoter region amplified from BAC. Digested with EcoRI/BamHI and cloned pBluescript (*Dr David. Millband*).
6	pDM50624-1 pGL3	507	DM50602A1 (GS 503) digested with KpnI/BamHI and inserted into pGL3 basic at KpnI/BglII -Basic-16b-Promoter (*Dr David. Millband*).

7	JLE1 pGL3-Basic ERE-16b	559	ERE region (Xho1/EcoR1) of MTG16b promoter from BAC368 PCR amplified and inserted into #507 pGL3-Basic-16b promoter at Xho1/EcoR1 sites (*Jacklyn Lee*).
8	pGL3-Basic-16b-Pro-DeltBCL6BS1	627	pBluescript-16b promoter R1 to BamH1 deleted through site directed mutagenesis to mutate putative BCL6-BS1 (GS#612). Kpn/BamHI fragment from (GS612 -DM5921B) into Kpn/BglII of pGL3- Basic (*Dr David. Millband*).
9	pcDNA3-BCL6-ZnF1-6mut	543-48	BCL6-znic finger mutants 1-6 cloned in pcDNA3 (Dr *Claudie Lemercier* (Mascle et al., 2003).
10	5j1 (pCMV-HA-BCL6WT)	670	BCL6-HA wild type generated by using 3n1 (473) and 3n4 (378) clone (Generated by *R Kumar* and *Ross. McKirdy*).
11	16a-L1GFP Fusion (F1-1)	863	16a leader sequence fragment 1 amplified from MTG16a-LNCX2 (GS#135) with LNCX2-F and MTG16R 378-ER1 reverse primers, cloned at BglII/EcoR1 site of pEGFP-N1vector.
12	16a-L2GFP Fusion (F2-1)	864	16a leader sequence fragment 2 amplified from MTG16a-LNCX2 (GS#135) with LNCX2-F and MTG16R 183 ER1 primer, cloned at bgl11-EcoR1 site of pEGFP-N1.

13	z3-1(pMSCVpuroD3'LTRD EGFP)gs1.	866	pMSCVpuroD3'LTRDHindIII-H1-hpM16-EMBO-F/R (Goardon et al., 2006) in gs1; pMSCV HindIII-H1-hpM16-EMBO- vector with EGFP ORF.
14	pcDNA3.1-Flag-HDAC1-7	489-95	FLAG-tagged HDAC1-7 were cloned in pcDNA3.1 (a kind gift by *Dr Kum Kum Khanna*).
15	pLNCX2-myc-MTG16b	134	MTG16b ORF with myc tag cloned into SalI/ClaI of LNCX2 {*Dr M. Kochetkova* {Kochetkova, 2002 #2}}.
16	pLNCX2-myc-MTG16a	135	MTG16a ORF with myc tag cloned into XhoI/ClaI of LNCX2 (*Dr M. Kochetkova*).
17	RMJ3; untagged MTG16b	164	MTG16b cloned into XbaI/EcoRI of pcDNA3.1 (*Ross. McKirdy*).
18	16a-L1GFP Fusion (F1-1)		16a leader sequence fragment 1 amplified from MTG16a-LNCX2 (GS#135) with LNCX2-F and MTG16R 378-ER1 reverse primers, cloned at BglII/EcoR1 site of pEGFP-C1vector.
19	16a-L2GFP Fusion (F2-1)		16a leader sequence fragment 2 amplified from MTG16a-LNCX2 (GS#135) with LNCX2-F and MTG16R 183 ER1 primer, cloned at bgl11-EcoR1 site of pEGFP-C1.
20	16aT-myc-GFP-pEGFP-N1		MTG16aT ORF amplified with Z16aT-BglII-myc-F / Z16a R-ERI and cloned in pEGFP-N1

21	16b-myc-GFP in pEGFP-N1		MTG16b ORF amplified with Z16b-BglII-myc-F and Z16a R-ERI cloned in pEGFP-N1.
22	P2 -pCMV-HA-PLZF	725	PLZF ORF amplified with PLZF-ERI-F/PLZF-BHI-R and cloned at EcoRI-BglII sites of pCMV-HA vector.
23	RMM3	171	MTG16hp I cloned into BglII/HindIII digested sa2 H1 (*Ross. McKirdy*).
24	RMM7	172	MTG16hp II cloned into BglII/HindIII digested sa2 H1 (*Ross. McKirdy*).

Table 2.3 List and recipes of various buffers used during this study.

Buffer name	Recipes
Lysis buffer 1 (MP lysis buffer)	(50 mM Tris-HCl (pH 7.5), 250 mM NaCl, 1% Triton X-100, 1 mM EDTA, 50 mM NaF, 0.1 mM Na_3VO_4)
Lysis buffer A (Cytosolic fractions)	(10 mM HEPES pH7.9, 10 mM KCl, 1.5 mM $MgCl_2$, 340 mM sucrose, 10% glycerol, 0.5 mM DTT, 0.1% Triton X-100)
Lysis buffer B (Nuclear fractions)	(20 mM HEPES pH7.9, 420 mM NaCl, 1.5 mM $MgCl_2$, 0.2 mM EDTA, 0.5 mM DTT, 25% glycerol)
IP lysis buffer	(50 mmol/L Tris-HCl (pH 8.0), 150 mmol/L NaCl, 1% Triton X-100)
Wash buffer 1	(50 mM Tris-HCl pH 8.0, 150 mM NaCl, 1% NP-40. 0.5% SDS and 0.1% sodium deoxycholate)
Low salt buffer	(20 mM Tris-HCl pH 7.5)
SDS-PAGE (sample loading buffer)	(0.0625 M Tris (pH 6.8), 2% SDS, 10% glycerol, 5% mercaptoethanol and 0.05% bromphenol blue)
5X RT buffer	(250 mM Tris-HCl pH 8.3, 375 mM KCl, 15 mM $MgCl_2$, 50 mM DTT)
Western Transfer buffer	(0.025M Tris-HCl, 0.192M glycines, 0.1%SDS)
SDS-PAGE buffer (pH 6.8)	(0.125 M Tris-HCl pH 6.8, 0.1% SDS)
SDS-PAGE buffer (pH 8.8)	(0.375 M Tris-HCl pH 6.8, 0.1% SDS)
TBE buffer	(90 mM Tris, 90 mM borate (pH 8.3), 2 mM EDTA)
TE buffer	(10 mM Tris, 1 mM EDTA, pH 8.0)
TBST 10X	(1.5 M NaCl, 0.2 M Tris HCl (pH 7.5), 50 ml 20% Tween 20)
PBS	(138 mM NaCl, 10mM sodium phosphate (pH 7.4), 2.7mM KCl)

2.6 - RT- PCR used for generating various expressions constructs

Various gene expression DNA constructs were generated by amplifying the open reading frame from cDNA libraries generated from normal tissues by using GC-RICH PCR amplification kit. 2µg of total RNA was used to generate cDNA with oligo $(dT)_{24}$ oligonucleotide in a 20 µl reaction volume. 1-2 µl of cDNA was amplified using the GC-RICH kit (Roche Applied Sciences, Indianapolis, IN). 2-3µl of cDNA was added to mixture 1 containing 0.01 µM dNTP's, 25 pmole of each forward and reverse primers, 5 µl of GC-RICH buffer-3 and water according to manufacturer instructions to make the final volume 35 µl. Mixture 2 was prepared by mixing 0.5 µl of GC-RICH enzyme with 10 µl of buffer 2 and 4 µl of water. Both reaction mixtures were combined and vortexed briefly. The reaction was PCR amplified at 95°C for 3 min followed by 40 cycles of 95°C for 30 s, 53-55°C for 40 s and 72°C for 3 min depending upon the size of the amplified product (generally 1 minute per kb), followed by extension at 72°C for 10 min. The amplified open reading frames of various genes indicated in Table 2.2 were digested with the restriction enzymes specified in Table 2.2, and were cloned into indicated plasmids. Integrity of the gene sequences were checked by sequencing.

2.7 - Sequencing

Sequence confirmation was carried out using the BigDye Terminator v3.1 sequencing kit (Applied Biosystems). Reactions were performed in 10 µl volumes containing 100-150 ng of double stranded plasmid DNA, 2.5 pmol of primer and 2 µl of Big Dye Terminator v3.1. The reactions mixes were vortexed and centrifuged. Thermal cycling was performed as: 25 cycles of 96°C for 10 s, 50°C for 5 s and 60°C for 4 min and reactions were held at 4°C until subsequent purification. The reaction products were precipitated by adding 80 µl of 75% isopropanol, incubating for 20 min at room

temperature in the dark, followed by centrifugation at 16,100 *g* for 20 min. After discarding the supernatant and adding another 250 µl of 75% isopropanol, the tubes were centrifuged at 16,100 *g* for 5 min. The supernatant was then aspirated, and the tubes were air dried for 15 min in the dark and kept at 4°C until sent to the DNA sequencing facility at the Institute of Medical and Veterinary Science (Adelaide, Australia) for sequence determination.

2.8 - Antibodies

Two rabbit polyclonal anti-CBFA2T3 antibodies RSH1 and PEP3 were used in this study. The sequence of CBFA2T3 proteins were aligned and presented in chapter 3 (Fig 3.1). RSH1 was generated by Dr Raman Kumar Sharma, using a unique C-terminal regions of CBFA2T3 proteins (Kumar et al., 2008) as marked by red line over the CBFA2T3 aligned sequences in Fig 3.1. PEP3 was commercially synthesized by Bethyl/DC laboratories Inc, USA. Sequences used to raise PEP3 were high-lighted by the black bar in Fig 3.1. The details of other antibodies used during the current study, available commercially or as generous gift from researchers are given in Table 2.4.

2.9 - Preparation of cell lysate and cellular fractions

To prepare total cellular lysates equal number of cells from various cell lines were lysed in lysis buffer 1 and 1× protease inhibitors (Roche Applied Sciences, Indianapolis, IN). Cells were incubated in lysis buffer for 8-10 minutes on ice and then sonicated for 3 pulses each of 15 second at 30% amplitude. The lysate was then centrifuged at 13000 rpm for 15-20 minutes.

Table 2.4 List of antibodies used during this study.

Antibody name	Origin	Source
α-MTG16 (RSH1)	rabbit	In house (DF Callen Lab)
α-MTG16 (PEP3)	rabbit	In house, Bethyl labs (USA)
α-β-actin	mouse	Sigma-Aldrich
α-HA (hemagglutinin)	rat	Roche
α-HA (hemagglutinin)	mouse	Roche
α-c-myc	mouse	IMVS
α-c-myc	rabbit	Sigma-Aldrich
α-Mek2	rabbit	Neomarkers
α-Lamin A/C	mouse	BD Biosciences
α-mSin3A	rabbit	Santa Cruz
α- BCL6	mouse	Neomarkers
α- BCL6	mouse	Neomarkers
α- BCL6	mouse	Dr G Roncador (Garcia et al., 2006)
α-Cdk2 AB-1	mouse	Neomarkers
α-cyclin D1	mouse	Santa Cruz
α-cyclin E	mouse	Santa Cruz
α-cyclin B1	mouse	Neomarkers
α-gamma tubulin (GTU-88)	mouse	Sigma-Aldrich
α-B23 (Nucleophosmin)	mouse	Sigma-Aldrich
α-p53 AB-5	mouse	Neomarkers
α-p21 AB-3	mouse	Neomarkers

α- FLAG	mouse	Sigma-Aldrich
α-glutamylated tubulin (GT335)	mouse	Dr Carnsten, J (Janke et al., 2008)
α- HSAS6	mouse	Dr Gonczy, P (Strnad et al., 2007)

To generate cytoplasmic and nuclear fractions from breast cancer cell lines, 1×10^7 cells from each cell line were collected by trypsinisation and washed 3 times with 1× PBS. Cells were resuspended in buffer A and 1× protease inhibitor cocktail. Cell suspensions were kept on ice for 8 min and then centrifuged at 1200× g at 4 ^{o}C. Supernatant was collected and marked as cytosolic fractions. To remove any left over cytosolic fractions, the pelleted nuclei were again washed with buffer A. Finally the nuclei pellet was resuspended in cold Buffer B (Wysocka et al., 2001) and incubated at 4^{o}C on a rotating wheel for 30 minutes. Lysates were sonicated three times at 30% amplitude for 10 second. Lysates were cleared by centrifugation at full (1600×g) and assayed for protein concentrations using the BCA protein assay kit as per the manufacturer instructions (Pierce). Equal amount of cytosolic and nuclear fractions together with proteins from myc-CBFA2T3a and untagged-CBFA2T3b (as a positive control) were analysed by western blot. For cytoplasmic and nuclear fraction marking MEK-2 and Lamin A/C antibodies were used during initial experiments. However due to unavailability of the MEK-2 antibody final data was produced using only Lamin A/C antibody.

2.10 - Western blot analysis

Equal quantities of protein from cell lysates were mixed with 1× protein loading buffer and were resolved on 8-10% SDS-PAGE at 130V for 2-3 hours (Laemmli, 1970; Laemmli et al., 1970) and transferred onto Hybond-C Extra membrane (Amersham Biosciences) overnight at 30V at 4^{o}C. Membranes were blocked in 10% milk in TBST for at least 45 minutes and subsequently probed with the relevant primary antibodies either overnight at 4 ^{o}C or for 3-4 hours at room temperature on rotating wheel. The membranes were washed with 1XTBST three times each for 10 minute. Membranes were then subjected to appropriate horseradish peroxidase-conjugated secondary

antibodies at room temperature for 1-2 hours. Finally the immune complexes were detected using an ECL and ECL Plus detection system (Amersham Biosciences) as described in standard protocols.

2.11 - Immunoprecipitation

Cellular lysates were prepared from cells 24 hours post transfection. After washing with 1× PBS three times the cells were lysed by tumbling on rotating wheel for 30 min at 4^{o}C in IP lysis buffer containing 1× complete protease inhibitor cocktail (Roche Diagnostics). Lysates were sonicated ×3 at 30% amplitude for 10 second each and cleared by centrifugation at 13000× rpm for 8 minutes. A small amount of cellular lysates were kept as inputs. The remaining cleared lysates were then divided into two aliquots, one for immunoprecipitation with antibody and second for mouse IgG control. Approximately 250 ng of appropriate antibody (for endogenous CBFA2T3 proteins anti-CBFA2T3 RSH1 antibody was used, while rabbit pre-immune serum was used as control in all immunoprecipitation and immunoflorescence experiments. Note: due to simplicity IgG was written in figures) and IgG was added to respective aliquots and were incubated on rotating wheel at 4^{o}C over night. 15 µl of protein A or G sepharose beads, precleaned with HEK293T protein lysates, were added to the supernatant-immune complexes for 3 hours. Beads were then washed 3× with IP lysis buffer, 3× with Wash buffer 1 and then 3× with Low salt buffer. Immune complexes were eluted with 50 µl of SDS loading buffer at 95 ^{o}C for 5 minutes. Equal volume of immunoprecipitated elutions from antibody immune complexes and IgG control were analysed on 8% SDS-PAGE gel together with of 1% of total lysate as inputs and no lysate control (beads immune complexes processed without any cellular lysate and eluted) and transferred to Hybond C membranes. Membranes were western blotted

using appropriate primary and secondary antibodies using procedure detailed in section 2.10.

2.12 – RNA Extraction and Real Time RT-PCR

Cells from different cell lines grown to 80-85% confluence (or after certain treatments) were resuspended into RNAlater (QIAGEN). Total RNA was isolated using RNeasy Mini Kit (QIAGEN) from the cell pellets according to manufacturer's instructions. 2 μg of total RNA was used to synthesis complementary DNA (cDNA) using MMLV (RNase H-) reverse transcriptase from Promega in accordance to the manufacturer's protocol. Briefly RNA was incubated with 0.5 μg of oligo $(dT)_{24}$ primer at 72°C for 4 mins followed by 4 minutes incubation at 4°C. Reverse transcription reaction mix contains 0.15 μM dNTPs, 0.5 μg of oligonucleotide, 5 μl of 5X RT buffer and 50-100 units of M-MLV RT (H^-) enzyme. The reaction protocol for reverse transcription was 90 minutes at 40°C followed by 15 mins incubation at 70°C.

Each real-time RT-PCR reaction contained 2 μl of cDNA, 6.25 pmole of relevant forward and reverse oligo primer and 5 μl of SYBR Green 1 PCR Master mix (PE Biosystems). Amplification was carried out on Rotor-Gene 3000 (Corbett Research) using the profile: 15 min activation of the polymerase at 95°C, 40 cycles of 15 sec at 94°C, 15 sec at 60°C and 30 sec at 72°C extension. Fluorescence data was acquired at 510nm during the 72°C extension phase of each cycle. Standard curves were generated using various standards of known RNA concentrations for quantitative real-time RT-PCR analysis. For all reactions *Cyclophilin-A* was used as housekeeping gene to normalize the expression of *CBFA2T3, CBFA2T1, CBFA2T2* and *CCND2*. Real-time PCR expression data was quantitated using the Rotor Gene System Software.

Normalised expression data was expressed relative to the expression levels in the HEK293T cells and presented as mean ± SEM (standard error of the mean) of triplicates.

2.13 – Immunofluorescence staining of exogenously expressed proteins

HeLa cells were seeded in Lab-Tek II Chamber Slides (Nalge Nunc, Naperville, IL) for immunofluorescence studies of transiently transfected DNA plasmids or for gene knock-down studies. Relevant plasmids were transfected using Lipofectamine 2000 (Invitrogen). Cells were fixed in 4% paraformaldehyde (15 mins, RT) or -20 °C methanol (10 mins at room temperature) and permeabilized in 0.4% Triton-X-100 (10 mins, RT). Cells were blocked with 5% goat serum at room temperature for 30-60 mins and then incubated with the relevant primary antibody in 1% goat serum (overnight, 4°C). following three time washes with 1X PBS for 10 minutes each cells were incubated with the appropriate Alexa Fluor-, rhodamine- or fluorescein-conjugated antibody (Molecular Probes, OR) 1:350 dilution in 1% goat serum (1-2 hour, RT) and mounted in VECTASHIELD mounting media with DAPI (Vector Laboratories, Burlingame, CA). Cells were imaged on a Bio-Rad Radiance 2100 Confocal Microscope and Olympus IX70 inverted microscope.

2.14 – Immunofluorescence studies of endogenously expressed proteins

10^5 cells from different cell lines (for example HeLa for centrosome analysis) were seeded overnight into each well of a 4 well chambered slide. Cells were fixed with iced cold methanol when stained with anti-γ-tubulin, anti-HSAS6 and anti-GT335 while for other proteins like endogenous CBFA2T3 (anti-CBFA2T3 RSH1 antibody) cells were fixed with 4% paraformaldehyde. The procedure was described in section 2.13.

2.15 – Immunofluorescence by Laser Scanning Confocal Microscopy (LSCM)

The images were produced using the Bio-Rad Radiance 2100 confocal microscope (The Hanson Detmold Imaging Core Facility, Institute for Medical and Veterinary Science, Adelaide, Australia) equipped with three lasers, Argon ion 488nm; Green HeNe 543 nm; Red Diode 637 nm and Olympus IX70 inverted microscope. The objective used was a 20× UPLAPO (NA= 0.70) or 40× UPLAPO with NA=1.15 water, or a 60× UPLAPO with NA=1.4 water. The single or dual labelled samples were imaged with two separate channels (PMT tubes) in a sequential setting. The Green fluorescence (GFP) was excited with Ar 488 nm laser line and the emission was viewed through a HQ515/30 nm narrow band barrier filter in PMT1. The red fluorescence (Alexa 546) was excited with Green HeNe 543 nm laser line and the emission was viewed through a long pass barrier filter (570LP) to allow only red light wavelengths longer than 570 nm to pass through PMT2. Automatically all signals from PMT1 and 2 were merged. The image data were stored on a CD for further analysis using a Confocal Assistant software program for the Microsoft® Windows™ (Todd Clark Brelje. USA).

Some of the work related to co localization of centrosomal proteins was imaged using a Nikon C1-Z confocal microscope. Nikon C1-Z was equipped with a Nikon E-2000 inverted microscope and three solid laser lines (Sapphire 488nm, Compass 532 nm and Compass 405 nm). A Nikon 20X UAPOW (NA= 0.70), 60XUAPOW (NA= 1.2) and 100X UAPO oil (NA= 1.4) objectives were used. The single and dual labelled samples were imaged with two separate channels (Photomultiplier tubes-PMT). Green fluorescence was excited with Ar 488nm laser line and the emission was viewed through BA 495-520nm narrow band barrier filter in PMT1. Red fluorescence was excited with Green HeNe 532 nm laser and viewed through a 570LP barrier filter in

PMT2. The DAPI was excited with near UV405 nm laser and passed through PMT3 only to allow blue light. All signals from PMT1, PMT2 and PMT3 were merged automatically with Nikon C1Z software.

2.16 – G1-S phase and G2-M phase cell synchronisation

MCF7 and MD-MBA-468 cells were synchronized at G_1-S phase using a double thymidine block. Equal numbers of cells were plated in 6cm culture dashes or in 6 well plates in the morning. Cells were grown in the presence of 2 mM thymidine for 15 hours for G_1-S phase synchronisation. Cells were washed and regrown in fresh medium without thymidine for a further 16 hours. To initiate a second block cells were cultured in the presence of 2 mM thymidine again for a further 15 hours. To release cells from second thymidine block cells were washed 2-3 times with pre-warmed fresh medium, and harvested at indicated time points.

For G_2-M phase synchronisation, cells were grown in the presence of 2mM thymidine for 16 hours washed thoroughly to release from the thymidine block, incubated in fresh medium for 5 hours, and then blocked in 2μM nocodazole for 6 hours. Cells were released from second block by three washes with fresh medium. Released cells were grown for various times before subsequent analysis.

Chapter 3 –CBFA2T3 isoforms are localized to different cellular compartments

3.1 Introduction

Molecular and cytogenetics analysis of breast tumour have revealed a frequent loss of 16q. 36-67% of primary sporadic breast cancers were reported to have loss of heterozygosity (LOH) of 16q (Tsuda et al., 1994). Physical map construction and expression analysis of some of the transcripts from 16q24.3 has identified 104 genes from a 2.4 Mb region. Three putative tumour suppressor genes were identified by expression analysis among a panel of breast cancer cell lines. CBFA2T3 is one of those identified tumour suppressors from chromosome band 16q24.3 (Powell et al., 2002). Transcript analysis of CBFA2T3 has shown that *CBFA2T3* expression is lost in breast tumours (Kochetkova et al., 2002). CBFA2T3 expression is retained in the B80-TERT cell line, which was derived from normal epithelial mammary cells.

CBFA2T3 (also known as MTG16 and ETO2) belongs to the CBFA2T family of proteins (see section 1.5). All members of this protein family share high homology. Proteins of this family including CBFA2T3 exist in the form of two splice variants known as isoform “a” and isoform “b”. CBFA2T3a encodes a 853 amino acid protein while CBFA2T3b encodes a 567 amino acid protein (Fig 3.1). The two isoforms differ from each other by differences in nucleotide sequences in the N-terminus region and by their association with different promoters. All members of the CBFA2T family are known nuclear transcription co-repressor proteins.

Aberrant promoter methylation was recognised as a known cause of down regulation of different tumour suppressor genes which results into inactivation of these genes (Baylin & Herman, 2000). The CBFA2T3b promoter region shows aberrant methylation of CpG dinucleotides

among a panel of breast cancer cell lines (Bais et al., 2004). This aberrant methylation of the CBFA2T3b promoter is associated with low levels of CBFA2T3 gene expression. So far no study has determined the methylation status of CBFA2T3a promoter. Previous study by Bais et al (2004) has indicated a potential requirement for the detailed study of CBFA2T3a promoter methylation status.

RUNX1 is a known transcription activator protein (Kitabayashi et al., 1998b; Linggi et al., 2002). The chromosomal translocation t(8;21) and t(16;21) resulted into the production of fusion proteins RUNX1-CBFA2T1 and RUNX1-CBFA2T3. The fusion protein from t(8;21) translocation instead of activation, results into the repression of RUNX1 target genes (Hug & Lazar, 2004). A similar scenario is found in treatment induced acute myeloid leukaemia which is associated with the chromosomal translocation t(16;21) resulting into RUNX1-CBFA2T3 fusion protein (Gamou et al., 1998). Further studies had shown that RUNX1-CBFA2T1 overexpression blocks parental 32D.3 myeloid progenitor cells in G1 phase of the cell cycle, while this effect was abolished when a mutant form of RUNX1-CBFA2T1 having Δ469 (removed *C-terminal* region of CBFA2T1 lacking binding sites for majority of corepressors including mSin3A, N-CoR and HDACs) was introduced in these cells. The observed effect was reported to be related to the recruitment of HDACs to RUNX1-CBFA2T1 protein and can be reverted to normal cell growth by treatment with Trichostatin A (TSA) (Amann et al., 2001).

The involvement of CBFA2T family proteins in proliferation and differentiation of erytheroid cells have also been shown by Lindberg *et.al*. Expression analysis of these proteins in leukemic cell lines and bone marrow cells had revealed that both *CBFA2T2* and *CBFA2T3* were ubiquitously expressed in leukemic cell lines, while *CBFA2T1* was expressed only in erytheroleukemic cell lines (Lindberg et al., 2005). Reduction in *CBFA2T2* and *CBFA2T3*

expression was reported in ATRA (*All Trans-Retinoic Acid*) responsive differentiation. In contrast the expression of these two homologues remained unaffected in vitamin D3 induced differentiation to monocyte cell lineage. It has also been shown that RUNX1-CBFA2T1 disrupts CBFA2T3 (ETO2) interaction with N-CoR which results into impaired granulocyte formation (Ibanez et al., 2004). CBFA2T3 role in erythropoiesis was further elaborated by Goardon et al, 2006. Overexpression and knock down studies of CBFA2T3 in erytheroid progenitor TF-1 cells had shown that, CBFA2T3 expression dynamics governs the proliferation and maturation process through TAL1 complex (Goardon et al., 2006). Expression of *RUNX* and *CBFA2T* family was further investigated by using an embryonic stem cell differentiation system, showing that the observed increase in *CBFA2T1* and *CBFA2T3* expression is correlated with the hematopoietic differentiation (Okumura et al., 2007). All these studies have suggested a variable expression of CBFA2T family members related to the maturation and differentiation of the cell lineage.

The cellular distribution of the CBFA2T family proteins has been extensively studied. Different localization studies indicate that CBFA2T proteins localize to the nucleus (Davis et al., 1999; Odaka et al., 2000). CBFA2T1 colocalizes with the BCL6 protein to nuclear speckles (Chevallier et al., 2004), which are known to be associated with sites of transcription repression (McGhee et al., 2003). CBFA2T3a overexpressed protein was reported to localize to the nucleolus, whereas the RUNX1-CBFA2T3 fusion is targeted to the nucleoplasm (Hoogeveen et al., 2002). The amino acid sequences present at the N terminal region of CBFA2T3a are responsible for targeting it to the nucleolus (Hoogeveen et al., 2002). Dual FRAP (Fluorescence Recovery after Photobleaching) studies have successfully demonstrated that CBFA2T1 and CBFA2T3 fusions affect the intracellular mobility of RUNX1-ETO fusion protein compared to the RUNX1 protein (Qiu et al., 2006). In COS-7 cells overexpressed CBFA2T1 and hSIN3B was shown to colocalize

to the nucleolus (Dhanda et al., 2008). In addition endogenous CBFA2T2a and CBFA2T3a proteins were also reported to colocalize with hSIN3B to the nucleolus of the K562 cells (an erytheroleukemic cell line derived from a CML patient) (Dhanda et al., 2008). These results are consistent with the localization of CBFA2T3a to the nucleolus.

Previous studies on CBFA2T3 expression were carried out at message level. There were some inconclusive reports about CBFA2T family proteins expression, due to the lack of specific antibodies for each CBFA2T family member. In addition, unpublished data from (D. F. Callen) has shown that N-terminal sequences of CBFA2T3a in the data bank are not complete hence the results regarding the "a" isoform localization of CBFA2T3 were based on incorrect version of the CBFA2T3aT construct and are misleading. The present study helps to address some of the relevant questions regarding the localization and expression analysis of CBFA2T3 proteins. CBFA2T3 isoforms were found to localize to different cellular compartments. It is proposed that as CBFA2T3a and CBFA2T3b isoforms exhibit differential subcellular localizations they may be involved in different cellular functions.

3.2 Materials and Methods

3.2.1 Cell lines and antibodies

The details of all human cell lines used in this study are outlined in Chapter 2 otherwise where it is necessary to mention a specific cell line it is indicated in the relevant section. The majority of the localization experiments with exogenously expressed proteins were carried out in HeLa cell line grown under conditions given in Chapter 2. Two affinity purified rabbit polyclonal antibodies RSH1 and PEP3 used in this study were raised against CBFA2T3 proteins, were available in house. RSH1 was generated by Dr Raman Kumar Sharma, using overlap PCR to amplify unique C-terminal regions of CBFA2T3 proteins (Kumar et al., 2008). PEP3 was raised against a peptide sequence from the C-terminus region of CBFA2T3 (Bethyl/DC laboratories Inc, USA). This region overlaps with the region used for raising RSH1. Further details about PEP3 are given in Chapter 5. All commercially available antibodies used during this study are described in Chapter 2, General Materials and Methods. During all experiments where PEP3 and RSH1 antibodies were used rabbit pre-immune sera was used as a control.

3.2.2 Plasmids

Myc tagged CBFA2T3a (an extended 5' sequence, see below) and CBFA2T3b (NM_175931.1) construct in pLNCX2 were previously generated by Breast Cancer Genetics lab (Kochetkova et al., 2002). EGFP-myc-CBFA2T3aT (CBFA2T3a as available in NCBI NM_005187.4, clone lacking extended N-terminus regions) was generated by PCR amplification using primers Z16aT-BglII-myc F #556 and Z16a R ERI # 541 (Table 2.2) from myc-CBFA2T3a DNA and was cloned inframe into the EcoR1 site of pEGFP-C1 vector. An extended N-terminal region for CBFA2T3a start site mapping was PCR amplified from Jurkat cell line cDNA (J-ZF2-R378) and was cloned in pGEMT vector. Integrity of the DNA sequences was confirmed by restriction digestion and sequencing analysis.

3.2.3 Primers used in chapter

Primers used during this study are described in details in Table 2.1 of Chapter 2. Their name and numbers are specified where they were used.

3.2.4 RNA preparation and RT-PCR for determination of CBFA2T3a start site

RNA was extracted (see Chapter 2 section 2.10) from MCF7, SKBR3 and Jurkat cell line using equal number of cells. cDNA was synthesized by incubating equal amount of RNA with the random hexamer primer in the presence of M-MLV reverse transcriptase H^- (Promega) (details in Chapter 2), a negative control sample (having RNA with no reverse transcriptase) was included together with water control. cDNA was amplified by gene specific primers sets MTG16a ZF1-MTG16a ZR1 and MTG16a ZF2- MTG16a ZR1 further referred as (ZF1-ZR1) and (ZF2-ZR1). These sets of primers spans to extended C-terminus region. In order to reconfirm these data primer sets spanning exon intron boundaries, ZF2-R378 and ZF2-R183 (reverse) were used for amplification. All amplifications were carried out with GC-RICH PCR system (Roche) under following conditions: 95 ^{0}C 3 min; 40 cycles of 95 ^{0}C 20 sec, 53 ^{0}C 20 sec, 72 ^{0}C 90 sec.

3.2.5 Real time RT-PCR for *CBFA2T3* expression analysis

RNA was prepared from a panel of breast cancer cell lines. Procedures for RNA, cDNA and RT-PCR were described in Chapter 2 (section 2.10). For each sample 2 µl of cDNA was used for amplification on a Rotor-Gene 3000 (Corbett Research). The reaction mix includes 10 µl of SYBR Green I PCR Master mix (PE Biosystems) and 6.25 p mole of each forward and reverse primer. Primer sets used for this experiment were as follow.

1) MTG16 EX4F2 - MTG16 EX6R1
2) MTG16 F1754 - MTG16-R1935
3) CYC F1 - CYC R1

Amplification profile was as follows: 95 ^{o}C for 15 minutes, followed by 40 cycles of 94 ^{o}C for 15 seconds, 60 ^{o}C for 15 seconds, and 72 ^{o}C for 30 seconds. Fluorescence data acquisition was carried out at 510 nm during 72 ^{o}C extension phase of each cycle. Melt curve analysis and agarose gel electrophoresis was performed following completion of the real-time PCR cycles. Internal cDNA standard curves were performed for quantification of mRNA. The results were normalized against *Cyclophilin A* gene, a house-keeping gene. Changes in *CBFA2T3* gene expression was calculated relative to the normal breast tissue cDNA as analysed during real-time RT-PCR experiment. All reactions were conducted in triplicates. Two independent experimental runs starting from cDNA synthesis were performed using the same RNA prep. Whole experiment with the new RNA preps was also repeated by (Paul M Neilson, PhD student).

3.2.6 Cellular lysate preparation and analysis for CBFA2T3 proteins expression

Equal numbers of cells from different cell lines, including finite life span human mammary epithelial cell lines 48SRT and 184AT, breast cancer cell lines (MCF7, ZR75-1, T47D, BT20, SKBR3, MDA-MB 468 and MDA-MB 231) and leukemic cell lines (Jurkat and Ramose) were collected from cultures at 85-90% confluence. Cells were washed with 1×PBS three times and lysed in 1× lysis buffer containing, 50 mmol/L Tris-HCl (PH 7.5), 250 mmol/L NaCl, 1% Triton X-100, 1 mmol/L EDTA, 50 mmol/L NaF, 0.1 mmol/L Na_3VO_4, 1 mmol/L DTT and 1× protease inhibitors for 10-15 min on ice. Cell lysates were then centrifuged at 1600× g to remove debris. Supernatant was kept for further analysis. Total protein contents were assayed using BCA protein assay kit from Pierce, Rockford IL. 40μg of protein was western blotted against anti-CBFA2T3 antibody RSH1. The details of SDS-PAGE analysis and western blotting are given in Chapter 2. Anti β-actin antibody was used to demonstrate equal loading among samples.

3.2.7 Immunoprecipitation of endogenous CBFA2T3 proteins

1×10^7 cells from MCF7, ZR75-1 and MDA-MB-468 cell lines with low passage number were collected. After washing with 1× PBS three times the cells were suspended in buffer containing 50 mmol/L Tris-HCl (pH 8.0), 150 mmol/L NaCl, 1% Triton X-100 and 1× complete protease inhibitor cocktail (Roche Diagnostics) for lysis. Lysates were prepared by tumbling on rotating wheel for 30 min at 4°C. Cellular lysates were sonicated ×3 at 30% amplitude for 10 second each and cleared by centrifugation at 1600× g for 8 minutes. Cleared lysates were divided into two aliquots, one for immunoprecipitation with RSH1 antibody and the second for rabbit IgG control (pre-immune sera). A small amount of lysates were kept as inputs before the addition of antibodies. Roughly 250 ng of rabbit polyclonal anti-CBFA2T3 antibody (RSH1) and rabbit IgG was added to respective aliquots and incubated over night on a rotating wheel at 4°C. 15 µl of protein A sepharose beads, precleaned with HEK293T protein, was added to the supernatant-immune complexes for 3 hours. Beads were then washed 3× with lysis buffer, 3× wash buffer 1 containing 50 mM Tris-HCl pH 8.0, 150 mM NaCl, 1% NP-40. 0.5% SDS and 0.1% sodium deoxycholate and then 3× with 20 mM Tris-HCl pH 7.5. Immune complexes were eluted with 50 µl of SDS loading buffer at 95 °C for 5 minutes. Equal volume of immunoprecipitated elutions from RSH1 and rabbit pre-immune sera control were analysed using 8% SDS-PAGE gel. Lanes with 1% inputs and no lysates were included as controls. The gel was transferred to a nitrocellulose membrane over night and western blotted against anti-CBFA2T3 antibody (RSH1) see section 2.9 (Chapter 2, General Material and Methods).

3.2.8 Cellular fraction preparation for CBFA2T3 proteins

Cellular fractions from breast cancer cell lines having low and high CBFA2T3 proteins expression were prepared. 1×10^7 cells from each cell line were collected and washed 3 times with 1× PBS. Cells were resuspended into buffer A containing 10 mM HEPES pH7.9, 10 mM

KCl, 1.5 mM $MgCl_2$, 340 mM sucrose, 10% glycerol, 0.5 mM DTT, 0.1% Triton X-100 and 1× protease inhibitor cocktail. Cells were kept on ice for 8 min and then centrifuged at 1100× g at 4 ^oC. Supernatant was collected and marked as cytosolic fractions. To remove any remaining cytosolic fractions, nuclei were again washed with buffer A. Finally the nuclei pellet was resuspended in cold Buffer B containing 20 mM HEPES pH7.9, 420 mM NaCl, 1.5 mM $MgCl_2$, 0.2 mM EDTA, 0.5 mM DTT, 25% glycerol (Wysocka et al., 2001) and incubated at 4^oC on a rotating wheel for 30 minutes. Lysates were sonicated at 30% amplitude for 10 second three times. Lysates were cleared by centrifugation at 1600× g and assayed for protein contents. Equal amount of cytosolic and nuclear fractions along with proteins from myc-CBFA2T3a and untagged-CBFA2T3b (as a positive control) were analysed for CBFA2T3 proteins using RSH1 antibody. Fractions were also probed with anti-Lamin A/C antibody, which was used as a marker for nuclear fractions.

3.2.9 Immunoflorescence staining of exogenously expressed CBFA2T3 proteins

Hela cells were grown overnight in Lab-Tek II Chamber slides (Nalge Nunc, Naperville, IL). Transient transfection of plasmids (name are specified where used) was carried out as described in Chapter 2. Twenty four hours post transfections cells were harvested, washed 3× with 1× PBS and were fixed with either with -20 ^oC methanol or 4% paraformaldehyde at room temperature for 10 minutes. Washed cells were permeabilized with 0.4% Triton X-100 (10 min) and were blocked with 5% goat serum in PBS (30 min), followed by incubation in primary anti-myc antibody in 1% goat serum over night at 4 ^oC. Next day, cells were washed 3 × with 1× PBS and were incubated with appropriate Alexa fluor, rhodamine or fluorescein-conjugated secondary antibodies (Molecular Probes, Oregon, USA) in 1% goat serum (1 hour, room temperature). Cells were 3× washed with 1× PBS and mounted in VECTASHIELD mounting media with

DAPI (Vector Laboratories, Burlingame, CA). Bio-Rad Radiance 2100 confocal microscope was used for imaging.

3.2.10 Co-staining of endogenous CBFA2T3 proteins with different cellular markers

Procedures for fixing and staining the cells were similar as described in section 3.2.9, except primary antibodies as specified in figure legends, followed by appropriate Alexa fluor-rhodamine or fluorescein labelled secondaries. Staining using the anti-CBFA2T3 antibody RSH1 was optimal when cells were fixed with 4% paraformaldehyde (10 min RT). The remaining method is similar as described in section 3.2.9.

3.2.11 Analysis of CBFA2T3 proteins expression during cell cycle

4×10^5 cells from MCF7 and MDA-MB-468 cell lines with low passage number were plated in 6 cm culture dishes early in the morning. Cells were blocked with 2 mM final concentration of thymidine for 15 hours at G1-S boundary. Cells were washed twice with pre-warmed media and incubated for 16 hours in fresh medium. Cells were then subjected to a second 15 hours block using 2mM thymidine. Followed by the release of the second thymidine block, cells were collected at regular intervals of time for 36 hours using Trypsin EDTA washed 2× with fresh medium and PBS. Pellets were stored frozen until analysed. Frozen cell pellets were lysed in equal volume of 1×MP lysis buffer (details given in Table 2.3) for 10-15 min on ice. For each time point two sets each of 40 μg protein were analysed on 8% SDS-PAGE and transferred to nitrocellulose membrane. Membranes were probed with anti-CBFA2T3 (RSH1), anti-cyclin-B and anti-β-actin antibodies.

3.3 Results

3.3.1 *In silico* analysis of CBFA2T3 proteins

The protein sequences for all three members including isoform 'a' and isoform 'b' of CBFA2T3 protein were aligned (Fig. 3.1) using ClustalX program (which is a window interface for the ClustalW multiple sequence alignment program available from www.igbmc.u-strasbg.fr/BioInfo/ (Thompson et al., 1997). Clustal W program writes file in postscript format read by GSview (Ghostscript) www.cs.wisc.edu/~ghost/ program. All three members of the family share regions of high homology as shown in Fig. 3.1. *In silico* analysis reveals the presence of an in frame extended N terminal sequence of the NCBI NM_005187.4 CBFA2T3a isoform. The only difference in CBFA2T3a and CBFA2T3b isoform exist in the N-terminus region while remaining protein sequences share high similarity with each other. Analysis to confirm this extended sequence is presented in the next section.

3.3.2 CBFA2T3a has actual start site upstream of the known NCBI start site

In silico analysis of CBFA2T3 family revealed the presence of a start site 531 bp upstream of the known start site in the (Accession number NM_005187) sequence found in GeneBank data base. A Kozak consensus sequence was determined in the upstream start site using program available from web (Kozak, 1986). The sequences present at 5' and 3' of upstream start site predict it as a strong Kozak consensus sequence than the existing NCBI start site. Further analysis revealed that no stop codon was present inframe between these two start sites. Instead three consecutive stop codons were present on 5'end of this upstream start site (99 bp upstream). This data provides a strong evidence that the true start site is the extended 5' site.

A
CBFA2T3a
CBFA2T3b
CBFA2T1
CBFA2T2
ruler

CBFA2T3a
CBFA2T3b
CBFA2T1
CBFA2T2
ruler

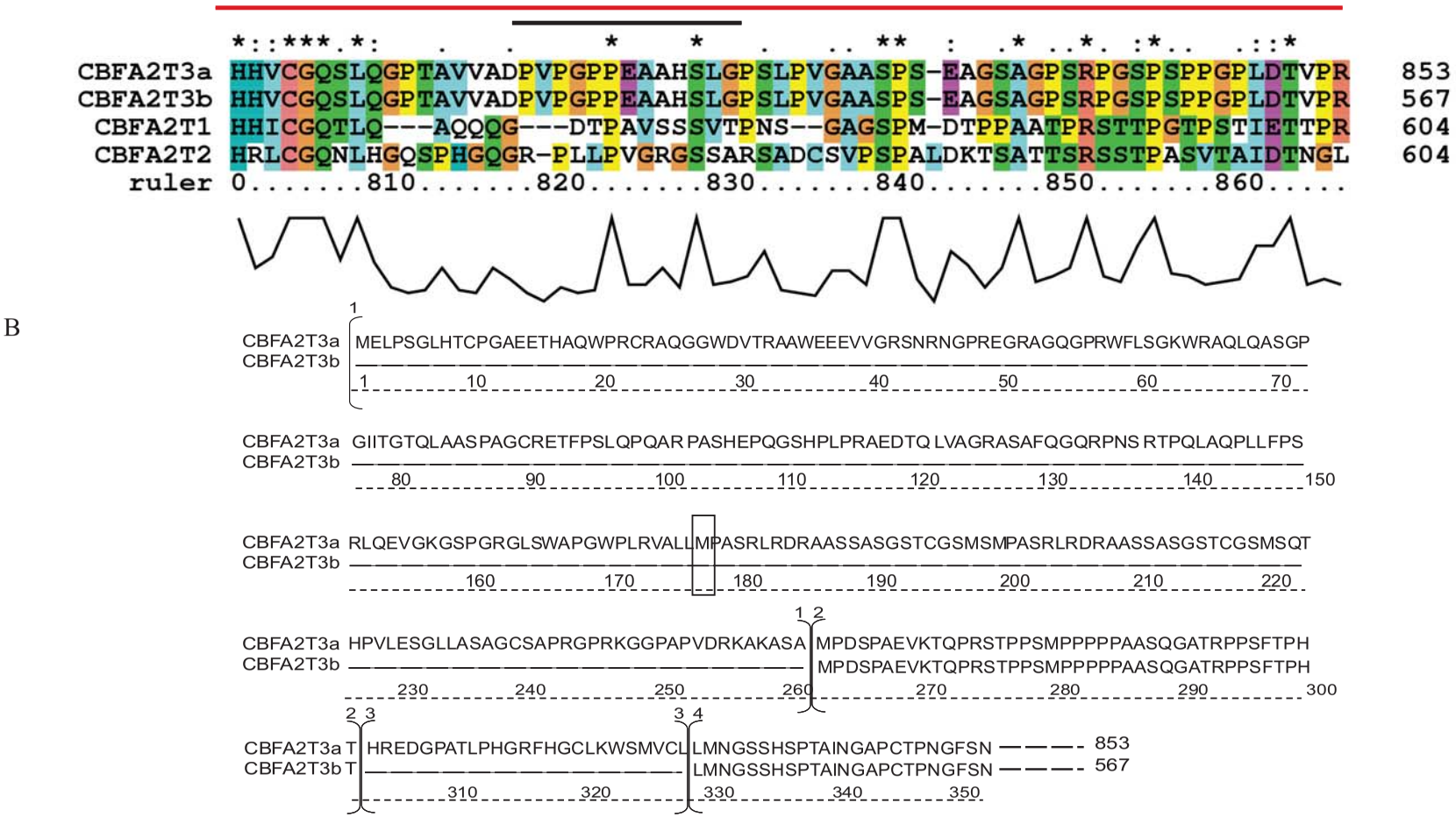

Figure 3.1. Alignment of CBFA2T3 isoforms along with other members of the CBFA2T proteins family

A. Homologus sequences for all members are marked with asterik. Regions used to raise two polyclonal antibodies are also marked with the coloured lines above the sequence (Red bar represent sequences used to raise RSH1 antibody, while black bar represents the sequence for PEP3 poly clonal peptide antibody. **B.** Alignment of C terminus sequences of CBFA2T3a and CBFA2T3b isoforms Box markes the start site present in CBFA2T3aT NM_005178. Total number of amino acids for each isoform is indecated at the end of dashed lines. Sequence from 330 amino acid onwards is common in both isoforms. Large bracket markes the exon boader as indicated by the numbers on the top.

To determine if this 5' extended sequence contains the actual start site, mRNA from different cell lines was analysed by RT-PCR. cDNA was prepared from MCF7, SKBR3 and Jurkat RNA, using either random hexamers or T_{24} poly A primers. Subsequently, the cDNA was amplified with a set of primers ZF1-ZR1 and ZF2-ZR1 spaning the 5' region which encompasses both start sites. The positioning of the different primers sets is shown in Fig 3.2A. Transcripts of specific sizes based on the presence or absence of intron are predicted as 635bp and 559bp respectively, were amplified from both sets of primers. A minimal amplification with ZF1-ZR1 primer set was observed for SKBR3 cell line under similar PCR conditions, while no product was amplified with second set of primers (Fig. 3.2B upper panel). On the other hand specific sized products were amplified from MCF7 and Jurkat cDNA. In subsequent experiment primers spaning introns (Fig 3.2A) were used which further confirms that these amplified products from N-terminus extended sequences were transcript of CBFA2T3a and were not from CBFA2T3a genomic sequences. Further ZF2-R378 primer set amplifies the sequence (922 bp) from the extended exon1 to exon3. A 922bp fragment (ZS1, amplified using primers ZF2-R378) was amplified from Jurkat cDNA (Fig. 3.2 B lower right panel) consistent with the expected size of cDNA.

Amplified transcripts from above mentioned RT-PCR were further investigated to confirm their integrity. Fragment ZS1 was also cloned into pGEMT vector. Purified DNA from this vector along with ZS1 was used for restriction digestion analysis. These fragments were digested by BamH1 and BamH1/Nco1 restriction enzyme. Both ZS1 released (592 bp and 330 bp) and pGEMT-ZS1 DNA (390bp) fragments upon digestion (Fig 3.2 C). Fragment ZS1 was further digested by Apa1, Sma1 and Dpn1 restriction enzymes. Dpn1 (596 and 326) and Sma1 (672 and 250) released fragments of expected sizes (Fig. 3.2D). Amplified ZS1 and ZS1 in pGEMT were completely sequenced. Sequencing data has confirmed the presence of the extended 5' sequences to the existing fragment of NM_005187.4 and presence of the upstream start site, 531bp

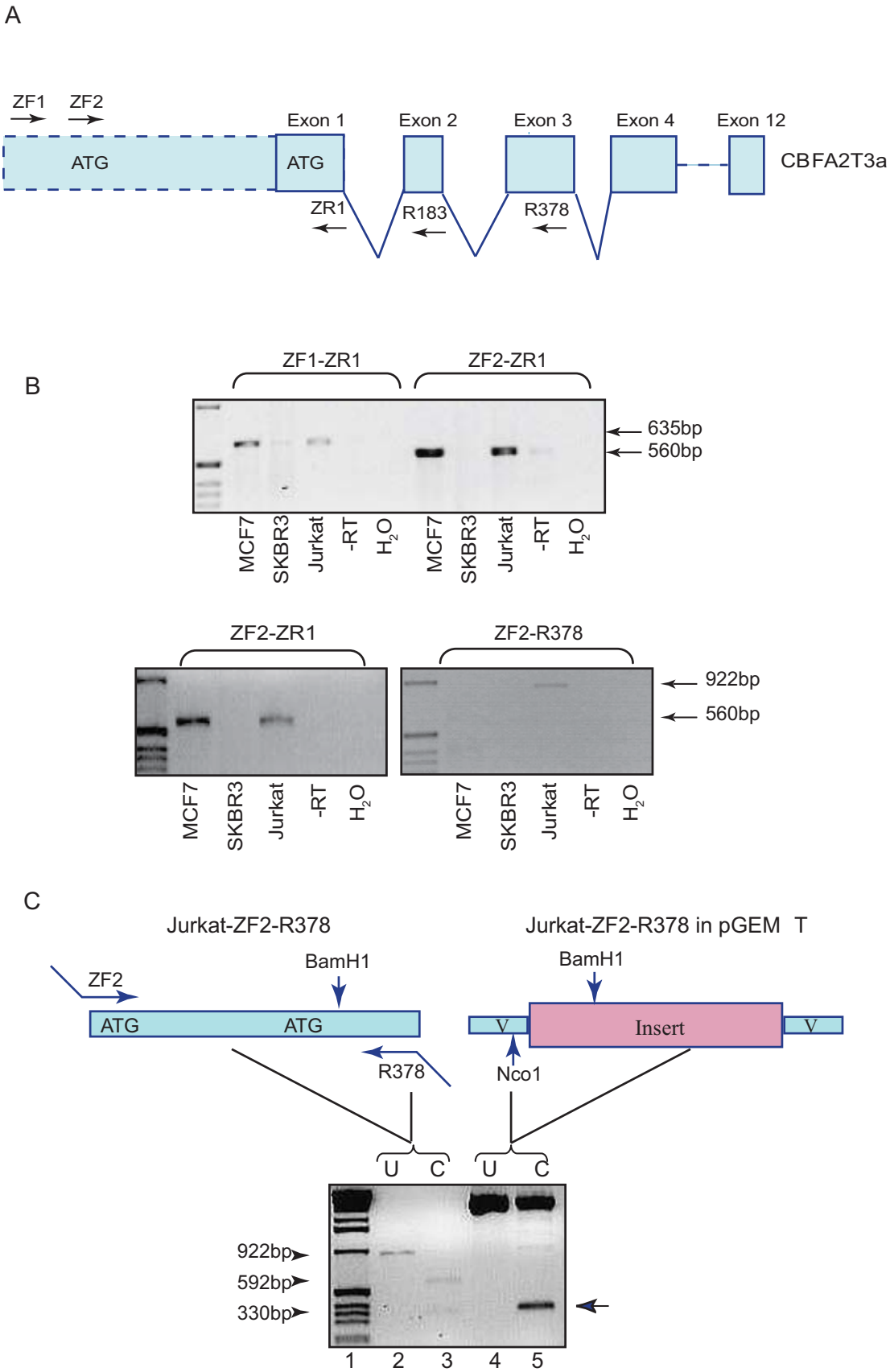
A
ZF1
ZF2
ATG
ATG
Exon 1
Exon 2
Exon 3
Exon 4
Exon 12
CBFA2T3a
ZR1
R183
R378
B
ZF1-ZR1
ZF2-ZR1
635bp
560bp
MCF7
SKBR3
Jurkat
-RT
H2O
ZF2-ZR1
ZF2-R378
922bp
560bp
C
Jurkat-ZF2-R378
Jurkat-ZF2-R378 in pGEM T
BamH1
ZF2
ATG
ATG
R378
V
Insert
V
Nco1
U
C
922bp
592bp
330bp
1
2
3
4
5

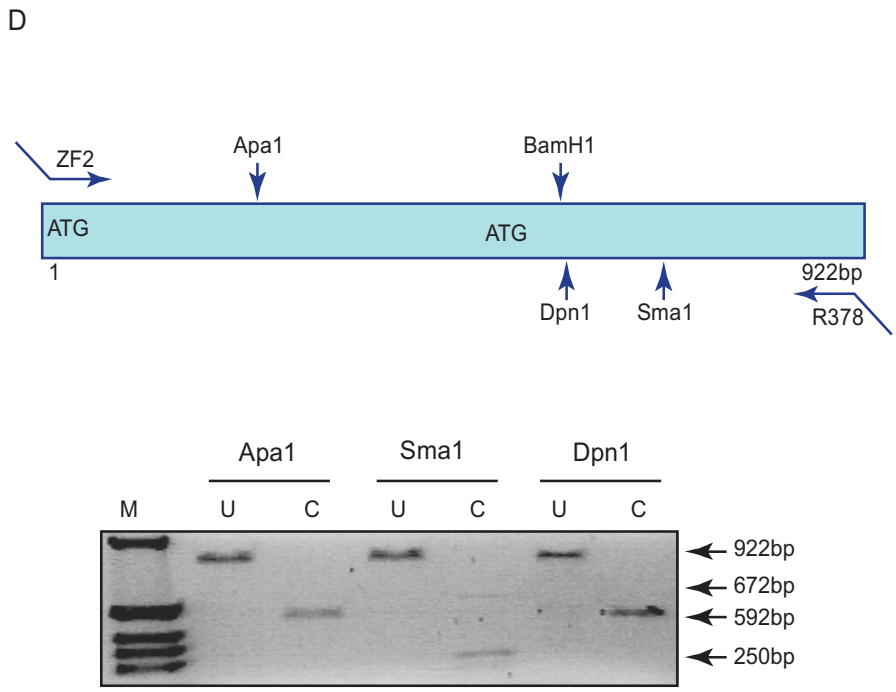

Figure. 3.2. CBFA2T3a has a Start site up stream of the known (NCBI) start site
A. Schematic presentation of CBFA2T3a N-terminus region showing the location of primers used for amplification. **B.** cDNA was prepared from MCF7, SKBR3 and Jurkat cell lines using random hexamer and T_{24} primers. ZF1-ZR1, ZF2-ZR1(upper panel) and ZF2-R378 (lower panel) primers sets were used to amplify cDNA. **B**. Represents the agarose gel analysis of RT-PCR from these cDNA. **C.** Amplified product ZF2-R378 from jurkat (lane 2 and 3) was cloned into pGEMT vector (lane 4 and 5) and digested with the restriction enzymes as shown in diagram. Note Insert in pGEMT is in reverse orientation. U = uncut DNA while C = cut DNA. Arrow head on left side marks specific sized band released from amplified fragment digestion, while arrow markes band released after digestion from cloned fragment in pGEMT. **D**.Restriction digestion of ZF2-R378 fragment with different enzymes as marked by sets.

upstream of the NCB1 start site (data not shown). The *in silico* analysis together with the RT-PCR data confirmed a 531 bp extended sequence of CBFA2T3a that results in a protein of an additional 153 amino acids to that of the NCBI sequence. In future experiments CBFA2T3a is always with this extended sequence while the shorter NCBI NM_005187.4 is termed CBFA2T3aT.

3.3.3 CBFA2T3 antibodies are specific to only CBFA2T3 proteins

Given that all three CBFA2T family proteins share a high homology, exploration of the role of these proteins in their endogenous environment was dependent on specific antibodies for protein members. The regions selected to raise polyclonal rabbit antibodies specific for the CBFA2T3 proteins were highlighted with colour bars over the aligned sequences in Fig 3.1. Two affinity purified polyclonal antibodies RSH1 (Kumar et al., 2008) and PEP3, were used throughout this study.

The specificity of CBFA2T3 antibodies to CBFA2T family members was confirmed by transfecting myc tagged CBFA2T family members into the HEK293T cell line. Equal amounts of protein from these lysates were western blotted against RSH1 and PEP3 antibodies. Western blotting with anti-myc antibody was also carried out as a control (Fig 3.3). Results showed that both RSH1 and PEP3 antibodies specifically detects only CBFA2T3 proteins, even though other members of CBFA2T family proteins share high homology. Both antibodies are predicted to detect endogenous CBFA2T3a and CBFA2T3b isoforms as they share n-terminal sequences. Data regarding endogenous CBFA2T3 expression is discussed in section 3.3.4b.

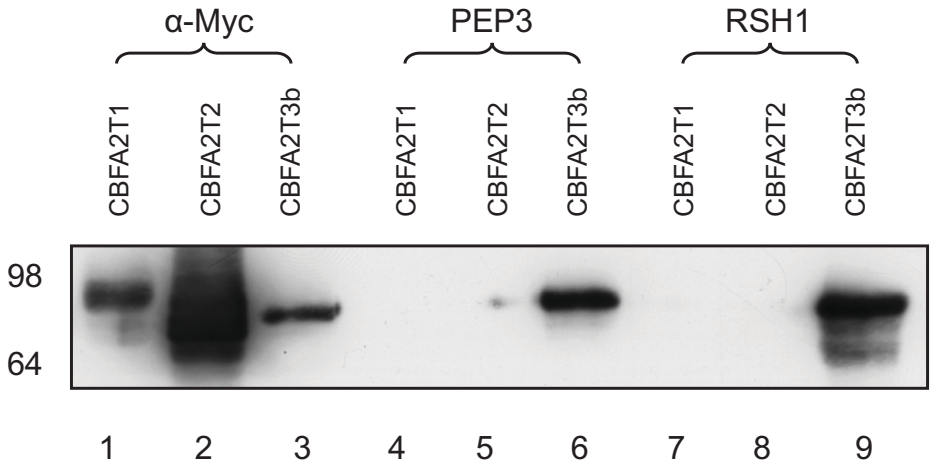

Figure 3.3. Anti CBFA2T3 antibodies specificity
293T cells were transfected with myc-CBFA2T1, myc-CBFA2T2 and myc-CBFA2T3 DNA. Equal amount of lysates from these transfected cells was blotted against α-Myc, RSH1 and PEP3 antibodies. Left side of the panel marks the molecular sizes of western magic marker.

3.3.4 CBFA2T3 expression in different breast cancer cell lines

3.3.4a) CBFA2T3 mRNA expression in different breast cancer cell lines

CBFA2T3 mRNA expression was determined in a panel of breast cell lines by real time RT-PCR. Cyclophilin A was used as an internal control. Total RNA from normal breast tissue purchased from a commercial source was included in this panel. The data presented here is from single experiment. Samples were run in triplicates. Bar diagram presents the relative CBFA2T3 expression. CBFA2T3 expression in cell lines from normal breast epithelial cells (HMEC and TERT-HMEC) was found comparable with CBFA2T3 expression in RNA from normal breast tissues. Furthermore, CBFA2T3 was found to be highly expressed in breast cancer cell lines like MCF7, T47D and BT20 while CBFA2T3 expression was strongly down regulated in MDA-MB-468 and MDA-MB-231 breast cancer cell lines.

3.3.4b) CBFA2T3 proteins expression in different cell lines

To gain an insight on CBFA2T3 protein expression, lysate was prepared from equal number of cells from a panel of cell lines. This panel was comprised of the finite lifespan human epithelial cells, non malignant immortalized mammary epithelial cells, breast cancer cells and some leukemic cell lines. Lysate from these cell lines along with myc-CBFA2T3a and untagged-CBFA2T3b proteins were subjected to western blotting with RSH1 antibody. Anti β-actin was used as a marker for equal loading (Fig 3.5 A).

The results showed that CBFA2T3b protein expression was high in a group of breast cancer cell lines, comprising MCF7, ZR75-1, T47D, positive for the ER (estrogens receptors). CBFA2T3b expression was not detected in SKBR3, MDA-MB-468 and MDA-MB-231 cell lines (Fig 3.5A). In contrast both leukemic cell lines, Jurkat and Ramose expressed high to moderate amount of CBFA2T3b protein.

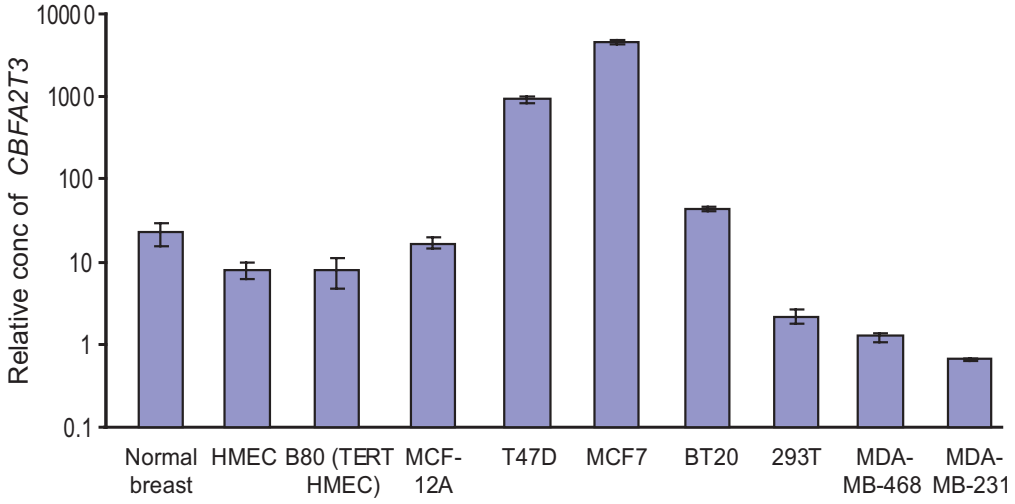

Figure 3.4. CBFA2T3 message expression in different cell lines
cDNA from equal amount of RNA prepared from a panel of cell lines comprising of normal and breast cancer cell lines. Amplified cDNA was subjected to real-time RT-PCR using *CBFA2T3* specific primers and was normalized relative to *Cyclophilin A* expressionin. Each bar of the histogram represents ±SEM. Samples were run in triplicates.

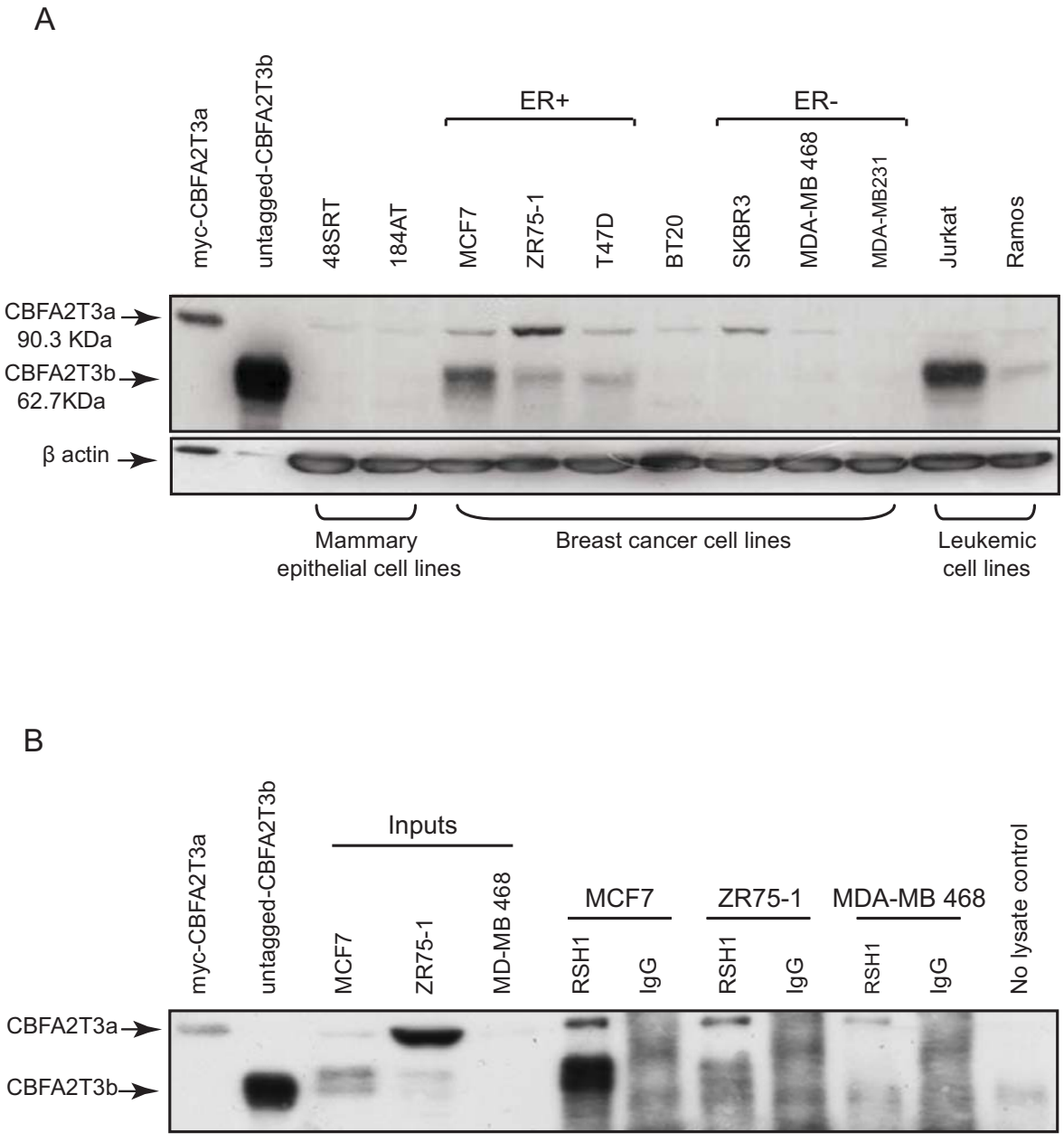

Figure 3.5. CBFA2T3 protein expression in different cell lines
A. Total lysate from equal number of cells from different cell lines was blotted against α-CBFA2T3 antibody and α-β actin. **B.** Immunoprecipitation of endogenous CBFA2T3 proteins from different cell lines. Lysate from equal number of cells from different cell lines was immunoprecipitated with RSH1 and rabbit pre-immune sera (labelled as IgG). Equal volume of elutions were blotted with RSH1 antibody.

Nevertheless, CBFA2T3a expression varied among all cell lines. It was noted that the cell lines with high cytoplasm to nucleus size ratio has moderate amount of CBFA2T3a expression as compared to the cell lines with low cytoplasmic index. In a broader aspect similar trends were observed for CBFA2T3 protein expression as was seen for *CBFA2T3* message analysis. Cell lines having high *CBFA2T3* mRNA transcript levels also have high CBFA2T3 protein content for example MCF7. While cell lines expressing low *CBFA2T3* mRNA like MDA-MB-231 and MDA-MB-468 also express CBFA2T3 proteins at lower levels. It is worthy to mention that the primer used for real-time RT-PCR can not differentiate the two isoforms of CBFA2T3, while analysis of CBFA2T3 proteins has made it clear that both CBFA2T3 isoforms "a" and "b" are differentially expressed in different cell lines. For example *CBFA2T3* message was found to be high in BT20 cell line. On the other hand western blot analysis of lysate revealed that BT20 cell line express moderate amount of CBFA2T3a, while CBFA2T3b is expressed at low levels.

Immunoprecipitation of CBFA2T3 proteins, from a panel of cell line having different levels of CBFA2T3 expression was then undertaken. Present approach helped to confirm that lower expression of CBFA2T3b was related to the reduce amount of CBFA2T3 proteins and is not due to the limited detectability of CBFA2T3 proteins. Cell lysates were prepared from equal number of cells from MCF7, ZR75-1 and MDA-MB-468 cell lines. 1% of the lysates was run as inputs, while quarter of the elutions immunoprecipitated with RSH1 antibody and rabbit IgG control were run alongside the inputs. An almost tenfold enrichment of CBFA2T3a and CBFA2T3b protein was observed in MCF7 cell line. These enrichments were specific since in elutions from IgG control no CBFA2T3 proteins binding to IgG bound beads was observed (Fig 3.5B). Enrichment of CBFA2T3 proteins was also observed from ZR75-1 cell lysates immunoprecipitated with RSH1 antibody. However due to reduce level of CBFA2T3b isoform in ZR75-1 cell line lesser enrichment of CBFA2T3b was observed as compared to MCF7 cell line.

No expression of CBFA2T3b was observed in immuno-precipitates from the MDA-MB-468 cell line (Fig 3.5B), although a faint band corresponding to the CBFA2T3a protein expression was observed. These results further supported that MDA-MB-468 had markedly reduced amount of CBFA2T3b protein expression.

3.3.5 CBFA2T3 proteins are localized to different cellular compartments

Cellular fractionation was used to define the location of CBFA2T3 isoforms. A panel of breast cancer cell lines having high and low expression of the CBFA2T3 isoforms were selected. Equal numbers of cells for each cell line were processed to extract cytosolic and nuclear fractions. Equal volumes of both fractions were western blotted using the anti-CBFA2T3 polyclonal antibody RSH1 to detect the CBFA2T3 proteins. The same blot was re-probed with anti-Lamin A+C antibody to assess possible cross contamination of the nuclear localized protein (Novelli et al., 2002). Surprisingly, the CBFA2T3a isoform related band was only found in the cytoplasmic fractions with no traces of CBFA2T3a observed in nuclear fractions from any of the cell line (Fig 3.6). This is in contrast to the previously published studies (Hoogeveen et al., 2002) where CBFA2T3a was localized to the nucleolus. However, CBFA2T3b was entirely found in the nuclear fraction which is consistent with the role of CBFA2T3b as a transcriptional co-suppressor. Localization of CBFA2T3b to the nuclear fraction was confirmed by the presence of lamin A+C protein (a nuclear protein) in the same fraction. The present data suggests that CBFA2T3 isoforms “a” and “b” are localized to the cytoplasmic and nuclear compartments respectively. These results were consistent for the three cell lines presented in the (Fig 3.6) and other breast cell lines analysed in this study (data not shown).

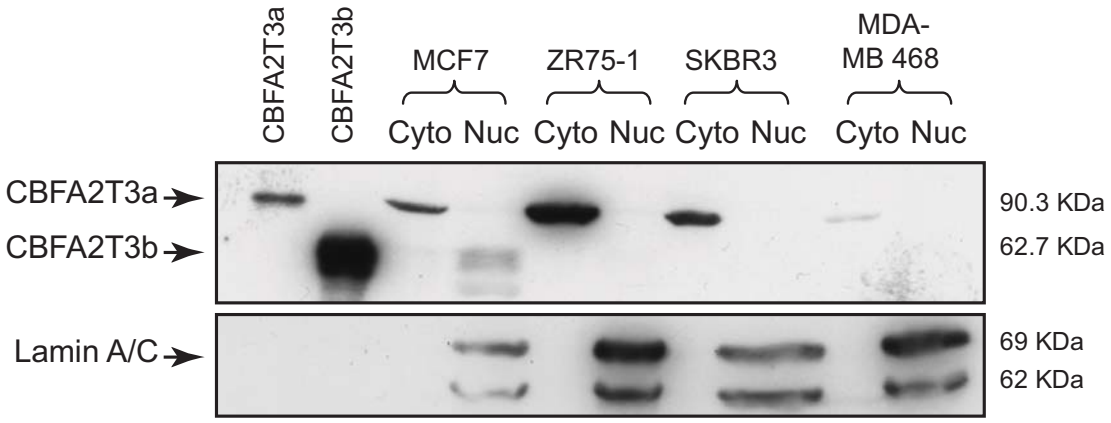

Figure 3.6. Differential compartmentalization of CBFA2T3a and CBFA2T3b

Cytosolic and nuclear fractions were prepared from four breast cancer cell lines, using same number of cells. Equal volume of protein was loaded for each fraction from all cell lines and was blotted with anti-CB FA2T3 (RSH1) antibody. Anti- Lamin A+C was used as marker for nuclear fractions as shown in lower panel.

3.3.6 Localization studies of exogenously expressed CBFA2T3 proteins

The previous cellular fraction studies showed the presence of CBFA2T3 isoforms in different cellular compartments. Fluorescent localization studies of exogenously expressed tagged version of these both isoforms were undertaken to further investigate their location and function.

Myc-tagged CBFA2T3a and CBFA2T3b constructs were transfected into the HeLa cell line. 24 hour post transfection cells were fixed and stained with Alexa fluor 488 labelled mouse anti myc IgG. HeLa cells were used for these studies as they are easily transfected and have superior morphology. In the majority of transfected cells CBFA2T3a was found to localize to the cytoplasm, while CBFA2T3b was found only in the nucleus (Fig 3.7A). Surprisingly a variation in CBFA2T3b localization pattern from diffused to sharp speckles was found among different cells, as was evident from two cells in panel from CBFA2T3b (Fig 3.7A lower panel merged image). A small percentage of cells with high levels of CBFA2T3b expression were found to have both nuclear and cytoplasmic localization (Fig 3.7B). However, CBFA2T3a showed exclusively cytoplasmic localization in cells having moderate to low levels of CBFA2T3a expression (comparable to endogenous level Fig 3.7B), while cells expressing high levels of CBFA2T3a have signal in both the cytoplasm and nucleus. These findings were consistent with the previous data from western blot analysis of cellular fractions.

CBFA2T3a full length protein localization was also compared with overexpressed CBFA2T3aT protein the truncated (NCBI version). Myc-tagged CBFA2T3a and myc-tagged CBFA2T3aT DNA were transfected into HeLa cells. Cells were stained with Alexa fluor 488 labelled mouse anti-myc IgG 24 hours post transfection. Structures of the CBFA2T3a and CBFA2T3aT are represented in Fig 3.8A, while the localization of both proteins was shown in Fig 3.8B.

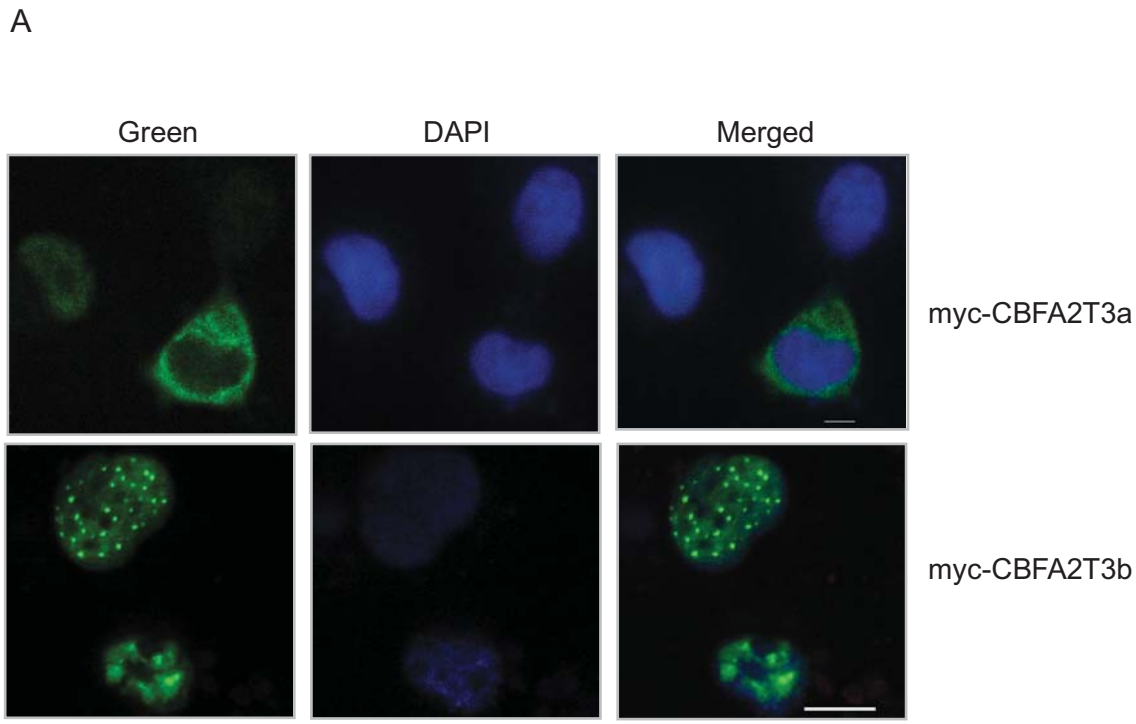

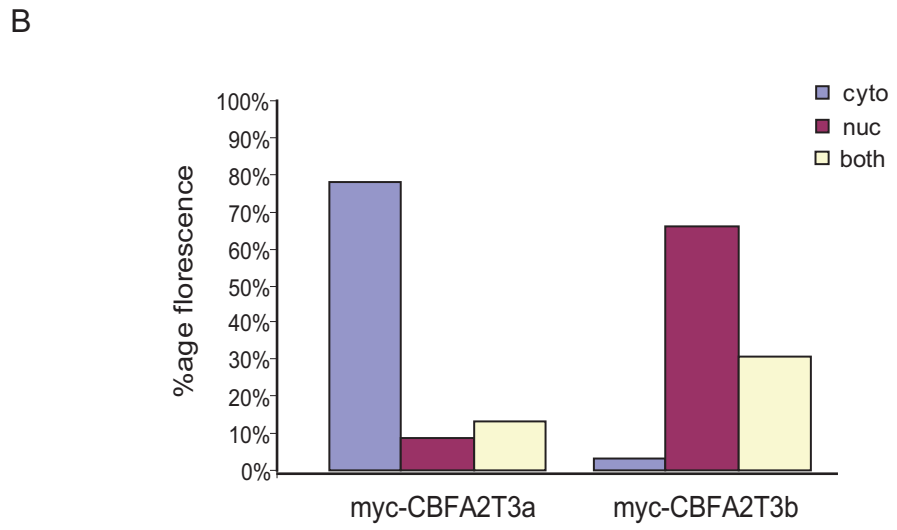

Figure 3.6. CBFA2T3 isoforms localize to different cellular compartments
HeLa cells were transfected with myc-CBFA2T3 and myc-CBFA2T3 DNA and stained with anti-myc antibody. Scale bar = 10μm in merged images. **B.** Histogram represents percentage flourescence for each isoforms per cellular compartment.

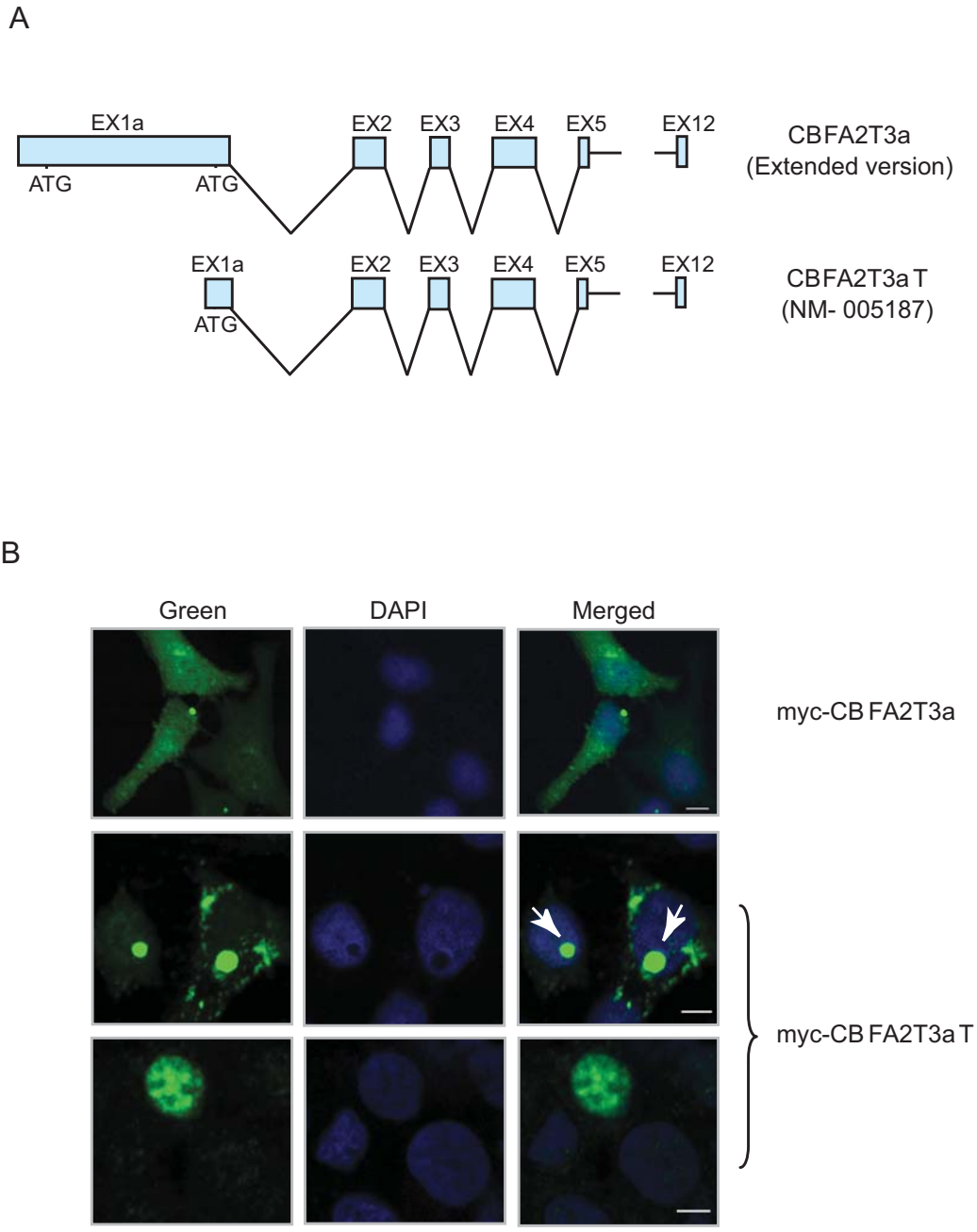

Figure. 3.8. Localization studies of CBFA2T3a isoform
A. Structure of CBFA2T3a (Extended version) and CBFA2T3aT (NM-005187.4). **B.** myc-CBFA2T3a and myc-CBFA2T3aT plasmids were transfected into HeLa cell line. Fixed cells were stained with mouse α-myc antibody conjugated with Alexa 488 IgG. Lower two panels represents myc-CBFA2T3aT localization. Arrow marks CBFA2T3aT localization to nucleolus in some cells. Scale bar = 10μm.

CBFA2T3a full length protein localized to cytoplasm and showed localization to one and two dots adjacent to nucleus which are predicted as centrosomes. In contrast to CBFA2T3a full length, CBFA2T3aT predominantly localized to the nucleus. Most of the cells transfected with CBFA2T3aT have diffused nucleoplasmic localization, while a small numbers of cells exhibit a nucleolus localization of CBFA2T3aT protein (Fig 3.8B).

3.3.7 Localization studies of endogenous CBFA2T3 proteins

Localization studies of endogenous CBFA2T3 proteins were also carried out in different cell lines. Anti-CBFA2T3 antibodies were titrated using different concentrations of antibodies to reduce the background for immunoflorescence studies. Staining with the pre-immune sera and no primary antibody control was performed as a control in all experiments. No fluorescent signal was observed when the cells were stained with the pre-immune sera from rabbits. In addition the background signal from secondary antibodies was further determined. No signal was detected under similar settings for no primary control (Fig 3.9). The results show that there is no back ground signal due to the rabbit IgG, the detected signal is only due to the binding of antibodies to the CBFA2T3 proteins. These findings were further confirmed in a separate experiment where antibodies were competed with the peptide immunogen used to raise the antibody to block the anti-CBFA2T3 antibodies binding to the cells. No signal was detected in experiments where competed immunogen was used for staining (Fig 3.9 second row).

Three breast cancer cell lines (MCF7, SKBR3 and MDA-MB-468) with varying CBFA2T3 expression as determined by western blot analysis (see Fig 3.5), were selected for the localization studies of endogenously expressed CBFA2T3 proteins. Fixed cells were stained with anti goat Alexa 488 conjugated to the anti CBFA2T3 antibodies (RSH1 and PEP3.

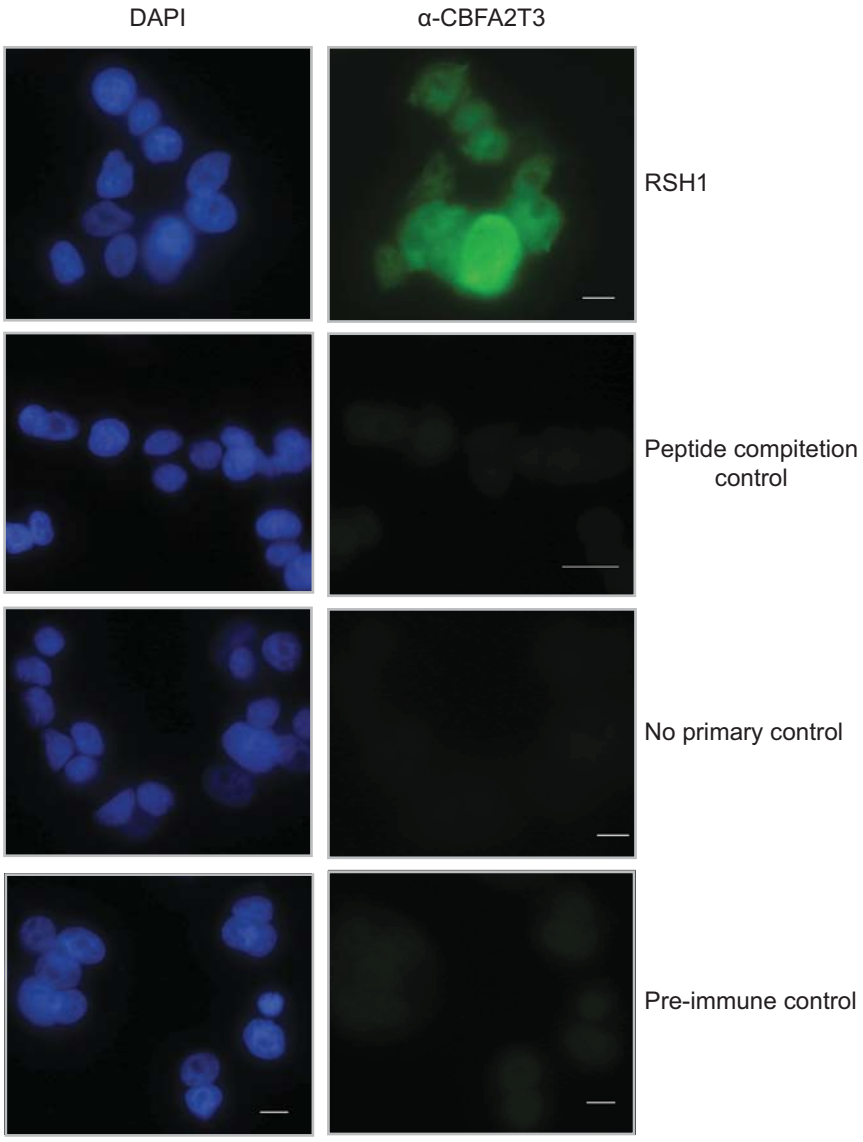

Figure. 3.9. Flourescence signals detected with α-CBFA2T3 antibody are specific toCBFA2T3 proteins
MCF7 cells were stained with rabbit α-CBFA2T3 (RSH1), RSH1 competed with the peptide sequences used to raise antibody and rabbit pre-immune serum. Cells were also treated with no primary antibody as a negative control. All specimens were subjected to anti-rabbit IgG conjugated with Alexa-488 secondary. Cells were counter stained with DAPI. Scale bar represents 10μm.

Fluorescent microscopy revealed high level of CBFA2T3 proteins expression in MCF7 cells (Fig 3.10). Some cells showed strong nuclear signal, while others have diminishing amount of the nuclear staining. Conversely, all cells showed a strong cytoplasmic staining (Fig 3.10 panel MCF7 single or merged images), which was consistent with western data. SKBR3 and MDA-MB-468 on the contrary have shown only cytoplasmic signal. A moderate to low levels of cytoplasmic staining pattern was observed in SKBR3 and MDA-MB-468 cell lines (Fig 3.10), while no nuclear staining was detected even when serial z-sections were taken (Fig 3.10). This is consistent with the western data where negligible levels of CBFA2T3b was detected in SKBR3 and MDA-MB-468 cell lines but a low levels of CBFA2T3a isoform was found. These findings are consistent with the hypothesis that CBFA2T3a isoform localizes to the cytoplasm. The SKBR3 and MDA-MB-468 cells also showed 1 or 2 strong spots in cytoplasm marked as arrow in the (Fig 3.10). These spots were confirmed later to be the centrosome when cells were counter stained with γ-tubulin, a known centrosomal marker, discussed in Chapter 4). Furthermore, all cell lines were also stained with the PEP3 antibody showed similar staining patterns as was observed with RSH1 staining, images from RSH1 stained cells were only shown here.

3.3.8 Endogenous CBFA2T3 proteins are cell cycle regulated

3.3.8a Co-localization studies of CBFA2T3 proteins with different cell cycle markers

Immunoflorescent data from CBFA2T3 protein localization in different cell lines revealed the presence of differences in expression level of CBFA2T3 proteins among an asynchronous population of cells. It is suggested that the observed differences in the expression of the CBFA2T3 proteins expression is due to cells being at different stages of the cell cycle. To explore this hypothesis, co-localization studies of CBFA2T3 proteins with different known cellular markers were conducted.

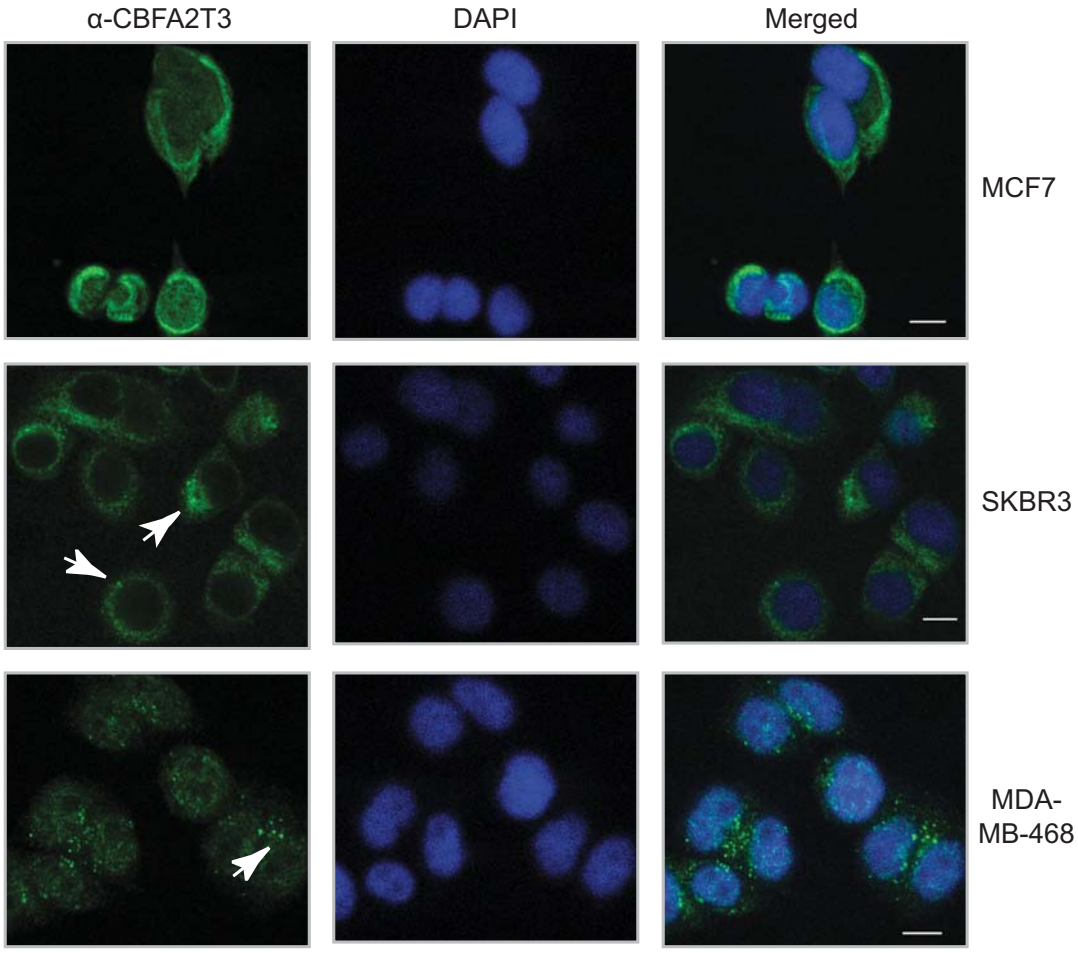

Figure 3.10. Localization studies of endogenous CBFA2T3 proteins from different breast cancer cell lines
Different breast cancer cell lines were stained with α-CB FA2T3 (RSH1) antibody. Cells were counter stained with DAPI (for marking nucleus). Scale bar in merged images = 10μm.

Asynchronous population of MCF7 cell line was co-stained with RSH1 (anti CBFA2T3 antibody) and antibodies specific for different cellular markers for the cell cycle cyclin-B (G2-M phase), cyclin-E (G1-S phase transition) and γ-tubulin. Fig 3.11A represented the images from the single antibodies showing that no bleach through signal was detected at wavelength for 488. Only specific signal was detected for example Alexa 594 labelled anti mouse antibodies showed red signal only at 532/543 wavelength in red panel, while no green signal was detected at this wave length. Fig 3.11 B represents the co-staining of cells with Alexa 488 labelled anti-mouse anti-CBFA2T3 IgGs and Alexa 594 labelled IgGs for cyclin-B, cyclin-E and γ-tubulin. For each antibody the labelling of 100-150 cells were scored. Only representative images are presented here. Consistent with previous findings a variable expression of CBFA2T3 proteins was noted (Fig 3.11A 1st row). Cells were stained for endogenous CBFA2T3 and cyclin-E and cyclin-B, an apparent correlation between cyclin-E and CBFA2T3 expression levels was observed but not for the cyclin-B (Fig 3.11B). As Cyclin-E (high expression during G1-S phase transition) and CBFA2T3 expression was found high in cells marked with arrows indicates the possibility that the cells were in late G1 or early S phase.

Images in lower two panels of Fig 3.11B were from co-staining of cells with anti-CBFA2T3 and anti-γ-tubulin antibodies. Surprisingly co-localization of CBFA2T3 protein with the γ-tubulin was found in small spots that are possibly centrosomes see Chapter 4 (Hollow arrow). A clear enlarged image will enable to clearly distinct co-localization of CBFA2T3 with γ-tubulin (Appendix 3). Therefore, it may be possible that seen variation in CBFA2T3 abundance during the cell cycle occurs at particular phases. This is further investigated in the next section.

A

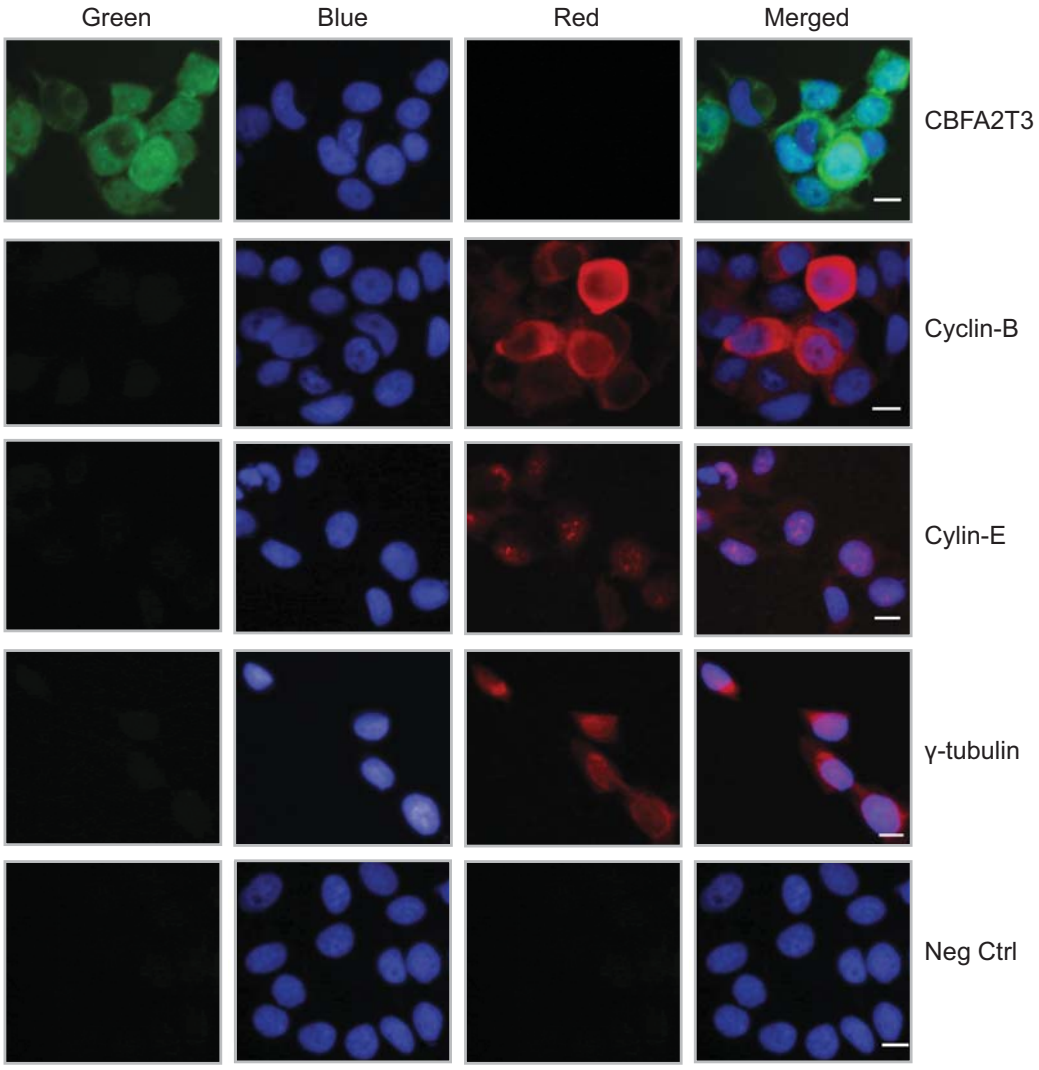

Figure. 3.11. CBFA2T3 proteins expression is cell cycle regulated
A. MCF7 cells were fixed and stained with antibodies as shown on the right side of each panel. Pre-immune sera and no primary were used as negative control. Anti-CBFA2T3 antibody was conjugated with rabbit Alexa fluor 488 (Green). Anti-cyclin-B, E and gamma-tubulin were conjugated with mouse Alexa fluor 594 (red). Cells were counter stained with DAPI (blue). Scale bar represents 10μm. All images for a particular wavelength where taken at same intensity.

B

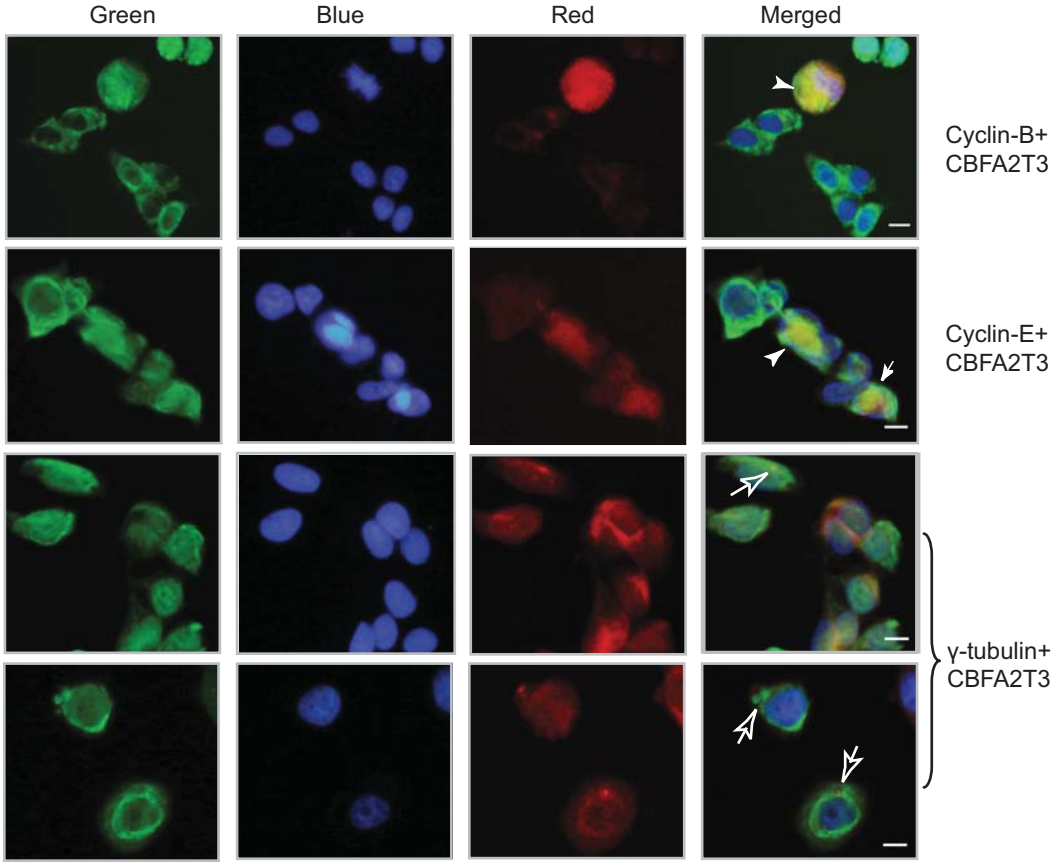

Figure. 3.11.B. CBFA2T3 proteins expression is cell cycle regulated
Images fr.om MCF7 cells costained with anti-CBFA2T3 and antibodies for different cellular markers. Solid arrow head indicate a metaphase where cyclin-B expression is high. Arrow in second merged panel points to cells having Cyclin-E and CBFA2T3 high expression. Hollow arrow head (orange signal) in lower two panels marks centrosomal co-localization of γ-tubulin with CBFA2T3. Scale bar is 10μm.

3.3.8b Cell cycle analysis of CBFA2T3 proteins from MCF7 and MDA-MB-468 cell lines

Analysis of CBFA2T3 proteins expression during the cell cycle was further determined by blocking the cells at the G1-S phase of the cell cycle. Two cell lines MCF7 and MDA-MB-468, with high and low CBFA2T3 expression, were selected for cell cycle analysis. MDA-MB-468 was selected to determine if there is variation in CBFA2T3a levels. Cells from a population of low passage number were double thymidine blocked and released (Chapter 2 section 2.14). Samples were taken at regular intervals of time and equal amounts of protein were analysed against RSH1, anti cyclin-B and β-actin antibodies by western blot for each time point (Fig 3.12A). The data is only presented for MCF7 cell line. The intensity of CBFA2T3a and CBFA2T3b band were also plotted against band intensity of cyclin-B (Fig 3.12B and C) respectively.

CBFA2T3b expression was found high after the release from thymidine block until the onset of mitosis. The current observation was based on the oscillation of cyclin-B levels from 10-12 hours. It was considered that mitosis was at 12 hour time point. CBFA2T3a and CBFA2T3b levels decreased to a minimum during the late S-G2 phase. Following mitosis from 10-12 hours CBFA2T3b expression decreased and this was paralleled by decreasing cyclin-B (Fig 3.12A and C). CBFA2T3b expression again rises during 12-20 hours period of time, which is the G1 phase of cell cycle. CBFA2T3a expression level was low as compared to “b” isoform. A little reduction in CBFA2T3a expression was observed when cells underwent mitosis at time point 8-10 hour (Fig 3.12 A and B), while during the rest of cell cycle the protein levels remained same. β-actin was found levelled for all time points indicating that the oscillation in CBFA2T3b and CBFA2T3a expression was not due to uneven loading of samples, but was the representation of actual CBFA2T3 proteins expression which varies among asynchronous population of cells.

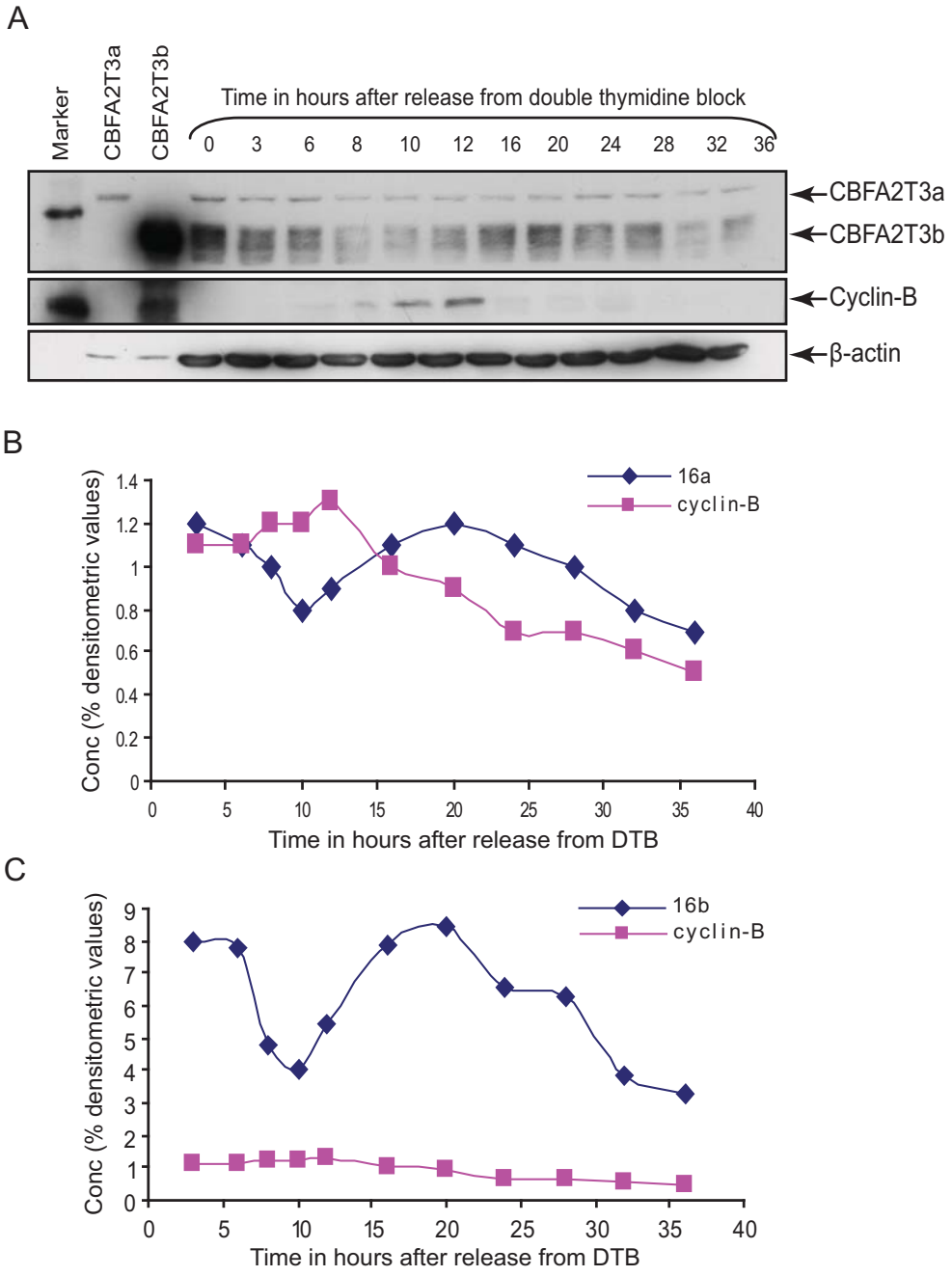

Figure. 3.12. Analysis of CBFA2T3 proteins during different stages of cell cycle

A. MCF7 cells were synchronized at G1-S boundry by double thymidine block. Samples were harvested at indicated time intervals. Equal amount of protein was analysed for CBFA2T3 and differnt cell cycle marker proteins by western blotting against those markers (Cyclin-B). β-actin was used as marker for loading control. **B.** Band intensities for CBFA2T3a and **C.** CBFA2T3b were measured using Alphaimager 2200 spot Denso tool, and are plotted against cyclin-B for di fferent time points. Time point 0 hrs was ignored due to intense background by positive control.

3.4 Discussion

The present study identified that the sequence for CBFA2T3a NCBI version NM_005187 was incomplete. An extended version of CBFA2T3a is established with a strong Kozak consensus sequence (Pedersen & Nielsen, 1997) present 531 bp upstream of the NM_005187.4 start site. A stronger Kozak sequence is associated with a "G" nucleotide at position +4 and A/G at position -3. The extended CBFA2T3a isoform upstream start site has a consensus sequence as -CCA$_{-3}$GGA$_{+1}$TGG$_{+4}$AGC- which is predicted as stronger start site (Kozak, 1986) than the published start site -CCTCATGCCG-. Furthermore, there is no stop codon present between these two start sites and hence the upstream start site was considered the more likely true start site for the CBFA2T3a isoform. The presence of upstream start site was then confirmed through RT-PCR amplification from cDNA derived from breast cancer and leukemic cell lines during this study (Fig 3.2A and B).

This alternate (upstream) start site results in an extended sequence of CBFA2T3a, which translated into a protein having 177 amino acids extra to the known NCBI version of CBFA2T3a (For simplicity NCBI version NM_005187 CBFA2T3a was referred as CBFA2T3aT, while isoform "a " with extended sequences in N-terminal region was called full length CBFA2T3a throughout this study). The extended 5' sequences resulted in a predicted protein of 853aa of 90 KDa size. This is consistent with the CBFA2T3a molecular weight size found on SDS-PAGE gel, as the α-CBFA2T3 RSH1 antibody detected an endogenous CBFA2T3a band at the same size as that of ectopically expressed CBFA2T3a (90KDa) with extra 177 amino acids.

Expression analysis of CBFA2T3 proteins among a panel of breast cancer cell lines showed

high to low levels of CBFA2T3b expression, which was consistent with the expression of *CBFA2T3* transcript among these cell lines. Cellular fractionation showed differential compartmentalization of the two isoforms. CBFA2T3a localizes to cytoplasmic fractions while CBFA2T3b showed a nuclear localization. Localization studies of exogenously expressed isoforms by immunofluorescence further confirmed the differential localization pattern of CBFA2T3a to cytoplasm and CBFA2T3b to nucleus.

CBFA2T3b isoform showed a diffuse nucleoplasmic to nuclear speckle localization which is consistent with its role as a transcription co-repressor (McGhee et al., 2003). Endogenous CBFA2T3a isoform from immortalized primary breast 48SRT and 184AT, breast cancer cell lines MCF7, ZR75-1, SKBR3 and leukemic cell lines Jurkat and Hut78 (data for Hut78 not shown) was found to have almost the same size (90 KDa) as myc-CBFA2T3a on SDS-PAGE gels (Fig 3.5). Anti-CBFA2T3 specific antibody (RSH1) has shown only the presence of CBFA2T3a and CBFA2T3b isoforms among different cell lines. This antibody specifically detected only CBFA2T3 proteins and had shown no cross reactivity with other CBFA2T protein members (CBFA2T1 and CBFA2T2) (Fig 3.3). The antibodies used in published studies were not sensitive enough to detect endogenous CBFA2T3 proteins (Hoogeveen et al., 2002). Hoogeveen et.al (2002) have carried out most of the experiments on exogenously overexpressed CBFA2T members. Presumably, due to the fact that the antibodies in previous studies were not sensitive enough to detect endogenous CBFA2T3 proteins and the data was derived from the NCBI truncated version of the protein. The larger size of the extended version has not been appreciated.

A previously published study concluded that CBFA2T3aT localized to the nucleolus (Hoogeveen et al., 2002). The N-terminal region of CBFA2T3aT was found to target CBFA2T3aT to

nucleolus. During the present study localization of myc-tagged CBFA2T3aT (NM_005187) was also investigated. Myc tagged CBFA2T3aT shows a variable localization from nucleoplasm to nucleolus (Fig 3.8) consistent with the published data (Hoogeveen et al., 2002). The CBFA2T3aT and CBFA2T3b are identical except the exon three and a part of exon one which presumably is responsible for driving the nucleolar localization of CBFA2T3aT. Since CBFA2T3a and CBFA2T3b are localized to different cellular compartments, and therefore the sequences responsible for cytoplasmic localization are likely to be in the extended 5' sequences unique to the extended version of CBFA2T3a. Detailed analysis suggests the presence of the nuclear export sequences with a putative role in cytoplasmic localization (see Chapter 4).

Hoogeveen et al (2002) also reported that in myeloid malignancies involving t(16;21) translocation, the AML-CBFA2T3 fusion protein in these malignancies is targeted to the nucleoplasm. Nucleolar CBFA2T3aT interacted with specific HDACs like HDAC1 and 3 but not to the cytoplasmic HDAC6. Furthermore, immuno-precipitations of the exogenously co-expressed CBFA2T family members showed heterodimerization of the CBFA2T proteins with each other. They also suggested that nucleolar CBFA2T3a can drag nucleoplasmic CBFA2T1 and CBFA2T2 to the nucleolus. Through interspecies heterokaryon test, authors had shown that CBFA2T3aT can shuttle through cytoplasm while other members of CBFA2T family lack this property (Hoogeveen et al., 2002). Although CBFA2T3aT lacks cytoplasmic localization, it can shuttle through the cytoplasm as was shown by interspecies heterokaryon test. The current property also supports the cytoplasmic localization of the full length version of CBFA2T3a with 5' extended sequences.

Two other reports (Dhanda et al., 2008; Lindberg et al., 2003) have shown that CBFA2T3aT localizes to the nucleolus and interacts with hSin3B. Both reports were based on overexpression of tagged proteins following transfection of CBFA2T3aT construct (NCBI NM_005187 version).

The antibody used by Lindberg et al (2003) was also unable to detect endogenous proteins. Only overexpressed proteins were detected by immunoprecipitation and western blot experiments. In addition, the antibody was raised against a peptide designed from 452-466 residues, the region which was common in both isoforms of CBFA2T3 proteins (Lindberg et al., 2003), hence should be capable of picking both isoforms. The same antibodies were used in a subsequent study by Dhanda et al (2008), where they demonstrated the nucleolar localization of endogenous CBFA2T3aT protein (Dhanda et al., 2008). The results from both studies were based on CBFA2T3aT overexpression, which does not have the correct CBFA2T3a sequence. Moreover the antibodies used for these proteins were not sensitive enough to differentially detect CBFA2T family member proteins.

During the period under investigation localization studies on endogenous CBFA2T3 proteins was also carried out. Localization study of endogenous CBFA2T3 proteins showed differential expression in an asynchronous population of cells (Fig 3.10 and 3.11A first panel). In addition co-localization of CBFA2T3 endogenous proteins were seen with the cellular markers as cyclin-B, cyclin-E suggesting that CBFA2T3 was likely to be cell cycle regulated (Fig 3.11 B). This was further investigated by protein expression analysis after using a double thymidine block to synchronise cells at G1-S interface. Maximum level of expression was observed in cells at G1-S phase of cell cycle. Expression of CBFA2T3b protein reduced to a minimal level at the M phase of cell cycle (Fig 3.11B and 3.12.A). Previous studies have shown that overexpression of RUNX1 results in accelerated entry into S phase of the cell cycle as compared to control vector, while RUNX1-CBFA2T1 overexpression leads to blockage of cells in G1 phase of cell cycle (Amann et al., 2001; Strom et al., 2000). Present study has also indicated the involvement of CBFA2T3 proteins in cellular processes during G1 phase of cell cycle as an increase in expression of CBFA2T3b was observed in G1 phase of the cell cycle (Fig 3.12).

CBFA2T3 expression was reported to be high in many human tissues except testis, ovary and kidney. Gamou et al (1998) showed that CBFA2T3 was ubiquitously expressed in leukemic cell lines while its expression was reduced in cells when induced for differentiation with ATRA (Gamou et al., 1998). Up regulation of *CBFA2T3b* in response to oestradiol in a screen for ER responsive genes in breast cancer cell line MCF7 has also been reported (Frasor et al., 2003). During this study, CBFA2T3 expression both message and protein was determined in breast cancer cell lines. A pattern of *CBFA2T3* expression seen at transcript level (Fig 3.4) was also reflected in CBFA2T3 protein expression (Fig 3.5A). CBFA2T3b protein expression was found high in breast cancer cell lines MCF7, T-47D and ZR75-1 which are positive for ER, while it was found low in breast cancer cell lines MDA-MB-468 and MDA-MB-231 which are ER negative (Fig 3.5A).

Current findings have confirmed that CBFA2T3a has an actual start site present upstream of the known sequences. Hence the sequences in data base are not correct for CBFA2T3a isoform. CBFA2T3a and CBFA2T3b isoforms are localized to different cellular compartments. CBFA2T3a exhibits cytoplasmic localization while CBFA2T3b showed nuclear localization pattern. CBFA2T3b expression varies among a panel of breast cancer cell lines and also among asynchronous population of cells from a single cell line. The impact of the localization on functional roles of these CBFA2T3 isoforms will be discussed in details in coming chapters of the current study.

Chapter 4 – CBFA2T3a is a novel centrosomal protein involved with centrosomal duplication

4.1 Introduction

The centrosome is a small non-membranous organelle in an animal cell which has fascinated scientists for 100 years. It is the centre for organizing microtubule nucleation, which is essential for regulating cell motility, adhesion and polarity. Because centrosomes are microtubule-organizing centres (MTOCs), their number and structure is tightly regulated during the cell cycle (Nigg, 2007; Tsou & Stearns, 2006b). Cells contain one centrosome during the early G1 phase of the cell cycle, but after G1-S phase transition the centrosome number doubles in each cell. At mitosis, centrosomes migrate to the spindle pole to mediate bipolar spindle assembly and ensure correct chromosomal segregation. The importance of the centrosome was first realized as a result of findings of centrosomal anomalies in cancer (Fukasawa, 2005; Lingle et al., 2002).

As far as structure is concerned, the centrosome is comprised of a pair of centrioles, a mother centriole and a daughter centriole, surrounded by a dense material called pericentriolar material (PCM) (Chretien et al., 1997). PCM in humans contains more than a hundred different proteins. Pericentrin and coiled-coil molecules are major constituents of PCM and function as docking partners for most of the cell cycle regulatory proteins (Andersen et al., 2003; Kramer et al., 2004; Sluder, 2005). In addition, PCM also contains molecules that mediate microtubule nucleation such as γ-tubulin. γ-tubulin interacts with various proteins to form two types of complexes called the γ-tubulin small complex (γTuSC) and the γ- tubulin ring complex (γTuRC).

γTuSC is comprised of two γ-tubulin units and one molecule each of Gamma Complex protein 2 and 3 (GCP2 and GCP3). Multiple γTuSC complexes, along with some additional proteins like GCP-4, -5, -6 and GCP-WD (NEDD1), assemble to form γTuRC complexes (Gunawardane et al., 2000; Murphy et al., 2001; Tassin et al., 1998). It has been reported that GCP-WD is required for targeting γTuRC to the centrosome, and that GCP-WD depletion inhibits centriole duplication (Haren et al., 2006). γTuRC complexes are involved in microtubule nucleation that originates from the centrosome. During mitosis the centrosome becomes enriched with γTuRC complexes while the level of other proteins, which are docking partners of γTuRC complexes, continue to vary throughout the cell cycle.

The centriole is an open cylinder composed of 9 microtubule triplets arranged in the form of a radial array. This canonical structure is 0.5 μm long and 0.2 μm in diameter (Paintrand et al., 1992). Centrioles are polarized along their distal and proximo-distal axes. Both mother and daughter centrioles are distinct from each other structurally as well as functionally. Only the mother centriole has appendages on the distal and sub-distal regions. These appendages dock microtubules and also anchor centrioles to the cell membrane (Ishikawa et al., 2005).

Centrosomes duplicate only once during the cell cycle during late G1 to early S phase, in order to maintain the integrity of bipolar spindles. Any defect in either centrosome number or structure will lead to mitotic abnormalities, leading to the genomic instability. Thus control of the centrosome number is crucial for normal cell division and proper chromosome segregation. Centrosomal duplication occurs in coordination with the cell cycle to avoid missegregations but how these are coordinated is still

mystery. The centrosome duplication cycle (Fig 4.1) has been divided into four discrete steps (Nigg, 2007): (1) disengagement of centrioles, (2) duplication of the two centrioles pair to yield two engaged pairs, (3) maturation of the daughter centrosomes (4) separation of two fully mature centrosome. Cells in G1 phase have a single centrosome, which contains two loosely joined mother centrioles. This configuration of centrioles is referred to as disengaged or licensed for duplication. During G1/S transition the formation of two procentrioles (new daughter centrioles) begins exactly at right angle to the mother centrioles. Both pairs of centrioles (comprising mother centriole and a new daughter centriole) at this stage remain in tightly closed orthogonal configurations and hence are termed engaged centrioles. Centriole duplication is dependent on CDK2/cyclin E activity, which is high during G1-S transition (Okuda et al., 2000). The procentrioles elongate until the late G2 phase. The engaged centrioles have an intrinsic block for reduplication until the next cell cycle. During the M phase both centrosomes separate and move to opposite poles. Interestingly, during this process or at the exit from mitosis, centrioles in each single centrosome again became disengaged to license duplication. Tsou et al. (2006) have shown the involvement of separase in centriole disengagement which allows centrosome duplication. Hence it was proposed that licensing of centrosome duplication is related to the anaphase stage when disengagement of centrioles happens in the presence of the separase enzyme (Tsou & Stearns, 2006a; Tsou & Stearns, 2006b).

It has been proposed that control over centrosome/centriole number is dependent on two controlling mechanisms, one within the cell cycle and the second by limiting the centriole copy number. A number of factors are responsible for the control within the cell cycle, including Cyclin Dependent Kinases (CDKs), Nucleophosmin (NPM/B23)

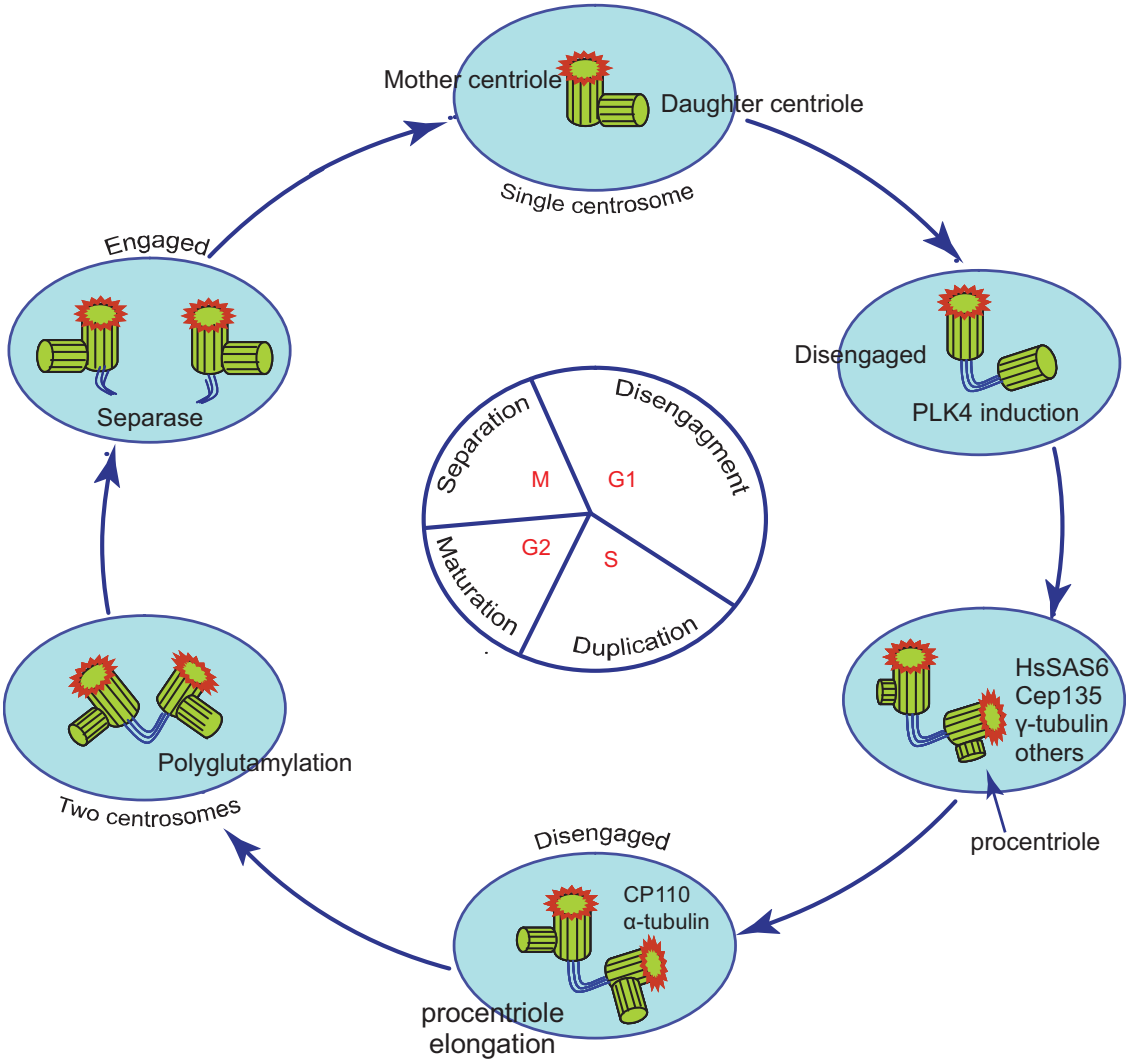

Figure 4.1. A model depicting the centrosome duplication cycle
Each centrosome during the normal cellular division passes through a series of changes leading to produce similar pair of centrosomes. These events are coordinated with cell cycle. The details of these events are described in the text, while a brief summary in schematic way is given in the current figure.

and separase activities (Okuda et al., 2000). Limiting centriole copy number is under the control of some intrinsic mechanisms from the centriole (Nigg, 2007). Normal centriole biogenesis involves the formation of seed for duplication by PLK4 kinase. PLK4 marks the site for procentriole formation on the mother centriole, possibly by phosphorylating an unknown substrate. The next step involves recruitment of proteins such as HsSAS-6, CPAP, Cep135 and γ-tubulin to the marked seed. Finally CP110 and α-tubulin mediate procentriole elongation, while polyglutamylation of tubulin stabilizes the newly formed centriole. It is now known that overexpression of PLK4 and HsSAS6 proteins induces multiple centriole formation (Kleylein-Sohn et al., 2007). These findings suggest that the PLK4 and HsSAS6 levels are tightly regulated for normal centriole biogenesis, and that any change to these initiates multiple centriole formation (Duensing et al., 2007; Kleylein-Sohn et al., 2007; Strnad et al., 2007). However, little is known about the substances present on the mother centriole. These suggest potential PLK4 substrates might have a crucial role in initiating centriole biogenesis.

In the present study, CBFA2T3a was identified as a novel centrosomal protein. Co-localization and immunoprecipitation has confirmed the interaction of CBFA2T3a with γ-tubulin. Moreover, a possible role was identified for CBFA2T3a in centrosome structure or function.

4.2 Materials and Methods

4.2.1 Cell lines and antibodies

The details of all human cell lines used in this study are outlined in Chapter 2 otherwise where it is necessary to mention a specific cell line it is indicated in the relevant section. The majority of the localization and shRNA experiments were conducted in HEK 293T and HeLa cell line grown under conditions given in Chapter 2. All commercially available antibodies used in this study are described in the General Materials and Methods (chapter 2). Two antibodies GT335 and α-Hs-SAS6 were a kind gift from Dr Carston Janke (France) and Dr Pierre Gonczy (Switzerland).

4.2.2 Plasmids

A variant of pEGFP-C1 or -N1 (Promega Inc) containing the full-length enhanced green fluorescent protein (EGFP) ORF either upstream (with a start codon but lacking a stop codon) or downstream (without a start codon but containing a stop codon) of the multiple cloning site was used to clone myc-CBFA2T3a full length, myc-leader sequence 1 (LS1) and myc-leader sequence 2 (LS2) fragments in both pEGFP-C1 and pEGFP-N1 vectors. Details of these fragments are shown in figure 4.2A. Integrity of these construct was confirmed by DNA sequencing (section 2.7 Chapter 2). Furthermore, pEGFP vector was used as a control during all experiments. To generate CBFA2T3 shRNAs, one reported (Goardon et al., 2006) and two other sets of short hairpin primers for CBFA2T3 were annealed and cloned at the BglII/HindIII site in the pMSCV vector, which also encodes EGFP for monitoring transfection efficiency (sequences for the hairpins are given in Table 2.1).

4.2.3 Immunofluorescence

The methods for immunoflorescence are described in Chapter 2 section 2.13. For the Hs-SAS6 antibody a modified method was used. Cells were fixed in cold methanol for 10 minutes, followed by incubation in a blocking solution A (1×PBS, 0.05% Triton X100, 1% BSA) for 30 min. After blocking, the cells were incubated in 1:60 dilution of Hs-SAS6 antibody in the solution A at 4 C^0 overnight. Cells were washed 4× with 1×PBS and then incubated with Alexa Fluor, rhodamine-, fluorescein-, or Cy5 conjugated secondary antibodies (1:300) for 1-2 hours at room temperature. Cells were then washed 4× with 1×PBS and mounted with VECTASHIELD mounting medium with DAPI (Vector Laboratories). Images were taken with Olympus 1X70 inverted microscope and a Bio-Rad Radiance 2100 confocal microscope equipped with three laser, Argon ion 488nm; Green HeNe 543nm; Red Diode 637nm. 300-400 cells where scored for metaphase and centrosomal abnormalities. While for all other co-localization studies 100-150 cells were scored in single experiment. To find the consistence of the data experiments were repeated at least twice. Images were processed using Adobe Photoshop software (Adobe Systems Inc., San Jose, CA).

4.2.4 Immunoprecipitation

For immunoprecipitation of endogenous CBFA2T3 proteins, 5×10^7 cells from MCF7 cell line were harvested as previously described (section 2.4). For overexpression studies cells were transfected with respective plasmids (section 2.1). The details of procedure for immunoprecipitation are given in section 2.11 in the General Material and Methods (chapter 2). Cleared lysate was incubated with α-CBFA2T3 RSH1 antibody for endogenous protein or with α-myc antibody for experiments where cells expressed a CBFA2T3 myc-EGFP fusion construct. The remaining procedure was the same as

described in section 2.11. Samples are eluted with SDS loading buffer and detected on western blots using appropriate antibodies.

4.2.5 Reverse transcription real time-PCR

RNA was prepared from HeLa cells expressing sh-CBFA2T3, sh-scrambled and mock using QIAGEN Mini RNA Kit (Quigen Inc. USA) as explained in Chapter 2 General Material and Method. cDNA was synthesized from RNA by oligo $(dT)_{24}$ primers using MMLV reverse transcriptase (RNase H^-). Real time-RT-PCR was used to monitor *CBFA2T3* mRNA with *Cyclophilin-A* levels used as an internal control.

4.3 Results

4.3.1 CBFA2T3a leader sequence has centrosomal localization signals

Previous localization (Section 3.3.6) and western data (Section 3.3.5) show that the CBFA2T3a isoform localized to the cytoplasm while the CBFA2T3b isoform localized to the nucleus. The different localizations of the two protein isoforms are presumably due to the differences in their N-terminus regions. *In silico* analysis of CBFA2T3 isoforms "a" and "b" revealed that CBFA2T3a has an extended N-terminus region. In addition to this extended exon 1, CBFA2T3a also has exon 3, which is lacking in the CBFA2T3b isoform (Fig 4.2 A). Analysis of this N terminus region revealed that it has two leucine-rich regions, each with a (**L X_3 LL X_{3-4} L)** putative nuclear export signal (NES). Region one is from 141-152 amino acids sequences followed by second leucine-rich region from 171-184 amino acids (Fig 4.15).

Different myc-CBFA2T3a full length and myc-CBFA2T3a fragment, myc-LS1, myc-LS2 (Fig-4.3.1A) were PCR amplified and cloned into the pEGFP-N1 and pEGFP-C1vectors to generate myc-EGFP fusion proteins. To determine the localization of these proteins in initial experiments, plasmids harboring myc-EGFP fusion constructs were transiently transfected into HEK293T or MCF7 cell lines. No change in localization of these proteins was observed due to the EGFP at N-terminus or either at the C-terminus of the constructs, confirming that the observed localization pattern is due to the signals from internal sequences of cloned fragments. CBFA2T3a-EGFP has exhibited the similar cytoplasmic/centrosomal localization pattern as shown by myc-CBFA2T3a. The presence of EGFP tag did not influence the localization of the CBFA2T3a protein as EGFP-CBFA2T3a has shown the pattern similar to myc-CBFA2T3a protein localization. Whereas myc-LSI-EGFP and myc-LS2-EGFP were exclusively localized

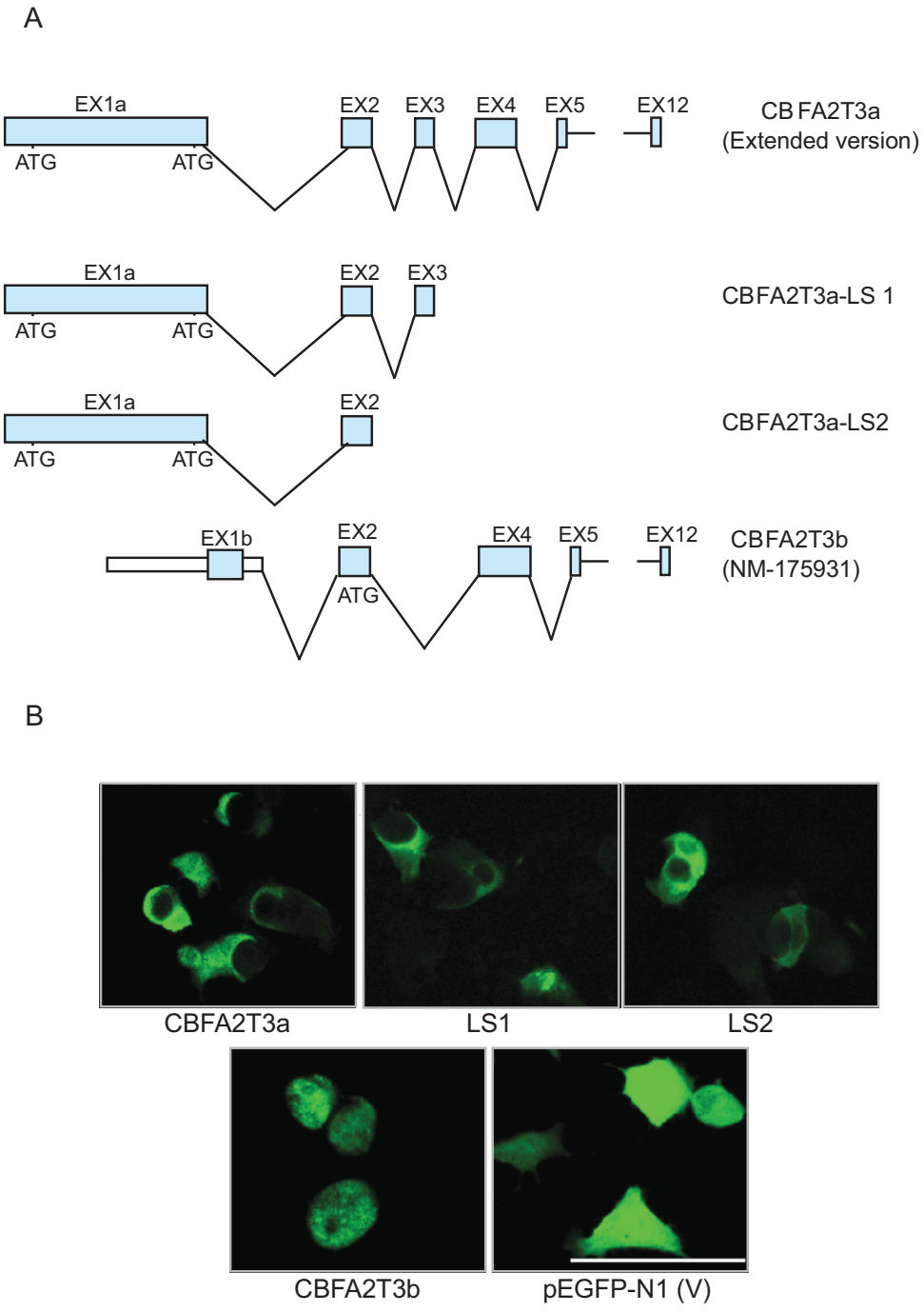

Figure 4.2. Structure and expression of different CBFA2T3 proteins
A. A diagram presenting exon structures of different CBFA2T3 isoforms showing variation in the N-terminus region. The exon structure of LS1 and LS2 clones are also shown. **B.** Flourescent images from transiently overexpressed different CBFA2T3 myc-EGFP fusion proteins in MCF7 cells. Scale bar = 10 µm.

to small distinct spots adjacent to or over nucleus (Fig 4.2 B) in the cytoplasm. It is important to note that cells with low levels of EGFP expression, comparable to the level of endogenous CBFA2T3 proteins have shown distinct spots (Fig Appendix 1).In contrast cells having higher EGFP expression have some cytoplasmic localization. Serial sections taken with CLSM revealed that these spots were not localized inside the nucleus and were very small in size (see appendix figure 4.1). Furthermore it was noted that in some cells there were two spots and these spots were positioned closely to each other, while in other cells these spots were at a distance from each other (Fig 4.4A arrow head). These spots in the cytoplasm suggested centrosomal localization. In contrast to CBFA2T3a, CBFA2T3b was localized to nuclear speckles and this pattern of localization was consistent with the previous finding (Chapter 3 Fig 3.7A).

4.3.2 Centrosomal localization of CBFA2T3a and leader sequence proteins

To confirm that CBFA2T3a and CBFA2T3a leader sequence clones were localized to centrosome, co-localization studies with other known markers for this organelle were performed. Co-localization studies were carried out with γ-tubulin, as this has been extensively used as centrosomal marker (Shinmura et al., 2007; Shinmura et al., 2005). Initial co-localization of CBFA2T3a and the leader sequence clones with γ-tubulin were determined in the MCF7 cell line. Subsequently, this was further confirmed in HeLa cell line which has the added advantage of superior morphology in fluorescent microscopy.

4.3.2a Interaction of endogenous CBFA2T3 proteins with γ-tubulin

CBFA2T3 and γ-tubulin co-localization studies were undertaken in the MCF7 cell line using anti-CBFA2T3 RSH1 and anti-γ-tubulin antibodies. It was found that endogenous

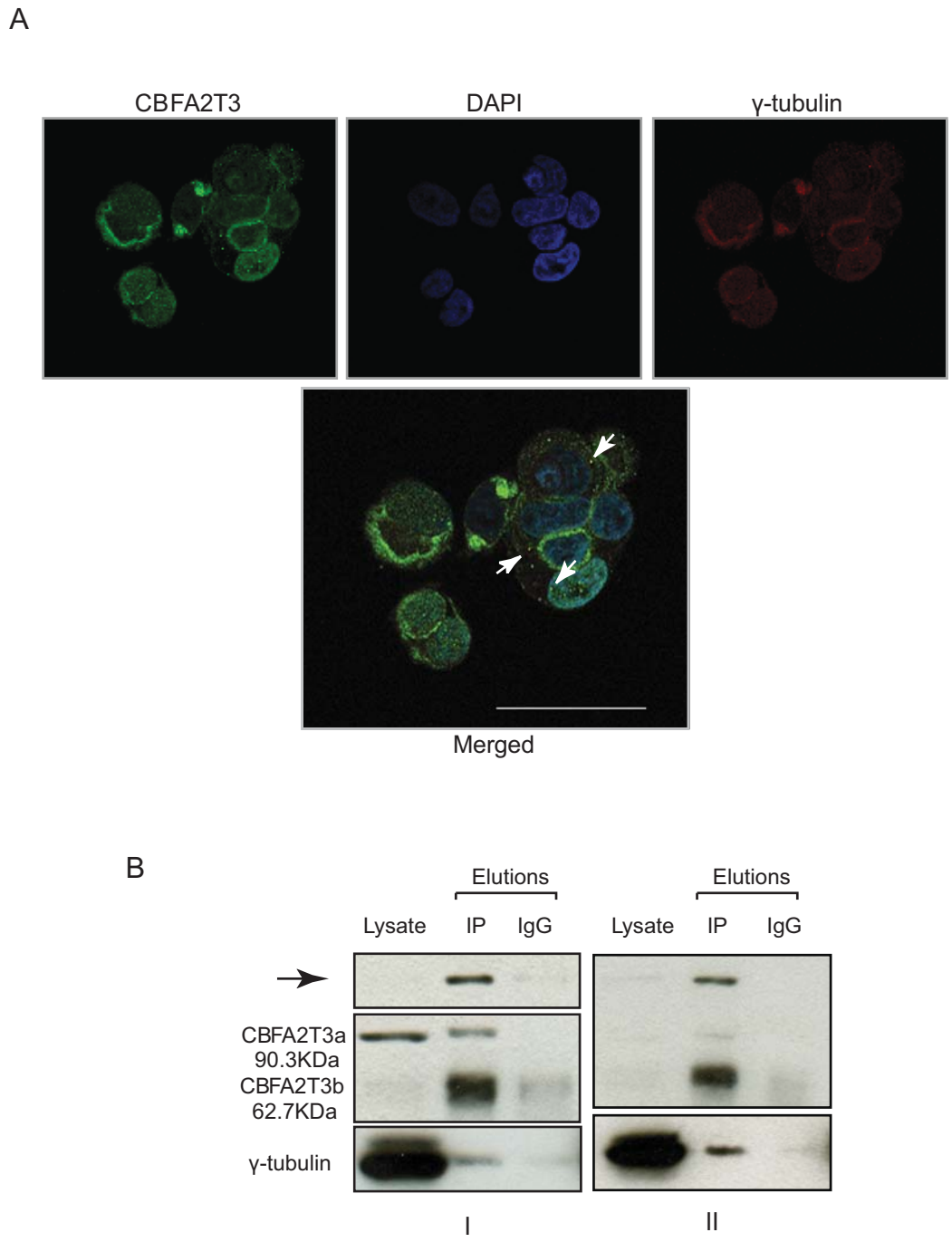

Figure 4.3. Endogenous CBFA2T3 co-localizes and interacts with the γ-tubulin
A. MCF7 cells were co-stained with anti-CBFA2T3 and anti-γ-tubulin antibodies**.** Arrows in merged image marks the co-localization of both proteins in the centrosomes. **B**. Endogenous CBFA2T3 proteins were immunoprecipitated with anti-CBFA2T3 antibody from the MCF7 cells. Lysates and elutions were western blotted with α-CBFA2T3 and α-γ-tubulin antibodies. Arrow corresponds to a high molecular weight protein often seen after immunoprecipitation. Data from two independent experiments I and II are presented.

CBFA2T3 proteins (as anti-CBFA2T3 antibody detects both CBFA2T3 isoforms) co-localized with γ-tubulin to the centrosome (Fig 4.3A). To verify CBFA2T3 interaction, immune complexes from MCF7 cell line were isolated using anti-CBFA2T3 RSH1antibody and western blotted against anti γ-tubulin and anti-CBFA2T3 RSH1 antibodies. Endogenous γ-tubulin was detected in immune complexes immunoprecipitated with α-CBFA2T3 antibody (Fig 4.3B). Given the fact that α-CBFA2T3 antibody can detect both CBFA2T3 isoforms, it was not possible to conclude which CBFA2T3 isoform was responsible for this interaction.

4.3.2b Interaction of exogenously expressed CBFA2T3a, LS1, LS2 and CBFA2T3b proteins with γ-tubulin

To further understand the interaction of CBFA2T3 isoforms with γ-tubulin, DNA from EGFP-myc fusion constructs of CBFA2T3a, LSI, LS2 and CBFA2T3b were transiently overexpressed in the HeLa cell line. Cells were immunostained with anti-γ-tubulin antibody. Immunofloresent signals from EGFP (green) and anti-γ-tubulin complexed with Alexa fluor 594 goat anti-mouse IgG (red) were detected using LCSM (Fig. 4.4A). It was found that γ-tubulin co-localized with EGFP-myc-CBFA2T3a, myc-LSI-EGFP and myc-LS2-EGFP (arrow heads in Fig. 4.4A). However, co-localization of EGFP-myc-CBFA2T3b with γ-tubulin was not observed. CBFA2T3b has shown the typical nuclear speckle localization while γ-tubulin signals can be visualised in centrosome outside the EGFP (green) or DNA signal (blue) in merged image (Fig 4.4A Panel CBFA2T3b marked with the solid arrow). The overlap in the localization patterns of these two proteins suggests that CBFA2T3a might associate with γ-tubulin and perhaps other centrosomal proteins.

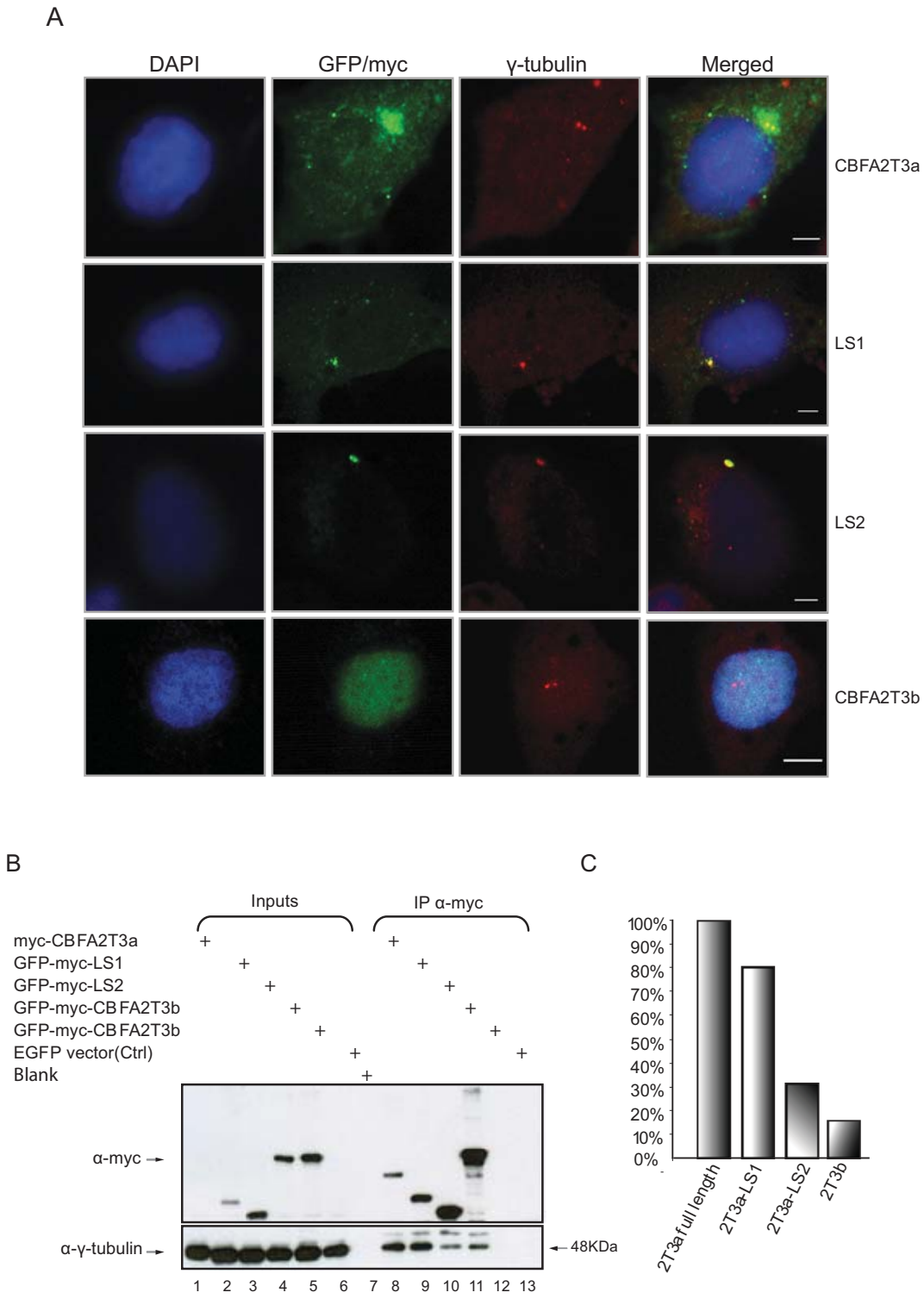

Fig 4.4. Co-localization and immunoprecipitation studies of CBFA2T3 Proteins
A. Different CBFA2T3 myc-EGFP fusion proteins were stained for endogenous γ-tubulin (red), while green represents signal from GFP-myc-fusions. Scale bar = 10 μm. **B.** CBFA2T3 myc-EGFP fusion protein lysates were immunoprecipitated with α-myc antibody and western blotted with α-myc and α-γ-tubulin antibodies. Arrow on the right side of the panel points to 48kDa γ-tubulin. **C.** Bar diagram presenting the intensity of γ-tubulin relative to the immunoprecipitated CBFA2T3 fragments.

To gain a further insight on the interaction of CBFA2T3a with γ-tubulin, the myc-EGFP-CBFA2T3 derived constructs (Fig. 4.2A) were transiently overexpressed in HEK293T cells and are analysed by immunoprecipitation. Protein-complexes were isolated with the α-myc antibody and analysed for endogenous γ-tubulin on western blots. These immunoprecipitation experiments show that CBFA2T3a and both the leader sequences LS1 and LS2 interact with γ-tubulin (Fig. 4.4B). Relative band intensities of γ-tubulin to CBFA2T3 immunoprecipitated proteins were presented as a bar diagram (Fig 4.4 C) indicating stronger interaction with full length CBFA2T3a and LS1, while the interaction is weaker for LS2 and CBFA2T3b. Interaction of CBFA2T3a, LS1 and LS2 with γ-tubulin confirmed that CBFA2T3a is a centrosomal protein. The data from comparison between the CBFA2T3a and CBFA2T3T localization (Fig 3.8 chapter 3) has further shown that CBFa2T3a localizes to the cytoplasm and particularly to the centrosome, while CBFA2T3aT is confined to the nucleoplasm. *In silico* analysis has shown the existence of differences only in *N-terminus* regions, the extended exon 1 sequences (Fig 4.14). The leucine-rich sequences, known to mediate centrosomal localization are present only in the extended exon 1.

Immunoprecipitation of overexpressed CBFA2T3 proteins has shown that CBFA2T3b proteins have greater binding efficiency with the anti-myc or anti-CBFA2T3 RSH1 antibodies as compared to the CBFA2T3a (Fig 4.4B). This might be due to the larger size of CBFA2T3a protein. A band showing interaction between γ-tubulin and the CBFA2T3b (lane 11 Fig 4.4B) was noticed only when protein-complexes were incubated for long periods with antibodies while no interaction with γ-tubulin was seen when the time of incubation was reduced (data not shown) indicating that the IP results for CBFA2T3b might be an artefact which was further supported by localization data.

Furthermore, the γ-tubulin signal in CBFA2T3b immunoprecipitates was linked with the observation of high molecular weight bands (Fig 4.4B lane 11 panel for α-myc), which is likely to correspond to hetrodimers or tetrameric forms of CBFA2T family proteins. These highly molecular sized bands were prominent when blots were exposed for longer periods of time (Fig 4.14B). it has been previously reported that CBFA2T family members can form dimers or tetramer both *in vivo* or *in-vitro* (Liu et al., 2007) (Hoogeveen et al., 2002).

The serial z-sections performed on CBFA2T3b overexpressing cells co-stained with anti- γ-tubulin have shown that CBFA2T3b did not co-localize with γ-tubulin (Fig 4.4A), the band observed in IP lane (Fig 4.4B lane 11 γ-tubulin panel) may be due to the oligomerization properties of these two isoforms. This was further confirmed by the absence of background binding of γ-tubulin to the beads (mouse IgG lane 12 and vector control lane 13).

4.3.3 Effects of CBFA2T3 knock down on normal centrosome biogenesis

Microscopy as well as immunoprecipitation of transiently expressed EGFP-myc fusion proteins of different CBFA2T3 clones demonstrated that CBFA2T3a colocalize with γ-tubulin to the centrosome. To further investigate the possible role of CBFA2T3 in the centrosome, CBFA2T3 specific knock down studies were performed.

A previously verified short hairpin RNA sequence (shRNA) targeting CBFA2T3 was used (Goardon et al., 2006). Experiments were also repeated with two additional shRNA sequences (hairpin I and II Table 2.1 Chapter 2) that have previously been shown to knockdown levels of CBFA2T3 proteins (David Millband, unpublished data).

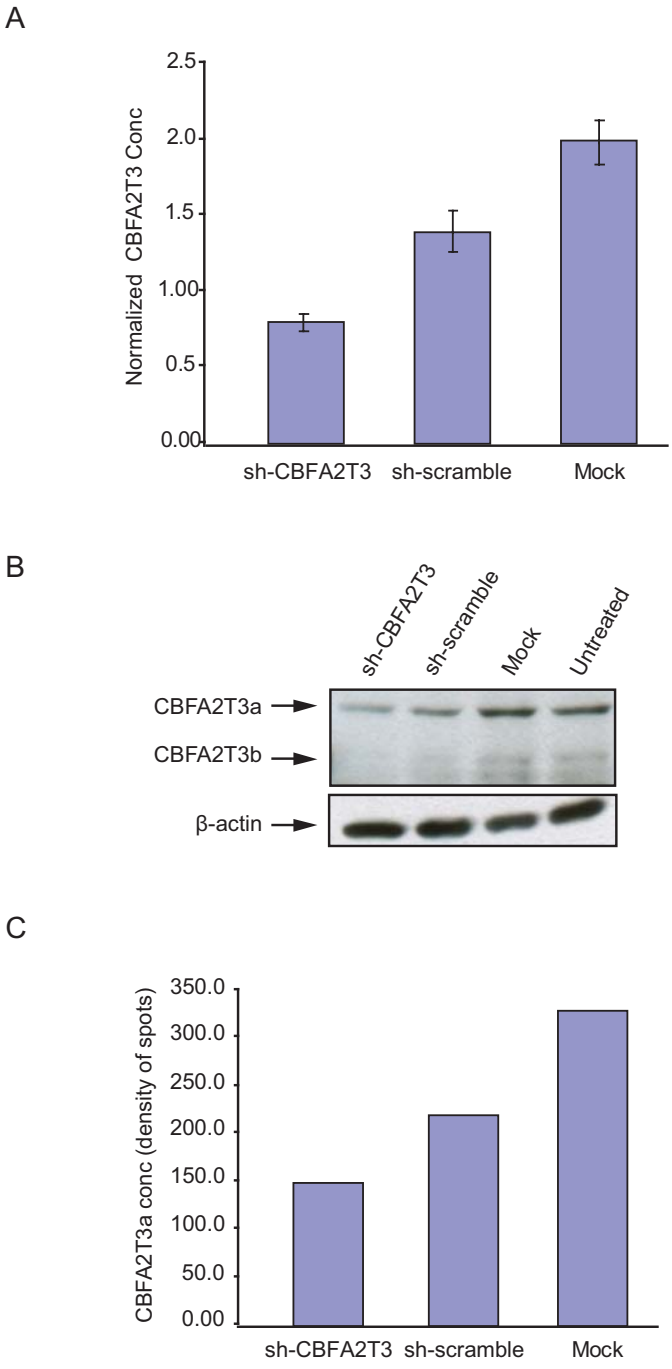

Figure 4.5. CBFA2T3 knock down in HeLa cell line
Cells were processed for protein and mRNA analysis after sh-CBFA2T3 and sh-scrambled treatment for 24 hrs. **A.** Relative conc of CBFA2T3 mRNA was quantified using real time RT- PCR with the *Cyclophilin-A* gene as a relative control. The bars represents ± SEM for each treatments. **B**. Lysates from the same experiment were blotted with α-CBFA2T3 and β-actin antibodies. **C**. The histogram represent CBFA2T3a amount for each treatment. The density of the bands from western data (B) for CBFA2T3a was measured using AlphaImager 2200 spot Denso tool.

Transient expression of these shRNA constructs for 24 hours resulted in reduction of endogenous CBFA2T3a and CBFA2T3b proteins. CBFA2T3a knockdown was detected at protein level by anti-CBFA2T3 antibody (Fig 4.5B). Due to low levels of CBFA2T3b, CBFA2T3b knock down was further assessed at the message level (Fig 4.5A). The results show a decrease in protein as well as mRNA level of both CBFA2T3 isoforms compared to the control scrambled shRNA treatment (Fig 4.5A, B and C).

4.3.3.1 Effect of CBFA2T3 knock down on centrosome number.

Given that immunoprecipitation data shows that CBFA2T3a localized to the centrosome and associate with γ-tubulin complexes in centrosomal fractions (Dr Raman Kumar data from glycerol gradient fractions unpublished), the structure and number of centrosomes was analyzed after CBFA2T3 knockdown by immunoflorescent staining with α-γ-tubulin antibody. Surprisingly, cells treated with CBFA2T3-specific shRNA treatment showed an increase in the centrosome number compared to the scrambled shRNA (Fig 4.6A). The amplified centrosomes are either in groups of three, four or more than five. Occasionally a Halo structure (group of three, five and more centrosomes) centrosome arranged like a flower petals (Fig 4.6A) were seen as described by (Kleylein-Sohn et al., 2007). Commonly three centrosomes were observed, while a small percentage of the cells showed Halo structures. More then 18% of cells were found with 3 centrosomes, while 4% cells had more than 4 centrosomes (Fig 4.5B). Similar findings were observed when the cells were treated with two different shRNA constructs for CBFA2T3 (Fig Appendix -2). Although the percentage of abnormalities was less which was found related with low transfection efficiency observed with the other shRNA constructs.

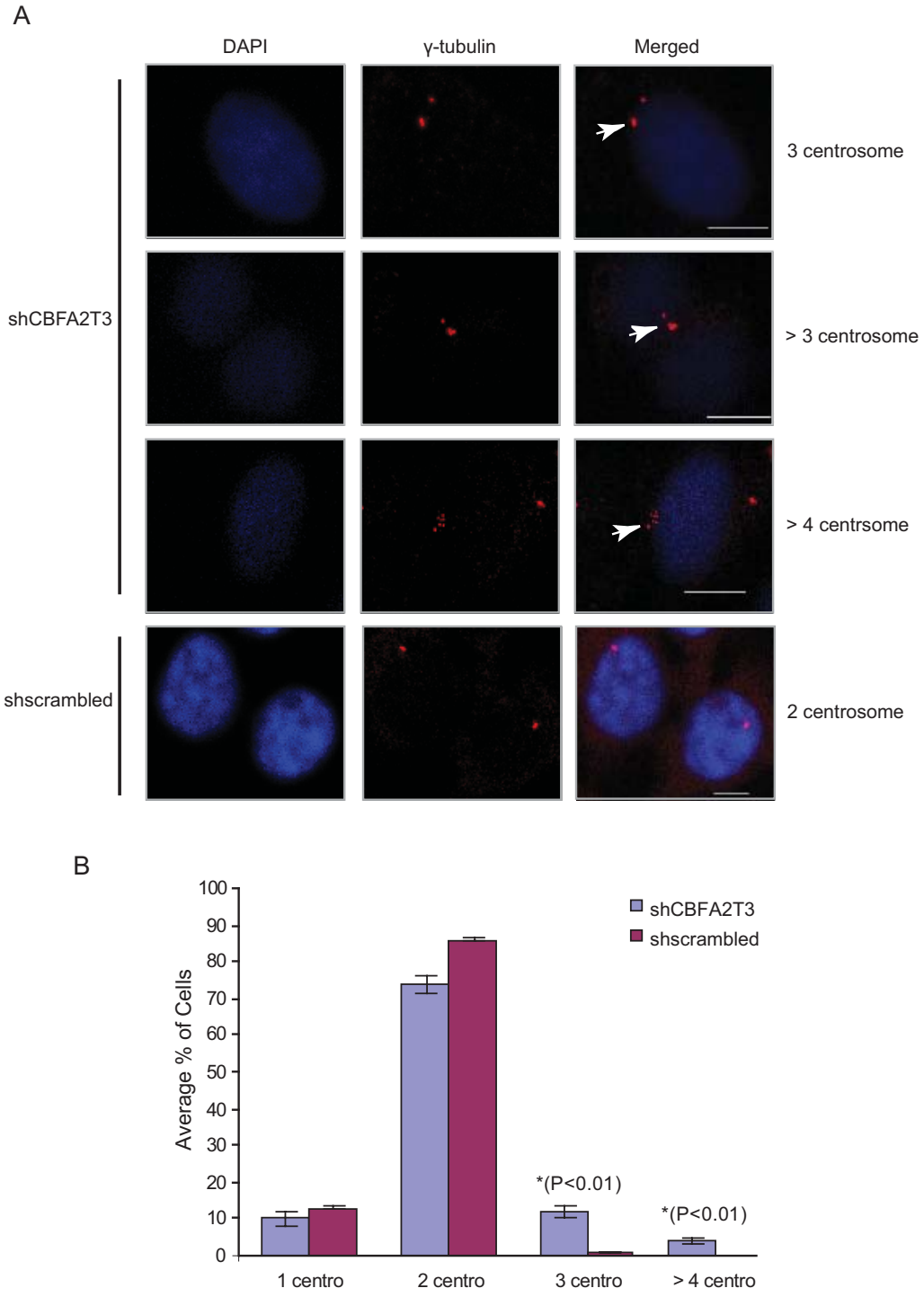

Figure 4.6. CBFA2T3 knockdown resulted into centrosome amplification
A. HeLa cells were stained with α-γ-tubulin antibody 24 hour post tranfectionof shCB FA2T3 and shscrambled constructs. Sets represent the examples of single and me rged images for each catagory (centrosome numbers) and treatments. Scale bar = 10 µm. **B**. Centrosome numbers were counted for 300-400 cells for each treatment from A. Each bar of the histogram is representative of ±SEM from three independent experiments calculated for di fferent catagories of centrosome numbers.

CBFA2T3 knockdown experiments were repeated in cell lines HEK 293T, HeLa and U2OS. The percentage of cells with more than two centrosome numbers was observed in both HEK293T and HeLa cell line (15% and 12% respectively) after shCBFA2T3 treatment. In the U2OS cell line 6% of the cells had more than two centrosome numbers as compared to scrambled control and there was no further increase in the percentage of cells with more than two centrosomes. The differences observed for the percentage of cells with more than two centrosome numbers among different cell lines was probably due to differential transfection efficiency of the cells particularly in U2OS cell line only 55% of cells were found transfected with shCBFA2T3 or shscrambled (Fig 4.7A) where as the transfection efficiency of shCBFA2T3 or shscrambled was about 95% in HeLa and HEK293T cell lines. The results from these experiments show that the observed increase in centrosome number after CBFA2T3 knock down is independent of the cell line or p53 status. As HEK293T has a wild type but inactive p53, HeLa cells express wild type p53 rapidly degraded by E6 but U2OS cell line has normal wild type active p53. The data from the CBFA2T3 knockdown in these cell lines has suggested that the seen effects of CBFA2T3 knockdown on centrosomal amplifications are independent of p53.

The effect of CBFA2T3 knock down on centrosome number in the HeLa cell line was further analyzed at different time points after transfection with shRNA. Cells were treated with shCBFA2T3 and shscrambled for 12, 24 and 48 hours. Centrosome numbers from these treatments were analyzed by staining with α-γ-tubulin antibody. There was a minimal increase in percent cells with increased centrosome numbers (13-14%) seen with the passage of time from 24 hours to 48 hours (Fig 4.7B). Only 1% of

A

Percent centrosome numbers 24 hours post transfection	shscramble			shCBFA2T3		
	1	2	>2	1	2	>2
293T	14%	86%	0%	12%	73%	15%
HeLa	12%	88%	0%	8%	80%	12%
U2OS	11%	89%	0%	13%	81%	6%

B

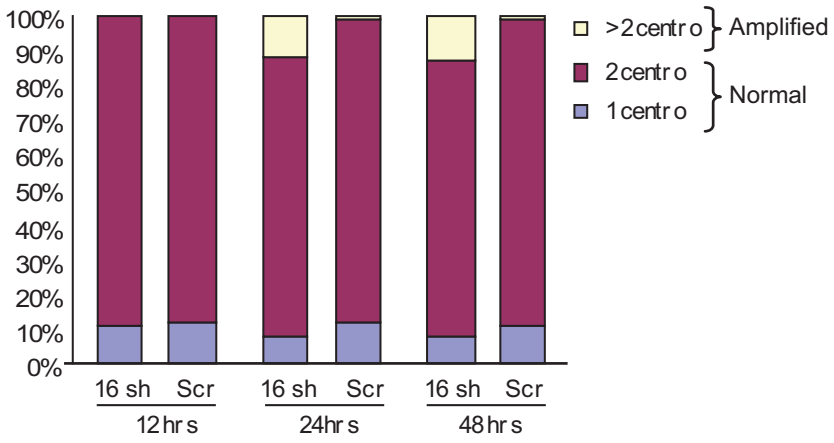

Figure 4.7. Effects of CBFA2T3 knockdowns on centrosome numbers
A. Three different cell lines 293T, Hela and U2OS were transfected with shCBFA2T3 and shscrambled plasmids for 24-28 hours. Cells were immuno stained with alexa 594 labelled γ-tubulin antibody to count centrosome numbers for all cell lines. Transfection efficiency was monitored by GFP expression. Note that thetransfection effeciency for U2OS cell line was 55% as compared to HeLa and HEK293T. **B.** Centrosomes were stained with γ-tubulin antibody post shCBFA2T3 (16sh) and shscrambled (Scr) treatments for 12, 24 and 48 hours. Percentage of different centrosome numbers were plotted for both treatments of each time point. More then 400 cells were counted for each catagory.

the total population of cells showed 3 centrosome numbers in the scrambled shRNA control at all time points (Fig 4.7B).

4.3.3.2 Increase in mitotic catastrophe following CBFA2T3 knock down.

Bipolar spindles are key components of normal cell division. Anomalies in this basic structure lead to the mis-segregations of chromosomes which increases genome instability (Lingle et al., 2002; Pihan et al., 1998). CBFA2T3 knockdown studies were carried out in the HEK293T and HeLa cell lines. Cells were treated with shRNA for CBFA2T3 and scrambled control constructs for 30-48 hours, fixed and immunostained with α-γ-tubulin to detect the centrosome or α-β-tubulin antibodies to stain the spindle. A dramatic increase in different metaphase anomalies was observed following CBFA2T3 shRNA treatment, while the numbers of metaphase abnormalities was negligible in the scramble shRNA control (Fig 4.8B).

Two major types of metaphase abnormalities were noticed. The majority of abnormal metaphases were pseudopolar, characterized by the formation of a plate-like structure on the spindle pole. This plate-like structure contains multiple centrosomes aligned in a single line (Fig 4.8A panel 3). The second major anomaly seen was multipolar metaphase spreads. These multipolar metaphases had either three polar or four polar spindle structures (Fig 4.8A panel 2). In addition to these, an elongation of the spindle structure was also noticed in some cells (data not shown).

40-45% of the metaphases in HeLa cells had pseudopoles 24 hr after transfection with CBFA2T3 shRNA, compared with the scrambled shRNA control where there was an absence of this abnormality (Fig 4.8B). In addition following CBFA2T3 shRNA

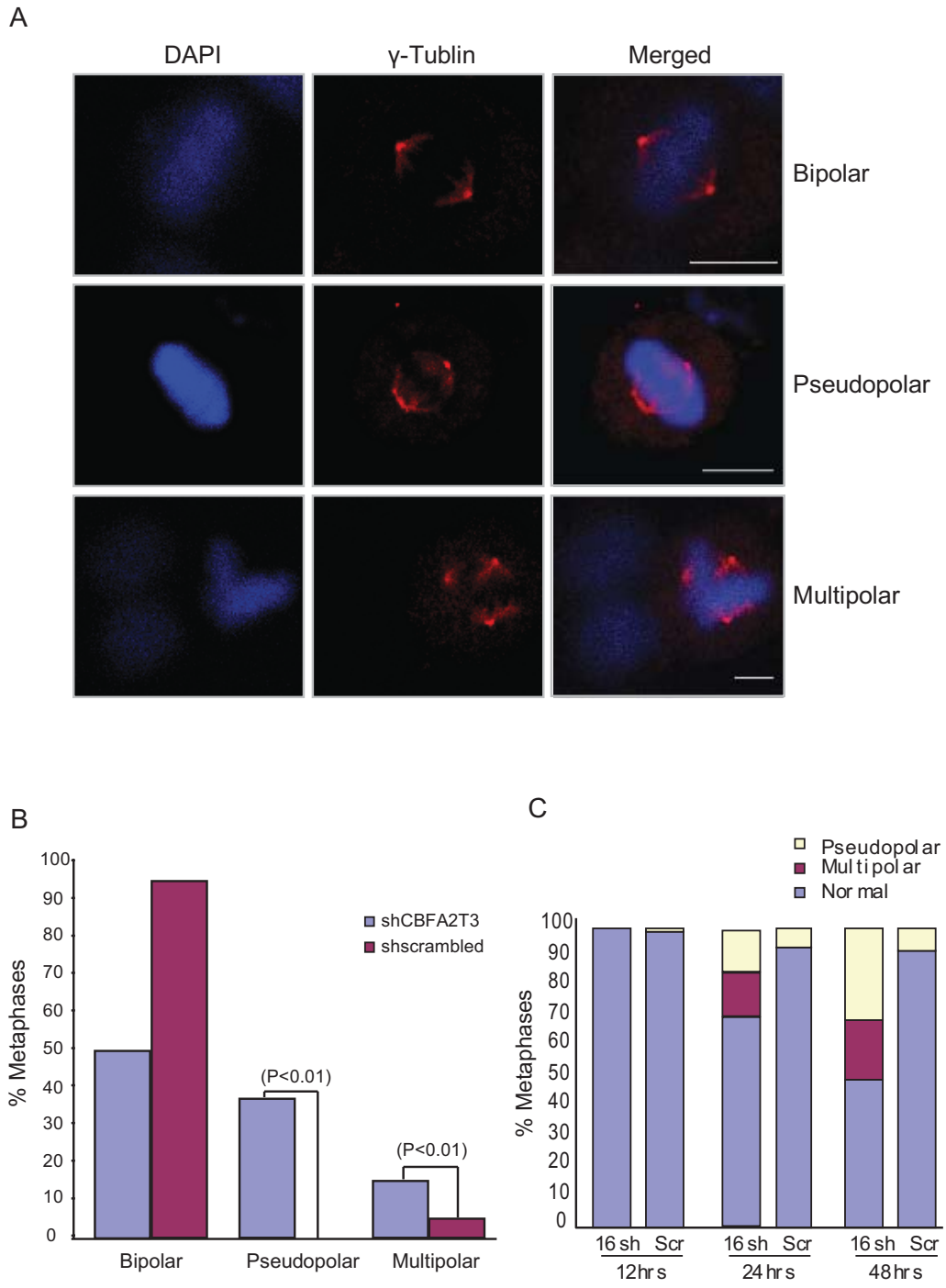

Figure 4.8. CBFA2T3 knock downs leads to mitotic catastrophe
A. HeLa cells were stained with α-γ-tubulin antibody. Each set is representative of the types of metaphases seen following shRNA treatment. Scale bar = 10 μm. **B**. Histogram bars represent the percent metaphases (bipolar, pseudopolar and multipolar) 48 hours post treatment. Data is represenative of a single experiment. More then 130-150 metaphase spreads were scored for each treatment. **C**. Histogram presenting % metaphases anomalies seen after staining with α-γ-tubulin after shRNA treatments for 12, 24 and 48 hours period of time.

treatment, 15% of the metaphases had multiple poles compared with the 4% of cells in scrambled shRNA (Fig 4.8B). These mitotic anomalies were further analyzed in HeLa cells treated with shRNA constructs for different periods of time. The percentage of pseudopolar and multipolar metaphases increased from 24 to 48 hours to the total of 50% of all metaphases following the shCBFA2T3 treatment compared with scramble shRNA treatment (Fig 4.8C). The current increased in % metaphase anomalies is likely to be due to the fact that cells with increased centrosome numbers in next round of cell cycle result in an increase in the metaphase catastrophe.

4.3.3.3 The effects of CBFA2T3 knock down on other cell cycle regulatory proteins involved in centrosome duplication.

Cell cycle proteins having a role in centrosome duplication were also analyzed by western blot analysis and immunoflorescent studies. Cellular lysates from shCBFA2T3 and shscrambled treatment in HeLa cells were probed with various cellular markers known for their role in centrosome duplication (Fig 4.10A). Data for the CBFA2T3 expression and loading control was presented earlier (Fig 4.5B) along with mRNA expression data (Fig 4.5A). This analysis was further expended to the lysates prepared from cell pellets harvested at different time points post shRNA treatments (Fig 4.10B).

The localization of B23/NPM (Nucleophosmin) protein was compared between scrambled and CBFA2T3 knock down samples from HeLa cells. B23 is a nucleolar protein which also associates with the centrosome. B23 has a role with the licensing of centrosome duplication as its disassociation from centrosome is reported to mark centriole biogenesis (Ma et al., 2006). B23 is also known for its role in pre-rRNA and pre-mRNA processing (Tarapore et al., 2006). Changes in B23 status is related to

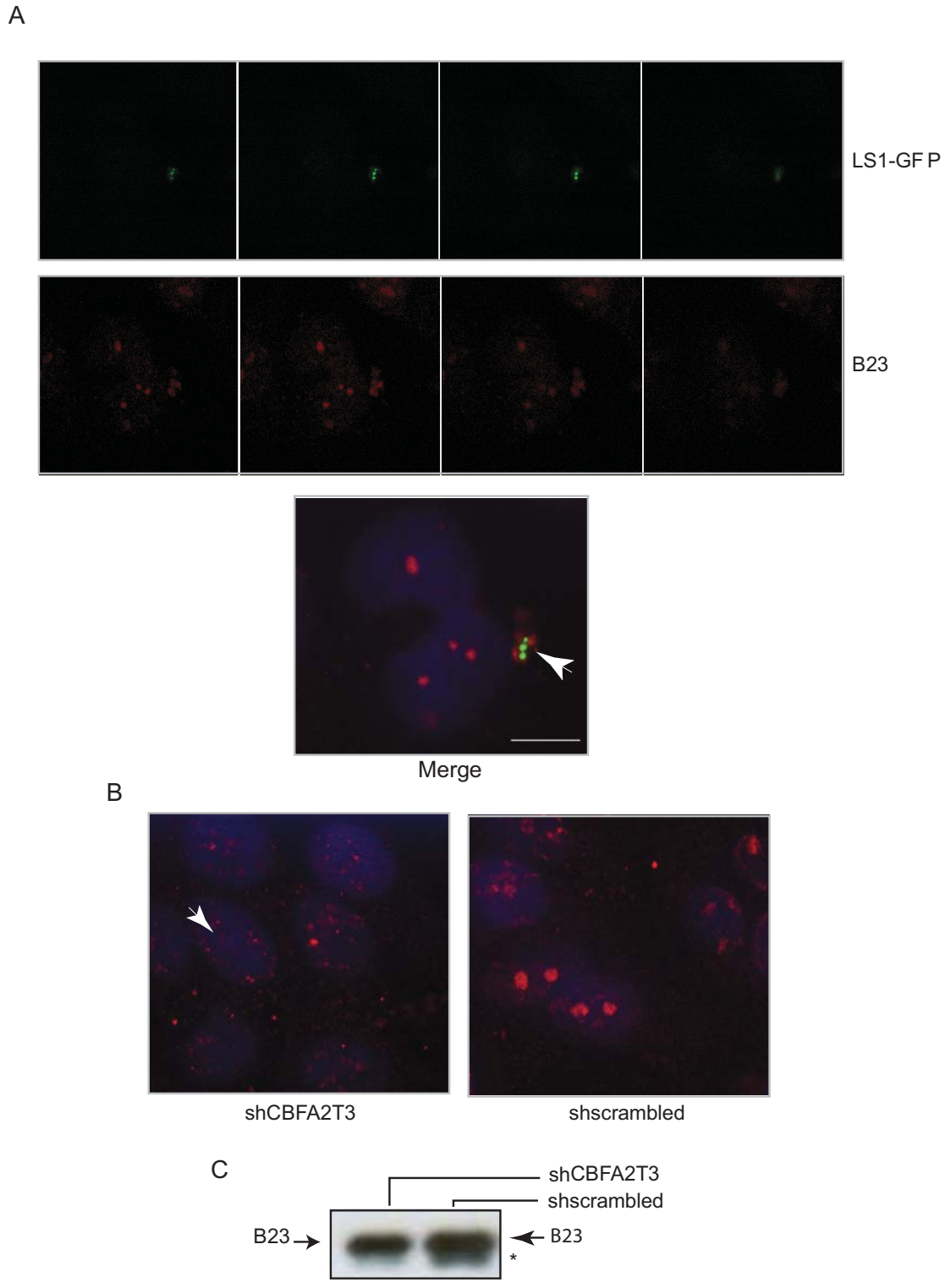

Figure 4.9. Changes in Nucleophosmin (B23) after CBFA2T3 knock down
A. Serial sections from myc-LS1-EGFP fusions stained with B23 antibody. **B**. HeLa cells were stained with B23 antibody post 24 hours treatment with sh-CBFA2T3 and sh-scrambled. **C**. Cell lysates from (B) were western blotted with B23 antibody. B23 proteins run in a doublet. Asteric marks the faster migrating band.

phosphorylation by CDK2/cyclin-E complexes (Okuda et al., 2000). A dispersed localization of B23 throughout the nucleus (arrow head Fig 4.9B) was found in HeLa cells treated with shCBFA2T3 while cells treated with shscrambled retain nucleolar localization of B23 (Fig 4.9B). Nuclear speckle localization of NPM/B23 is already known to be related to its phosphorylation at Thr-^{199} (Tarapore et al., 2006). NPM/B23 phosphorylation at Thr-^{199} is reported to be critical for its role in centrosome duplication (Ma et al., 2006). Western analysis of B23 protein (Fig 4.10A and B) also revealed a change in size from a diffuse doublet to a single compact band (Fig 4.9C and 4.10A) which is suggested to correspond to the phosphorylated status of B23. A shift in balance between phosphorylated and non-phosphorylated form of B23, toward the more phosphorylated B23 is known to impart centrosome licensing for duplication. Further experiments were not possible due to non-availability of the phospho specific antibodies.

A change in CDK2 status was also observed. There was an increase in the faster migrating band (lower band, is more pronounced in Fig 4.10A CDK2 panel) for shCBFA2T3 as compared to scramble control. The faster migrating band for CDK2 corresponds to protein phosphorylated at Thr-160, which is associated with high CDK2 activity (Ukomadu & Dutta, 2003) (western panel for CDK2 bands became dim or lost their prominence after scanning Fig 4.10A and B). Similar results were observed when the lysates from shCBFA2T3 and shscrambled harvested at different time points were analysed (Fig 4.10B).

The association of CBFA2T3 with CDK2 was further investigated. *In silico* analysis has revealed a putative CDK2 binding motif in CBFA2T3a 160-166aa (SPGRGL)

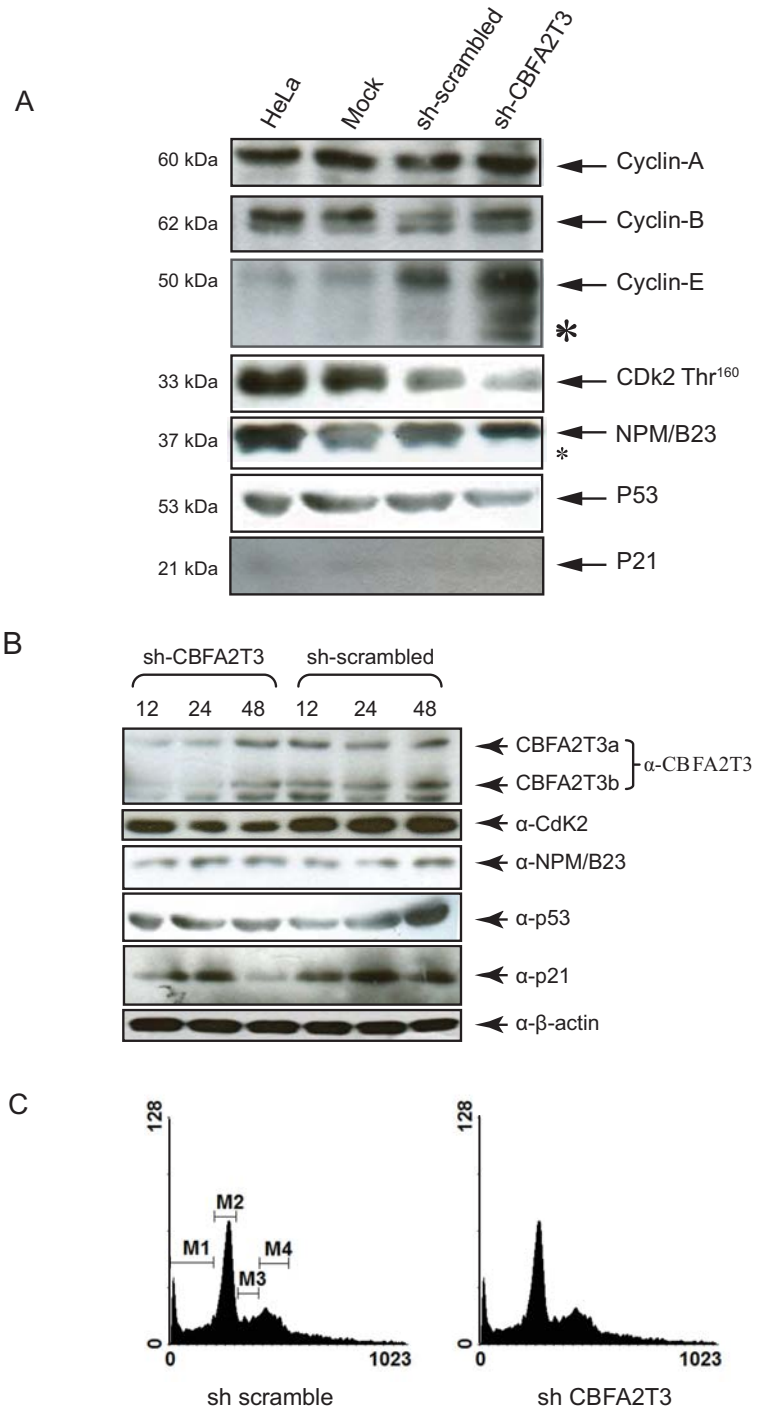

Figure 4.10. Effects of CBFA2T3 knockdown on different cellular proteins
A. HEK293T cells were treated with shCBFA2T3 and shscrambled for 24 hours. Equal amount of protein for each treatment was western blotted against di fferent cellular markers, indicated on the right side of each panel. **B.** Analysis of HeLa cell lysates post CBFA2T3 knockdowns for 24 and 48 hour treatment. **C.** Cells from sh-CBFA2T3 and sh-scramble treatment in HeLa were analysed by FACs 24 hour post treatment.

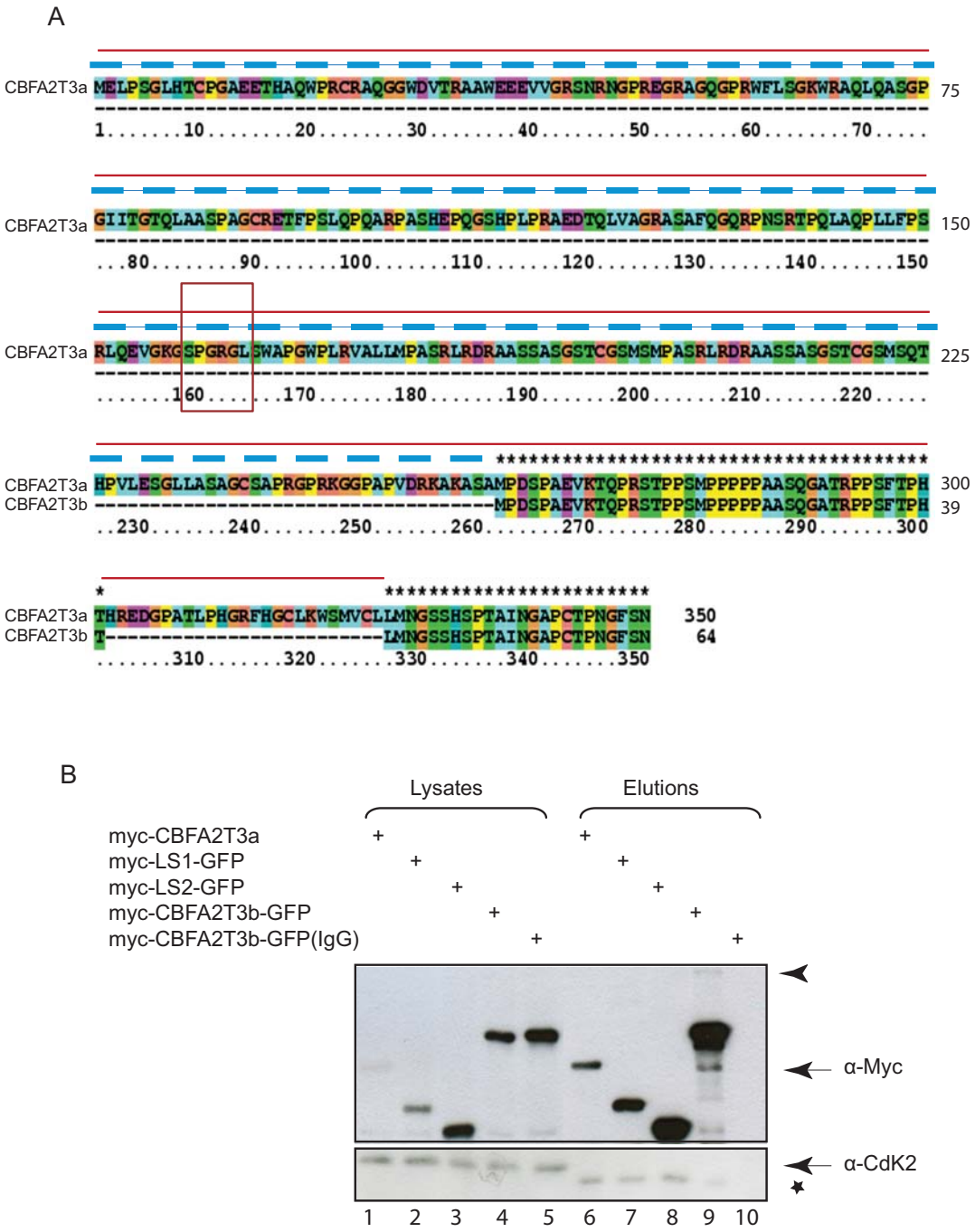

Figure 4.11. CBFA2T3 interaction with CdK2

A. Alignment of CBFA2T3a and b isoform from 1-350 aa. Red line markers sequence for LS1, while dashed blue line represent sequence for LS2. Boxed amino acids are the putative CdK2 binding site. **B.** Myc-CBFA2T3a full length, Myc-leader sequence-GFP and GFP-myc-CBFA2T3b constructs were overexpressed in HEK-293T cell line. Lysates from these transfections were subjected to immunoprecipitation with α-myc antibody and immunobloted against α-myc and α-CdK2 antibody. Arrow head points to the high molecular weight band often observed with CBFA2T3b IP lane, while asterik mark IgG.

(Takeda et al., 2001) (Fig 4.14 A red box). This putative bipartite motif for CDK2 (S/TPXR) also has a Cy motif (RXL) in the form of last three amino acids, while there are multiple Cy motifs also present in downstream sequence of CBFA2T3a which is similar to CBFA2T3b. HEK293T cells were transfected with respective DNA from different CBFA2T3 isoforms (Fig 4.11B). Lysates were immunoprecipitated with α-myc antibodies and western blotted with α-myc and α-CdK2 antibodies (Fig 4.11B). No interaction of CDK2 with CBFA2T3a and the N-terminus region of CBFA2T3a were found. These results might be due to low levels of CDK2 proteins and should be repeated along with a positive control to confirm the current findings. However, presence of high molecular size bands (as mentioned earlier for CBFA2T3 homo and hetrodimers) in lane 9 (upper panel) was worthy of note.

An increase in cyclin-E levels was observed after shRNA treatments, although the presence of low molecular weight bands was only observed in shCBFA2T3 lane. These lower bands may correspond to the low molecular weight isoforms of cyclin-E (Harwell et al., 2000; Porter & Keyomarsi, 2000) which are related to aggressive properties of cancer. Cyclin-A level was similar throughout treatments. The cell cycle profile for both shRNA treatments showed similar patterns (Fig 4.13 B) indicating that cells were at similar phase of the cell cycle. P53 levels remain unchanged, while at 48 hour time point level of p21 dropped in shCBFA2T3 treated cells as compared to shscrambled treatment (Fig 4.8 C). Further more, an increase in cell death was also noticed with the passage of time.

4.3.4 Increased centrosome numbers after CBFA2T3 knockdown are mature centrosomes and are not the results of centriole splitting

To confirm the observed amplification in centrosome number was due to the actual biogenesis of the daughter centrosomes, cells were stained with the antibody GT335. GT335 recognizes polyglutamylated α- or β-tubulin. α-tubulin is the major component of the daughter centrioles and these side chains are modified by poly-glutamylation to stabilize the centriolar microtubules (Bobinnec et al., 1998). Polyglutamylation of the tubulin only occurs when the daughter centriole reaches maturity. Cells stained with GT335 antibody for 24 hour following transfection of shRNA constructs revealed a similar increase in the centrosome number, as was observed when the cells were stained with α-γ-tubulin antibody after CBFA2T3 knockdown. Indeed the observed amplified centrosomes were actually mature centrosomes formed through complete centriole biogenesis and not the results of centrioles splitting (Fig 4.12A).

Further staining of cells expressing the LS1-EGFP fusion protein shows co-localization with the GT335 marker (Fig 4.12B). In the picture (Fig 4.12B Merged image, inset), the daughter centriole (arrowhead) biogenesis has initiated next to the mother centriole (arrow). The daughter centriole has not yet reached maturity, which is indicated by the lack of GT335 (red signal) on the daughter centriole. Only two red dots were seen with GT335, while in the LS1-EGFP (green) or merged panel there were two small green dots at right angle to the yellow signal (four green dots). This observation leads to the conclusion that CBFA2T3a initially localizes to the mother centriole, but is also present in procentrioles (seeds for daughter centriole formation). Its presence at newly formed procentrioles was observed even before procentrioles reaches maturity i.e negative for GT335.

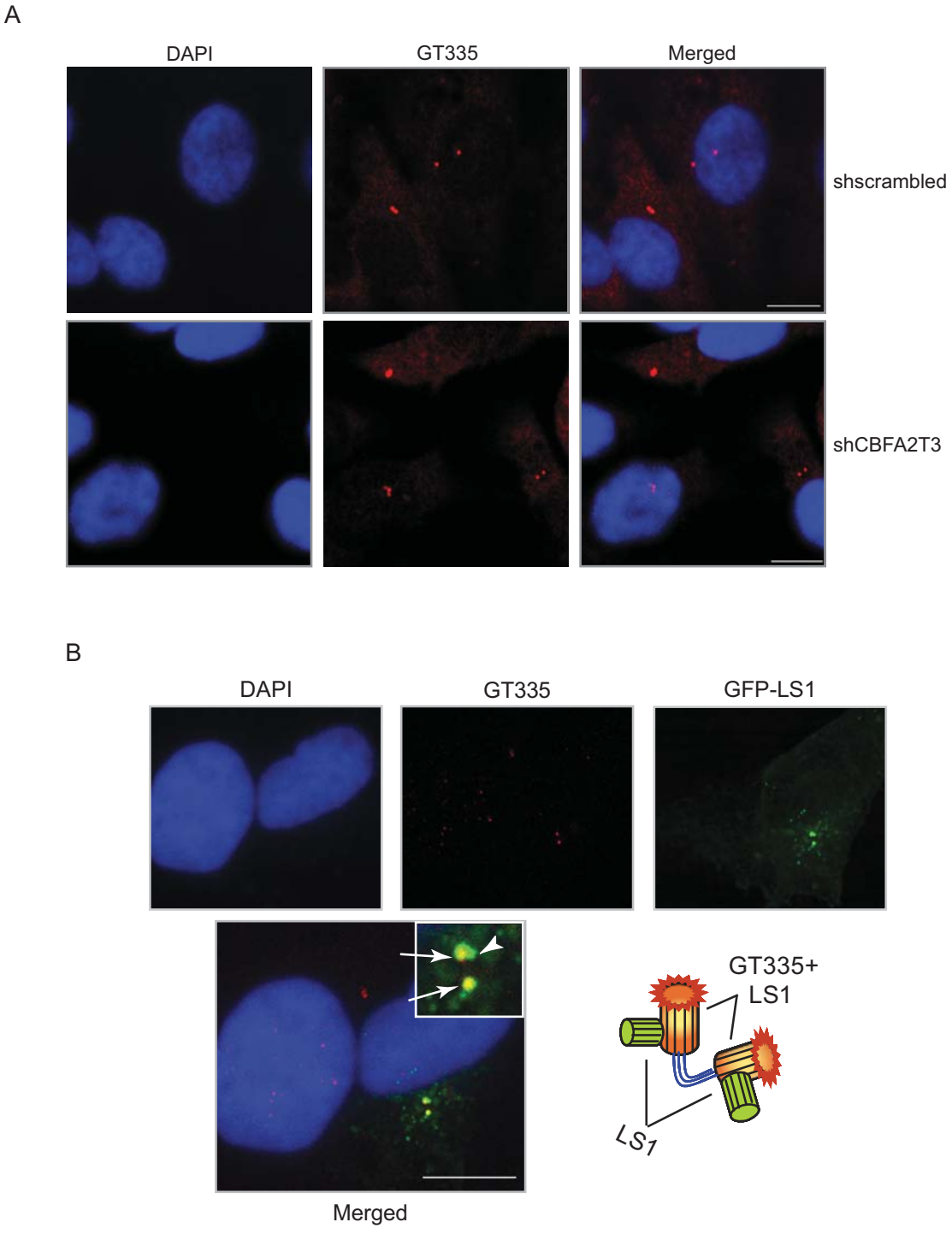

Figure 4.12. Observed amplified centrosomes are mature centrioles
A. HeLa cells transiently expressing sh-CBFA2T3 and sh-scrambled were stained with GT335 antibody. **B.** Flourescent images from cells expressing myc-LSI-GFP fusion stained with GT335 antibody. Arrow represents the mother centriole, arrow head indicates the formation of procentriole. Scale bar = 10 μm, inset = 5x zoomed.

4.3.5 CBFA2T3a co-localizes with Hs-SAS6 protein for centriole biogenesis.

To further validate that the observed centrosomal amplification following CBFA2T3 knockdown is related to actual centriole biogenesis, co-localization studies of LS1-EGFP were carried out with Hs-SAS6 protein. A recent report has shown that Hs-SAS6 presence on the mother centriole axis is necessary to start the formation of daughter centrioles (Strnad et al., 2007). Hs-SAS6 protein remains there (between mother and daughter centriole) until the procentrioles reaches maturity and become disengaged during late mitosis or early G1 (Kleylein-Sohn et al., 2007).

Centrosomes were stained with α-Hs-SAS6 and α-γ-tubulin antibodies 24 hours post shRNA transfection in U2OS cells. α-γ-tubulin was used to marker the centrosome numbers. It was noted that Hs-SAS6 co-localized with γ-tubulin to the multi-spots representing the abnormal centrosome Halo structure (Fig 4.13A). This co-localization was only observed in engaged centrioles (Fig 4.13A arrow head, closely associated centrioles (Kleylein-Sohn et al., 2007)) was clearly evident in the inset 1 of the merged image. These two proteins did not co-localize in disengaged or dispersed centrioles (Fig 4.13A arrow and lower inset, dissociated centrioles). The present results confirm that the multiple centrosomes observed following CBFA2T3 knockdown are mature centrosomes formed following complete centriole biogenesis.

Localization of CBFA2T3a with HsSAS6 protein was further investigated using overexpressed LS1-EGFP and endogenous HsSAS6 proteins during procentrioles formation. Co-staining of these two proteins has shown that LS1, used for its increased transfection efficiency, localized to the mother centriole (Fig 4.14A myc-LS1-EGFP),

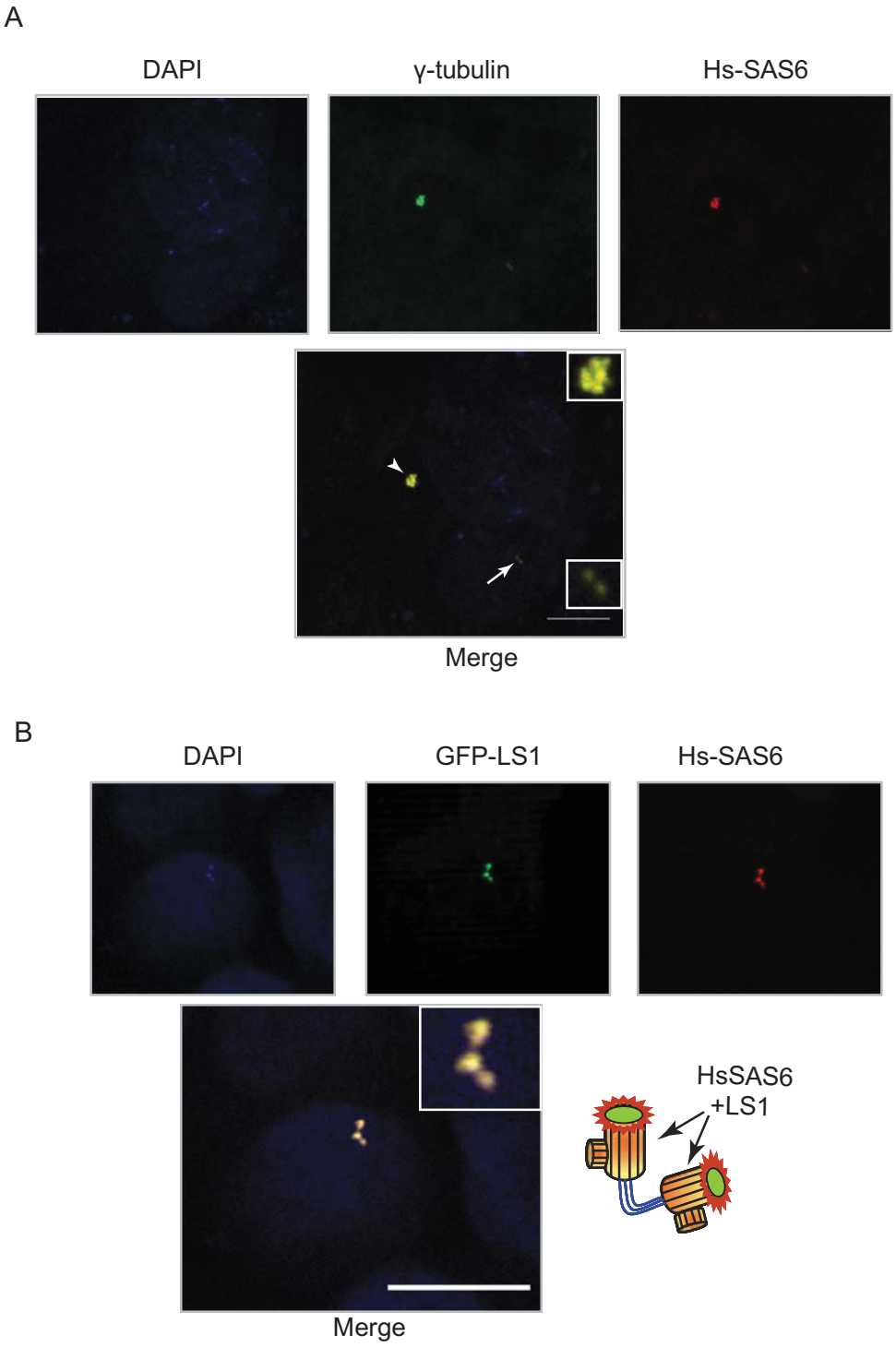

Figure 4.13. Colocalization Studies of CBFA2T3 and HsSAS6 proteins
A. shRNA construct for CBFA2T3 and scrambled were transiently overexpressed in U2OS cells. Cells were co-stained with α-HsSAS6 and α-γ-tubulin antibodies. Inset in the merged image (arrow head) represents a Halo structure, while the arrow marks the normal centrioles. **B.** myc-LS1-EGFP fusion was expressed in HeLa cell line and immunostained with α-HsSAS6 antibody. Green signal is from EGFP. Scale bar = 10 μm, inset is = 5x magnified.

while Hs-SAS6 is detected adjacent to the mother centriole surrounding the green signal. Localization of the LS1 to the parental and to the daughter centriole (Figs 4.12, 4.13 and 4.14) has indicated its potential critical role in centrosome biogenesis. This was further supported by co-localization of LS1 with HsSAS6, since HsSAS6 has a crucial role in centriole biogenesis, and the observed amplification of centrosomes post CBFA2T3 knockdown indicates the involvement of CBFA2T3a in centriole biogenesis.

4.3.6 Co-localization studies of CBFA2T3 proteins after shCBFA2T3 treatment

Experiments were carried out to determine if even a small amount of CBFA2T3a is still present on centrioles after CBFA2T3 knock down. HeLa cells were treated with shCBFA2T3 and shscrambled for 24 hours. Cells were co-stained with anti-CBFA2T3 RSH1 for the endogenous CBFA2T3 and anti-GT335 for marking centrosomes. CBFA2T3 protein levels were markedly down in cells treated with shCBFA2T3 compared to shscrambled or non-transfected cells. But still two CBFA2T3 dots were detected on the centrosomes (Fig 4.14B green), while in GT335 staining (Fig 4.14B red) three centrosomes were detected. These results have shown the limited availability of CBFA2T3a for the newly generated centrioles, while on the other hand showed the presence of previously transcribed CBFA2T3a to the parent centrosomes. Note that more back ground signal was seen in green channel due to the loose EGFP transcribed independently from other promoter along with shCBFA2T3 and shscrambled.

4.4 Discussion

In this study, CBFA2T3a, an isoform of CBFA2T3 was identified as a novel centrosomal protein. Localization and knock down studies with CBFA2T3 provided evidence to substantiate a role for CBFA2T3a in the centrosome duplication. *In silico*

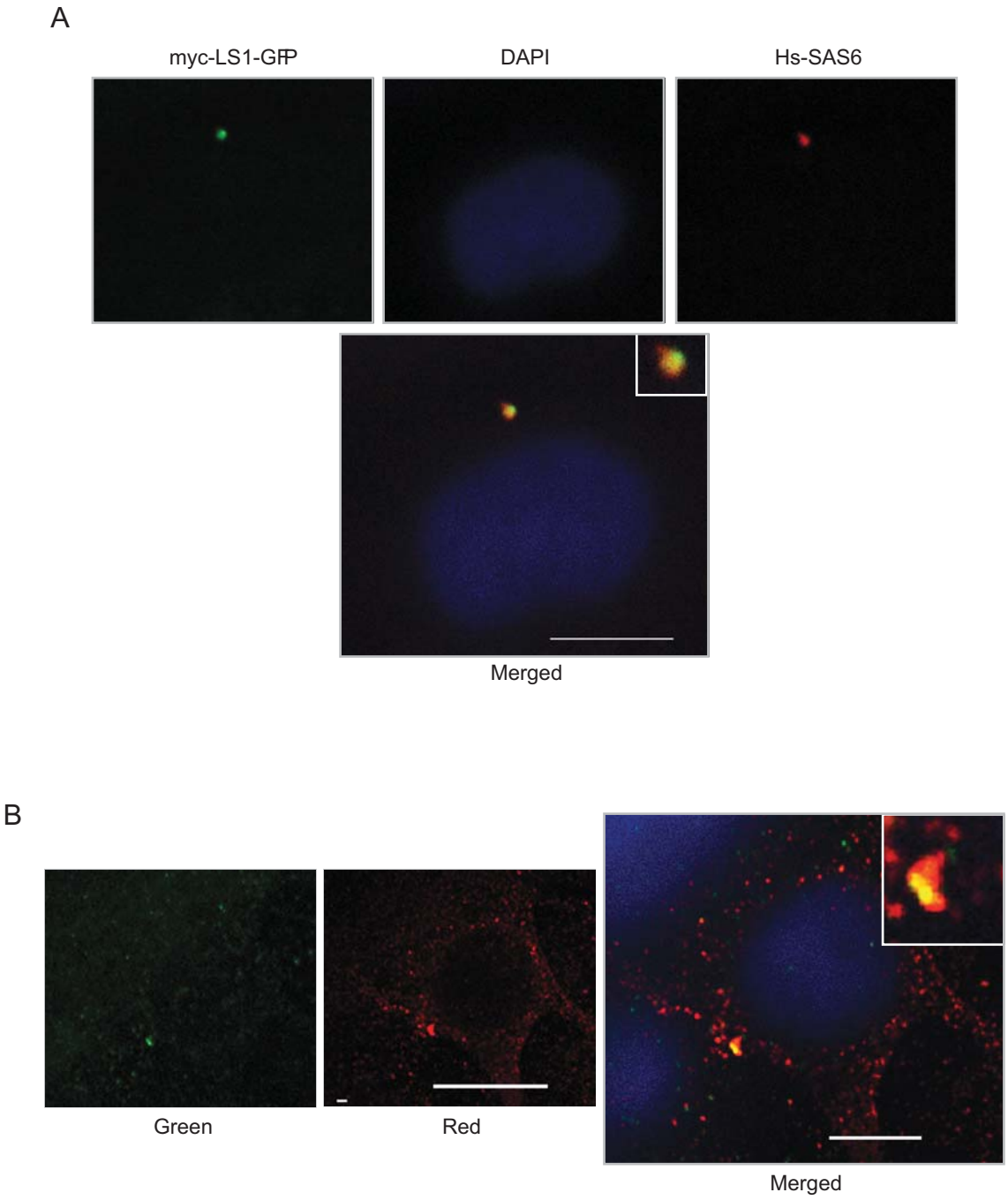

Figure 4.14. A. CBFA2T3a/LS1 colocalization with Hs-SAS6.
myc-LS1-GFP expressed in HeLa cells co-stained with Hs-SAS6 antibodies.
B. CBFA2T3 localization to centrosome after CBFA2T3 knockdown.
HeLa cells were co stained with α-CBFA2T3 and α-GT335 antibodies after sh-CBFA2T3 treatment for 24 hours. Different panels represents Green (CBFA2T3), red (GT335) and merged images. Scale bar = 10 μm.

analysis of CBFA2T3 proteins revealed differences in the N-terminus region between two isoforms "a" and "b". The extended CBFA2T3a isoform has an additional 261 amino acids to the CBFA2T3b isoform. The details of the differences in isoform sequences are discussed in Chapter 3 of this thesis. Analysis of the CBFA2T3a protein sequences in the N-terminus region has shown the presence of two putative NESs (Fig 4.15). The alignment of NESs identified in different tumour suppressor proteins is also shown in Fig 4.15. These NESs are related to CRM1 nuclear export activity (Fabbro & Henderson, 2003; Thompson et al., 2005). It has been shown that mutation or deletion of these NES sequences results in the retention of proteins in the nucleus (Kanno et al., 2007; Matsumoto & Maller, 2004). It should be noted that these putative NES sequences are only present in full length CBFA2T3a and in the LS1 and LS2 protein fragments. All these CBFA2T3a protein fragments exhibited cytoplasmic/centrosomal localization (Fig 4.4A), in contrast to the CBFA2T3b isoform which was localized in the nucleus (Fig 4.4A).

The CBFA2T3b isoform exhibited strong nuclear localization, which was presumably due to the presence of nuclear localization sequences (NLS) localized at amino acid 292-331 (Odaka et al., 2000). Although CBFA2T3a also has these NLSs, it is suggested that the N-terminal NESs are sufficient to localize the protein to the cytoplasm (Fig 4.4A). LS1 and LS2 both showed strong cytoplasmic localization and particularly to centrosomes. Both these leader sequence constructs from CBFA2T3a lack NLSs and have NESs. It is a common finding that most proteins with NESs also localize to the centrosomes (for example cyclin-E and BRCA1). In general a specific centrosome targeting sequences has not been described. Matsumoto et al. (2004) identified a 20 amino acid sequence for cyclin E protein that functions as a centrosomal localization

P53	340	**M F R E L N E A L E L K**	354
BRCA1	22	**L E C P I C L E L**	30
BRCA1	86	**L L K I I C A F Q L**	95
BRCA2	1382	**D L S D L T F L E V A**	1398
CBFA2T3a	141	**Q L A Q P L L F P S R L**	152
CBFA2T3a	171	**P L R V A L L M P A S R L**	184
Consensus		**L X1-3 L X2-3 L X L X**	

Figure 4.15 CBFA2T3a Putative nuclear export sequences
Comparison of putative nuclear export sequences in different known centrosomal proteins to that of CBFA2T3a N terminus. Residue critical for NES activity are indicated in red. (Kanno, Y et al: 2007; Fabbro, M et al: 2003).

sequence (CLS) (Matsumoto & Maller, 2004 207). Consensus CLSs for other proteins have not been found, but it has been noted that proteins having leucine-rich regions often localize to the centrosome. CBFA2T3a has two putative leucine-rich regions from amino acid sequences 141-152 and 171-184 that are not present in CBFA2T3b. CBFA2T3a localization studies have demonstrated that CBFA2T3a also localizes to the centrosome (Fig 4.4A and appendix 4.1).These localization findings were further supported by the results of immunoprecipitation (Fig 4.4B). Immunoprecipitation of different CBFA2T3a myc-EGFP fusion proteins demonstrated an interaction of CBFA2T3a with γ-tubulin, a centrosomal protein which is the part of γ-TuRC complexes. It was found that the CBFA2T3a full length and leader sequence fragments LS1 and LS2 both co-immunoprecipitated with the centrosomal γ-tubulin, which was evident from the presence of γ-tubulin band of 48 KDa in immunoprecipitated fractions (Fig 4.4 B). Further, analysis of glycerol gradient fractions has confirmed that CBFA2T3a and γ-tubulin proteins were found in centrosomal fractions, while CBFA2T3b was confined to fractions having nuclear proteins (Dr Kumar's unpublished data). The results from immunoflorescent studies and immunoprecipitation (Section 4.3.2) confirm that CBFA2T3a is localized to the centrosome and associates with centrosomal γ-tubulin complexes. This evidence strongly implicates CBFA2T3a as a centrosomal protein.

The role of CBFA2T3a in centrosome structure or function was further investigated by using CBFA2T3 specific shRNAs to knock down these proteins in different cell lines. One previously reported (Goardon et al., 2006) and two other independent shRNA's were used during the current study. As these shRNAs can knockdown both CBFA2T3 isoforms, CBFA2T3 knockdown experiments were carried out in cell lines having

minimum level of CBFA2T3b isoform expression. A two fold decrease in CBFA2T3 proteins and mRNA level was observed post transfection of shRNA constructs, compared to treatment of cells with shscrambled (Fig 4.5A and B). It was noted that longer exposure to shCBFA2T3 resulted in an increase in cell death. Attempts were made to generate a stable CBFA2T3 knockdown cell line. However, cells selected after retroviral transduction of CBFA2T3 shRNA constructs did not survive (D F Callen unpublished data). To confirm these results one approach would be to generate CBFA2T3a specific siRNAs, however this may be difficult due to the high homology among the two isoforms which limits the sequence available to design the siRNAs.

The present study demonstrates an increase in centrosome number when CBFA2T3 proteins were knocked down in cells compared to the cells treated with the scrambled control. A significant increase in the cell population with more then two centrosomes was observed following CBFA2T3 knock down (Fig 4.6A). A similar increase in centrosome number was observed when the effect of endogenous BRCA1 was blocked either by siRNA or BIF peptide (Sankaran et al., 2006) in human mammary epithelial cells. In addition, it is reported that abnormal centrosome number is also related to the p53 protein, as p53 plays a role in centrosome duplication control (Shinmura et al., 2007). p53 directly control CDK2/cyclin E levels through its target p21 (Mantel et al., 1999). Since centrosomal amplification is p53 dependent, a normal p53 function is required for normal centrosome duplication. Keeping this in mind, CBFA2T3 knockdown experiments were repeated in three different cell lines, HEK293T with p53 under SV40-T antigen control, HeLa having normal but low expression of p53 (ATCC data sheet), U2OS cells with wild type p53. Centrosomal amplification was observed in all cell lines independent of the p53 status (Fig 4.7A). Level of p53 and p21 were

monitored in these cell lines after CBFA2T3 knock down. No significant change at protein level was observed for p53, while p21 was not detected after CBFA2T3 knockdown (Figure 4.10A and B). These facts further supported the notion that there is an intrinsic control of centrosome duplication within the centrosome. It is possible that CBFA2T3a itself is that control, or may have a role in this control.

Effects of CBFA2T3 knock down on different cell cycle regulatory proteins were also investigated. Analysis of cell lysates prepared post shRNA treatments for different cellular proteins showed changes in some of the known markers for centrosome duplication. Western blot with α-B23 revealed a change in B23 status (Fig 4.10A and B). A single band was observed in shCBFA2T3 treated cells, while shscrambled and mock treatment B23 protein appears as two bands (Fig 4.10A). B23 is a multimeric protein having two isoforms, B23.1 and B23.2. These two isoforms change their localization and dimer forming characteristics upon various post translational modifications, like phosphorylation. B23.1 is phosphorylated by cyclin B, which results in loss of the RNA binding property during mitosis, and as a consequence of this phosphorylated B23 protein disperses throughout the cytoplasm (Okuwaki et al., 2002).

Localization of B23 to the middle region of both centrioles is crucial for centrosome duplication. Its association with the centriole prevents centrosome duplication (Okuda et al., 2000). B23 disassociates from the centriole upon phosphorylation by CDK2/cyclin E complexes on Thr-^{199} (Okuda et al., 2000; Tokuyama et al., 2001). A predominant change in localization of the B23 protein was seen after CBFA2T3 knock down (Fig 4.9B). Due to nonavailability of phospho specific antibodies it was not possible to state that the change in status of B23 was specifically due to its phosphorylation at Thr-^{199}, S^{4}

(Zhang et al., 2004) or on any other reported sites although localization data (Fig 4.12 B) has indicated a change in its localization which was previously known to be linked with Thr-^{199} phosphorylation (Tarapore et al., 2006). However a change in CDK2 activation status was also evident from the western blot with a anti-CDK2 antibody. CDK2 activity is dependent on phosphorylation on Thr-^{160}, which corresponds to a faster migrating band on a gel blotted with CDK2 antibody (Ukomadu & Dutta, 2003). The increase in CDK2 activity seen in shCBFA2T3 cell lysates in the present study is consistent with the previous findings.

Cell cycle analysis of these shRNA treated cells was crucial to identify changes in normal cell cycle profile which were responsible for the observed centrosomal amplification. Cell cycle profile showed a similarity in cell cycle pattern of the shCBFA2T3 and shscrambled treated cells. More than 30% of cells in both treatments were in the G1 phase of the cell cycle. No significant difference in cell populations for the G1/S phase of the cell cycle was observed between the two treatments. Overall, the cell cycle profile for shCBFA2T3 and shscrambled were similar (Fig 4.10C). No blockage of the cell cycle was observed at any stage. It is already known that prolonged blockage of cells in G1/S phase transition results in centrosomal amplification. The results from the present study support the idea that CBFA2T3 knock down effects on the centrosome are not due to other cellular events related to the cell cycle, but are the direct effect of knock down of the proteins of both isoforms. It is possible that the CBFA2T3a isoform has some controlling role in normal centriole biogenesis and that CBFA2T3a loss resulted in the observed abnormal centriole biogenesis.

Co-localization studies of CBFA2T3a/LS1 with various centrosomal proteins were also carried out during this study. LS1-EGFP colocalizes with the HsSAS6 protein which has a crucial role in centriole biogenesis (Strnad et al., 2007). During normal centriole biogenesis a single daughter centriole is formed next to the mother centriole. Thus the increase in centrosome number is related to the generation of multiple procentrioles on the single mother centriole. Recent reports have shown that the PLK4 kinase initiates the formation of this procentriole on a marked site on the axis of the mother centriole (Duensing et al., 2007; Kleylein-Sohn et al., 2007). Subsequent steps involve the recruitment of Hs-SAS6 and other proteins to assemble γ-TuRC complexes along with other members to form a complete daughter centriole. Indeed overexpression of the PLK4 protein has been shown to induce the formation of multiple centrioles on the nascent mother centriole (Habedanck et al., 2005). In the present study CBFA2T3a LS1 co-localization with Hs-SAS6 showed that these two proteins are adjacent to each other (Fig 4.13B). Hs-SAS6 protein is actually covering the EGFP signal from LS1 (Fig 4.14A). Moreover biogenesis of multiple centrioles on the mother centriole induced by CBFA2T3 knockdown shows Hs-SAS6 presence in the multiple centrioles in the cells with engaged centrioles (Fig 4.13A arrow head), while no Hs-SAS6 signal was detected in cells having dispersed or disengaged centrioles (Fig 4.13A arrow). This observation was consistent with the previously published results (Kleylein-Sohn et al., 2007; Strnad et al., 2007). It was also reported that PLK4 and Hs-SAS6 overexpression induces multiple seeds for procentriole formation on the mother centriole (Kleylein-Sohn et al., 2007).

In summary the results of this study showed CBFA2T3a localization to the centrosome, and its interaction with γ-tubulin particularly centrosomal γ-tubulin. The present study

has demonstrated that CBFA2T3 knock down can also induce the formation of multiple centrioles on the nascent mother centriole. The shRNA experiments have shown an increase in the centrosome number. In addition to centrosome amplification, effects were also observed on different cell cycle regulatory proteins having a role in the centrosomal duplication cycle. Keeping in mind that CBFA2T3 is a transcription co-repressor (Kochetkova et al., 2002), likelihood remains that CBFA2T3b or CBFA2T3a might be part of the E2F transcription regulation machinery. E2F is involved in cyclin E and CDK2 up-regulation (Morris et al., 2000). Up-regulated levels of cyclin E–CDK2 complexes facilitate the repetition of the centrosomal duplication cycle without DNA replication. Up-regulation of cyclin-E/CDK2 was also observed during the present study. In contrast no change was observed in cell cycle profile. Thus the results support the idea that CBFA2T3a is probably the substrate involved in the formation of the procentrioles on the mother centriole or have a controlling role in daughter centriole formation. It is possible that changes in CBFA2T3a levels might facilitate the formation of the seeds for centriole biogenesis. There is still a need to further investigate a possible role of CBFA2T3 with E2F transcription regulation.

Chapter 5 – Expression analysis of CBFA2T3 proteins in breast tumour sections

5.1 Introduction:

Breast cancer is a complex disease, characterized by heterogeneity of the cancer cells with genetic changes. These genetic alterations lead to the development of aggressive forms of breast cancer having a greater potential for metastasis to distant organs (Loeb, 2001). To date several different clinical and pathological markers have been used to determine tumour stage and prognosis. In addition to those conventional markers (age, tumour size, tumour grade, node involvement), different hormone receptor markers (ER and PR) and HER-2 status are also used for tumour characterization and to predict response to treatment. Involvement of hormone in the development of tumour phenotype is well known now. Tumour progression is thought to follow a path of hormone dependent type to hormone independent type (Khan et al., 1998).

Breast tumours can be characterized into four distinct hormonal molecular phenotypes on the basis of gene expression microarray data, which includes Luminal A, Luminal B, HER-2 type and Basal type (Perou et al., 1999; Sorlie et al., 2001; Sorlie et al., 2003). Lately it has been shown that these molecularly defined phenotypes showed significant prevalence in different types of breast tumours (Tamimi et al., 2008). Breast tumours of the luminal A type are frequently observed in invasive cancers, while HER-2 type tumours are frequently prevalent in DCIS tumours and basal type phenotypes are more prevalent in invasive tumours. Mostly high grade DCIS or invasive tumours were HER-

2 type and basal like tumours as compared to low or intermediate grade tumours (Tamimi et al., 2008).

LOH is a major event detected in sporadic cancers. LOH of specific chromosome regions is associated with cancers. LOH on 16q24.3 was reported in several cancer types including breast cancer (Cleton-Jansen et al., 2001; Sato et al., 1998). Melchor, et.al (2007) have recently investigated the frequency of 16q loss in sporadic and familial breast tumours (Melchor et al., 2007). The role of estrogen receptor in development of particular tumour pathways was determined among familial and sporadic breast lesions by using CGH technique. Distinct genetic alterations were found in ER^+ or ER^- tumours irrespective of the BRAC1 and BRAC2 status. 16q loss was the classical alteration found in ER^+ tumours that were typically low grade tumours, while ER^- tumours present several genomic aberrations such as 3p25.3-p21.3, -5q, -12q14-q15 and -12q23.1-q23.31 (Melchor et al., 2007).

CBFA2T3 was identified as a breast tumour suppressor gene from chromosome region 16q24.3 (Kochetkova et al., 2002). Aberrant loss of *CBFA2T3* expression was found by RNA *in-situ* hybridization in breast tumours while normal epithelial lining of breast ducts retain *CBFA2T3* expression. CBFA2T3 function as transcriptional corepressor. ZNF652, a novel zinc finger protein, was identified as a partner of CBFA2T3 transcriptional repressor complexes. Low expression of ZNF652 is reported in primary tumours and cancer cell lines. A role for ZNF652-CBFA2T3 complexes has been shown in breast cancer oncogenesis (Kumar et al., 2006). Down regulation of ZNF652 expression was also reported in breast tumour specimens and breast cancer cell lines (Kumar et al., 2008; Kumar et al., 2006).

The present study was designed to determine the expression of CBFA2T3 and ZNF652 proteins in different breast tumour phenotypes. Initial studies were carried out on both proteins but due to the shortage of the resources the final experiment was only completed on the CBFA2T3 protein. In order to evaluate CBFA2T3 as a prognostic marker, the expression data of CBFA2T3 was analysed to determine any association with known clinical and pathological markers.

5.2 Materials and Methods

5.2.1 Materials

Anti-CBFA2T3 antibody PEP3 was raised and purified against the C-terminus sequence of CBFA2T3 proteins by Bethyl laboratories USA, while anti-CBFA2T3-RSH1 and anti-ZNF652-RSH9 was available in-house (details in Chapter 2 General Material and Methods). 3,3'-diaminobenzidine tetra hydrochloride (DAB) was purchased from Sigma chemical Co. Streptavidin-HRP conjugated complexes, biotinylated goat anti-rabbit IgG secondary antibody or anti-mouse IgG secondary antibody were from Dako Scientific Inc.

5.2.2 Patients and Tissue Samples

Use of various human tissues for immunohistochemistry was approved by the Human Ethics Committee of the Royal Adelaide Hospital. Optimization of immunohistochemistry with anti-CBFA2T3 and anti-ZNF652 antibodies were undertaken on normal or benign sections of formalin fixed paraffin embedded breast tissues provided by Pathology Laboratories, Institute of Medicine and Veterinary Sciences (IMVS) Adelaide. Subsequently three independent breast tumour tissue microarray (TMA) sections were used for expression studies. TMA, from Melbourne Tissue Bank (a cohort of 30 tumours), a Test TMA from Garvan Institute Sydney (a cohort of 31 tumours) and TMA BR701 (a cohort of 70 patients) was purchased from US Biomax, USA. The clinical details available were from pathology reports. Some samples were excluded from analysis due to unavailability of some clinical data.

5.2.3 Optimization of different buffer conditions for antigen retrieval

Initial experiments were carried out to determine anti-CBFA2T3 antibody reactivity on formalin fixed, paraffin embedded tissue sections. Data from initial experiments demonstrated that tissue staining using anti-CBFA2T3 antibodies required antigen retrieval by either microwave or by pressure cooker treatment. Microwave was used in all subsequent experiments due to ease of the use and greater reliability. To determine the best buffers for antigen retrieval, two different dilutions of different buffers were used (details given in results).

5.2.4 Antibody specificity in tumour sections

Specificities of all CBFA2T3 antibodies on western blot are shown in Chapter 3 (Fig 3.3). The specificity of the PEP3 antibody was determined by peptide competition. Equal amount of antibody was competed with increasing concentrations of the peptide immunogen (10×, 20× and 40×) against which it was raised for 3 hour at room temperature before use in immunohistochemistry. Competed peptide, along with anti-CBFA2T3 (PEP3) antibody was then used to stain normal breast tissue sections after antigen retrieval. Detail procedure for immuno histochemical staining will be given in the following sections.

5.2.5 Immunohistochemical staining of breast tissue

4μm sections freshly cut sections from archival formalin-fixed paraffin embedded breast tissue were mounted on Histogrip coated slides. Sections were then baked for 2-3 hours or overnight at 50-60^{0}C, and then were deparaffinised in xylene (3×), dehydrated with absolute ethanol (3×) and washed three times with 1×PBS for 5 min each. Endogenous peroxidase was blocked by 0.3% H_2O_2 in PBS for 5 min. Sections were further washed

by 1×PBS three times for 5 min each. Initial experiments were conducted to compare antigen retrieval using Dako low pH buffer, Dako high pH buffer, Citrate buffer pH6.5 and 1mM EDTA buffer. Subsequently 1mM EDTA pH 8.0 buffer was used for all immunohistochemistry experiments with anti-CBFA2T3 antibody. 1mM EDTA pH 8.0 was prepared fresh or either checked for pH. Antigen retrieval was by microwaving slides in 1mMEDTA pH 8.0 buffer at 4 min 900 W, 20 min 350 W followed by three washes with PBS. Sections were incubated with 5% goat serum in order to block the nonspecific binding of antibody. The sections were incubated overnight at 4^0C with a 1:150 dilution of the PEP3 anti-CBFA2T3 antibody in a humid chamber followed by biotinylated anti-rabbit IgG secondary antibody (1/400, 2 hr RT, Dako) and peroxidase conjugated streptavidin (1/500, 1 hr RT, Dako), 10 min incubation with 3,39-diaminobenzidine tetrahydrochloride (DAB) containing 10mM of Imidazole per ml. Note that each step was followed by 3× washes of 5 minute each with 1×PBS. Tissue was then counterstained with weak (1:10) Lillie-Mayer's haematoxylin 2-3 minutes, washed with water, dehydrated through graded alcohol and cleared by xylene, and mounted in DPX.

5.2.6 Evaluation of the staining and scoring method

For the assessment of positive staining, tissue sections from normal breast or benign tumour sections were included with the breast cancer tissues as a positive control in all experiments. In addition, a negative control, where the section was stained with normal rabbit IgG or pre-immune serum of the same concentration as the polyclonal antibody, was also included. Images were captured either by *Video-pro* soft ware by Leading edge Adelaide or a Nano-zoomer Digital imaging system by Hamamatsu Co. Japan. Scanning of the individual cores was carried out with the help of NDP.view computer assisted

program provided with the Nano-zoomer. CBFA2T3 immuno reactivity was assessed separately in the nucleus and cytoplasm of the cancer and normal duct epithelial cells by scoring the percentage of cells with each of the staining categories on a scale of +++ (very dark staining), ++, + (moderate to week) and 0 (absence of staining). For the majority of sections 200-300 cells or more were scored per tumour section. The clinical and marker data of the breast cancer samples were provided by the suppliers of the TMAs. Tumours were categorized as having high CBFA2T3 positive if 70% (+++, ++ and + all) positive staining or negative having ≥ 30% cells with negative CBFA2T3 expression. Scoring of the CBFA2T3 positivity was then assessed by a second independent person.

CBFA2T3 cytoplasmic staining was also assessed to analyse CBFA2T3a expression with the known tumour markers as CBFA2T3a localized to cytoplasm only. Cytoplasmic staining was assessed either positive or negative as CBFA2T3 immuno-reactivity in the cytoplasm was found uniform through out the population of a tumour sample.

5.2.7 Statistical analysis

Statistical analysis for the BR701 TMA was performed by Dr Carmela Ricciardelli using SSPS 13 for windows software (SSPS Inc, Chicago, IL) Pearson Chi square or Fisher's exact tests were performed to determine the relationship between different clinical markers and CBFA2T3 expression. The p value <0.05 was used to assess the significance.

5.2.8 Immunofluorescence (γ-tubulin) and immunohistochemical (CBFA2T3) studies on BR701 TMA

Deparaffinised and dehydrated tumour sections were immersed in -20^{0}C cold methanol for 8 minutes. Samples were then processed for endogenous peroxidase quenching and antigen retrieval as described in section 5.2.4. Samples were then blocked with 5% goat serum for 30 minutes and treated with primary antibodies (1/100 rabbit polyclonal PEP3 anti-CBFA2T3 and 1/300 mouse monoclonal anti-γ-tubulin antibodies0 in 1% goat serum in humid chamber for 24 hour at 4^{0}C. 3× washes were given with 1×PBS on the following day. Sections were then subjected to secondary antibodies (biotinylated anti-rabbit IgG secondary antibody (1/400) and anti mouse-Alexa-fluor 594 (1/300) in 1% goat serum for 2 hr at RT. This was followed by 3× wash with 1×PBS and incubation with peroxidase conjugated streptavidin (1/500, 1 hr RT), 10 min incubation with 3, 39-diaminobenzidine tetrahydrochloride (DAB) containing 10mM of Imidazole per ml. slides were washed, dehydrated through graded alcohol and cleared by xylene, and mounted in VECTASHIELD mounting media with DAPI for staining nuclei. CBFA2T3 expression was assessed by taking images with Nano zoomer imaging system, while Laser scan confocal microscopy was carried out to take images for fluorescent labelled γ-tubulin as centrosomal marker.

5.3 Results

5.3.1 Optimization of conditions for antigen retrieval and antibodies

In order to screen for the best staining results different antigen retrieval buffers were investigated in this study. Details of all buffers and respective antibody dilutions are given in (Table 5.1). CBFA2T3 protein immuno reactivity with PEP3 antibody was graded from negative to positive depending upon the intensity of the staining. It was found that RSH1 antibody gave a good staining with citrate and EDTA buffer, while no signal was detected with Dako low PH and high PH antigen retrieval buffers. On the other hand α-CBFA2T3 PEP3 antibody gave a strong immuno-reactive staining with the EDTA buffer when imadazol was used along with DAB. In contrast sufficient to moderate staining was noticed with out imadazol. A further improvement in signal intensities was found when PEP3 was used at 1/150 rather then at 1/250 dilution of PEP3 antibody. For all subsequent experiments, PEP3 antibody with these conditions was used. For the α-ZNF652 antibody RSH9 the best results were obtained with 1:200 dilution using EDTA buffer PH 8.0 for antigen retrieval.

5.3.2 Assessment of anti-CBFA2T3 (PEP3) antibody specificity

Tissue sections from normal breast or benign tumour sections were stained with PEP3 antibody. Images from normal breast ducts are presented in Fig 5.1A. CBFA2T3 nuclear staining was found highly variable, ranging from cells with strong signal intensities to moderately expressing cells and to even cells with no overall expression of nuclear CBFA2T3 in the same mammary duct. Normally 70-80% of the epithelial cells of the normal breast ducts express high level of CBFA2T3 nuclear protein, scored as +++. The remaining 20-25% cells showed lower expression of nuclear CBFA2T3

Table 5.1. Assesment of antibody sensitivity and retrivel solutions.

Antibodies Concentrations	Buffer used for Antigen Retrival			
	Citrate (PH6.5)	EDTA (PH8.0)	Dako low PH	Dako high PH
CBFA2T3				
RSH1 (1:100)	+	+	-	-
(1:200)	+/-	+/-	-	-
PEP3 (1:150)	+	++	-	-
+Imadazol	+	+++	-	-
(1:250)	+/-	+	-	-
+Imadazol	+	+	-	-
ZNF652				
RSH9 (1:200)	++	+++	+	++

\+ = Sufficient staining

++ = Good staining

+++ = Strong staining

\- = No signal

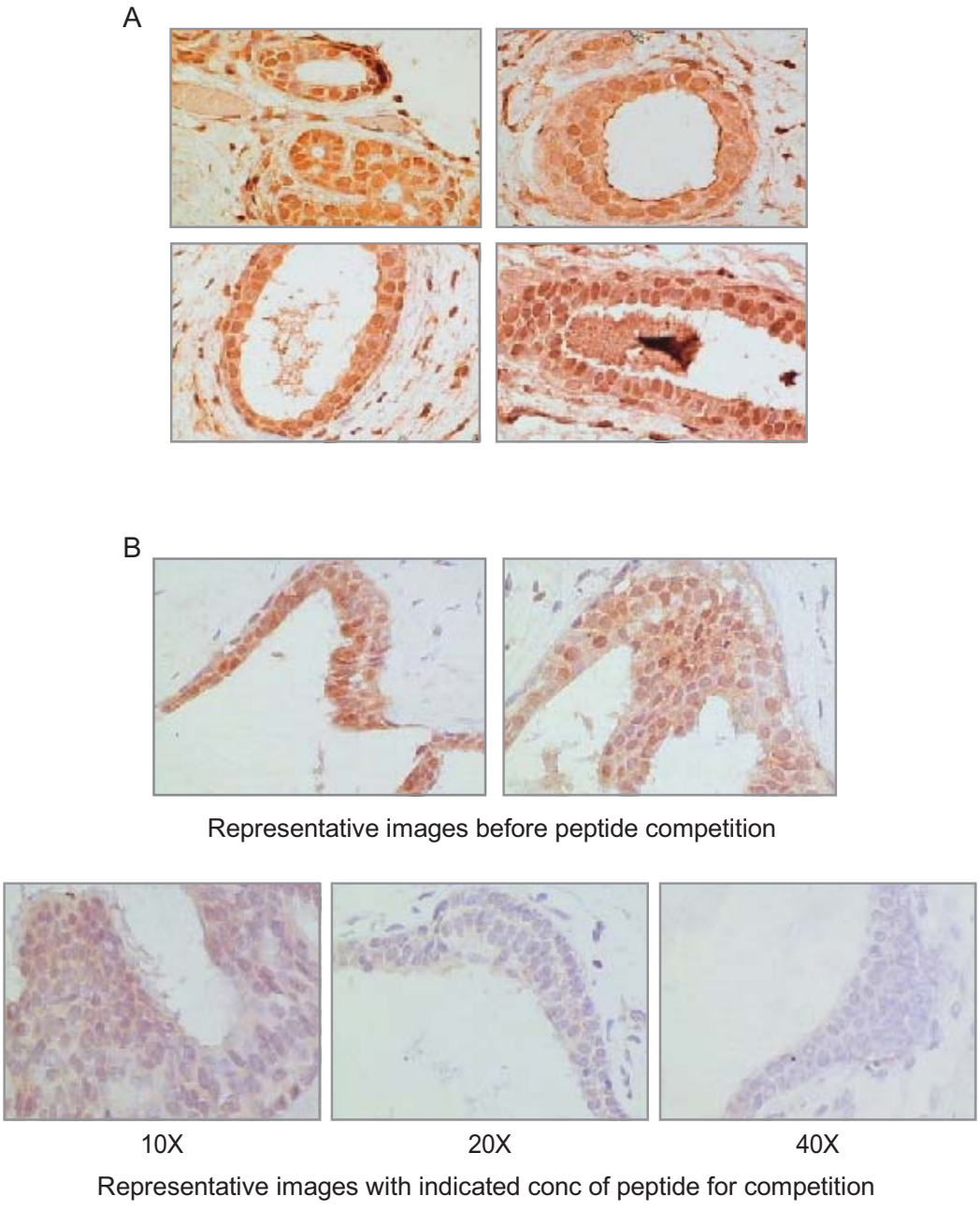

Figure 5.1. CBFA2T3 antibody specifically detects CBFA2T3 proteins in tumour sections **A.** Representative images of normal mammary ducts stained with PEP3 antibody. A slight variation in intensity of the stain (as evident from the panel) was observed from experiment to experiment. **B.** PEP3 antibody was competed against an increasing concentration of peptide against which it was raised. Fig B represents the images stained with PEP3 antibody before and after the peptide competition. Images were taken at 40X lense power.

protein. A small proportion (< 4%) of the total epithelial cells was negative for CBFA2T3 expression in the nucleus.

Specificity of the anti-CBFA2T3 PEP3 antibody in tissue sections was assessed by a competition experiment, performed by using the peptide against which the antibody was raised. Competed and non-competed antibodies were used subsequently for staining. A decrease in signal intensity with the increasing concentration of peptide used was observed for CBFA2T3 immuno-reactivity (Fig 5.1B). No signal was detected with 40×conc of peptide, while a very weak cytoplasmic staining was only detectable with 20× conc. Current data shows that the observed staining was due to the immuno reactivity of CBFA2T3 protein with antibody. When antibody was competed with the immunogen used to raise the antibody the loss of immuno-reactivity was noticed inside the cells of breast tissue sections, hence proving that the detected staining is specific for the CBFA2T3 proteins.

5.3.3 CBFA2T3 expression analysis in TMAs from Garvan institute Sydney and Melbourne Tissue Bank

Expression of CBFA2T3 proteins were assessed among a panel of breast cancer and some normal breast sections. TMA was acquired from Garvan Institute Sydney for staining with anti-CBFA2T3 antibody containing the tumour and normal breast tissues (4 cores for each patient). Similarly a small cohort of breast tumour sections, comprising of 16 patients (2 cores for each patient), was sourced from Melbourne Tissue Bank and stained with CBFA2T3 antibody. Four cases of normal breast tissues were also stained. Samples were scored for staining intensity, of the CBFA2T3 antibody

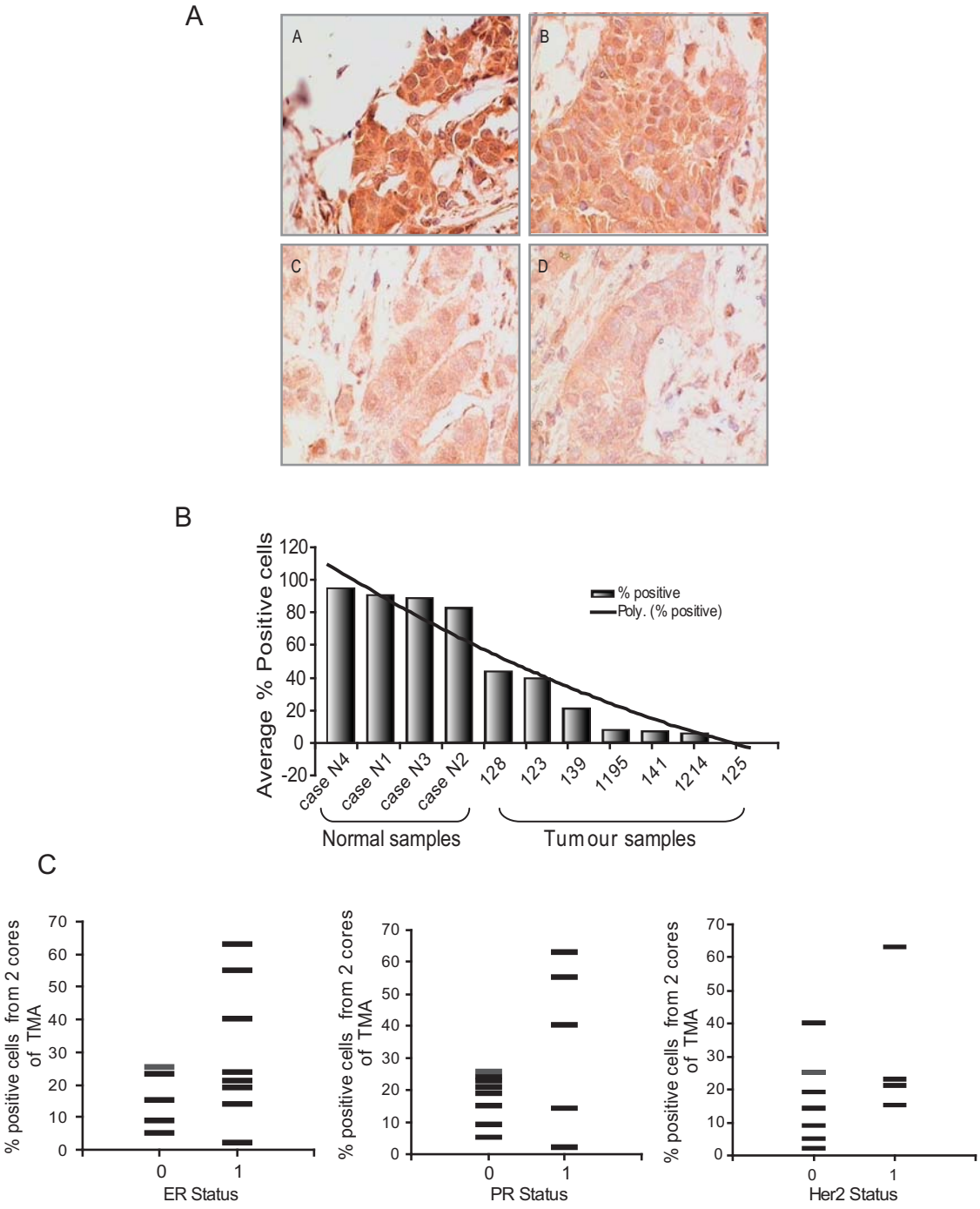

Figure 5.2 CBFA2T3 expression among tissues from Breast Tumours.
A. Representative images from breast tumour TMA from Garvan Institute stained with anti-CBFA2T3 PEP3 antibody. **B.** Graphic presentation of average +++, ++ and + % positive cells for CBFA2T3 nuclear staining. **C.** Graphical presentation of CBFA2T3 % positivity for each tumour verses harmonal status for that tumour form Melbourne Tissue Bank TMA. Value 0 and 1 along x-axis represents negative and positive hormonal status.

immuno-reactivity in these sections compared to normal breast sections. The criteria of scoring (cut off values for CBFA2T3) were kept similar for both TMA. Few selected images from tumours with high and low levels of CBFA2T3 expression were presented in Fig 5.2A. CBFA2T3 positivity in terms of % cells with +++, ++ and + expression (average of 4 cores) for each patient of breast cancer TMA from Garvan Institute Sydney was plotted (Fig 5.2B). CBFA2T3 expression (% positive cells) was found reduced in tumour samples (ranging from 0-45%) as compared to the normal ducts (85-100%) from control breast sections. Similar trend was also observed among breast tumour sections from Melbourne TMA. Graphical presentations of CBFA2T3 % positivity from Melbourne TMA against hormonal status of the patient were given here (Fig 5.2C). The ER^- tumours were found to have less then 30% CBFA2T3 positive cells. In contrast ER^+ tumours have variable CBFA2T3 expression from 15% to 65% in terms of CBFA2T3 expressing cells. These differences in CBFA2T3 expression among ER^+ and ER^- tumours are statistically significant, (Student *t-test*, p= 0.048* two tailed). No significant difference was observed with the PR and HER-2 status.

The data from Garvan TMA could not be meaningfully analysed due to the small number of samples. However it is presented in the form of a table (Fig 5.3C).

5.3.4 ZNF652 expression analysis in a test TMA from Garvan institute Sydney

A TMA from Garvan Institute Sydney was stained with anti-ZNF652 antibody RSH9. The TMA comprised 2 cores each from 18 patients. Four tissue sections from normal breast were also stained with RSH9 as positive control. ZNF652 expression was found high in 90-95% of the cells from normal breast ducts (Fig 5.3A upper panel A and B),

A

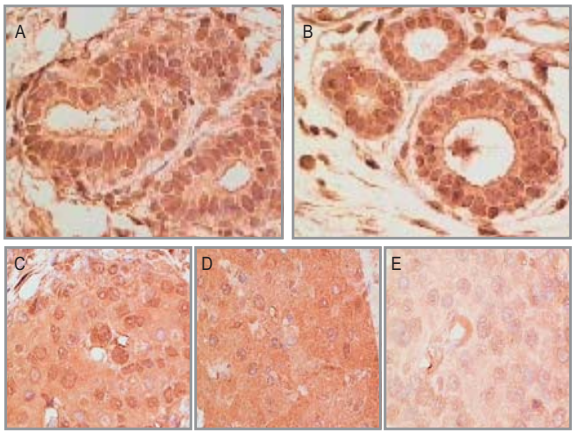

B

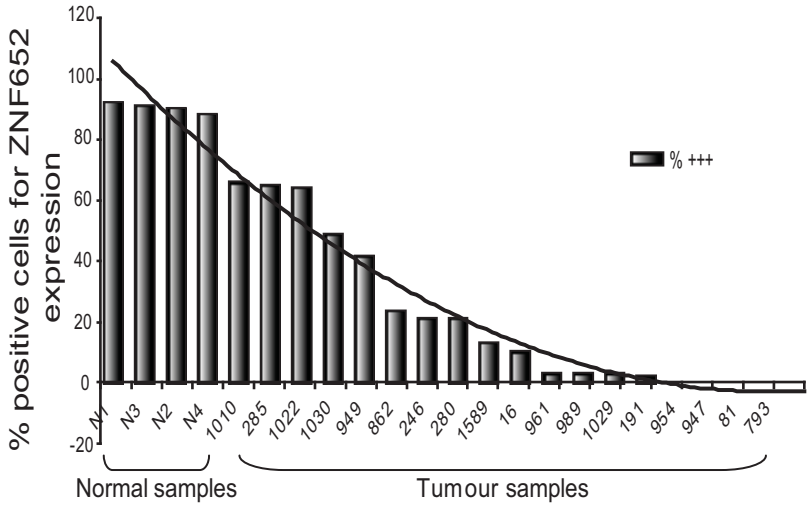

C

		ER n(-ve) and n(+ve) *p value*	PR n(-ve) and n(+ve) *p value*	Her2 n(-ve) and n(+ve) *p value*
TMA from Garvan	ZNF652	5/18 13/18 (*p*=0.458)	6/18 12/18 (*p*=0.110)	15/18 3/18 (*p*=0.148)
	CBFA2T3	0/7 7/7 *NA*	2/7 5/7 (*p*=0.698)	6/7 1/7 (*p*=0.362)
CBFA2T3 Malbourne Tissue Bank		5/13 8/13 (*p*=0.048)*	7/12 5/12 (*p*=0.123)	7/11 4/11 (*p*=0.845)

Figure 5.3 ZNF652 expression in normal and cancerous breast tissues.
A. Representative images from TMA stained with anti-ZNF652 RSH9 antibody. **B.** Graphic presentation of average +++ % positive cells for ZNF652 nuclear staining. Note. Images were taken at 40X zoom conditions. N represents the normal breast tissue section stained, while patient numbers for different cores of TMA are indicated under each bar. **C.** Data from Garvan and Melbourn Tissue Bank TMAs was analysed using *t-test*. Number of sample per catagory and *p* values from two tailed analysis were given in table. * marks $p < 0.05$ and is significant. Note. Only Hormonal status of the samples was available for these TMA's.

while the expression was found reduced in tumour samples (Fig 5.3A lower panel C, D and E). ZNF652 expression (+++ nuclear staining), varying from 0-65% was observed among breast tumour sections. Graphical presentation of the percentage of cells positive for ZNF652 nuclear expression among tumour sections for TMA is given in Fig 5.3B. The significance of differences between the mean values of ZNF 652 % nuclear staining for hormone negative and positive categories was calculated by Student *t-test* for independent samples. The results from all TMAs for both CBFA2T3 and ZNF652 are summarized in Fig 5.3C in the form of a table. The data for ZNF652 analysis from Garvan TMA showed the presence of a no significant differences in hormone negative and positive tumours for ZNF652 % +++ expression. However, the p value of 0.055 (one tailed analysis) does suggest a trend may exist. No significant difference between the mean values of ZNF652 % +++ expression was observed for ER and HER-2 status.

5.3.5 CBFA2T3 expression analysis in BR701 TMA from US Biomax, Inc.

The TMA BR701 comprised a larger cohort of infiltrating ductal carcinoma of the breast and was sourced to extend the previous studies. BR701 comprised breast tumour sections from 70 patients with a single core for each patient. BR701 along with four benign breast tumour sections with normal or benign breast ducts were stained with anti-CBFA2T3 PEP3 antibody. The cores were in the form of 10 columns (1-10) and 7 rows named A-G as shown in the general scan of stained TMA slide in Fig 5.4. Stained slides were scanned at 40x magnification. An overview of TMA stained with PEP3 antibody was captured under 0.42x zoom condition and is presented in Fig 5.4. Images were captured with both 40x and 63x objectives. Some of the representative images from different cores having either high or low expression of CBFA2T3 are shown (Fig 5.5A, B and C). Scoring for CBFA2T3 expression was based on the same criteria as

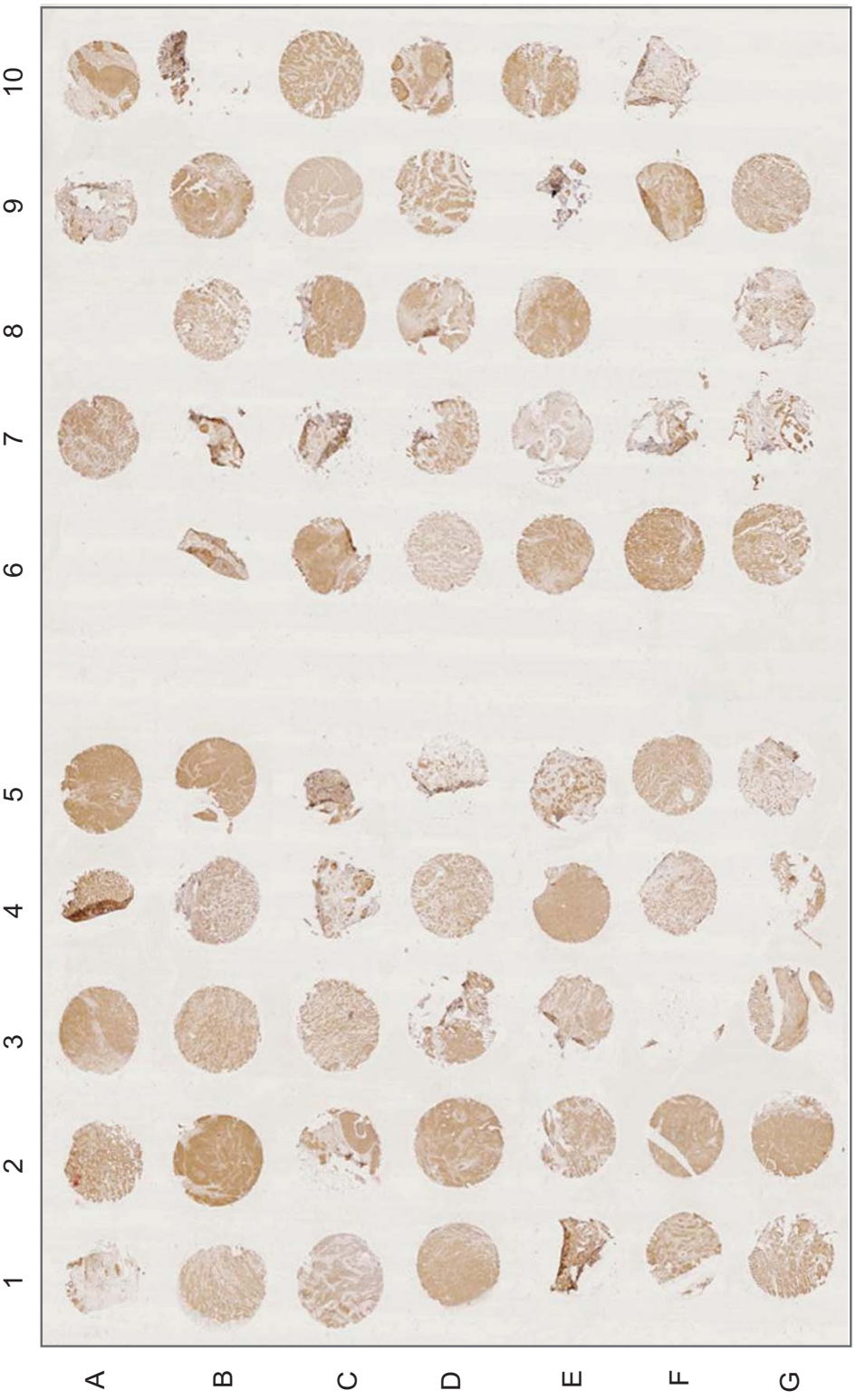

Figure 5.4 Analysis of CBFA2T3 proteins expression in breast tumour sections
A comercially available TMA (BR701. US. Biomax. co) was stained with anti-CBFA2T3 antibody PEP3. TMA was scaned at 40X zoom conditions on Hamamatsu Nano zoomer. Present image represents 0.42X.

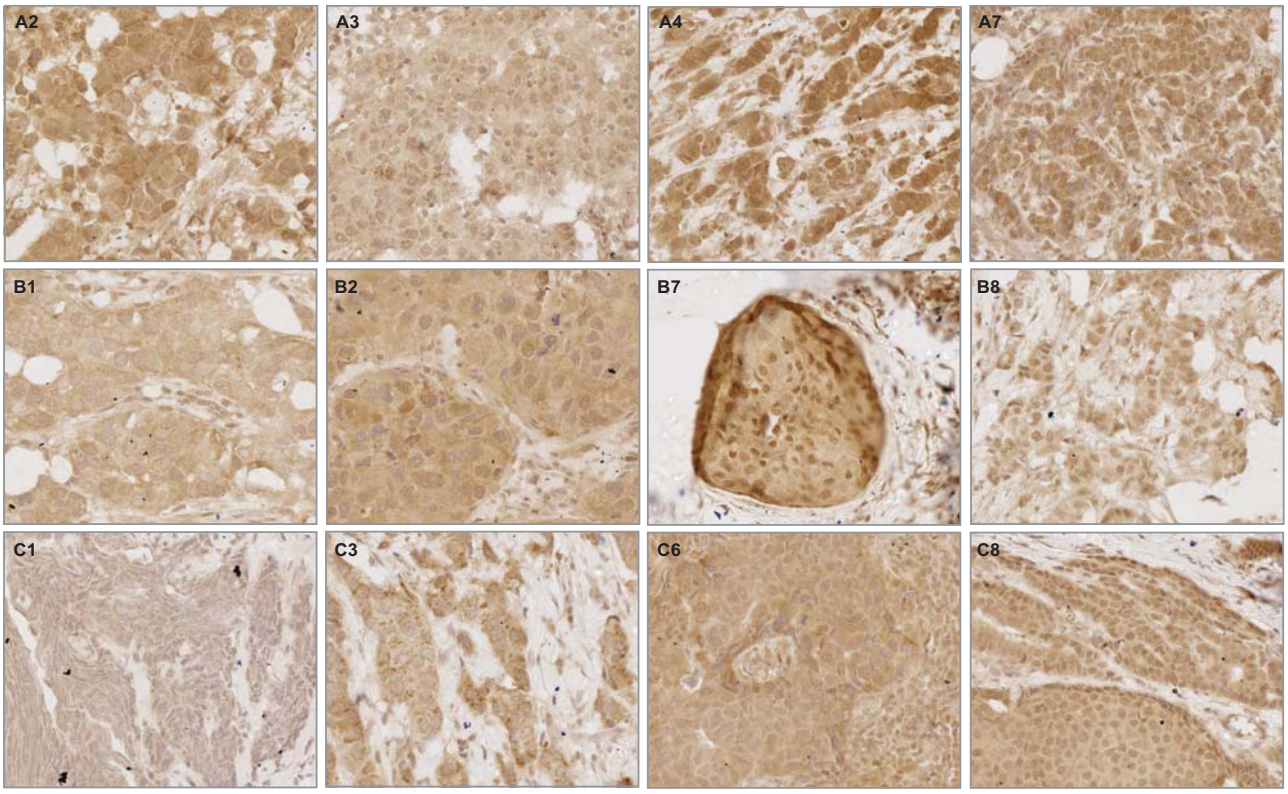
A2
A3
A4
A7
B1
B2
B7
B8
C1
C3
C6
C8

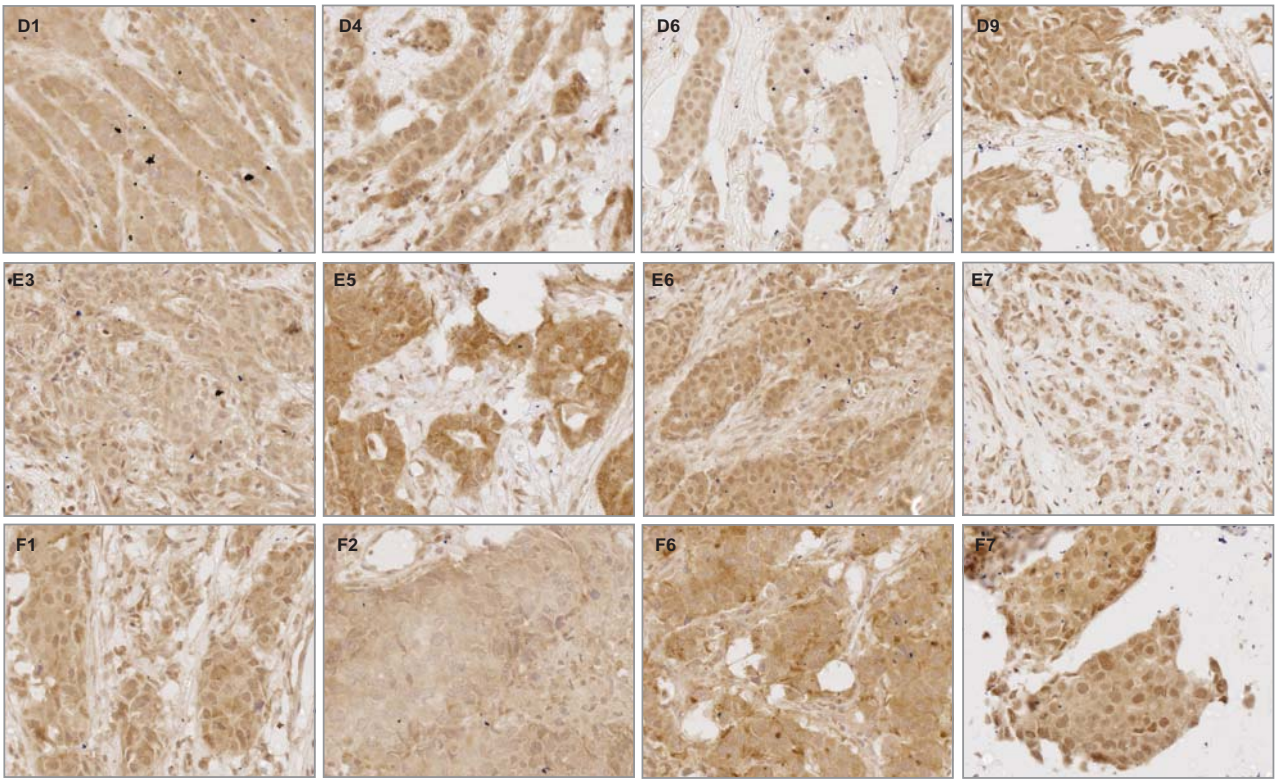
D1
D4
D6
D9
E3
E5
E6
E7
F1
F2
F6
F7

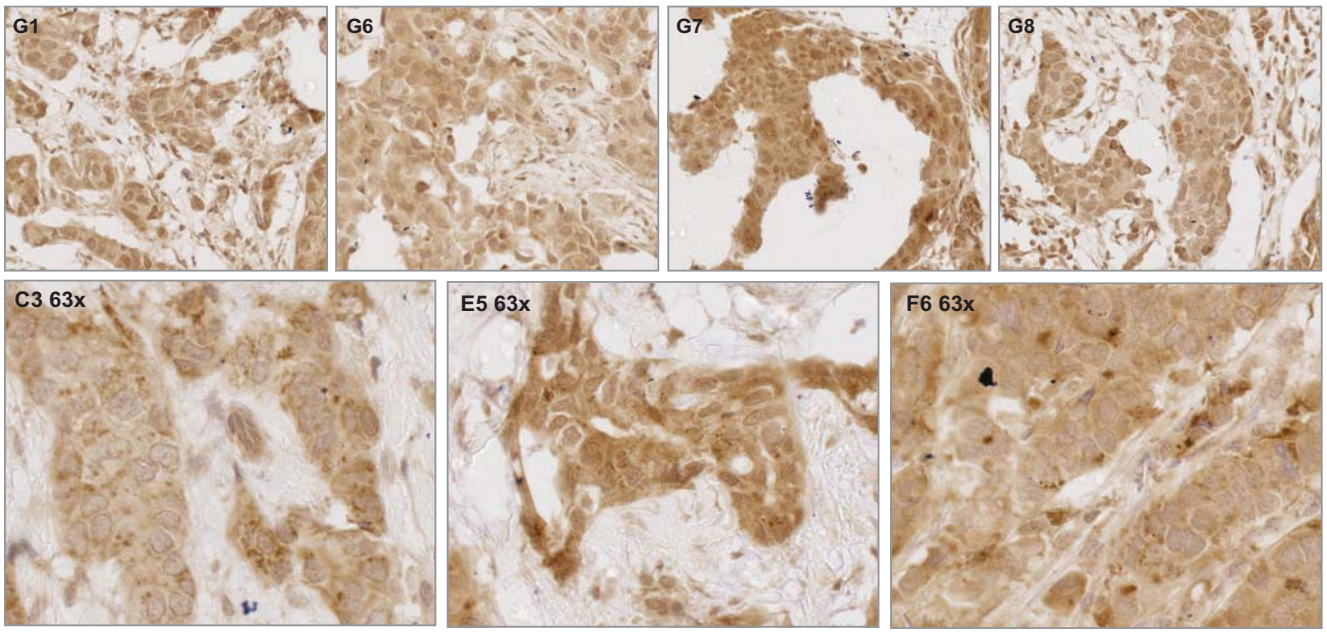

Figure 5.5 Representative images of Breast tumour sections from BR701 TMA stained with PEP3 antibody.
Images were taken at 40X zoom conditions. Only four images for each row of tumour sections was presented here, while their number was given above each image. Last row represents images from C3, E5 and F6 zoomed at 63X lens power to show multi dark spots (centrosomes).

mentioned in section 5.2.6 of this chapter. 200-400 cells for CBFA2T3 expression (+++, ++, +, -) were scored to calculate % positive cells for all categories.

The clinical data along with histological grading, TNM grading, ER, PR and HER-2 status is given in Table 5.2 and was provided by Biomax-US. Clinical and pathological data for the nuclear grade and tumour size was not available for at least 40% of the tumours and were excluded from the analysis. Nuclear data was analysed with a cut off values for determining the levels of staining that is considered being positive for CBFA2T3. The selected cuts off value for positive tumours, with > 70% cells with (+++, ++ and +) nuclear expression or negative ≤ 30% cells without CBFA2T3 nuclear expression. CBFA2T3 cytoplasmic (since CBFA2T3a isoform localizes to cytoplasm, thus cytoplasmic staining was considered to represent CBFA2T3a expression). CBFA2T3a expression was found uniform across a particular section. Thus the sections were considered positive for CBFA2T3a if the cells showed staining or considered negative if no staining was observed.

5.3.6 Relationship of CBFA2T3 expression with the molecular phenotypes of breast tumours.

The expression of nuclear CBFA2T3 using the two different cut off values (Table 5.4 and 5.6 respectively) together with the CBFA2T3 cytoplasmic expression were analysed to determine any relationship with the documented clinical molecular phenotypes of the tumours (Perou et al., 2000), and the expression of the available hormonal tumour markers ER, PR and HER-2 (Hu et al., 2006; Sorlie et al., 2003; Tamimi et al., 2008).

Characteristics	
Median age (range)	70(24-81) years
Nuclear Grade	70
N1	25
N2	18
N3	3
Unknown	24
Histological Tumour grade	70
Grade I	3
Grade II	31
Grade III	31
Unknown	5
Tumour size	14
<20mm	14
>20mm	
Unknown	56
TNM grading	
T-primary tumour	
T0	0
T1	16
T2	43
T3	4
T4	7
N-regional lymph node	
N0	23
N1	36
N2	10
M-Distant metastasis	
Mx (cant be assessed)	1
M1	6
M0- No metastasis	62
Hormonal Status	
Estrogene	
ER+	41
ER-	24
Unknown	5
Progesteron	
PR+	39
PR-	26
Unknown	5
Her-2 (neu or C-erbB-2)	
Her-2+	34
Her-2-	27
Unkown	9

Table 5.2 Clinical and Pathological Characteristics of 70 Patients from TMA BR701

The clinical data is in the form of (TNM, lymph node counts, Black 's nuclear grade, Bloom and Richardson Histological grade and IHC results for ER, PR and Her-2 proteins.

		Group I (ER+, PR+, HER2-)	Group II (ER+, PR+, HER2+)	Group III (ER-, PR-, HER2+)	Group IV (ER-, PR-, HER2-)
CBFA2T3b 70% cut-off	Positive	18/19 (94.7%)	13/23 (56.52%)	10/12 (83.3%)	9/9 (100%)
	Negative	1/19 (5.29%)	10/23 (43.47%)	2/12 (16.6%)	0/9 (0%)
CBFA2T3b 5% +++	Positive	15/19 (78.9%)	13/23 (56.5%)	6/12 (50%)	6/9 (66.6%)
	Negative	4/19 (21.0%)	10/23 (43.47%)	6/12 (50%)	3/9 (33.3%)
CBFA2T3a cytoplasmic	Positive	7/19 (36.8%)	7/23 (30.43%)	4/12 (33.3%)	1/9 (11.11%)
	Negative	12/19 (63.15%)	16/23 (69.56%)	8/12 (66.6%)	8/9 (88.89%)

Table 5.3 comparison of CBFA2T3 expression among different molecular sub-types of IDC tumours .

Tumour sections from BR701 TMA stained with anti-CBFA2T3 antibody were sorted into four different groups on the bases of three different tumour markers ER, PR and HER-2. Table presents the number and %age in brackets for CBFA2T3 (nuclear stained) positive cells 70% cut off value, > 5%+++ nuclear staining and CBFA2T3a cytoplasmic staining.

The data was compared for all three categories for CBFA2T3 expression (Table 5.3) and molecularly defined phenotypes of breast cancer. Up to 94% of luminal A like tumours which are ER positive tumours have CBFA2T3 positive nuclear expression, while only 36.4% luminal A like tumours showed CBFA2T3 cytoplasmic staining (Table 5.3). 100% of basal like (Triple -ve) tumours expressed nuclear CBFA2T3 protein, while this percentage reduces to 83% in HER-2 like tumours for the CBFA2T3 expression (Table 5.3 A). Contrary to this CBFA2T3 cytoplasmic (CBFA2T3a) expression was found lost in 88% of the Basal like tumours. No grouping of Luminal B like tumours was seen on the basis of CBFA2T3 positivity or negativity.

5.3.7 CBFA2T3 nuclear expression correlation with clinical and pathological markers.

The various clinical and pathological markers available on the breast TMA BR701 were assessed for any association with CBFA2T3 expression. Data was analysed using SSP 13 statistical analysis program using the cut off value for CBFA2T3 nuclear expression (70% cells positive for +++, ++ and + CBFA2T3 expression) and CBFA2T3 cytoplasmic expression (+ and -). Relative proportion of patients in numbers positive and negative for CBFA2T3 nuclear expression and *p* values for each category were given in Table 5.4.

An association of CBFA2T3 expression with molecular subtypes and HER-2 status of the tumours was observed when CBFA2T3 expression with 70% cut-off value was analysed against these markers. CBFA2T3 expression was found high in Luminal A (Group I) like and Basal like tumours (Group IV) ranging from 94-100%. Expression of HER-2 has an inverse association with CBFA2T3 expression. 96% tumours (26 out of 27) negative for HER-2 expression were positive for high levels of CBFA2T3

CBFA2T3 positive tumours with cut-off value > 70% +ve nuclear expression

Characteristics	CBFA2T3 positive	CBFA2T3 negative	p value
	Proportion in numbers (%)		
Median age 55 (years)			
+	4/15 (27%)	11/15 (73%)	
-	9/51 (17%)	42/51 (83%)	0.471
Histological Tumour grade			
Bloom's and Richardson modified (BR)			
grade I	2/3	1/3	
grade II	22/29 (75%)	7/29 (25%)	
grade III	27/29 (93%)	2/29 (7%)	0.050 *
Lymph node			
+	26/34 (76%)	8/34(24%)	
-	19/21 (90%)	2/21 (10%)	0.287
TNM grading			
(Grading for tumour invasion)			
T1	12/13 (92%)	1/13 (8%)	
T2	11/41 (26%)	30/41 (74%)	
T3	3/3 (100%)	0/3 (0%)	
T4	6/7 (85%)	1/7 (15%)	0.351
N-regional lymph node			
L_0	20/23 (86%)	3/23 (14%)	
L1	24/32 (75%)	8/32 (25%)	
L2	7/9 (77%)	2/9 (23%)	0.547
Molecular subtypes [a]			
Group I	18/19 (94%)	1/19 (6%)	
Group II	14/22 (63%)	8/22 (37%)	
Group III	9/11 (81%)	2/11 (19%)	
Group IV	9/9 (100%)	0/9 (0%)	0.028 *
Hormonal Status			
Estrogen			
ER+	30/41 (73%)	11/41 (27%)	
ER-	20/22 (90%)	2/22 (10%)	0.116
Progesterone			
PR+	28/35 (80%)	7/35 (20%)	
PR-	22/28 (78%)	6/28 (22%)	1.00
Her-2 (neu or C-erbB-2)			
Her-2+	21/31 (67%)	10/31 (33%)	
Her-2-	26/27 (96%)	1/27 (4%)	0.007**
Centrosome amplification			
Cen no. 2	42/52(80.7%)	8/52 (19.3%)	
Cen no.>2	10/15 (66.6%)	5/15 (33.3%)	0.268

Table 5.4 Association of CB FA2T3 nuclea r expression with Clinical and Pathological characteristics of 70 Patients f rom TMA BR701.

Different known clinical marker data was analysed against CB FA2T3 expression using SSPS statistical analysis tool. Chi-Square values and probabilities by Fisher exact test for each parameter were given in the table. * Marks significant results ($P < 0.05$).

[a] (marks the Breast cancer subtypes on the bases of hormonal status).

CBFA2T3a (cytoplasmic) % positive or negative tumours

Characteristics	CBFA2T3 positive	CBFA2T3 negative	p value
	Proportion in numbers (%)		
Median age 55 (years)			
+	7/15 (46.6%)	8/15 (53.3%)	
-	13/51 (25.4%)	38/51 (74.6%)	0.199
Histological Tumour grade			
Bloom's and Richardson modified (BR)			
grade I	1/3	2/3	
grade II	9/29 (31%)	20/29 (69%)	
grade III	9/30 (30%)	21/30 (70%)	0.898
Lymph node			
+	11/35 (31.4%)	24/35 (68.5%)	
-	7/21 (33.3%)	14/21 (66.6%)	0.779
TNM grading			
(Grading for tumour invasion)			
T1	2/13 (15.3%)	11/13 (84.6%)	
T2	12/42 (28.6%)	30/42 (71.4%)	
T3	0/3 (0%)	3/3 (100%)	
T4	5/7 (71.4%)	2/7 (28.6%)	0.024*
N-regional lymph node			
L_0	6/23 (26.08%)	17/23 (73.9%)	
L1	8/32 (25%)	24/32 (75%)	
L2	5/10 (50%)	5/10 (50%)	0.268
Molecular subtypes [a]			
Group I	7/19 (36.8%)	12/19 (63.15%)	
Group II	7/23 (30.4%)	16/23 (69.6%)	
Group III	4/12 (33.3%)	8/12 (66.6%)	
Group IV	1/9 (11.1%)	8/9 (88.9%)	0.593
Hormonal Status			
Estrogen			
ER+	12/41 (29.2%)	29/41 (70.7%)	
ER-	6/22 (27.2%)	16/22 (72.8%)	1.00
Progesterone			
PR+	9/35 (25.7%)	26/35 (74.2%)	
PR-	22/28 (78%)	6/28 (22%)	0.589
Her-2 (neu or C-erbB-2)			
Her-2+	9/31 (29.0%)	22/31 (71%)	
Her-2-	8/27 (29.6%)	19/27 (70.4%)	1.00
Centrosome amplification			
Cen no. 2	30/49 (61.2%)	19/49(39.8%)	
Cen no.>2	2/15 (13.3%)	13/15 (86.6%)	0.002*

Table 5.5 CB FA2T3 cytoplasmic exp ression association with Clinical and Pathological Markers.

Cells with CB FA2T3 cytoplasmic expression was taken as positive and negative vise versa. Statistical significance was calculated by Chi squared and Fisher Exact Test.* Marks significant results with $p < 0.05$.

expression (Table 5.4). Significance of difference was calculated by Chi squared or Fisher *t-test* analysis tools and was compared with CBFA2T3 cytoplasmic expression (Table 5.6). Histological tumour grades showed a week association (p= 0.050 with 70% cut off) with CBFA2T3 nuclear expression. Significant correlation of CBFA2T3 expression with molecular subtypes (p= 0.028) and HER-2 status (p= 0.007) was observed with 70% CBFA2T3 positive cut-off value.

5.3.8 CBFA2T3 cytoplasmic expression association with clinical markers

CBFA2T3 cytoplasmic staining was assessed to determine any correlation between known clinical markers and CBFA2T3 cytoplasmic staining according to the scoring mentioned in section 5.25. The staining pattern in the cytoplasm was found to be uniform between cells in a section. Tumours were characterized as either positive (if showed staining) or negative (no staining) for CBFA2T3 cytoplasmic staining. High grade tumours, according to TNM grading for tumour invasion showed an inverse association with the CBFA2T3 cytoplasmic pattern. T1, T2 and T3 grade tumours {84.6% (11/13), 71.4% (30/42) and 100% (3/3) respectively} were found negative for CBFA2T3 cytoplasmic staining. While T4 grade tumours 71.4% (5 out off 7) were found positive for CBFA2T3 cytoplasmic staining.

A small proportion of tumours (15 in number) were found with centrosomal anomalies (increase in centrosome numbers or defects in both centrosome structure and size) in 6-30% cells. It was noticed that 86.6% of tumours negative for CBFA2T3 cytoplasmic expression have centrosome abnormalities. While only 13.3% of tumours with increased centrosome numbers were found positive to cytoplasmic CBFA2T3 expression. Chi squared test revealed a significant correlation (p= 0.002) of centrosome

Characteristics	CBFA2T3 (nuclear) ≥ 70% positive cut-off	CBFA2T3a (cytoplasmic)
Median age (range)		
	(*p*= 0.471)	(*p*= 0.199)
Histological Tumour grade Bloom's and Richardson modified (BR)		
	(*p*= 0.050)*	(*p*= 0.898)
Lymph node		
	(*p*= 0.287)	(*p*= 0.779)
TNM grading (Grading for tumour invasion)		
T-primary tumour		
	(*p*= 0.351)	(*p*= 0.024)*
N-regional lymph node		
	(*p*= 0.547)	(*p*= 0.268)
Molecular subtypes [a]		
	(*p*= 0.012)*	(*p*= 0.593)
Hormonal Status		
Estrogen		
	(*p*= 0.116)	(*p*= 1.00)
Progesterone		
	(*p*= 1.00)	(*p*= 0.589)
Her-2 (neu or C-erbB-2)		
	(*p*= 0.007)*	(*p*= 1.00)
Centrosome amplification		
	(*p*= 0.268)	(*p*= 0.002)*

Table 5.6 Comparison of two cut-off values for CBFA2T3 nuclear expression assosiation with Clinical and Pathological markers.
p values calculated for >70% nuclear positive CBFA2T3 (Table 5.4)and CBFA2T3a cytoplasmic (Table 5.5) with the clinical markers are summerized here. * Marks significant results where $p < 0.05$. [a] (marks the Breast cancer subtype based on the hormonal status).

anomalies with the CBFA2T3 cytoplasmic expression.

5.3.9 Immunoflorescent staining of BR701 TMA with γ-tubulin confirmed that the observed structures with anti-CBFA2T3 antibody are centrosomes.

Increase in centrosome numbers or defects in structures seen among the tumours from BR701 TMA were further confirmed by co-staining with anti-γ-tubulin. All sections were also stained with streptavidin labelled anti-CBFA2T3 (PEP3) antibody. Representative images from the tumours and normal breast ducts along with the negative control for fluorescently labelled γ-tubulin are given in Fig 5.6. Co-localization of CBFA2T3 with the γ-tubulin was seen in tumours as well as the normal breast ducts. Due to unavailability of monochrome camera on confocal microscope the imaging of both signals (DAB labelled CBFA2T3 and florescent labelled γ-tubulin) was not possible for the same field (as the florescent imaging and phase contrast imaging was only possible at different focal plans which makes it impossible to have focused image with two different labelling at the same focal plan). Thus only fluorescent images for anti-γ-tubulin labelled tumours (Fig 5.6A-D) and normal breast ducts (Fig 5.6E-F) were presented here. While representative images for CBFA2T3 staining for the centrosomal abnormalities were shown in (Fig 5.5C with the core numbers C3, E5 and F6). Immunofluorescent staining confirmed that the observed structures with anti-CBFA2T3 antibody are centrosomes.

Discussion

This study determined the relative expression of CBFA2T3 proteins in breast tumour sections available in the form of TMA. CBFA2T3 is expressed in epithelial lining of normal breast ducts but was found down regulated in tumours. CBFA2T3 expression

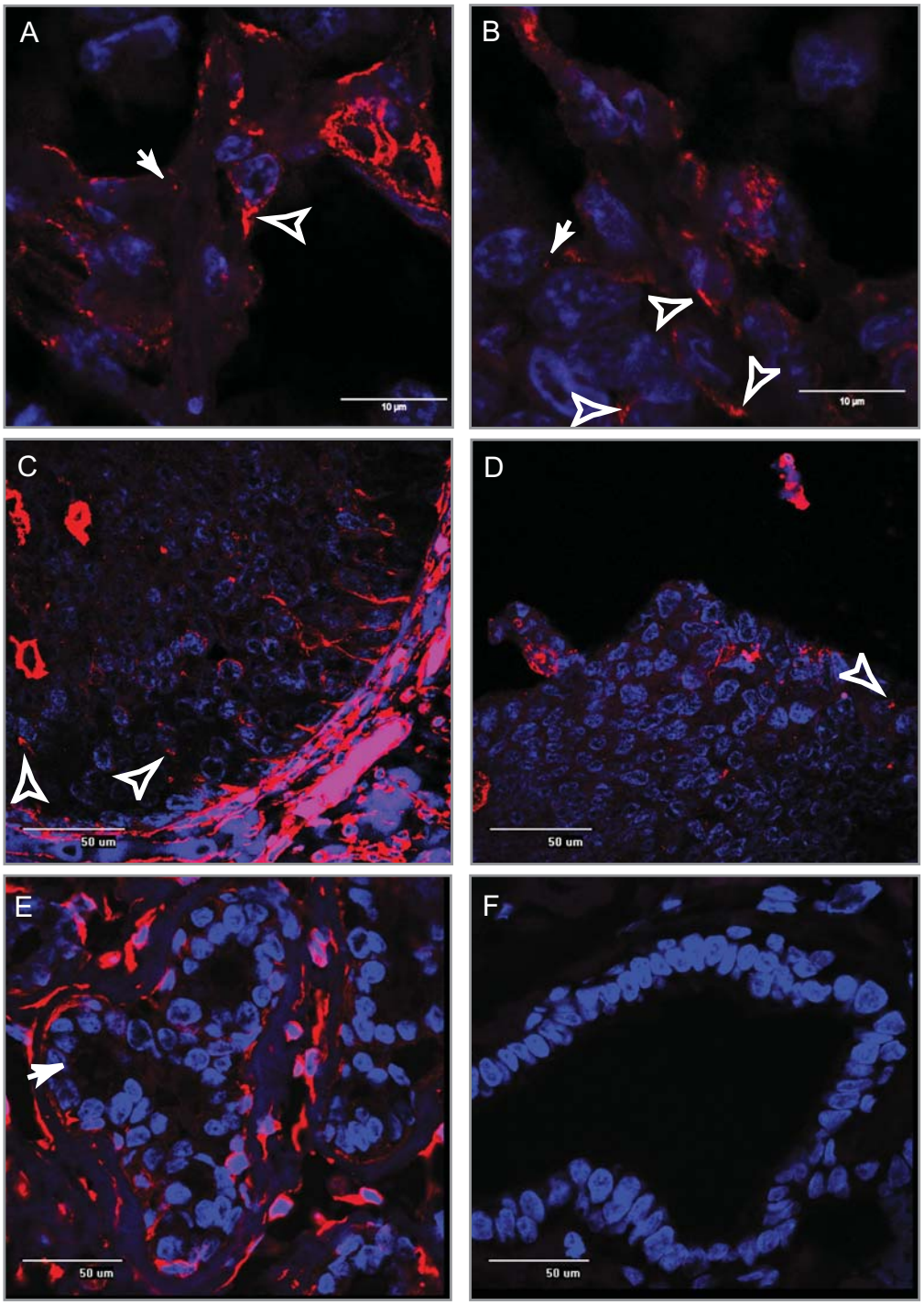

Figure 5.6 Images from BR701 TMA stained with γ-tubulin antibody. BR701 TMA was stained with Alexa-594 labelled γ-tubulin and streptavidin-biotin labelled α-CBFA2T3 (PEP3) antibodies (same slide). fluoresecent imaging was performed using confocal microscope. **A-D.** Representative images from tumour sections with amplified centrosomes. **E.** Normal ducts containing section stained with γ-tubulin. **F.** Negative control.Solid arrow marks normal centrosome, while hollow arrow head stands for abnormal centrosomes. C-F images taken at 60X while A and B are 3 time zoomed with 60X.

was initially analysed in separately sourced TMAs, consisting of small cohorts of breast tumours. Final experiment was conducted on a breast TMA (BR701) sourced commercially comprising of 70 breast tumours. CBFA2T3 expression, under cut-off value (70% positive) for the nuclear CBFA2T3 and cytoplasmic CBFA2T3 was assessed for any correlation with the available clinical data. Statistical analysis of the data from breast TMA sections reveal the presence of an inverse relation between CBFA2T3 nuclear expression and HER-2 status with 70% positive cut-off value. CBFA2T3 nuclear expression was also found significantly associated with molecular subtypes and histological tumour grade. Moreover, an association of CBFA2T3 cytoplasmic expression with the tumour invasion characteristics (TNM staging) and centrosomal abnormalities among a cohort of breast tumour sections from BR701 TMA was found during current study.

Previous data from Kochetkova et al (2002) has shown the down regulation of *CBFA2T3* message in breast tumours, while *CBFA2T3* retains its expression in epithelial lining of the normal breast ducts (Kochetkova et al., 2002). A similar scenario was observed with the CBFA2T3 proteins expression (immortalized mammary epithelial HEMC, HEMC-tert, MCF-10, MCF-12 and mammary epithelial cell lines 48SRT and 184AT) during the present study which follows the same pattern as was observed with mRNA expression discussed in Chapter 3. CBFA2T3 expression for both isoforms was found high in normal breast ducts, while a variable expression from high to low or absence of expression was observed in the breast tumours.

No significant association of CBFA2T3 expression with the median age of patients, ER and PR status was observed in TMA BR701, comprising of a bigger cohort of 70 patients during the current study. However among a small cohort of patients from

Melbourne tissue bank TMA, a significant association of CBFA2T3 nuclear positivity was found with the ER status (p= 0.048) (Fig 5.3C). A similar trend was also noticed, although no significant association of CBFA2T3 expression with ER was found in the bigger cohort of tumour tissues (BR701 TMA). The current scenario urged the need to further analyse CBFA2T3 expression for better understating, in a bigger cohort of breast tumour sections. Expression analysis of CBFA2T3 proteins among a panel of cell lines from this study (Chapter 3 Fig 3.5A) showed similar findings, as CBFA2T3 expression was high in cell lines positive for ER expression or vice versa. In a gene microarray study, *CBFA2T3* was found as an ER responsive gene (Frasor et al., 2003). *In silico* analysis of the CBFA2T3 promoter region has shown the presence of two canonical ERE (ER response element) (Fig 6.5 Chapter 6). However further experiments were required to determine CBFA2T3 expression regulation by ER pathways.

A significant association of CBFA2T3 nuclear expression with molecular subtypes was seen in the current study (Table 5.4). CBFA2T3 nuclear expression (70% positive) was found high in ER positive and HER-2 negative tumours. While 100% of Basal like tumours negative for ER, PR and HER-2 expression were also found negative for CBFA2T3 nuclear expression (Table 5.3). An inverse association of CBFA2T3 nuclear expression (70% positive cut-off) with HER-2 expression (p= 0.007) was observed among tumour sections from BR701 TMA. 96% of tumours which were negative for HER-2 expression were found positive for CBFA2T3 nuclear expression (Table 5.5). No significant association of CBFA2T3 cytoplasmic expression was observed for ER, PR and HER-2 levels. The data for other members of ErbB or HER family was not available for the current TMA. HER family members are known (EGFR, HER-2, HER-3 and HER-4) for their co-expression in breast tumours (Abd El-Rehim et al., 2004; Barnes et al., 2005; Witton et al., 2003). HER family members are known to form homo

or hetro-dimmers as discussed in Chapter 1 (Karamouzis et al., 2007). A strong association of HER-2 and HER-3 or HER-2 and HER-4 was reported in node positive breast tumours (Hudelist et al., 2003) but this association was generally lost in node negative tumours. HER-4, a member of HER family proteins interacts and co-localize with CBFA2T3 through its intracellular domain in nuclear compartment. Reporter assays have shown the blockage of CBFA2T3 mediated repression by overexpression of HER-4, indicating a plausible role for CBFA2T3 in HER-4 pathways in breast cancer (Linggi et al., 2006). Co-regulation of ER receptors by HER-4 was earlier reported. Upon induction with estrogen, ERα binds with HER-4 proteins to the promoter regions of selective ER inducible genes. Knockdown of HER-4 in T47D cell line inhibits the growth promoting action of estrogen (Zhu et al., 2006). These independent reports have shown an association of HER-4 with ER and CBFA2T3 proteins.

An association of HER-2, a member of HER family proteins which may exist as a hetrodimer with HER-4, was found with CBFA2T3 nuclear expression during this study. Abd El Rehim et.al (2004) data has indicated the coexistence of HER family proteins as 49.5% of HER-2 positive tumours over express HER-4 or 34.6% of HER-4 positive tumours do express HER-2 (Abd El-Rehim et al., 2004). An inverse association of HER-4 with ER status was reported earlier (Vogt et al., 1998). HER-2 expression is known to predict poor overall or disease free survival, while CBFA2T3 expression is found related to good prognosis. Current data from this study has shown a significant association of CBFA2T3 expression with the tumour molecular subtypes and HER-2 status (Table 5.4). As 67% of Her-2 positive tumours are positive for CBFA2T3 nuclear expression, while all Her-2 negative tumours are found positive for CBFA2T3 expression. These results indicate the possibility that CBFA2T3 expression (known for

good prognosis prediction) may divide HER-2 group (with poor survival rate) in a better prognostic sub group.

During this study a strong association of tumours invasion characteristics (p= 0.028) and centrosomal abnormalities (p= 0.005) was observed with CBFA2T3 cytoplasmic expression. 86% of the tumours negative for the CBFA2T3 cytoplasmic expression were found with increased centrosomal number and volume. Previous reports has shown that centrosome abnormalities either structural or numerical results in chromosomal instability, which is the leading cause of tumour heterogeneity and metastasis in many types of tumours (Lingle et al., 2002; Pihan et al., 1998; Pihan et al., 2001; Sato et al., 2001). These abnormalities are reported to arise independently of the ER and P53 status and are found associated with mitotic and spindle abnormalities in breast tumours leading to more aggressive tumour development (D'Assoro et al., 2002). A significant association of structural centrosomal abnormalities with HER-2 overexpression, negative ER status was recently reported (Guo et al., 2007). A similar outcome was observed during this study. Breast tumour sections from patients positive for HER-2 expression (11 out of 15 patients) had centrosome amplifications. While only 4 patients with centrosomal amplification were found negative for HER-2 and positive for ER and PR. A significant association of CBFA2T3 cytoplasmic expression with invasive tumours was also observed (Table 5.5). T3 and T4 grade tumours were found 100% positive for CBFA2T3a cytoplasmic expression. These findings were consistent with the previous reports, where an increased expression of CBFA2T3 was reported in high grade tumours.

ZNF652 expression analysis in breast tumour sections was also carried out in a small cohort of TMA from Garvan Institute Sydney. ZNF652 expression was found down

regulated in various tumour sections, which was consistent with the previous findings from our group. In a cDNA profiling array Kumar *et.al* has shown a down regulation of ZNF652 expression in breast, vulva, prostate and pancreatic cancers as compared to normal tissues (Kumar et al., 2006). No significance association of ZNF652 was observed with any clinical marker. Reduced expression of ZNF652 protein has been shown in vulvar squamous cell carcinomas. No association of ZNF652 expression with known tumour markers for vulvar carcinoma was found (Holm et al., 2008). David F Callen has shown association of ZNF652 high level and AR expression with increased relapse risk in organ defined prostate cancer (manuscript in preparation).

Data from the present study have shown a potential for CBFA2T3 expression to sub divide HER-2 group into a better prognostic group, as CBFA2T3 expression is related with better prognosis. There is a likelihood that CBFA2T3 may evolve as a prognostic marker for HER-2 group. A bigger study with the patient survival data is required to support these findings for CBFA2T3. In addition expression analysis of HER family proteins, particularly HER4 and ZNF652 in the same cohort of breast cancer samples will help to clarify these complex pathways.

Chapter 6 –Role of CBFA2T3 protein as a transcriptional corepressor

6.1 Introduction:

CBFA2T3, a member of the CBFA2T protein family, has been identified as a transcriptional corepressor (Kochetkova et al., 2002). Both CBFA2T1 and CBFA2T3 show a high degree of homology, and function as transcription repressors by recruiting various proteins including various co-repressors and histone deacetylases to repress the transcription of different target genes. The CBFA2T family of proteins are non-DNA binding proteins and bind to transcription factors like BCL6, ZNF652, Gfi1 and PLZF to repress the transcription of target genes.

The interaction of CBFA2T1 with PLZF and BCL6, which are involved in promyelocytic leukaemia and B-cell lymphoma development respectively are already known (Chevallier et al., 2004; Melnick et al., 2000b). RUNX1-CBFA2T1 fusion protein (product of t(8:21) translocation in leukaemia: discussed in Chapter 1) has been shown to support proliferation and inhibits senescence in leukaemia cell lines (Martinez et al., 2004). It has been suggested that BCL6 and PLZF are both regulators of the cell cycle (Albagli et al., 1999; McConnell et al., 2003; Sanchez-Beato et al., 2003). Recently, up regulation of the BCL6 gene has been reported in invasive breast tumours and its expression was found correlated to the expression of cyclin D2 (Bos et al., 2003). This report suggests a potential involvement of BCL6 in breast tumour development. The knowledge that tumour suppressor genes play an important role in cellular proliferation by inhibiting the effect of genes involved in abnormal

proliferation, such an oncogenes, helped to hypothesize the role of BCL6 in the cell cycle maintenance mediated by CBFA2T3.

Although CBFA2T1 has been shown to interact with BCL6 and PLZF, a possible interaction of CBFA2T3 with these transcription factors has not been investigated. The majority of the available information regarding these transcriptional repressor complexes relates to CBFA2T1. Due to the similarities between CBFA2T1 and CBFA2T3 in their gene sequences and structures it is likely that CBFA2T3 also interacts with the BCL6 and PLZF. Since CBFA2T3 has been proposed as a breast cancer tumour suppressor then this function may be mediated through BCL6 (Kochetkova et al., 2002). The knowledge that interaction between various cellular proteins are cell type or time specific helped to hypothesize that CBFA2T3-BCL6 or CBFA2T3-PLZF interaction might be cell type specific. These interactions might be different in nature to the interaction between CBFA2T1-BCL6 and CBFA2T1-PLZF. Further more information on these transcriptional repressor complexes might help to elaborate their role in the development of breast cancer.

6.2 Materials and methods

6.2.1 Cell lines and antibodies

Most of the overexpression experiments were conducted in the HEK293T cell line where the cell line has not been used it is indicated in the relevant section. HEK293T and MCF7 cell lines were grown under conditions given in Chapter 2. Anti-BCL6 antibody GI 191E/A8 was a kind gift by Dr G Roncador, from Spanish National Cancer Centre (CNIO) Madrid, Spain (Garcia et al., 2006). All commercially available antibodies used in this study are described in Chapter 2.

6.2.2 Plasmids

Plasmid constructs with Myc-CBFA2T1, Myc-CBFA2T2, Myc-CBFA2T3 and HA-BCL6 (Chapter 2 General Material and Methods, Table 2.2) were already available in the lab. HA-PLZF was PCR amplified from a cDNA library generated from brain tissue using a primer set (PLZF-ER1-F and PLZF-BH1-R Chapter 2 Table 2.1). The amplified product was cloned inframe at EcoR1-BamH1 site of pCMV-HA vector. All constructs of the CBFA2T3 promoter region were designed and generated by Dr David Millband and Jaclyn Lee. HA-BCL6 zinc finger mutant constructs (B6ZM1-6) were a kind gift from Dr Claudie Lemercier (Mascle et al., 2003). Flag-tagged HDACs 1-7 were generously given by Dr Kum Kum Khana (Queensland Institute of Medical Research-QMIR).

6.2.3 Primers used in this chapter

Different sets of primers (Table 2.1 Chapter 2) were designed to specifically amplify each of the three CBFA2T family member's transcript form HEK293T cells. Specificity of these primers sets was checked. All sequences are given in Table 2.1.

6.2.4 Myc tagged CBFA2T interaction studies with HA-BCL6 and HA-PLZF

Initial experiments were undertaken to achieve equal levels of expression of each of the ectopically expressed CBFA2T family member by varying the amounts of transfected plasmids. This proved to be difficult since CBFA2T1 always expressed at low levels, while CBFA2T2 and CBFA2T3 showed high expression even if the concentration of transfected DNA was low. Myc-CBFA2T1 (6μg), myc-CBFA2T2 (2 μg), myc-CBFA2T3 (2.5 μg), HA-BCL6 (2.5 μg) and HA-PLZF (2.5 μg) were transfected into HEK293T cells each of two wells of 6 well plates. The total DNA content for each transfection was kept constant (4 μg per well, except for CBFA2T1 which totalled 4.25 μg) by adding appropriate amount of empty vector DNA. The details of single and multiple transfections are given in Fig 6.1A and B. The procedure for transfection and immunoprecipitation is described in General Material and Method section 2.2 and 2.10.

6.2.5 BCL6 protein expression in breast cancer cell lines

Equal concentration of cellular lysates, prepared from a panel of normal and breast cancer cell lines (Section 3.2.6 Chapter 3), were western blotted against anti-BCL6 antibody GI 191E/A8 and anti-β actin antibody.

6.2.6 Real-time RT-PCR for measuring the effects of ectopically expressed BCL6 on the endogenous *CBFA2T* transcripts

Increasing amounts of BCL6 (as shown in Fig 6.3B) were transfected into the HEK293T cell line using the standard protocol in Chapter 2, section 2.2. 24 hours post transfection RNA was prepared from each transfection and cDNA was generated which was subsequently subjected to real-time RT-PCR using the relevant sets of primers. The relative levels of the transcripts *CBFA2T3, CBFA2T1, CBFA2T2* and *Cyclophilin A* were determined (see Chapter 2 section 2.12). The levels of *CBFA2T* transcripts were

normalized with the levels of the house keeping gene *Cyclophilin A*. The expression in different treatments was expressed relative to that of the HEK293T expression and presented as mean ± SEM of triplicates. A negative control consisting of BCL6 in reverse orientation (RBCL6) (4 μg) was also transfected and analysed.

6.2.7 Effects of BCL6 on endogenous CBFA2T3 proteins expression

HA-BCL6 was ectopically expressed in the MCF7 cell line that expresses detectable level of CBFA2T3. MCF7 cells were plated on two of 6 well plates at 1×10^5 cells per well. A glass cover slips was added to one plate and subsequently was used for the immunoflorescent staining and second plate was used for preparation of cellular lysates. Cells transfected with HA-BCL6 were fixed with -20^{o}C methanol for 8 minutes and stained with immuno-fluorophore labelled rat anti-HA and rabbit anti-CBFA2T3 (RSH1) antibodies. Details of procedure are given in Chapter 2 section 2.12. Images were captured using a confocal microscope. Signal intensities of 10 randomly selected cells for anti-CBFA2T3 labelled (green), expressing moderate amount of HA-BCL6, were measured using ImageJ (Java based image analysis software) available free of charge from www://rsb.info.nih.gov/ij/. The average intensities of these cells were compared with the average intensities of non HA-BCL6 expressing cells stained for endogenous CBFA2T3. To calculate the significance of differences between two sets of samples the data was analysed using the Student *t-test*.

Increasing amount of HA-BCL6 ranging from 0.5μg, 1.0μg, 2.0μg to 4.0μg (per well of 6 well plate) were transfected in to the MCF7 cell line. 24 hours post transfection equal volumes of cellular lysates were prepared and analysed for CBFA2T3 expression by immuno blotting with anti-CBFA2T3 (RSH1) antibody and anti-β actin antibody.

6.2.8 Dual luciferase reporter assays for measuring the effects of BCL6 on CBFA2T3b promoter

CBFA2T3b promoter constructs were generated (from BAC 368P13) with B6BS (BCL6 binding site) and ERE (estrogen receptors response elements) (Driscoll et al., 1998) driving the luciferase gene in the PGL3 basic reporter construct. Schematic presentation of these constructs is given in Fig 6.5 A. 2×10^4 HEK293T cells in 96 well plates were transfected with 200ng of B6BS or ERE-B6BS construct, with 300ng of RBCL6, and 20ng of pRLTK plasmid as an internal control. 24 hours later cells were lysed and assayed using a dual luciferase reporter assay system from Promega. Luciferase activity was normalized with *Renilla* luciferase and plotted as relative light units (RLU). In experiments to determine the additive effects of ER on BCL6 regulation to CBFA2T3b promoter CHO cells were grown for 48 hour in charcoal stripped media. 1×10^5 cells were co-transfected with 200ng of CBFA2T3b promoter, B6BS-ERE (GS#559), 300ng RBCL6 or 300ng BCL6, and 100ng of pSG5-ER-α (ER+) or empty vector (ER-). 8-9 hours later cells were stimulated with oestradiol E2 (2 nM) or ethanol as a control. Reporter assays were performed as described earlier. Dual luciferase assays were performed using wild type CBFA2T3b promoter containing B6BS-ERE sites (named WP16-B6BS-ERE) or mutant CBFA2T3b promoter construct in which B6BS1 was mutated through site directed mutagenesis (named Mt2BS1).

6.2.9 Effects of BCL6 zinc finger mutants on CBFA2T3 proteins

HA-BCL6 zinc finger mutant constructs B6ZM1 to B6ZM6 were kindly provided by Dr Claudie Lemercier, France. Paired cysteines residues (X-C-X_2-C-X_3) in each of these zinc fingers were mutated to glycines (X-G-X_2-G-$X_{3)}$ (Mascle et al., 2003). 4µg of HA-BCL6 zinc finger mutant constructs (B6ZM1-6) were transfected in HEK293T cell line

per well of a 6 well plate. The wild type HA-BCL6 construct was used as a negative control. Equal amounts of lysate from each transfection was analysed for endogenous CBFA2T3 expression by immuno blotting with anti-CBFA2T3 RSH1 antibody and anti-β actin antibody.

6.2.10 CBFA2T3b additive effects on BCL6 mediated repression of *Cyclin-D2*

HEK293T cells were plated in 6 well plates at 85-90% confluence. Cells were co-transfected with either 900ng of myc-tagged CBFA2T1 or 900ng of CBFA2T3a or 150ng of CBFA2T3b and 50ng of either HA-tagged RBCL6 or BCL6. The net DNA concentration per transfection was adjusted to 1100ng per well by adding remaining amount of empty vector. Cells were washed with 1×PBS and resuspended into 100µl of PBS. 75µl of this cell suspension was used to prepare RNA, while cellular lysates were prepared from the remaining. cDNA was prepared from extracted RNA and was analysed for the expression of *Cyclin-D2* and *Cyclophilin A* by real-time quantitative PCR (General Material and Methods, Chapter 2 section 2.11). Each sample was analysed in triplicates. Relative concentration of *Cyclin-D2* was calculated for each treatment of BCL6 and RBCL6 as mentioned in Fig 6.6 A. Relative concentration of *Cyclin D2* for each categories of BCL6 treatment was normalized against RBCL6 treatment for that particular category and was plotted as ±S.E (Fig 6.6 B). To demonstrate transfected indicated levels of expression of myc-CBFA2T members, lysates were analysed with anti-myc, anti-HA and anti-β actin antibodies.

6.2.11 CBFA2T3 interaction with Sin3A

Endogenous CBFA2T3 protein complexes were purified from the MCF7 cell line, using the RSH1 antibody (Chapter 2 section 2.10). 2% of the original lysate was analysed as

input and one third of the elution were western blotted with the anti-CBFA2T3 antibody RSH1 and the anti-Sin3A antibody.

6.2.12 Interaction of CBFA2T3a with HDACs proteins

2µg of myc-CBFA2T3a and 2µg of either Flag-HDAC1 to HDAC7 was co-transfected into HEK293T cells. Immune complexes were purified 24 hours later, using anti-myc antibody conjugated protein G beads. 1% of the original lysate and one third of elusions were western blotted against anti-myc and anti-Flag antibodies.

6.3 Results

6.3.1 CBFA2T3 protein interaction with the DNA binding zinc finger proteins BCL6 and PLZF.

The CBFA2T family of proteins interact with different DNA binding zinc finger proteins to mediate the transcription repression of target genes. In addition to these DNA binding proteins, interaction with different HDACs and corepressors like mSin3A and NCoR were also reported in the transcription repressor complexes. CBFA2T1 was reported to interact with the known DNA binding proteins BCL6 (Chevallier et al., 2004), PLZF (Melnick et al., 2000b) and Gfi1 (McGhee et al., 2003). The interaction of Gfi-1 with CBFA2T3a protein was also reported by McGhee *et al*, 2003. Our lab previously identified a novel zinc finger protein ZNF652 as a binding partner of CBFA2T3b from a yeast two hybrid screen (Kumar et al., 2006). As CBFA2T family proteins share high homology, we therefore hypothesized that other known DNA binding proteins which interacts with CBFA2T1 may also interact with CBFA2T3b.

Human myc tagged-CBFA2T1, CBFA2T2 and CBFA2T3b clones were available in the laboratory. HA-BCL6 and HA-PLZF were generated during this study (details in section 6.2.1). Different amounts of CBFA2T1, CBFA2T2 and CBFA2T3 constructs were co transfected with equal amount of BCL6 or PLZF in HEK293T cells. Lysates from single and double transfections were immunoprecipitated with anti- myc antibody and western blotted against both anti-HA and anti-myc antibodies. Initial experiments were performed to conduct two ways IP's but immunoprecipitation of HA-tag was found not as successful as that of myc-tagged proteins. To enrich protein complexes different sets of conditions (magnetic beads, Protein A or G coupled beads etc) were tried. The data presented in this section is from the final experiment with the most

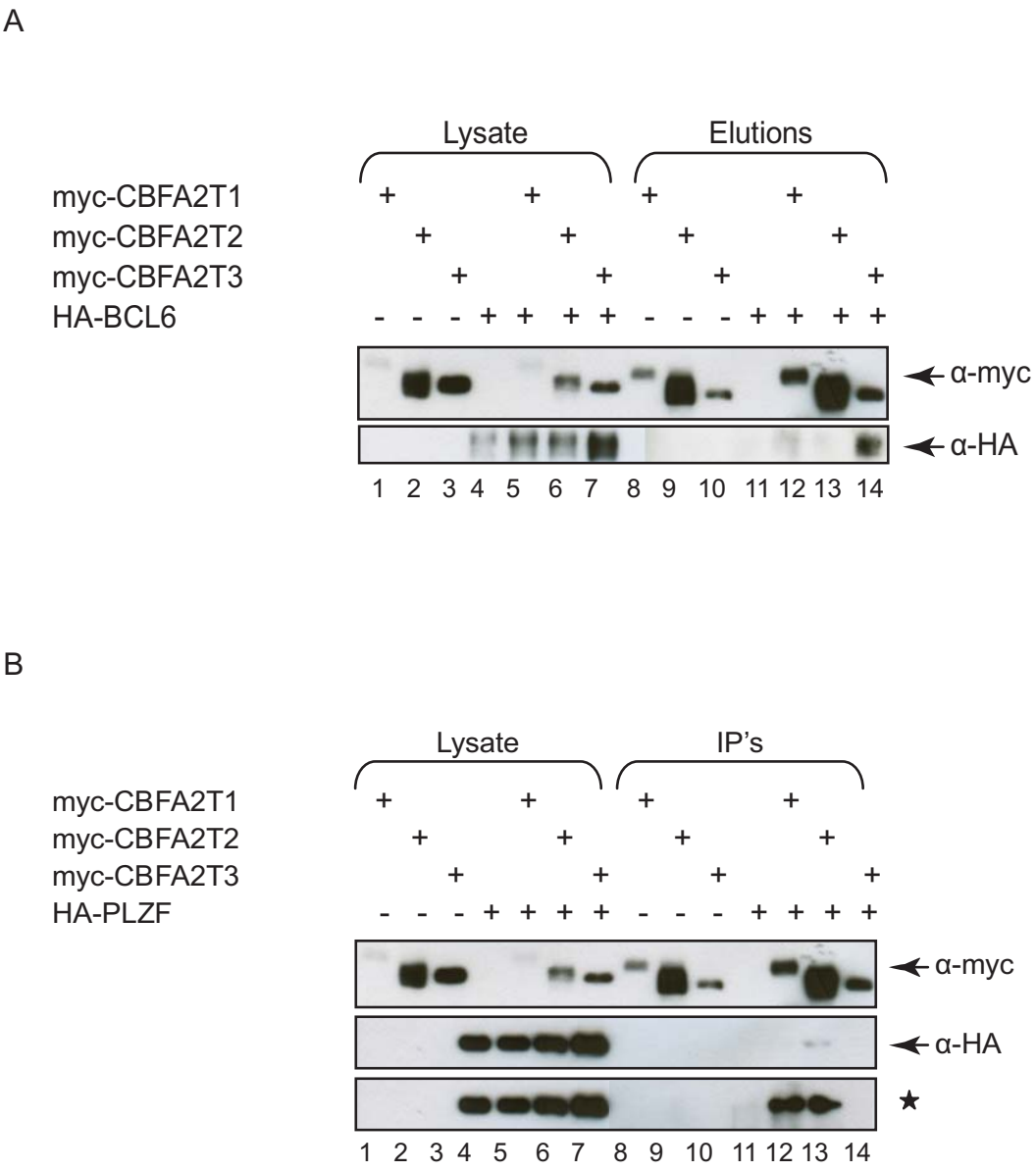

Figure 6.1. CBFA2T3 interaction with two DNA binding proteins: BCL6 and PLZF
HEK 293T cells were co-transfected with myc-CBFA2T family with HA-BCL6 or HA-PLZF DNA as shown shematically in figure **A** and **B** respectively. Cell lysates were subjected to immuno-precipitation with α-myc antibody 24 hours post transfection. 1% of lysate and 1/4th of elutions were western blotted with α-myc and α-HA antibodies. Net amount of DNA per transfection was kept similar for each transfection catagory by co transfecting appropriate amount of vector DNA. Asteric in **B** markes the exposure with α-HA antibody using ECL plus kit.

favourable sets of conditions. Immunoprecipitation of BCL6 proteins with CBFA2T family members are presented in Fig 6.1A, while Fig 6.1B shows immunoprecipitation with PLZF.

Despite the variable expression of CBFA2T family members in the inputs, equal level of CBFA2T1 and CBFA2T3 proteins were observed in elutions (Fig 6.1A panel α-myc). BCL6 protein interaction with CBFA2T3b protein was found stronger (lane 14) as compared to the interaction of BCL6 with the CBFA2T1 protein (lane 12) (Fig 6.1A panel α-HA). Although the expression of CBFA2T1 in the inputs was far less then the CBFA2T3, the immunoprecipitated amounts of CBFA2T1 and CBFA2T3 were found comparable. CBFA2T1 was used as a positive control as CBFA2T1 interaction with BCL6 and PLZF is already known. No interaction of BCL6 was observed with CBFA2T2 (lane 11).

Immunoprecipitation of PLZF with the CBFA2T family of proteins shows that the CBFA2T3b protein does not interacts with PLZF, as indicated in lane 14 of Fig 6.1B. On the other hand, a strong interaction of both CBFA2T1 and CBFA2T2 proteins with PLZF was observed. These interactions were confirmed in repeat experiments at least six times. A strong interaction of CBFA2T3 with BCL6 was consistently observed, while no interaction was seen with PLZF.

6.3.2 Expression analysis of endogenous BCL6 protein in a panel of breast cancer cell lines.

various studies have shown the expression of BCL6 protein in various erytheroid lineages or leukemic cell lines (Garcia et al., 2006) but the expression of BCL6 in breast

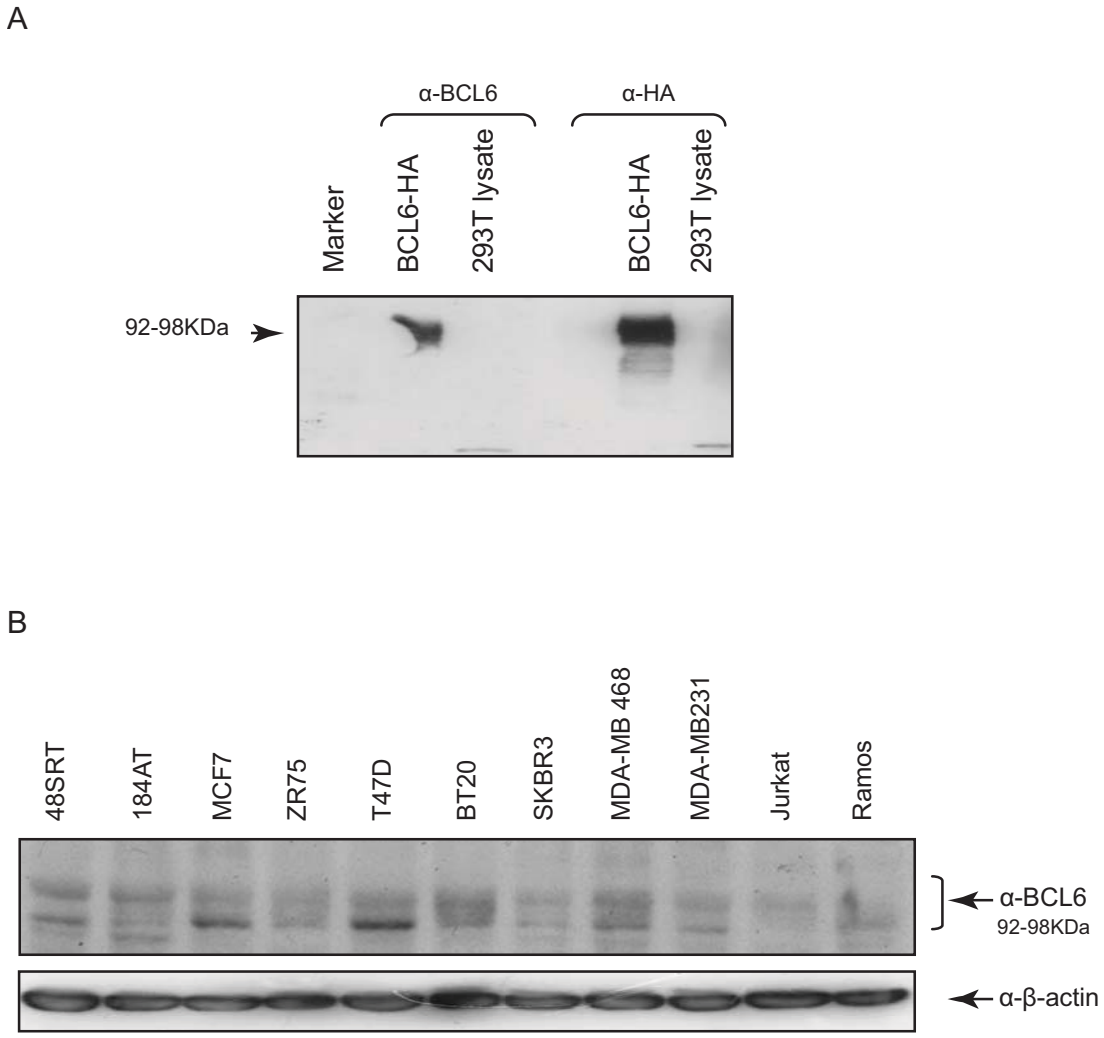

Figure. 6.2. BCL6 protein expression in different cell lines
A. α-BCL6 antibody specificity was determined by western blotting cell lysates from HA-tagged BCL6 and HEK293T with anti-BCL6 (GI 191E/A8) and anti-HA antibodies. **B.** Cell lysates from same number of cells from different cell lines were prepared. Equal amount of protein was blotted against anti-BCL6 antibody. β-actin was used as loading control. Note. several diffused bands were present dependending upon the status of BCL6 when run on 8% SDS page gel.

cancer cell lines has not been reported to date. Present study was conducted to determine if BCL6 expression in breast cancer cell lines is possibly related to the expression of CBFA2T3.

The specificity of the -BCL6 antibody was determined using western blot of cell lysates from HEK293T cells expressing HA-tagged BCL6 construct. HEK293T lysate was also included to test for non specific binding of the anti-BCL6 antibody. Transfected HA-BCL6 was detected by both anti-HA and the anti-BCL6 antibodies (GI 191E/A8) (Fig 6.2 A). No bands were observed in HEK293T cellular lysate. This may be due to low levels of expression of BCL6 protein in the currently analysed cell line. As anti-BCL6 antibody specifically detects only BCL6 protein this antibody can be used for further analysis.

Modifications of the BCL6 protein by acetylation and phosphorylation have been reported. BCL6 protein phosphorylation marks it for degradation during the cell cycle (Niu et al., 1998; Phan et al., 2007). These modifications result in an appearance of a diffuse protein band or a doublet when expressed *in vivo* or *ex vivo* (Niu et al., 1998; Pantano et al., 2006). Cellular lysates prepared from an equal number of cells among a panel of cell lines were western blotted against the anti-BCL6 antibody (Fig 6.2 B upper panel) and anti-β actin (lower panel). BCL6 antibody detected diffused bands ranging from 92-98 KDa as indicated in Fig (6.2 B). Human immortalized normal breast derived cell lines 48SRT and 184AT both express nearly equal amount of 92KDa and 98KDa BCL6 proteins. The cell lines MCF7 and T47D (with high CBFA2T3b expression) possessed high levels of BCL6 low molecular weight band. While BT20 and MDA-MB 468 (with low CBFA2T3 expression) express similar amount of high and low molecular

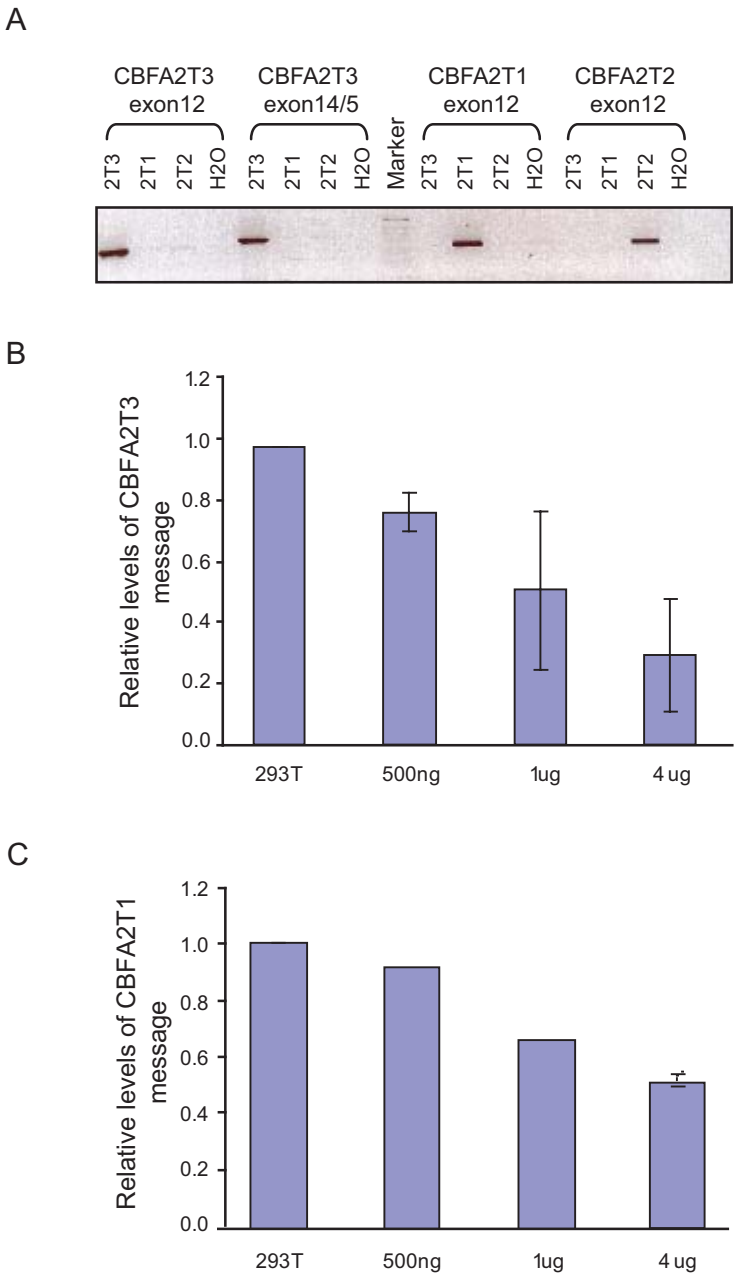

Figure 6.3. Effects of BCL6 on endogenous CBFA2T1 and CBFA2T3 message levels. **A.** Specificity of primers sets used for real time RT-PCR for CBFA2T family members was checked by optimizing conditions to specifically detect only transfected individual CBFA2T members. Increasing amount of HA-BCL6 was transfected into HEK293T cells in 6 well plate. HA-RBCL6 was used as negative control. 24 hours post transfection RNA was prepared from these cells. cDNA from the respective RNA was used for real-time RT-PCR for CBFA2T3 and CBFA2T1. *Cyclophilin A* was amplified as a internal control and all message levels were expressed relative to the levels of *Cylophilin A*.**B.** Histogram showing the effects of BCL6 on relative amount of CBFA2T3 relatized to293T. **C.** Effect of BCL6 on Relative amount of CBFA2T1. Bars represents ± SEM calculated from two independent experiments.

weight BCL6 proteins. Contrary to these a faint band corresponding to 98KDa was only observed in Jurkat cell line, whereas Ramos cell line had shown only the 92KDa protein band (Fig 6.2 B upper panel). Differences in the expression of both molecular sizes 92KDa and 98KDa proteins were observed in spite of equal loading which was evident from β-actin level. It is suggested that the variation in the intensity of the two bands reflects the BCL6 modifications present in that particular cell line which might have an impact on levels of CBFA2T3 expression or vice versa. This needs to be further investigated in the future.

6.3.3 Effects of overexpressed BCL6 on CBFA2T3 message.

Data from the current study has shown that BCL6 and CBFA2T3 proteins interact in immuno-precipitation experiments using the epitope tagged overexpressed HA-BCL6 and myc-CBFA2T3 proteins (Section 6.3.1 Fig 6.1A). *In silico* analysis of the putative CBFA2T3 promoter region shows the presence of the two potential BCL6 binding sites (results will be discussed later in section 6.3.8). Those findings led us to hypothesise the possible effects of overexpressing BCL6 on levels of CBFA2T3 message and protein.

To investigate effects of BCL6 on CBFA2T3, HEK293T cells were transfected with increasing amounts of BCL6 (Fig 6.3). Cells were harvested and resuspended into RNAlater (QIAGEN Ltd) for RNA stabilization 24 hours post transfection. Synthesised cDNA was analysed by for real-time semi-quantitative RT-PCR using primer sets able to specifically detect *CBFA2T1*, *CBFA2T2,* and *CBFA2T3* while *Cyclophilin A* amplification was used as internal control (Fig 6.3A). The levels of *CBFA2T1* and *CBFA2T3* message, relative to the *Cyclophilin A* control were calculated. For each set of transfection, either *CBFA2T1* or *CBFA2T3* the levels of the message are expressed relative to the non transfected control (Fig 6.3B and C). The data presented here is from

two independent experiments only, while the same trend was observed in 5-6 experimental repeats. A significant dose dependent decrease in the relative levels of *CBFA2T3* calculated by t test analysis (p= 0.002) was observed when the BCL6 amount was increased from 500ng to 4 μg. Similar effects were also noticed on *CBFA2T1* message with increasing amount of BCL6 (Fig 6.3B and C). A 2.5 fold decrease in *CBFA2T3* concentration was observed with an increase in BCL6 amount (Fig 6.3B). On the other hand, a 1.8 fold reduction in the relative concentration of *CBFA2T1* was seen with the increase in BCL6 concentration (Fig 6.3C). The results, suggest that the expression of *CBFA2T3* is at least, if not more, sensitive to repression by BCL6 than CBFA2T1. RBCL6 was used as a transfection control in concentration equivalent to the highest conc of BCL6 (4μg).

6.3.4 Overexpression of BCL6 protein results into reduction in endogenous levels of CBFA2T3 proteins.

The finding that BCL6 protein represses the expression of *CBFA2T3* levels developed the need to evaluate these finding at the protein level. Two approaches were used to examine the effects of BCL6 expression on endogenous CBFA2T3 protein. The first was to observe these effects at the single cell level through immunoflorescence studies. The second was to determine the results of CBFA2T3 repression at the protein level. The data from these experiments is presented in this section.

The MCF7 cell line, which expresses detectable levels of CBFA2T3 proteins, was transfected with HA-BCL6 construct. Cells were fixed and co-stained with immuno-fluorophore labelled anti-CBFA2T3 (RSH1) and anti-HA antibodies, 24 hour post transfection. Representative images from single and double labelled cells are presented

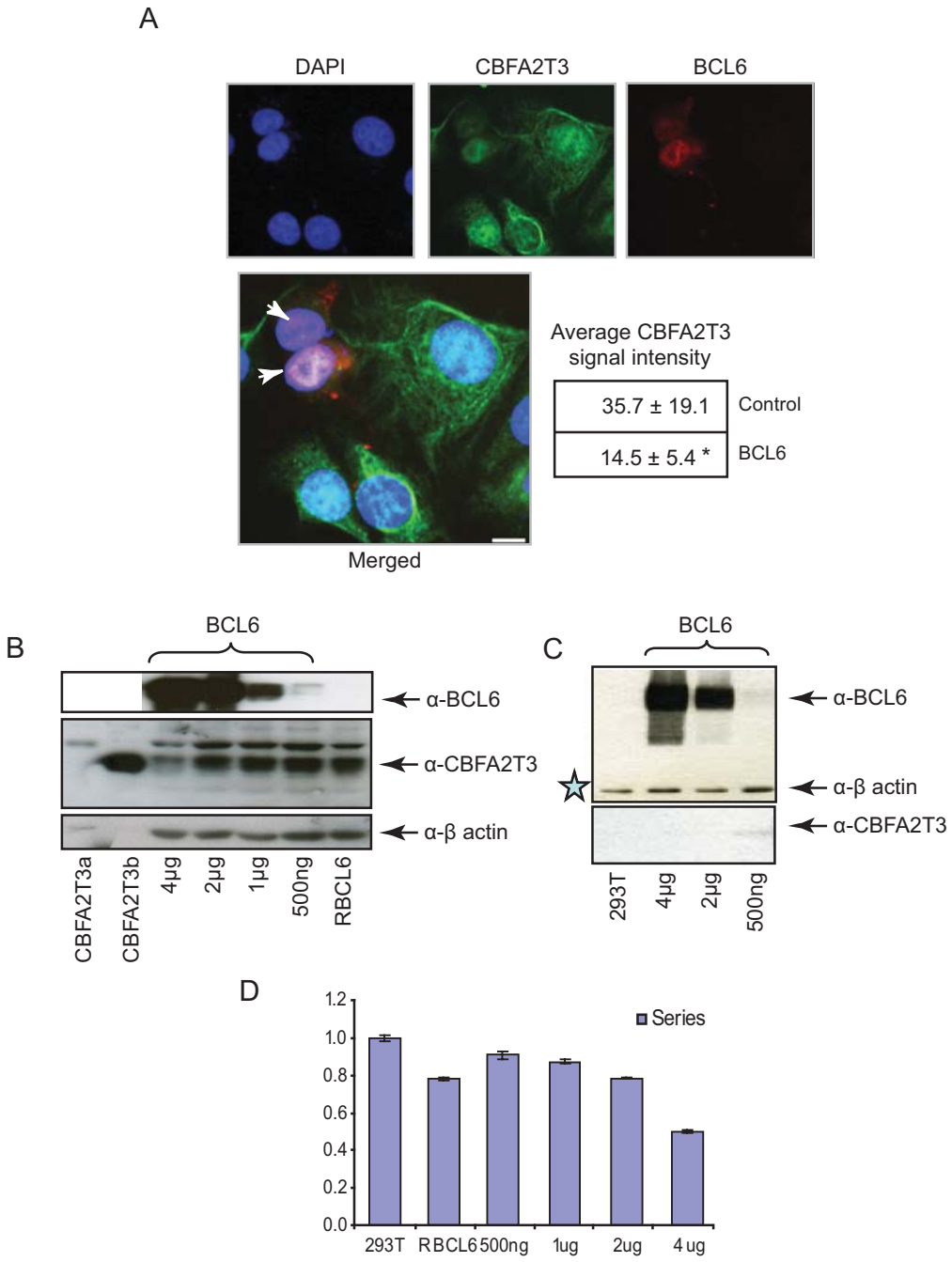

Figure. 6.4. Bcl6 repress endogenous CBFA2T3 proteins
A. HA-BCL6 was transfected transfected into MCF7, a cell line that expresses high level of CBFA2T3 proteins. Cells were fixed and co-stained with α-CBFA2T3 and α-HA antibodies. The avergae signal intensity for randomly picked BCL6 tansfected cells was quantified against non BCL6 transfected cells (n=10). *, Error represents 95% confidence interval. Scale bar, 10 µm. **B.** Increasing amount of BCL6-HA along with 4.0µg of RBCL6 was transfected into MCF7. Cell lysates were analysed for BCL6 effects on CBFA2T3 protein expression by western blot. β-actin was used as controle for equal loading. The effects of BCL6 overexpression on endogenous CBFA2T3 protein (**C)** and message (**D)** measured by real time RT-PCR in 293T cell line. Star in **C.** marks lower amount of protein in 293T lane.

(Fig 6.4A). CBFA2T3 proteins were found to have variable expression in MCF7 cell line. Cells were found with high cytoplasmic and nuclear CBFA2T3 expression, on the other hand some cells express low amount of nuclear CBFA2T3 (Fig 6.4A panel Green with α-CBFA2T3 antibody). Two cells with overexpressed HA-BCL6 protein are shown in Fig 6.4 (labelled red). It was noted that cells with overexpressed BCL6 protein, showed reduced levels of endogenous CBFA2T3 proteins, as was evident in both cells marked with arrow in merged image (Fig 6.4A merged). Similar trend was noticed during a series of experiments. Signal intensities for only 10 cells transfected with BCL6 labelled with Alexa-fluorophore 488 CBFA2T3 were measured from a single image (in order to reduce variation among different images) taken at confocal microscope using IMAGE J analysis software. These intensities were compared with the signal intensities of the non-BCL6 transfected cells from the same captured image. The differences among the signal intensities for these two categories were found significant (p= 0.0001). Average intensities for both sets of data were presented as a mean ±SE in the form of a table (Fig 6.4A).

Measurement of immunoflorescence of individual cells showed a decrease in endogenous CBFA2T3 proteins when BCL6 is overexpressed. To further confirm these results western blot analysis of the total protein lysates following HA-BCL6 expression was performed. MCF7 cells were transfected with increasing amounts of HA-BCL6 (Fig 6.4B) in 6 well plates. BCL6 in reverse orientation (RBCL6) was used as a control. Equal amount of cellular lysates were blotted against α-CBFA2T3 and α-HA antibodies (Fig 6.4B). A marginal decrease in levels of the CBFA2T3 “b” isoform was observed when 2ug of HA tagged BCL6 was overexpressed in the MCF7 cell line (Fig 6.4B). However, 4μg of transfected BCL6 resulted into a decrease in levels of both CBFA2T3 isoforms i.e. isoform “a” and isoform “b”, while β-actin level indicated approximately

equal loading for all treatments. Highest amount of RBCL6 (4μg) was overexpressed as a transfection control during the current experiment and there was no effect observed on endogenous CBFA2T3 levels (Fig 6.4B). These effects were also observed when BCL6 was overexpressed in independent experiments using the HEK293T cell line (Fig 6.4C). Although the level of endogenous CBFA2T3 proteins in HEK293T cell line was low, a decrease in CBFA2T3b level was observed from 500ng-1μg BCL6 treatment. CBFA2T3 expression in 293T lysate was not detected due to less protein loading (marked by star in Fig 6.4C). Effects of BCL6 on *CBFA2T3* concentration was further investigated in these samples by real-time RT-PCR. A consistent decrease in CBFA2T3 levels both at protein and message was observed in all experiments.

6.3.5 BCL6 protein along with the ER regulates CBFA2T3 promoter

6.3.5a Transcriptional repression of CBFA2T3 by BCL6

In silico analysis of CBFA2T3 " a" and "b" promoter region (3212 base pair upstream of the start site) revealed the presence of two putative BCL6 binding sites (Phan & Dalla-Favera, 2004) at -1222 and -2122 base pairs in the CBFA2T3b promoter region (Fig 6.5A). CBFA2T3a promoter has also shown the presence of one putative BCL6 binding site at -1971 base pairs upstream of the CBFA2T3a start site (reported through this thesis). But in the period under report only the effects of BCL6 on the CBFA2T3b promoter was investigated. Further upstream to these putative BCL6 binding sites at -2605 and -2903 base pairs from start site were present two putative estrogen receptor response elements (ERE) (Driscoll et al., 1998; Krieg et al., 2004). The sequences of these putative BCL6 binding sites (BSB1 and BSB2) along with ERE (ERE1 and ERE2) are shown in Fig 6.5A. Details of the plasmids were given in section 6.2.1 Material and Methods.

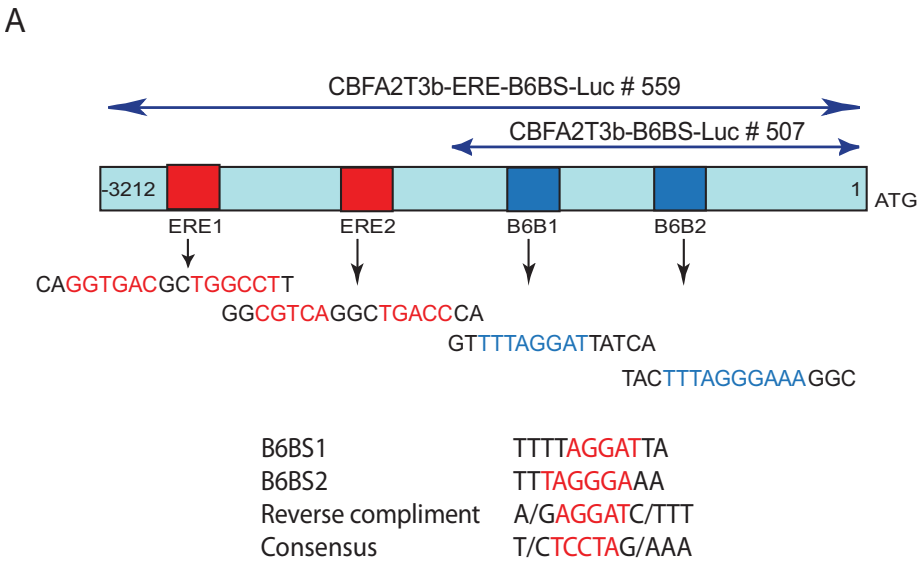
A
CBFA2T3b-ERE-B6BS-Luc # 559
CBFA2T3b-B6BS-Luc # 507
-3212
1
ATG
ERE1
ERE2
B6B1
B6B2
CAGGTGACGCTGGCCTT
GGCGTCAGGCTGACCCA
GTTTTAGGATTATCA
TACTTTAGGGAAAGGC
B6BS1 TTTTAGGATTA
B6BS2 TTTAGGGAAA
Reverse compliment A/GAGGATC/TTT
Consensus T/CTCCTAG/AAA

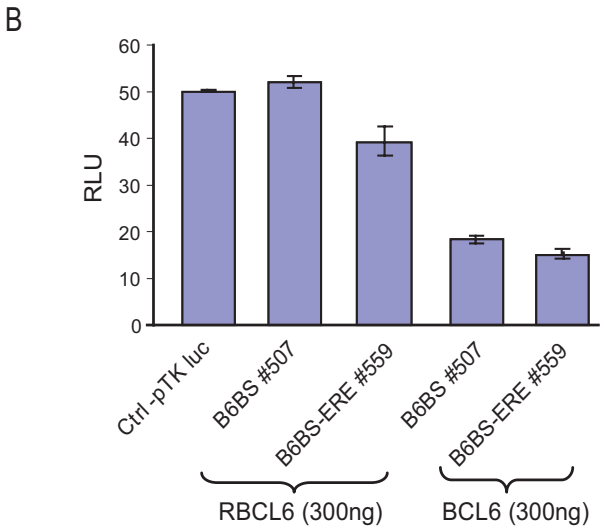
B
RLU
60
50
40
30
20
10
0
Ctrl -pTK luc
B6BS #507
B6BS-ERE #559
B6BS #507
B6BS-ERE #559
RBCL6 (300ng)
BCL6 (300ng)

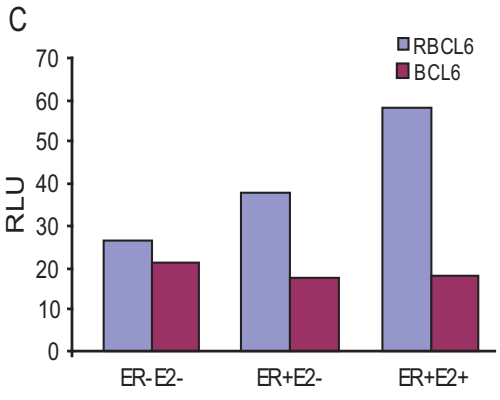
C
RLU
70
60
50
40
30
20
10
0
RBCL6
BCL6
ER-E2-
ER+E2-
ER+E2+

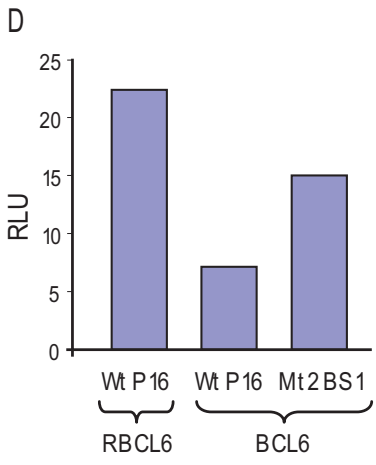
D
RLU
25
20
15
10
5
0
Wt P16
Wt P16
Mt2 BS1
RBCL6
BCL6

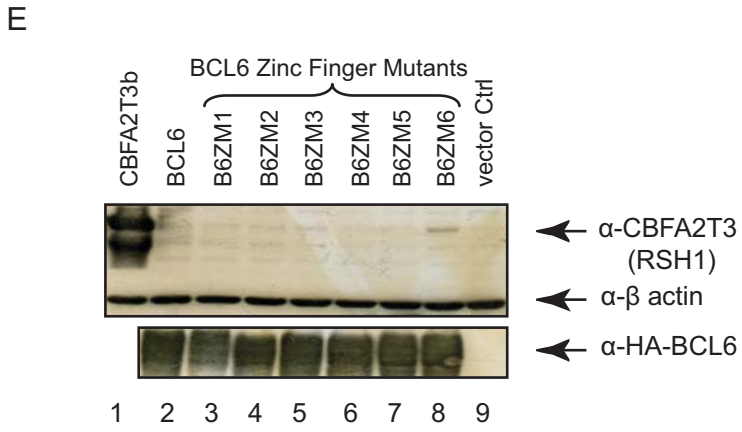

Figure 6.5. BCL6 along with ER regulates CBFA2T3b promoter activity. CBFA2T3b promoter region 3.2 Kb upstream of startsite was cloned from BAC 368P13 into pGL3 Basic upstream of the luciferase reporter gene. **A.** Schematic presentation of CBFA2T3 promoter region with marked putative ERE and BCL6 binding sites (reverse complimemtary sequences and consensus B6BS sequences were given. **B.** Effects of BCL6 on CBFA2T3 reporter in HEK293T cells was compared with reverse BCL6 and was presented as a reduced luciferase activity. **C.** Effects of BCL6 and ERα on the CBFA2T3 promoter stimulated with 2nM estradiol. **D.** B6BS1 in CBFA2T3 promoter was deleted by site directed mutagenesis. CBFA2T3b-ERE-B6Bs-Luc and CBFA2T3b-ERE-B6BS1 reporter constructs were co-transfected with RBCL6 and BCL6 in CHO cell line. Reporter activity was measured in terms of relative luciferase units (RLU) and plotted for each category. **E.** BCL6 zinc finger mutant constructs and full length BCL6 were overexpressed in HEK293T cell line. Lysates were probed with anti-HA, anti-CBFA2T3 and anti-β actin antibodies. Note that the data presented as **C, D** and **E** was from preliminary experiments which should be repeated in future studies.

To demonstrate if BCL6 can influence the transcription of CBFA2T3b dual luciferase assays were performed using the wild type CBFA2T3b promoter. Initial experiments were conducted on two promoter constructs, one with the putative BCL6 binding sites only (#507 B6BS) and second having both ERE and the putative BCL6 binding sites (#559 ERE-B6BS). Co-expression of BCL6 in both these CBFA2T3 promoter constructs resulted in a marked decrease in transcriptional activity (2.4 fold decrease in case of ERE-B6BS construct # 559), which was measured in terms of relative luciferase units (RLU) compared to the control transfection (Fig 6.5 B). RBCL6 showed marginal effects on luciferase activity. The results from the current experiment show that it is likely that BCL6 represses CBFA2T3 transcription by binding to these B6SB sites in CBFA2T3b promoter. In each experiment samples were transfected in duplicates and similar trend were observed in 3 independent experiments. The putative BCL6 binding sites in the CBFA2T3b promoter were further investigated by mutagenesis studies. Putative BCL6 binding site 1 (B6BS1) was deleted by site directed mutagenesis studies (performed by Dr David Millband) and was confirmed by sequencing.

Dual luciferase assay were performed to determined the effects of BCL6 and RBCL6 on CBFA2T3 wild type (P16Wt) and BCL6 binding site 1 deletion promoter (Mt2BS1) constructs and is presented in terms of relative luciferase units (Fig 6.5D). A 4 fold reduction in CBFA2T3 promoter activity was observed when BCL6 is co-expressed as compared to the RBCL6. A decrease (almost half) in repression of luciferase transcription mediated by BCL6 was observed when BCL6 binding site 1 was mutated (Fig 6.5D Mt2BS1). The current findings suggest that at least one of these BCL6 binding sites of the CBFA2T3b promoter are genuine and BCL6 mediate repression of CBFA2T3b transcription by binding to these sequences (TTTAGGAT in B6BS1) in CBFA2T3 promoter. Experiments to test the second site (B6BS2) were not completed

during the current study. The results presented are preliminary as the experiments were not repeated. Completion of these experiments for CBFA2T3b and CBFA2T3a promoter in future will help to determine the repression caused by BCL6 to CBFA2T3 transcription, which will lead to better understating of the CBFA2T3 transcription regulation.

6.3.5b CBFA2T3 transcription is up regulated by ER

To investigate the possibility that estrogen regulates CBFA2T3 transcription, CBFA2T3 promoter construct containing ERE-B6BS sites was co-transfected with either RBCL6 or BCL6, together with and without ERα. Cells were stimulated with 2nM oestradiol (E2) and ethanol (as a control) 8-9 hours post transfection. Transcriptional activity of the pGL2-promoter CBFA2T3-ERE-B6BS1-Luc reporter construct was measured 24 hour post-transfections by determining the dual luciferase activity for each treatment (Fig 6.5 C). Transactivation of CBFA2T3b promoter-Luc reporter was enhanced with the increased level of ERα (ER+ without E2) as compared to untreated sample (ERα E2-) in RBCL6 transfections. Transactivation of CBFA2T3b-promoter-Luc construct was found almost double when the cells were further stimulated with oestradiol (ERα + and E2+) as compared to ERα - and E2- cells with RBCL6 (series 1 RB6. Fig 6.5C). Repression to CBFA2T3-promoter-Luc activity was observed when BCL6 was co-expressed with CBFA2T3-promoter-ERE-B6BS-Luc sites (series 2 B6 Fig 6.5C). Increase in CBFA2T3b-promoter activity in the presence of ERα and oestradiol (E2) indicates a potential regulatory role of estrogen in CBFA2T3b transcription. Although the reported experiment was conducted on cells plated for 24 hours in charcoal-stripped media, transactivation of the CBFA2T3b-promoter construct, even in the absence of oestradiol, was observed. This indicates a need to repeat these experiments on cells cultured for longer time in charcoal-stripped media to reduce the levels of endogenous

estrogen. Furthermore, the effects of ERα in a dose dependent manner should be studied on the CBFA2T3b-Promoter-Luc construct.

6.3.5c BCL6 zinc finger 6 mutant enhances endogenous CBFA2T3 levels

The interaction of BCL6 with CBFA2T1 is mediated through the fourth zinc finger of BCL6 (Chevallier et al., 2004). BCL6 zinc fingers 3 to 6 are reported to also interact with HDAC5 and HDAC7 (Lemercier et al., 2002). BCL6 repression of its target genes is reported to be mediated through these zinc finger regions as abrogation of this repression was seen when these zinc finger regions were mutated, as ability of BCL6 binding to its targets was found lost in BCL6 zinc finger region mutants (Mascle et al., 2003). It is likely that interaction of BCL6 with the CBFA2T3 protein is also mediated through its zinc finger regions and this was investigated by determining the expression of CBFA2T3 proteins after overexpressing BCL6 proteins containing mutations in individual zinc finger regions.

BCL6 zinc finger mutants 1 to 6 (B6ZM1-B6ZM6 details given in material and method section 6.2.9) were transfected into HEK293T cells in 6 well plates. Equal amount of cellular lysates from these were western blotted against anti-HA and anti-CBFA2T3 (RSH1) antibodies. Analysis of cellular lysates shows a significant increase in endogenous CBFA2T3b protein with B6ZM6 expression (Fig 6.5 E lane 8). While no significant effect was seen with other mutants. β-actin and HA-B6ZM1-6 levels were found similar for all treatments. Current data further support the previous findings related to repressive effects of BCL6 on CBFA2T3 expression. De-repression of the CBFA2T3b reporter activity was seen when B6BS1 site in CBFA2T3 promoter was mutated (Fig 6.5 D). A marginal increase in the levels of endogenous CBFA2T3b was also noticed when mutant 6 carrying point mutations in two cysteines (CX2C) of BCL6

zinc finger regions was over expressed in HEK293T cells (Fig 6.5 E). Effects of zinc finger 6 mutant have clearly demonstrated that zinc finger 6 of BCL6 protein is responsible for binding to CBFA2T3 promoter.

6.3.6 Additive effects of CBFA2T3 proteins to BCL6 repression to *cyclin-D2*

BCL6 is a transcriptional repressor of many known genes like *TP53* (Phan & Dalla-Favera, 2004)*, MIP1α*, *Blimp1, Cyclin-D2* (Shaffer et al., 2000). BCL6 recruits corepressor such as CBFA2T1, a member of the CBFA2T family to mediate repression of its targets (Chevallier et al., 2004). We hypothesised that as CBFA2T3 is also a known transcriptional co repressor and is homologous to CBFA2T1, it also might be a component of BCL6 transcriptional repressor complex. As discussed in chapter 3 the CBFA2T3 isoforms "a" and "b" localized to different cellular compartments and therefore, we suggest that they have selective effects on BCL6 mediated repression.

To demonstrate the effects of the two isoforms of CBFA2T3 on BCL6 transcriptional activity the CBFA2T3 isoforms and CBFA2T1b used as a positive control were expressed in cells expressing a minimal amount of BCL6 (comparable to endogenous BCL6) and RBCL6. A schematic presentation of all treatments and western blot analysis of the expression of CBFA2T and BCL6 proteins are given in Fig 6.6A. Expression of CBFA2T members was fairly similar in BCL6 verses the RBCL6 (control) treatment. β-actin was found comparable in all sample. 24 hour post transfection the relative effects of the CBFA2T family of proteins on the expression of *Cyclin-D2* by real-time RT-PCR. *Cyclin-D2* concentration was normalized to *Cyclophilin A* conc (as an internal control). Normalized conc of *Cyclin-D2* in BCL6 treated cells relative to RBCL6 treatment was plotted in Fig 6.6B. A significant decrease in *Cyclin-D2* conc (p= 0.0023) was seen when the cells were co-transfected

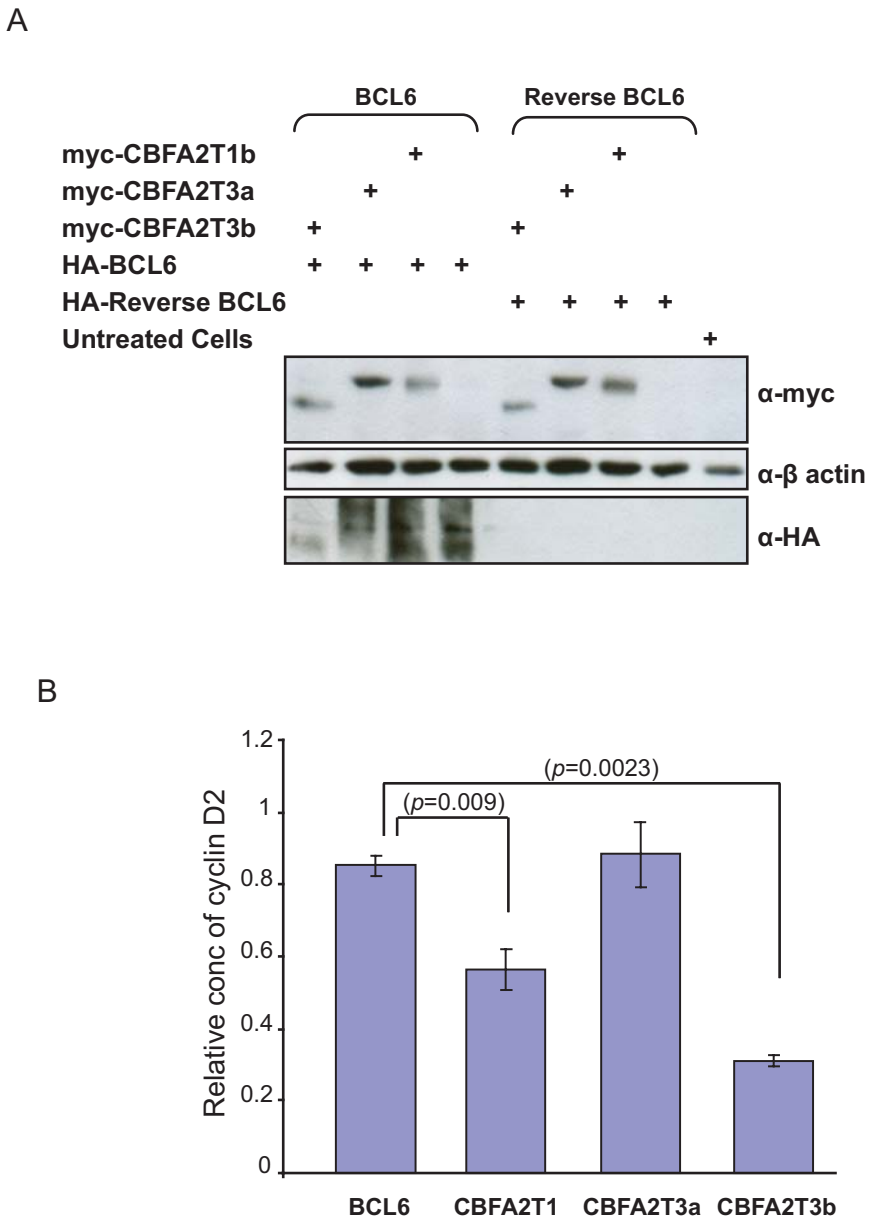

Figure 6.6 Additive effect of CBFA2T family proteins on BCL6 repression to its target *Cyclin D2*

HEK293T cells were transfected with respective plasmids for CBFA2T family plus reverse BCL6 or BCL6. cells were harvested 24 hour post transfection. 75% cells were kept for RNA extraction and rest for western analysis. **A.** Cell lysates were blotted against α-myc (CBFA2T proteins), α-HA (BCL6) and β actin antibodies. **B**. RNA from transfected cells (A) was subjected to reverse transcription followed by quantitative real-time RT-PCR for *Cyclin D2* and *Cyclophilin A* amplification as an internal control. Each treatment was replicated 3x and the experiment was repeated twice. *Cyclin D2* concentration for BCL6 treatments were relative to reverse BCL6 treatments. Statistical significance was calculated by applying student *t-test.*

with CBFA2T3b. While on the other hand no additive effect to BCL6 mediated repression was observed when CBFA2T3a was co-expressed (Fig 6.6B). These findings further support the data from the current study that CBFA2T3a is localized to cytosole and is functionally distinct from CBFA2T3b which is a known transcriptional co repressor. In other words, both the localization data and the differential affects of. CBFA2T3 isoforms on *Cyclin-D2* repression, suggests that CBFA2T3a is not part of the BCL6 repressor complexes and only the CBFA2T3b isoform interacts and functions as a co repressor with BCL6 transcriptional repressor complexes

6.3.7 Sin3A is a part of endogenous CBFA2T3 repression complexes

Sin3 proteins, mainly Sin3A and Sin3B, modulate the transcription of genes by interacting with other transcriptional repressors or co-repressors. The murine homologue of CBFA2T1 is known to associate with Sin3A and Sin3B (Dhanda et al., 2008; Lutterbach et al., 1998b). While ETO2 the murine homologue of CBFA2T3, does not interact with the Sin3A (Amann et al., 2001). No association of CBFA2T3 and mSin3A was detected by endogenous immunoprecipitation but overexpressed CBFA2T3 was shown to interact with Sin3B (Dhanda et al., 2008). Attempts were made to analyse interaction of endogenous Sin3A and CBFA2T3 proteins.

Alignment of the murine and human CBFA2T3 and human CBFA2T1 proteins is presented in Fig 6.7A. Reported regions of interaction to PLZF and Sin3A were marked as red and blue boxes respectively. Blue box marks the minimal region mediating CBFA2T1 interaction with Sin3A (Amann et al., 2001). The anti-CBFA2T3 RSH1 antibody available in laboratory can specifically detect and immunoprecipitates endogenous CBFA2T3 proteins. CBFA2T3 immune complexes were immunoprecipitated from MCF7 cell line by using RSH1 and pre immune sera. Cellular

lysates (2% of the total lysate as an input) and immunoprecipitates were western blotted against anti-CBFA2T3 and anti-Sin3A antibodies (Fig 6.7). A band of specific size (140 kDa) was detected with anti-Sin3A antibody. Due to the high concentration of Sin3A in inputs lower exposure is presented here. A Pre-immune serum was used as a negative control. No binding of CBFA2T3 or Sin3A was seen with the negative control (data not shown). Current data shows that CBFA2T3 proteins immunoprecipitated from MCF7 cell line does interact with Sin3A. Experiments with overexpressed CBFA2T3b and Sin3A will further gave insight on these repressor complexes.

The data regarding CBFA2T3b (overexpressed) interaction with various class I and class II type HDAC proteins is already available (Amann et al., 2001). Immunoprecipitation experiments were conducted to determine if CBFA2T3a (full length) interacts with the various HDAC proteins. Although data was available for HDAC1, 2, 3, 4 and 6 interactions with CBFA2T3a (Hoogeveen et al., 2002) however, this was based on ectopic expression of the shorter version of the CBFA2T3a protein, the previous findings are summarized in Fig 6.8B.

Immunoprecipitation of CBFA2T3a full length with ectopically expressed class I and class II HDAC proteins demonstrated CBFA2T3a interacts with class I HDAC 1, 2 and 3 during current study. Previous data from Hoogven et al (2002) has shown that CBFA2T3a (shorter version) does not interacts with cytoplasmic HDAC4 (Hoogeveen et al., 2002). Contrary to the previous findings, CBFA2T3a full length interacts with both class II type HDAC4 and HDAC5 proteins (Fig 6.8A). These results further support the finding that the full length CBFA2T3a localizes to the cytoplasmic fractions as shuttling between nucleus to cytoplasm is a well known characteristic of both HDAC4 and HDAC5 (Wade, 2001). No interaction of HDAC6 and HDAC7 with

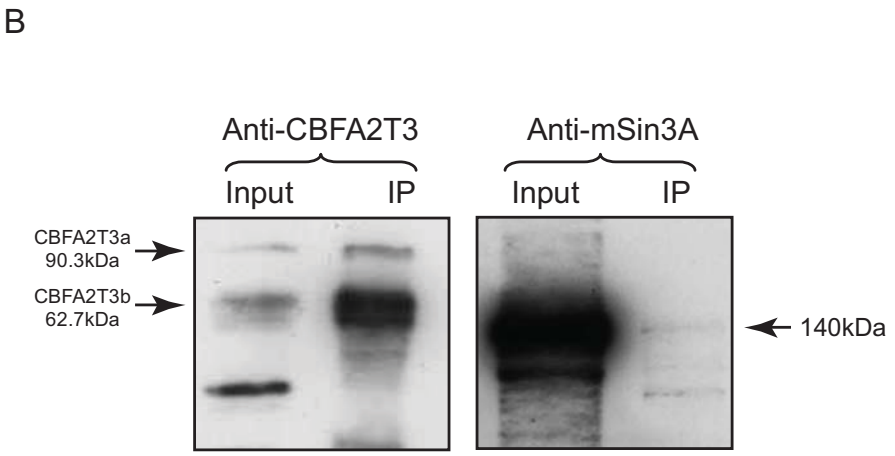

Figure 6.7 CBFA2T3 interacts with endogenous Sin3A protein.
A. Alignment of CBFA2T3 with murine homologue mETO2 and CBFA2T1. Protein sequences from three CBFA2T family members were aligned using Clustal-X and maps were generated using ghost script program. Homology among these proteins is marked by star above the sequences or graphed as curves below the amino acid sequences. The region previously reported in mouse involved in interaction with PLZF and SIN3A are marked as red and blue boxes. Orange line marked HHR domain of CBFA2T family proteins. **B.** Endogenous CBFA2T3 proteins were immunoprecipitated from the MCF7 cell line using anti-CBFA2T3 (RSH1) antibody. Lysates and elutions were probed with RSH1, anti-mSin3A antibodies. Western blot probed with anti-mSin3A antibody along with RSH1 were shown here. rabbit pre-immune sera was used as IP's control the control was clear, no binding of any back ground was seen (data not presented).

A

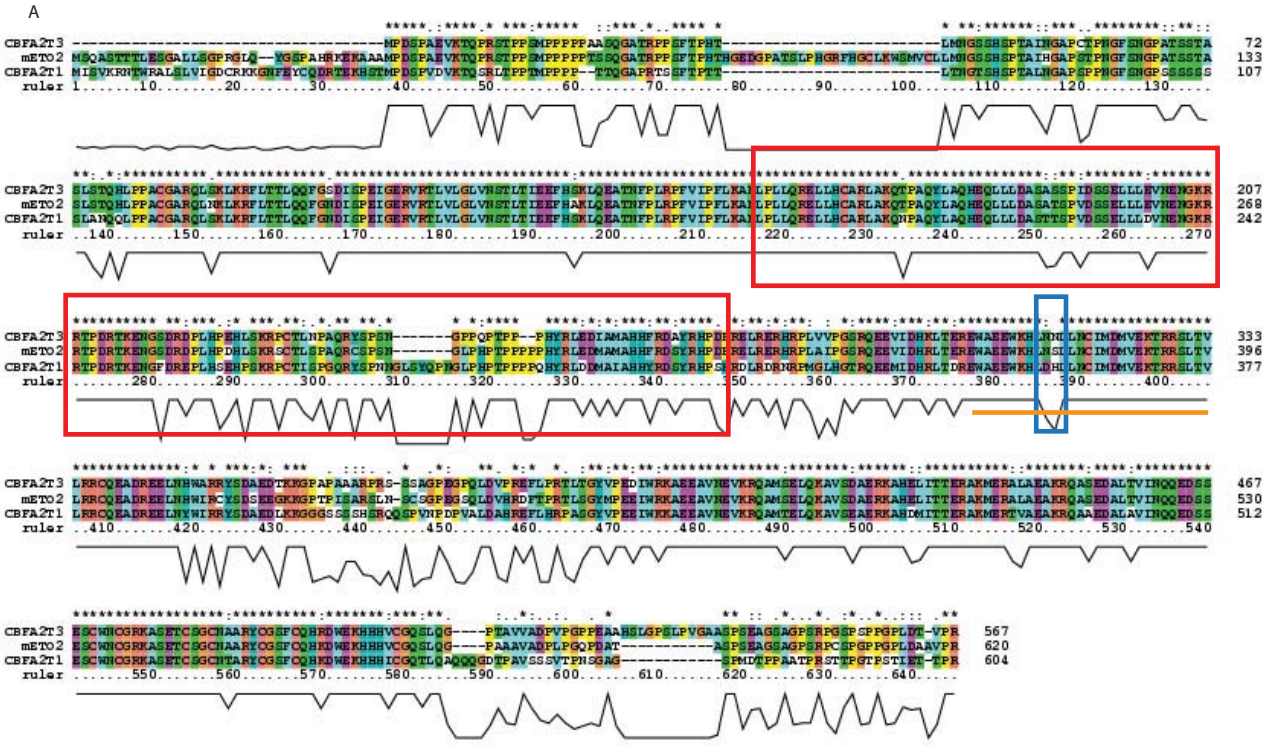

A

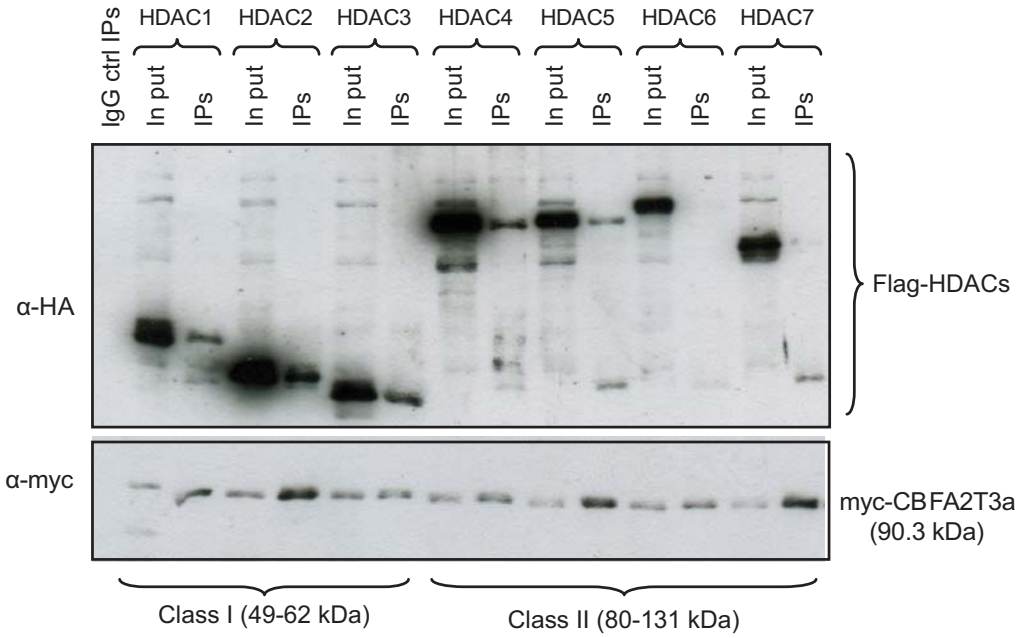

B

	HDAC1	HDAC2	HDAC3	HDAC4	HDAC5	HDAC6	HDAC7
CBFA2T3a (Hoogven *et al*)	+	+	+	-	NT	-	NT
CBFA2T3a present study	+	+	+	+	+	-	week
CBFA2T3b (Amann *et al*)	+	+	+	-	-	+	-

Figure 6.8 CBFA2T3a interacts with Class I and Class II type HDAC proteins.

A. myc-CBFA2T3a and HA-HDAC1-7 were co transfected in HEK 293T cells. Cells were lysed in equal volume of lysate 24 hours post transfection and were subjected to immuno-precipitation with anti-myc conjugated protein G beads for 3 hours. 1% lysate (Input) and 1/3 of elutions (IP's) for each HDAC set were blotted against anti-myc and anti-HA antibodies. **B.** Summary of CBFA2T3a and CBFA2T3b interaction with class I (1, 2, 3 and 8) and class II HDAC's (4, 5, 6 and 7). NT specifies (not tested), while - markes no interaction.

CBFA2T3a was observed in this study (Fig 6.8A). The data regarding all HDAC interaction with CBFA2T3a and b are summarized in a table (Fig 6.8B).

6.4 Discussion

CBFA2T3 is a known transcriptional co-repressor, which interacts with a novel zinc finger protein, ZNF652 (Kumar et al., 2006). CBFA2T3 interaction with two other known zinc finger containing DNA binding proteins, BCL6 and PLZF was analysed by immunoprecipitation studies conducted during the period under report. Experiments were conducted for two ways immunoprecipitation. HA-BCL6 immunoprecipitation were found unsuccessful might be due to the folding of the protein which might had made HA-BCL6 inaccessible by antibodies. Final experiments were conducted using myc-CBFA2T3b immunoprecipitation followed by western blotting for both tagged proteins. Data shows CBFA2T3b interaction with BCL6 while no interaction was observed with PLZF (Fig 6.1A and B). This was functionally confirmed since CBFA2T3b has shown an additive effect on transcription repression of the BCL6 target genes *Cyclin-D2* (Fig 6.6B). In addition, BCL6 represses transcription of *CBFA2T3* (Fig 6.3B). Thus BCL6 not only recruits CBFA2T3b for the repression of its targets but itself also represses CBFA2T3 transcription. A strong interaction of BCL6 protein with CBFA2T3b protein was found during this study (Fig 6.1 A). BCL6 is a known partner for CBFA2T1, a member of the CBFA2T family proteins. BCL6 interaction with CBFA2T1 is through its zinc finger 4 region and NHR2 domain of CBFA2T1 protein. This interaction has additive repressive effects on known targets of BCL6 (Chevallier et al., 2004). CBFA2T1 was also reported to interact with PLZF (Melnick et al., 2000b). In contrast to this no interaction of PLZF was found with CBFA2T3b during this study (fig 6.1B).

BCL6 and PLZF together with CBFA2T1 form a transcriptional repressor complex and recruits additional transcriptional co-repressors like NCoR, SMRT (Melnick et al., 2002), Sin3A and B , CBFA2T1 (Lutterbach et al., 1998b) and various HDAC's (Lemercier et al., 2002) to repress their target genes. The interaction of the CBFA2T1 with all these transcriptional corepressor and histone deacetylases has been reported (see section 1.51 Chapter 1). Interestingly, the Sin3A and B form complexes with CBFA2T1 (Lutterbach et al., 1998b), while the murine homologue of CBFA2T3 was reported to have no interaction with Sin 3A (Amann et al., 2001). Contrary to the above findings, human CBFA2T3 with Sin3A were co-immunoprecipitated from the MCF7 cell line during this study (Fig 6.7), although a very week band was seen in the immunoprecipitates. Detection of various proteins like HDAC, Sin3A from endogenous immune complexes was not possible due to the low sensitivity of available antibodies. Due to the above reason it was impossible to conduct two ways IP's. Future experiments with overexpressed human Sin3A and CBFA2T3b will gave some insight on these immune complexes.

Interactions of HDAC1, 2, 3, 6 and 8 with CBFA2T3b was already published (Amann et al., 2001). Some data regarding HDAC interaction with CBFA2T3a was also available, but the experiments used CBFA2T3aT (the shorter version of CBFA2T3a). CBFA2T3a interaction with Class I (HDAC1, 2, 3 and 8) and Class II (HDAC4, 5, 6 and 7, defined and differentiated by the presence of N-terminus sequences), has been checked through immunoprecipitation experiments during this study. A strong interaction of HDAC4 and HDAC5 with CBFA2T3a was found. CBFA2T3aT (shorter version of CBFA2T3) was earlier reported to interact with HDAC 1, 2 and 3 of class I type (Hoogeveen et al., 2002). Contrary to Hoogeveen et al (2002) interaction of CBFA2T3a with HDAC1, HDAC2 and HDAC3 class I and HDAC4 and HDAC5 class

II type HDACs was found in the present study (Fig 6.8). Wade et al (2001) have reviewed the shuttling of HDAC4 and 5 from nucleus to cytoplasm as a result of a differentiation signal. For instance, phosphorylation of HDAC4 by calmodulin-dependent kinase (CaMK) leads to HDAC4 binding to the 14-3-3 protein, which results into its export from the nucleus. In the cytoplasm HDAC4 was phosphorylated at different site by Ras signalling pathways, which lead to its active transport back into nucleus to repress differentiation related targets (Grozinger & Schreiber, 2000; McKinsey et al., 2000; Wade, 2001). Previous findings about CBFA2T3a localization has shown that 10-12% of the cells overexpressing CBFA2T3a showed cytoplasmic localization or to both cytoplasm and nucleus, while in 85-90% cells CBFA2T3a was found confined to cytoplasm only (Fig 3.7B Chapter 3). These findings were further supported by CBFA2T3a interaction with Class II type HDAC4 and HDAC5 known for there nuclear cytoplasmic shuttling characteristics.

BCL6 is a transcriptional repressor known for the repression of its targets involved in various cellular processes like proliferation, differentiation (Shaffer et al., 2000) and apoptosis (Baron et al., 2007). To date many targets of BCL6 have been identified. BCL6 recruits many proteins or co-factors to repress its targets, CBFA2T1 is one of them (Chevallier et al., 2004). During this study we found CBFA2T3b as a cofactor for BCL6 mediated repression to *Cyclin-D2* (Fig 6.6), while no effect was seen when CBFA2T3a was co-expressed with BCL6 protein. This finding not only indicates the differential behaviour of CBFA2T3 isoforms due to the differential localization in cells, inspite of high homology in structure but also showed the selective recruitment of CBFA2T3 isoforms by BCL6 proteins to repress *Cyclin D2* transcription.

BCL6 repression to the target genes is mediated through its binding to specific sequences present either in their promoter region or in entire genome (Baron et al., 2002; Shaffer et al., 2000; Tunyaplin et al., 2004). BCL6 protein was known to suppress *Tp53* expression (Phan & Dalla-Favera, 2004). Suppression of BCL6 expression by siRNA leads to an increase in massage and protein levels of p53 (Phan & Dalla-Favera, 2004). BCL6 not only regulates p53 levels but also itself is regulated by p53 (Margalit et al., 2006). CBFA2T3b was found as a target for BCL6 during the current study. Repression of *CBFA2T3* message and protein was seen following expression of increasing amount of the BCL6 (Fig 6.3 and 6.4). Two potential BCL6 binding sites (B6BS) were found in the CBFA2T3b promoter region (Fig 6.5 A). Reporter assays have shown the repression of CBFA2T3b promoter by BCL6 (Fig 6.5). Mutation of BCL6 binding site B6BS1 (TTTAGGAT) in CBFA2T3b promoter region has reduced BCL6 mediated repression by half. In addition, induction of CBFA2T3b expression was observed when ZFM6 (zinc finger mutant 6 for BCL6) was expressed in HEK293T cells (Fig 6.5 E). As mentioned earlier, BCL6 contact with its targets and other repressor proteins are mediated by its zinc finger regions. Chevallier et.al (2004) have earlier reported BCL6 interaction with CBFA2T1 through its zinc finger 4 (Chevallier et al., 2004). Data from the current study has shown the repression of CBFA2T3 protein by BCL6 mediated through its binding with zinc finger 6. Point mutations in two cysteines of zinc finger 6 results in abrogation of this repression, which was evident by an increase in endogenous CBFA2T3b protein by overexpressing BCL6-ZFM6 in HEK293T cells (Fig 6.5 E). There is likely hood that BCL6 ZFM6 is competing with the endogenous BCL6 for its repression to CBFA2T3 protein.

Increased expression of BCL6 protein is reported in 16% of breast cancers and is associated with Cyclin-D1, p53 and HIF-1α overexpression (Bos et al., 2003). Another

study by Logarajah S. et. al (2003) has shown the overexpression of BCL6 in 68% of high grade aggressive breast ductal carcinomas. Furthermore they have shown that BCL6 prevents expression of milk protein β-casein and duct formation when overexpressed in mammary epithelial cell line EpH4 (Logarajah et al., 2003). BCL6 is also reported to repress AP-1 mediated activation of inflammatory genes (Vasanwala et al., 2002). Another report has suggested a possible interaction of AP-1 with BCL6 in breast cancer patients resistant to tamoxifen (Altundag et al., 2004). 75% of the breast cancer tumours are found positive for ER expression. ER and AP-1 interaction are reported to regulate many genes involved in cellular process as proliferation, differentiation, motility and apoptosis. *In silico* analysis has shown the presence of two putative canonical estrogen response elements (ERE) in the CBFA2T3 promoter region (Fig 6.5 A). Further the effect of BCL6 has been demonstrated on CBFA2T3b promoter containing ERE sites. A 3 fold increase in promoter activity was seen when reverse BCL6 is co overexpressed with ER and stimulated with oestradiol as compared to BCL6 expressing cells (Fig 6.5 C). Previous data from current study has also shown that CBFA2T3 expression is high in cell lines positive for ER indicating a possible role of ER in CBFA2T3 regulation. Careful analysis of the CBFA2T3b promoter region has indicated the presence of putative AP-1 binding site (TGAcGC / TGAcgctgGC) hidden inside the ERE1 site (GGTGACGCTGGCCT) in CBFA2T3b promoter (Fig 6.5 A). Present data has shown the regulation of CBFA2T3b transcription by BCL6 and also has indicated a putative involvement of ER and AP-1 transcription factors in CBFA2T3b regulation. To conclusively demonstrate the role of these elements in CBFA2T3b regulation, experiments in future are required to be repeated in charcoal-striped media or BCL6 null cell.

Chapter 7 - General discussion and concluding remarks

Cancer is a complex of diseases characterized by proliferation of abnormal cells which arise from genetic alterations either due to the effects of environmental carcinogen or from the normal metabolic processes. These cancerous cells are able to bypass the cellular processes like apoptosis and possess the ability to invade tissues resulting in the metastasis.

There were 100,000 new cases of cancer diagnosed in Australia in 2005. This number is growing by more then 3000 cases per year. Breast cancer is a major cancer in females, 12,170 cases (incidence rate in 2005) accounted for over 27% of all diagnosed cases of cancer. During 2006-2010 breast cancer increased at a rate of 0.1% per year resulting in 12,773 in 2006 to 14,017 cases till 2010, an increase of 311 new cases per year (Cancer in Australia: an overview, 2008 by Australian Institute of Health and Welfare: AIHW, Statistics and Information agency based on AACR data). Breast cancer was the most common cause of cancer related deaths (2707 deaths) in females until 2005. However, the death rate from breast cancer decreased by -0.3 since this time due to the availability of new therapeutics.

Loss of heterozygosity (LOH) of various regions harbouring tumour suppressor alleles is the most common chromosomal change observed among sporadic breast cancer. LOH of chromosome band 16q was reported in 37-67% of primary sporadic breast cancer cases. CBFA2T3 was identified as a breast tumour suppressor gene from chromosome band 16q24.3 (Powell et al., 2002). CBFA2T3 is a member of CBFA2T family of

homologous proteins together with CBFA2T1 and CBFA2T2. These proteins are comprised of four domains NHR1-4, called nervy domains due to their homology to the nervy protein of Drosophila. CBFA2T1 and CBFA2T3 are known transcriptional co-repressor proteins that together with other known DNA binding proteins (for example BCL6, PLZF, Gfi1 and ZNF652) binds to the promoters of target genes to repress transcription (Chevallier et al., 2004; Kochetkova et al., 2002; Kumar et al., 2008). The Majority of available information on these repression complexes concerns CBFA2T1 but is also relevant to CBFA2T3 due to their shared high homology. A little is known about the expression and function of CBFA2T3 isoforms in breast cancer development. The worked described in this thesis was undertaken with the objective of examining the location and function of CBFA2T3 isoforms. These studies will contribute to an understanding of the CBFA2T3 functional pathways.

CBFA2T3 has two isoforms, CBFA2T3a and CBFA2T3b, our polyclonal antibodies were able to detect these endogenous isoforms. Variable expression of CBFA2T3 proteins was observed among a panel of cell lines and this was consistent with the variation in *CBFA2T3* mRNA expression. In a small panel of cell lines, CBFA2T3 expression was found high in the ER+ cell lines and found low in ER- cell lines. The results presented in this thesis show that the accepted NCBI sequences for CBFA2T3a isoform notated as CBFA2T3aT was incomplete. In silico and RT-PCR approaches established a new sequence of CBFA2T3a that extended the transcript further 5' resulting in a new transcription start site and an extended protein isoform of 853aa. The size of this extended protein (90 kDa) was consistent with that of the endogenous isoform detected by our anti-CBFA2T3 antibodies.

A distinct cytoplasmic localization pattern of CBFA2T3a full length was observed which contrasts with the known nucleolar localization of CBFA2T3aT (Hoogeveen et al., 2002) (from NCBI data base). Immunofloresent studies of exogenously overexpressed CBFA2T3 isoforms determined that CBFA2T3a localize to the cytoplasm, while CBFA2T3b showed nuclear speckle localization (Fig 3.7). A diffuse to distinct nuclear speckle localization pattern was observed for CBFA2T3b proteins supporting its function as a transcriptional corepressor. These results were further confirmed by cellular fractionation studies of different breast cancer cell lines showing differential compartmentalization of the CBFA2T3a to cytoplasmic fractions and CBFA2T3b to the nuclear extracts (Fig 3.6).

Localization pattern of the two CBFA2T3 isoforms was likely to be attributed by the elements in the extra sequence of the N-terminal region of the exon 1 or the additional exon 3 regions which are present in CBFA2T3a isoform but are missing from CBFA2T3b. The remaining sequences of the CBFA2T3 isoforms are identical (Fig 3.1).

During these CBFA2T3 isoform studies, it was noted that there existed a potential localization to centrosomes. This was further investigated by constructing GFP-myc tagged CBFA2T3a *N-terminal* constructs. These GFP fused *N-terminal* sequences of CBFA2T3a (LS1 and LS2) showed a localization to centrosomes which was confirmed by co-localization studies with other centrosomal markers γ-tubulin, glutamylated γ-tubulin and HSAS-6 proteins (Fig 4.10 and 4.11). These results were further investigated by immunoprecipitation studies on endogenous and over-expressed CBFA2T3 proteins showing interaction and co-localization of CBFA2T3a, LS1 and LS2 with γ-tubulin (Fig 4.3 and 4.4).

Knockdown of both CBFA2T3 isoforms using three different shRNA's and siRNA shows a significant increase in cells with centrosomal abnormalities and an associated increase in metaphase abnormalities (Fig 4.6 and 4.7). Changes into the B23 and cyclin E, cellular proteins involved with centrosomal duplication cycle and G1-S phase transitions respectively were also observed in CBFA2T3 specific shRNA treatments compared with the scrambled or mock treatment (Fig 4.13). Attempts were made to do localization studies of endogenous CBFA2T3 after knockdown. Marked reduction in cytoplasmic and nuclear CBFA2T3 levels were observed. Present findings have suggested a potential role for CBFA2T3a in centrosomal duplication.

The relationship of CBFA2T3 expression with various markers and clinical characteristics of breast cancer was then determined and are given in Chapter 5. CBFA2T3 proteins were highly expressed in the cells of the epithelial lining of normal breast ducts. A decrease in CBFA2T3 nuclear and cytoplasmic expression was observed in breast tumours. Data for known tumour markers was analysed using cut off value of greater than 70% positive cells for nuclear and for cytoplasmic CBFA2T3 expression. A significant correlation of CBFA2T3 cytoplasmic expression with TNM staging and centrosome amplification was observed (Table 5.5). A significant inverse correlation of molecular subtypes, histological stage of the tumour and HER-2 was seen with CBFA2T3 nuclear expression (Table 5.4). It has been reported that CBFA2T3b interacts with ErbB4/ HER-4, another member of the HER family of proteins (Linggi & Carpenter, 2006). Since HER family proteins are known to exist in the form of homo and hetrodimers it is possible that CBFA2T3 is indirectly is involved in HER-2 pathways (Table 5.4). Future studies on TMAs from a larger cohort of breast tumours together with patient survival data is required to further support the findings reported in

this thesis. The current data suggests a subdivision of HER-2 tumours where those with CBFA2T3 expression are associated with better prognosis. Future studies will confirm these findings and will provide further data regarding use of CBFA2T3 as a prognostic marker.

CBFA2T1 and CBFA2T3 are known transcriptional co-repressor proteins. Different DNA binding proteins like BCL6, PLZF, Gfi1 were known partners of CBFA2T1 repressor complexes (Chevallier et al., 2004; McGhee et al., 2003), while ZNF652 was identified to preferentially interact with CBFA2T3 (Kumar et al., 2008; Kumar et al., 2006). CBFA2T3 interaction with BCL6 and PLZF were investigated during the current study (Fig 6.1). Data from this thesis shows CBFA2T3 interacts with the BCL6 protein, while no interaction with PLZF was observed. During this study real-time RT-PCR established that the nuclear localized isoform CBFA2T3b has a repressive effect on the BCL6 target *cyclin D2,* while the cytoplasmic localized CBFA2T3a isoform has no effect on expression of BCL6 targets (Fig 6.6). BCL6 was also identified as a repressor of CBFA2T3 transcription during the current study. *In silico* analysis of the CBFA2T3b promoter shows the presence of two putative BCL6 binding sites. Reporter assays shows repression of CBFA2T3b transcription is mediated through at least one of these BCL6 binding sites (Fig 6.5). Further characterization of the CBFA2T3 repressor complexes established that Sin3A is present, in contrast to the previously published data (Amann et al., 2001).

In summary this thesis describes novel distinctive features of the two CBFA2T3 isoforms which helped and are summarized in a model of CBFA2T3 function (Fig 7.1).

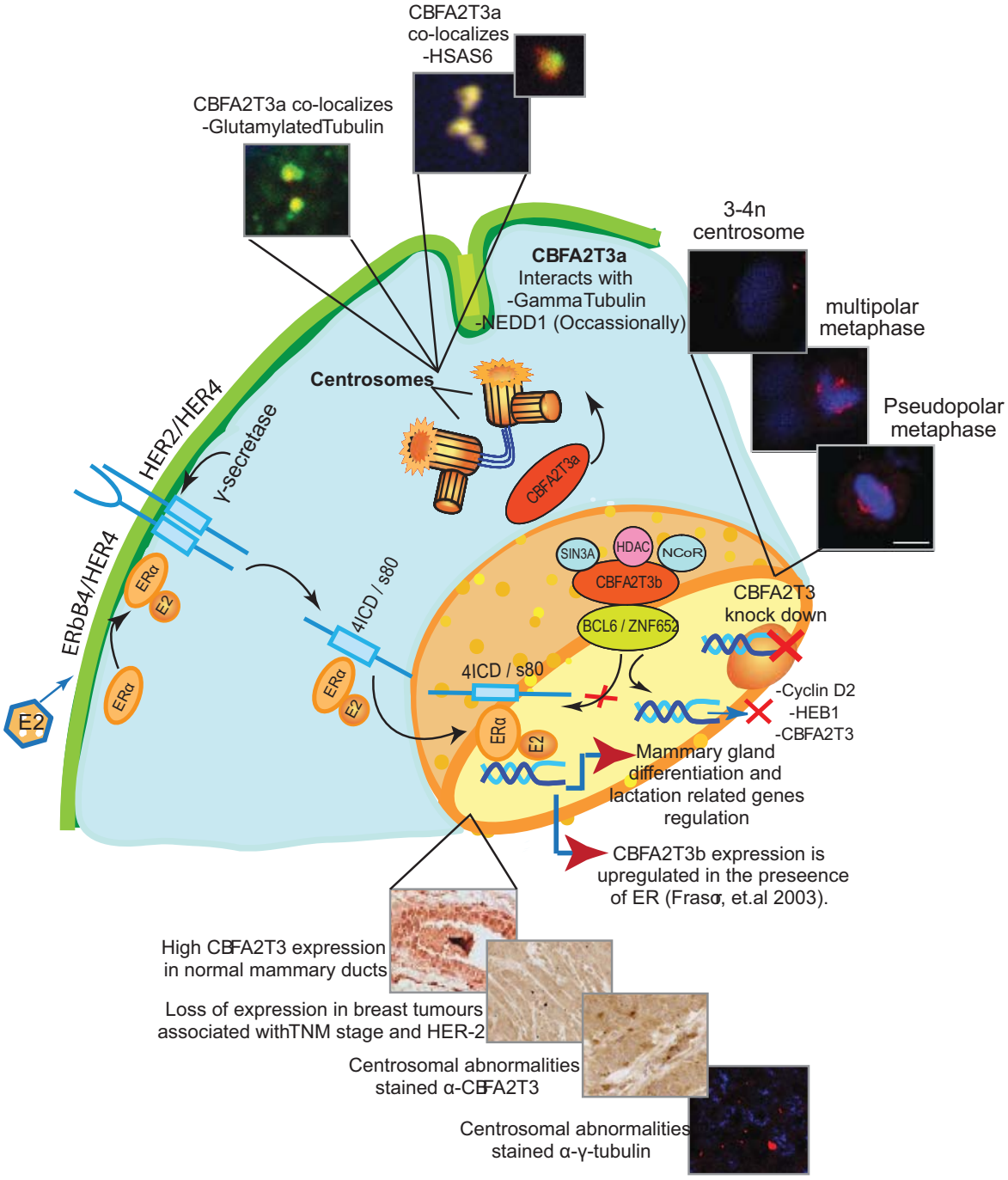

Figure 7.1 A model depicting the role of CBFA2T3 isoforms in breast epithelial cell.

CBFA2T3 isoforms were found to localize to different cellular compartments. Both isoforms were involved in different cellular functions. The presented model aims to summaries all available data and findings from the current study. Co-regulation of ERbB4 by estrogen recepotor was reported by Yun Zhu et.al, Cancer Research 2006, 66: (16). August 15. CBFA2T3b interaction with ERbB4/ HER4 (4ICD/s80) was reported by Linggi and Carpentar, The JBC 2006, 281: (35) pp.25373-80.

These features are

(i) The differential compartmentalization of CBFA2T3a to cytoplasmic fraction and CBFA2T3b to nuclear fractions

(ii) Presence of the centrosomal targeting sequences in the *N-terminal* region of CBFA2T3a

(iii) Possible involvement of CBFA2T3a in centrosome duplication

(iv) CBFA2T3b localization to nuclear speckles is related to its function as a transcriptional co-repressor of the BCL6 target *cyclin D2*

(v) CBFA2T3 expression is down regulated in breast tumour sections and showed a significant correlation with TNM staging, HER-2 positivity and centrosomal abnormalities

The current study provides an insight into the discrete role of CBFA2T3a in centrosome function, in contrast to CBFA2T3b which function as a typical transcriptional co repressor. Moreover, it has opened an area for future research for example (1) searching for targets or more interacting partners of the CBFA2T3a isoform, (2) determining the effects of CBFA2T3a specific knockdowns on the various centrosomal proteins, (3) analysis of CBFA2T3 proteins expression in breast tumours section where patient survival data is available, (4) analysis of the CBFA2T3b promoter to find regulatory proteins additional to BCL6 which will help to elucidate CBFA2T3 regulatory pathways. These findings will eventually lead to understand the role of CBFA2T3 proteins in tumour development and eventually for developing new therapeutics for cancer treatment.

References

Abd El-Rehim, D.M., Pinder, S.E., Paish, C.E., Bell, J.A., Rampaul, R.S., Blamey, R.W., Robertson, J.F., Nicholson, R.I. & Ellis, I.O. Expression and co-expression of the members of the epidermal growth factor receptor (EGFR) family in invasive breast carcinoma. (2004). *Br J Cancer*, **91,** 1532-42.

Albagli, O., Lantoine, D., Quief, S., Quignon, F., Englert, C., Kerckaert, J.P., Montarras, D., Pinset, C. & Lindon, C. Overexpressed BCL6 (LAZ3) oncoprotein triggers apoptosis, delays S phase progression and associates with replication foci. (1999). *Oncogene*, **18,** 5063-75.

Allred, D.C., Mohsin, S.K. & Fuqua, S.A. Histological and biological evolution of human premalignant breast disease. (2001). *Endocr Relat Cancer*, **8,** 47-61.

Altundag, K., Altundag, O., Gunduz, M. & Arun, B. Possible interaction between activator protein-1 and proto-oncogene B-cell lymphoma gene 6 in breast cancer patients resistant to tamoxifen. (2004). *Med Hypotheses*, **63,** 823-6.

Amann, J.M., Nip, J., Strom, D.K., Lutterbach, B., Harada, H., Lenny, N., Downing, J.R., Meyers, S. & Hiebert, S.W. ETO, a target of t(8;21) in acute leukemia, makes distinct contacts with multiple histone deacetylases and binds mSin3A through its oligomerization domain. (2001). *Mol Cell Biol*, **21,** 6470-83.

Andersen, J.S., Wilkinson, C.J., Mayor, T., Mortensen, P., Nigg, E.A. & Mann, M. Proteomic characterization of the human centrosome by protein correlation profiling. (2003). *Nature*, **426,** 570-4.

Badra, F.A., Karamouzis, M.V., Ravazoula, P., Likaki-Karatza, E., Tzorakoleftherakis, E., Koukouras, D., Iconomou, G., Xiros, N., Siablis, D., Papavassiliou, A.G. & Kalofonos, H.P. Non-palpable breast carcinomas: correlation of mammographically detected malignant-appearing microcalcifications and epidermal growth factor receptor (EGFR) family expression. (2006). *Cancer Lett*, **244,** 34-41.

Bais, A.J., Gardner, A.E., McKenzie, O.L., Callen, D.F., Sutherland, G.R. & Kremmidiotis, G. Aberrant CBFA2T3B gene promoter methylation in breast tumors. (2004). *Mol Cancer*, **3,** 22.

Barnes, N.L., Khavari, S., Boland, G.P., Cramer, A., Knox, W.F. & Bundred, N.J. Absence of HER4 expression predicts recurrence of ductal carcinoma in situ of the breast. (2005). *Clin Cancer Res*, **11,** 2163-8.

Baron, B.W., Anastasi, J., Thirman, M.J., Furukawa, Y., Fears, S., Kim, D.C., Simone, F., Birkenbach, M., Montag, A., Sadhu, A., Zeleznik-Le, N. & McKeithan, T.W. The human programmed cell death-2 (PDCD2) gene is a target of BCL6

repression: implications for a role of BCL6 in the down-regulation of apoptosis. (2002). *Proc Natl Acad Sci U S A*, **99,** 2860-5.

Baron, B.W., Zeleznik-Le, N., Baron, M.J., Theisler, C., Huo, D., Krasowski, M.D., Thirman, M.J., Baron, R.M. & Baron, J.M. Repression of the PDCD2 gene by BCL6 and the implications for the pathogenesis of human B and T cell lymphomas. (2007). *Proc Natl Acad Sci U S A*, **104,** 7449-54.

Baylin, S.B. & Herman, J.G. DNA hypermethylation in tumorigenesis: epigenetics joins genetics. (2000). *Trends Genet*, **16,** 168-74.

Bieche, I. & Lidereau, R. Genetic alterations in breast cancer. (1995). *Genes Chromosomes Cancer*, **14,** 227-51.

Bobinnec, Y., Moudjou, M., Fouquet, J.P., Desbruyeres, E., Edde, B. & Bornens, M. Glutamylation of centriole and cytoplasmic tubulin in proliferating non-neuronal cells. (1998). *Cell Motil Cytoskeleton*, **39,** 223-32.

Bonneterre, J., Thurlimann, B., Robertson, J.F., Krzakowski, M., Mauriac, L., Koralewski, P., Vergote, I., Webster, A., Steinberg, M. & von Euler, M. Anastrozole versus tamoxifen as first-line therapy for advanced breast cancer in 668 postmenopausal women: results of the Tamoxifen or Arimidex Randomized Group Efficacy and Tolerability study. (2000). *J Clin Oncol*, **18,** 3748-57.

Bos, R., van Diest, P.J., van der Groep, P., Greijer, A.E., Hermsen, M.A., Heijnen, I., Meijer, G.A., Baak, J.P., Pinedo, H.M., van der Wall, E. & Shvarts, A. Protein expression of B-cell lymphoma gene 6 (BCL-6) in invasive breast cancer is associated with cyclin D1 and hypoxia-inducible factor-1alpha (HIF-1alpha). (2003). *Oncogene*, **22,** 8948-51.

Calabi, F. & Cilli, V. CBFA2T1, a gene rearranged in human leukemia, is a member of a multigene family. (1998). *Genomics*, **52,** 332-41.

Caldon, C.E., Daly, R.J., Sutherland, R.L. & Musgrove, E.A. Cell cycle control in breast cancer cells. (2006). *J Cell Biochem*, **97,** 261-74.

Caligo, M.A., Polidoro, L., Ghimenti, C., Campani, D., Cecchetti, D. & Bevilacqua, G. A region on the long arm of chromosome 16 is frequently deleted in metastatic node-negative breast cancer. (1998). *Int J Oncol*, **13,** 177-82.

Callahan, R. & Campbell, G. Mutations in human breast cancer: an overview. (1989). *J Natl Cancer Inst*, **81,** 1780-6.

Callahan, R., Cropp, C., Sheng, Z.M., Merlo, G., Steeg, P., Liscia, D. & Lidereau, R. Definition of regions of the human genome affected by loss of heterozygosity in primary human breast tumors. (1993). *J Cell Biochem Suppl*, **17G,** 167-72.

Carey, L.A., Perou, C.M., Livasy, C.A., Dressler, L.G., Cowan, D., Conway, K., Karaca, G., Troester, M.A., Tse, C.K., Edmiston, S., Deming, S.L., Geradts, J., Cheang, M.C., Nielsen, T.O., Moorman, P.G., Earp, H.S. & Millikan, R.C.

Race, breast cancer subtypes, and survival in the Carolina Breast Cancer Study. (2006). *Jama*, **295,** 2492-502.

Chang, C.C., Ye, B.H., Chaganti, R.S. & Dalla-Favera, R. BCL-6, a POZ/zinc-finger protein, is a sequence-specific transcriptional repressor. (1996). *Proc Natl Acad Sci U S A*, **93,** 6947-52.

Chen, C.M., Chen, H.L., Hsiau, T.H., Hsiau, A.H., Shi, H., Brock, G.J., Wei, S.H., Caldwell, C.W., Yan, P.S. & Huang, T.H. Methylation target array for rapid analysis of CpG island hypermethylation in multiple tissue genomes. (2003). *Am J Pathol*, **163,** 37-45.

Chen, Z., Brand, N.J., Chen, A., Chen, S.J., Tong, J.H., Wang, Z.Y., Waxman, S. & Zelent, A. Fusion between a novel Kruppel-like zinc finger gene and the retinoic acid receptor-alpha locus due to a variant t(11;17) translocation associated with acute promyelocytic leukaemia. (1993). *Embo J*, **12,** 1161-7.

Chevallier, N., Corcoran, C.M., Lennon, C., Hyjek, E., Chadburn, A., Bardwell, V.J., Licht, J.D. & Melnick, A. ETO protein of t(8;21) AML is a corepressor for Bcl-6 B-cell lymphoma oncoprotein. (2004). *Blood*, **103,** 1454-63.

Chretien, D., Buendia, B., Fuller, S.D. & Karsenti, E. Reconstruction of the centrosome cycle from cryoelectron micrographs. (1997). *J Struct Biol*, **120,** 117-33.

Citri, A., Skaria, K.B. & Yarden, Y. The deaf and the dumb: the biology of ErbB-2 and ErbB-3. (2003). *Exp Cell Res*, **284,** 54-65.

Cleton-Jansen, A.M., Callen, D.F., Seshadri, R., Goldup, S., McCallum, B., Crawford, J., Powell, J.A., Settasatian, C., van Beerendonk, H., Moerland, E.W., Smit, V.T., Harris, W.H., Millis, R., Morgan, N.V., Barnes, D., Mathew, C.G. & Cornelisse, C.J. Loss of heterozygosity mapping at chromosome arm 16q in 712 breast tumors reveals factors that influence delineation of candidate regions. (2001). *Cancer Res*, **61,** 1171-7.

Cleton-Jansen, A.M., Moerland, E.W., Kuipers-Dijkshoorn, N.J., Callen, D.F., Sutherland, G.R., Hansen, B., Devilee, P. & Cornelisse, C.J. At least two different regions are involved in allelic imbalance on chromosome arm 16q in breast cancer. (1994). *Genes Chromosomes Cancer*, **9,** 101-7.

Cornelis, R.S., van Vliet, M., Vos, C.B., Cleton-Jansen, A.M., van de Vijver, M.J., Peterse, J.L., Khan, P.M., Borresen, A.L., Cornelisse, C.J. & Devilee, P. Evidence for a gene on 17p13.3, distal to TP53, as a target for allele loss in breast tumors without p53 mutations. (1994). *Cancer Res*, **54,** 4200-6.

Cui, X., Schiff, R., Arpino, G., Osborne, C.K. & Lee, A.V. Biology of progesterone receptor loss in breast cancer and its implications for endocrine therapy. (2005). *J Clin Oncol*, **23,** 7721-35.

D'Assoro, A.B., Barrett, S.L., Folk, C., Negron, V.C., Boeneman, K., Busby, R., Whitehead, C., Stivala, F., Lingle, W.L. & Salisbury, J.L. Amplified

centrosomes in breast cancer: a potential indicator of tumor aggressiveness. (2002). *Breast Cancer Res Treat*, **75,** 25-34.

David, G., Alland, L., Hong, S.H., Wong, C.W., DePinho, R.A. & Dejean, A. Histone deacetylase associated with mSin3A mediates repression by the acute promyelocytic leukemia-associated PLZF protein. (1998). *Oncogene*, **16,** 2549-56.

Davis, J.N., McGhee, L. & Meyers, S. The ETO (MTG8) gene family. (2003). *Gene*, **303,** 1-10.

Davis, J.N., Williams, B.J., Herron, J.T., Galiano, F.J. & Meyers, S. ETO-2, a new member of the ETO-family of nuclear proteins. (1999). *Oncogene*, **18,** 1375-83.

De Paola, F., Vecci, A.M., Granato, A.M., Liverani, M., Monti, F., Innoceta, A.M., Gianni, L., Saragoni, L., Ricci, M., Falcini, F., Amadori, D. & Volpi, A. p27/kip1 expression in normal epithelium, benign and neoplastic breast lesions. (2002). *J Pathol*, **196,** 26-31.

Dent, A.L., Shaffer, A.L., Yu, X., Allman, D. & Staudt, L.M. Control of inflammation, cytokine expression, and germinal center formation by BCL-6. (1997). *Science*, **276,** 589-92.

Dhanda, R.S., Lindberg, S.R. & Olsson, I. The human SIN3B corepressor forms a nucleolar complex with leukemia-associated ETO homologues. (2008). *BMC Mol Biol*, **9,** 8.

Driouch, K., Dorion-Bonnet, F., Briffod, M., Champeme, M.H., Longy, M. & Lidereau, R. Loss of heterozygosity on chromosome arm 16q in breast cancer metastases. (1997). *Genes Chromosomes Cancer*, **19,** 185-91.

Driscoll, M.D., Sathya, G., Muyan, M., Klinge, C.M., Hilf, R. & Bambara, R.A. Sequence requirements for estrogen receptor binding to estrogen response elements. (1998). *J Biol Chem*, **273,** 29321-30.

Duensing, A., Liu, Y., Perdreau, S.A., Kleylein-Sohn, J., Nigg, E.A. & Duensing, S. Centriole overduplication through the concurrent formation of multiple daughter centrioles at single maternal templates. (2007). *Oncogene*, **26,** 6280-8.

Eccles, D.M., Russell, S.E., Haites, N.E., Atkinson, R., Bell, D.W., Gruber, L., Hickey, I., Kelly, K., Kitchener, H., Leonard, R. & et al. Early loss of heterozygosity on 17q in ovarian cancer. The Abe Ovarian Cancer Genetics Group. (1992). *Oncogene*, **7,** 2069-72.

Erickson, P., Gao, J., Chang, K.S., Look, T., Whisenant, E., Raimondi, S., Lasher, R., Trujillo, J., Rowley, J. & Drabkin, H. Identification of breakpoints in t(8;21) acute myelogenous leukemia and isolation of a fusion transcript, AML1/ETO, with similarity to Drosophila segmentation gene, runt. (1992). *Blood*, **80,** 1825-31.

Erickson, P.F., Robinson, M., Owens, G. & Drabkin, H.A. The ETO portion of acute myeloid leukemia t(8;21) fusion transcript encodes a highly evolutionarily conserved, putative transcription factor. (1994). *Cancer Res*, **54,** 1782-6.

Fabbro, M. & Henderson, B.R. Regulation of tumor suppressors by nuclear-cytoplasmic shuttling. (2003). *Exp Cell Res*, **282,** 59-69.

Fan, S., Wang, J., Yuan, R., Ma, Y., Meng, Q., Erdos, M.R., Pestell, R.G., Yuan, F., Auborn, K.J., Goldberg, I.D. & Rosen, E.M. BRCA1 inhibition of estrogen receptor signaling in transfected cells. (1999). *Science*, **284,** 1354-6.

Fearon, E.R. & Vogelstein, B. A genetic model for colorectal tumorigenesis. (1990). *Cell*, **61,** 759-67.

Feinberg, A.P., Ohlsson, R. & Henikoff, S. The epigenetic progenitor origin of human cancer. (2006). *Nat Rev Genet*, **7,** 21-33.

Feinberg, A.P. & Tycko, B. The history of cancer epigenetics. (2004). *Nat Rev Cancer*, **4,** 143-53.

Feinstein, P.G., Kornfeld, K., Hogness, D.S. & Mann, R.S. Identification of homeotic target genes in Drosophila melanogaster including nervy, a proto-oncogene homologue. (1995). *Genetics*, **140,** 573-86.

Fracchiolla, N.S., Colombo, G., Finelli, P., Maiolo, A.T. & Neri, A. EHT, a new member of the MTG8/ETO gene family, maps on 20q11 region and is deleted in acute myeloid leukemias. (1998). *Blood*, **92,** 3481-4.

Frasor, J., Danes, J.M., Komm, B., Chang, K.C., Lyttle, C.R. & Katzenellenbogen, B.S. Profiling of estrogen up- and down-regulated gene expression in human breast cancer cells: insights into gene networks and pathways underlying estrogenic control of proliferation and cell phenotype. (2003). *Endocrinology*, **144,** 4562-74.

Fu, M., Wang, C., Li, Z., Sakamaki, T. & Pestell, R.G. Minireview: Cyclin D1: normal and abnormal functions. (2004). *Endocrinology*, **145,** 5439-47.

Fukasawa, K. Centrosome amplification, chromosome instability and cancer development. (2005). *Cancer Lett*, **230,** 6-19.

Gamou, T., Kitamura, E., Hosoda, F., Shimizu, K., Shinohara, K., Hayashi, Y., Nagase, T., Yokoyama, Y. & Ohki, M. The partner gene of AML1 in t(16;21) myeloid malignancies is a novel member of the MTG8(ETO) family. (1998). *Blood*, **91,** 4028-37.

Garcia, J.F., Maestre, L., Lucas, E., Sanchez-Verde, L., Romero-Chala, S., Piris, M.A. & Roncador, G. Genetic immunization: a new monoclonal antibody for the detection of BCL-6 protein in paraffin sections. (2006). *J Histochem Cytochem*, **54,** 31-8.

Gelmetti, V., Zhang, J., Fanelli, M., Minucci, S., Pelicci, P.G. & Lazar, M.A. Aberrant recruitment of the nuclear receptor corepressor-histone deacetylase complex by the acute myeloid leukemia fusion partner ETO. (1998). *Mol Cell Biol*, **18,** 7185-91.

Goardon, N., Lambert, J.A., Rodriguez, P., Nissaire, P., Herblot, S., Thibault, P., Dumenil, D., Strouboulis, J., Romeo, P.H. & Hoang, T. ETO2 coordinates cellular proliferation and differentiation during erythropoiesis. (2006). *Embo J*, **25,** 357-66.

Godfrey, T.E., Cher, M.L., Chhabra, V. & Jensen, R.H. Allelic imbalance mapping of chromosome 16 shows two regions of common deletion in prostate adenocarcinoma. (1997). *Cancer Genet Cytogenet*, **98,** 36-42.

Goodwin, P.J. & Boyd, N.F. Mammographic parenchymal pattern and breast cancer risk: a critical appraisal of the evidence. (1988). *Am J Epidemiol*, **127,** 1097-108.

Gross, C.T. & McGinnis, W. DEAF-1, a novel protein that binds an essential region in a Deformed response element. (1996). *Embo J*, **15,** 1961-70.

Grozinger, C.M. & Schreiber, S.L. Regulation of histone deacetylase 4 and 5 and transcriptional activity by 14-3-3-dependent cellular localization. (2000). *Proc Natl Acad Sci U S A*, **97,** 7835-40.

Gunawardane, R.N., Martin, O.C., Cao, K., Zhang, L., Dej, K., Iwamatsu, A. & Zheng, Y. Characterization and reconstitution of Drosophila gamma-tubulin ring complex subunits. (2000). *J Cell Biol*, **151,** 1513-24.

Guo, H.Q., Gao, M., Ma, J., Xiao, T., Zhao, L.L., Gao, Y. & Pan, Q.J. Analysis of the cellular centrosome in fine-needle aspirations of the breast. (2007). *Breast Cancer Res*, **9,** R48.

Habedanck, R., Stierhof, Y.D., Wilkinson, C.J. & Nigg, E.A. The Polo kinase Plk4 functions in centriole duplication. (2005). *Nat Cell Biol*, **7,** 1140-6.

Hall, J.M., Lee, M.K., Newman, B., Morrow, J.E., Anderson, L.A., Huey, B. & King, M.C. Linkage of early-onset familial breast cancer to chromosome 17q21. (1990). *Science*, **250,** 1684-9.

Haren, L., Remy, M.H., Bazin, I., Callebaut, I., Wright, M. & Merdes, A. NEDD1-dependent recruitment of the gamma-tubulin ring complex to the centrosome is necessary for centriole duplication and spindle assembly. (2006). *J Cell Biol*, **172,** 505-15.

Harris, M.B., Chang, C.C., Berton, M.T., Danial, N.N., Zhang, J., Kuehner, D., Ye, B.H., Kvatyuk, M., Pandolfi, P.P., Cattoretti, G., Dalla-Favera, R. & Rothman, P.B. Transcriptional repression of Stat6-dependent interleukin-4-induced genes by BCL-6: specific regulation of iepsilon transcription and immunoglobulin E switching. (1999). *Mol Cell Biol*, **19,** 7264-75.

Harwell, R.M., Porter, D.C., Danes, C. & Keyomarsi, K. Processing of cyclin E differs between normal and tumor breast cells. (2000). *Cancer Res*, **60,** 481-9.

Herman, J.G. & Baylin, S.B. Gene silencing in cancer in association with promoter hypermethylation. (2003). *N Engl J Med*, **349,** 2042-54.

Herschkowitz, J.I., He, X., Fan, C. & Perou, C.M. The functional loss of the retinoblastoma tumour suppressor is a common event in basal-like and luminal B breast carcinomas. (2008). *Breast Cancer Res*, **10,** R75.

Hiebert, S.W., Lutterbach, B. & Amann, J. Role of co-repressors in transcriptional repression mediated by the t(8;21), t(16;21), t(12;21), and inv(16) fusion proteins. (2001). *Curr Opin Hematol*, **8,** 197-200.

Hildebrand, D., Tiefenbach, J., Heinzel, T., Grez, M. & Maurer, A.B. Multiple regions of ETO cooperate in transcriptional repression. (2001). *J Biol Chem*, **276,** 9889-95.

Holm, R., Knopp, S., Kumar, R., Lee, J., Nesland, J.M., Trope, C. & Callen, D.F. Expression of ZNF652, a novel zinc finger protein, in vulvar carcinomas and its relation to prognosis. (2008). *J Clin Pathol*, **61,** 59-63.

Hong, S.H., David, G., Wong, C.W., Dejean, A. & Privalsky, M.L. SMRT corepressor interacts with PLZF and with the PML-retinoic acid receptor alpha (RARalpha) and PLZF-RARalpha oncoproteins associated with acute promyelocytic leukemia. (1997). *Proc Natl Acad Sci U S A*, **94,** 9028-33.

Hoogeveen, A.T., Rossetti, S., Stoyanova, V., Schonkeren, J., Fenaroli, A., Schiaffonati, L., van Unen, L. & Sacchi, N. The transcriptional corepressor MTG16a contains a novel nucleolar targeting sequence deranged in t (16; 21)-positive myeloid malignancies. (2002). *Oncogene*, **21,** 6703-12.

Hopp, T.A., Weiss, H.L., Hilsenbeck, S.G., Cui, Y., Allred, D.C., Horwitz, K.B. & Fuqua, S.A. Breast cancer patients with progesterone receptor PR-A-rich tumors have poorer disease-free survival rates. (2004). *Clin Cancer Res*, **10,** 2751-60.

Horlein, A.J., Naar, A.M., Heinzel, T., Torchia, J., Gloss, B., Kurokawa, R., Ryan, A., Kamei, Y., Soderstrom, M., Glass, C.K. & et al. Ligand-independent repression by the thyroid hormone receptor mediated by a nuclear receptor co-repressor. (1995). *Nature*, **377,** 397-404.

Hu, Z., Fan, C., Oh, D.S., Marron, J.S., He, X., Qaqish, B.F., Livasy, C., Carey, L.A., Reynolds, E., Dressler, L., Nobel, A., Parker, J., Ewend, M.G., Sawyer, L.R., Wu, J., Liu, Y., Nanda, R., Tretiakova, M., Ruiz Orrico, A., Dreher, D., Palazzo, J.P., Perreard, L., Nelson, E., Mone, M., Hansen, H., Mullins, M., Quackenbush, J.F., Ellis, M.J., Olopade, O.I., Bernard, P.S. & Perou, C.M. The molecular portraits of breast tumors are conserved across microarray platforms. (2006). *BMC Genomics*, **7,** 96.

Hudelist, G., Singer, C.F., Manavi, M., Pischinger, K., Kubista, E. & Czerwenka, K. Co-expression of ErbB-family members in human breast cancer: Her-2/neu is the preferred dimerization candidate in nodal-positive tumors. (2003). *Breast Cancer Res Treat*, **80,** 353-61.

Hug, B.A. & Lazar, M.A. ETO interacting proteins. (2004). *Oncogene*, **23,** 4270-4.

Hug, B.A., Lazar, M.A., Peterson, L.F., Zhang, D.E., Nimer, S.D., Moore, M.A., Tonks, A., Tonks, A.J., Pearn, L., Pearce, L., Hoy, T., Couzens, S., Fisher, J., Burnett, A.K., Darley, R.L., Lindberg, S.R., Olsson, A., Persson, A.M. & Olsson, I. ETO interacting proteins (2004). *Oncogene*, **23,** 4270-4274.

Hulten, M.A., Hill, S.M. & Rodgers, C.S. Chromosomes 1 and 16 in sporadic breast cancer. (1993). *Genes Chromosomes Cancer*, **8,** 204.

Huynh, K.D. & Bardwell, V.J. The BCL-6 POZ domain and other POZ domains interact with the co-repressors N-CoR and SMRT. (1998). *Oncogene*, **17,** 2473-84.

Huynh, K.D., Fischle, W., Verdin, E. & Bardwell, V.J. BCoR, a novel corepressor involved in BCL-6 repression. (2000). *Genes Dev*, **14,** 1810-23.

Ibanez, V., Sharma, A., Buonamici, S., Verma, A., Kalakonda, S., Wang, J., Kadkol, S. & Sauntharajah, Y. AML1-ETO decreases ETO-2 (MTG16) interactions with nuclear receptor corepressor, an effect that impairs granulocyte differentiation. (2004). *Cancer Res*, **64,** 4547-54.

Ishikawa, H., Kubo, A. & Tsukita, S. Odf2-deficient mother centrioles lack distal/subdistal appendages and the ability to generate primary cilia. (2005). *Nat Cell Biol*, **7,** 517-24.

Janke, C., Rogowski, K. & van Dijk, J. Polyglutamylation: a fine-regulator of protein function? 'Protein Modifications: beyond the usual suspects' review series. (2008). *EMBO Rep*, **9,** 636-41.

Jones, P.A. & Baylin, S.B. The fundamental role of epigenetic events in cancer. (2002). *Nat Rev Genet*, **3,** 415-28.

Kanno, Y., Suzuki, M., Miyazaki, Y., Matsuzaki, M., Nakahama, T., Kurose, K., Sawada, J. & Inouye, Y. Difference in nucleocytoplasmic shuttling sequences of rat and human constitutive active/androstane receptor. (2007). *Biochim Biophys Acta*, **1773,** 934-44.

Karamouzis, M.V., Badra, F.A. & Papavassiliou, A.G. Breast cancer: the upgraded role of HER-3 and HER-4. (2007). *Int J Biochem Cell Biol*, **39,** 851-6.

Keyomarsi, K., Tucker, S.L., Buchholz, T.A., Callister, M., Ding, Y., Hortobagyi, G.N., Bedrosian, I., Knickerbocker, C., Toyofuku, W., Lowe, M., Herliczek, T.W. &

Bacus, S.S. Cyclin E and survival in patients with breast cancer. (2002). *N Engl J Med*, **347,** 1566-75.

Khan, S.A., Rogers, M.A., Khurana, K.K., Meguid, M.M. & Numann, P.J. Estrogen receptor expression in benign breast epithelium and breast cancer risk. (1998). *J Natl Cancer Inst*, **90,** 37-42.

Kinzler, K.W. & Vogelstein, B. Cancer-susceptibility genes. Gatekeepers and caretakers. (1997). *Nature*, **386,** 761, 763.

Kitabayashi, I., Ida, K., Morohoshi, F., Yokoyama, A., Mitsuhashi, N., Shimizu, K., Nomura, N., Hayashi, Y. & Ohki, M. The AML1-MTG8 leukemic fusion protein forms a complex with a novel member of the MTG8(ETO/CDR) family, MTGR1. (1998a). *Mol Cell Biol*, **18,** 846-58.

Kitabayashi, I., Yokoyama, A., Shimizu, K. & Ohki, M. Interaction and functional cooperation of the leukemia-associated factors AML1 and p300 in myeloid cell differentiation. (1998b). *Embo J*, **17,** 2994-3004.

Kleylein-Sohn, J., Westendorf, J., Le Clech, M., Habedanck, R., Stierhof, Y.D. & Nigg, E.A. Plk4-induced centriole biogenesis in human cells. (2007). *Dev Cell*, **13,** 190-202.

Ko, M.J., Murata, K., Hwang, D.S. & Parvin, J.D. Inhibition of BRCA1 in breast cell lines causes the centrosome duplication cycle to be disconnected from the cell cycle. (2006). *Oncogene*, **25,** 298-303.

Kochetkova, M., McKenzie, O.L., Bais, A.J., Martin, J.M., Secker, G.A., Seshadri, R., Powell, J.A., Hinze, S.J., Gardner, A.E., Spendlove, H.E., O'Callaghan, N.J., Cleton-Jansen, A.M., Cornelisse, C., Whitmore, S.A., Crawford, J., Kremmidiotis, G., Sutherland, G.R. & Callen, D.F. CBFA2T3 (MTG16) is a putative breast tumor suppressor gene from the breast cancer loss of heterozygosity region at 16q24.3. (2002). *Cancer Res*, **62,** 4599-604.

Koepp, D.M., Harper, J.W. & Elledge, S.J. How the cyclin became a cyclin: regulated proteolysis in the cell cycle. (1999). *Cell*, **97,** 431-4.

Kozak, M. Point mutations define a sequence flanking the AUG initiator codon that modulates translation by eukaryotic ribosomes. (1986). *Cell*, **44,** 283-92.

Kramer, A., Mailand, N., Lukas, C., Syljuasen, R.G., Wilkinson, C.J., Nigg, E.A., Bartek, J. & Lukas, J. Centrosome-associated Chk1 prevents premature activation of cyclin-B-Cdk1 kinase. (2004). *Nat Cell Biol*, **6,** 884-91.

Krieg, A.J., Krieg, S.A., Ahn, B.S. & Shapiro, D.J. Interplay between estrogen response element sequence and ligands controls in vivo binding of estrogen receptor to regulated genes. (2004). *J Biol Chem*, **279,** 5025-34.

Kumar, R., Cheney, K.M., McKirdy, R., Neilsen, P.M., Schulz, R.B., Lee, J., Cohen, J., Booker, G.W. & Callen, D.F. CBFA2T3-ZNF652 corepressor complex regulates transcription of the E-box gene HEB. (2008). *J Biol Chem*.

Kumar, R., Manning, J., Spendlove, H.E., Kremmidiotis, G., McKirdy, R., Lee, J., Millband, D.N., Cheney, K.M., Stampfer, M.R., Dwivedi, P.P., Morris, H.A. & Callen, D.F. ZNF652, a novel zinc finger protein, interacts with the putative breast tumor suppressor CBFA2T3 to repress transcription. (2006). *Mol Cancer Res*, **4,** 655-65.

Kumar, R., Neilsen, P.M., Crawford, J., McKirdy, R., Lee, J., Powell, J.A., Saif, Z., Martin, J.M., Lombaerts, M., Cornelisse, C.J., Cleton-Jansen, A.M. & Callen, D.F. FBXO31 is the chromosome 16q24.3 senescence gene, a candidate breast tumor suppressor, and a component of an SCF complex. (2005). *Cancer Res*, **65,** 11304-13.

Laemmli, U.K. Cleavage of structural proteins during the assembly of the head of bacteriophage T4. (1970). *Nature*, **227,** 680-5.

Laemmli, U.K., Beguin, F. & Gujer-Kellenberger, G. A factor preventing the major head protein of bacteriophage T4 from random aggregation. (1970). *J Mol Biol*, **47,** 69-85.

Lemercier, C., Brocard, M.P., Puvion-Dutilleul, F., Kao, H.Y., Albagli, O. & Khochbin, S. Class II histone deacetylases are directly recruited by BCL6 transcriptional repressor. (2002). *J Biol Chem*, **277,** 22045-52.

Lenny, N., Meyers, S. & Hiebert, S.W. Functional domains of the t(8;21) fusion protein, AML-1/ETO. (1995). *Oncogene*, **11,** 1761-9.

Lin, R.J., Nagy, L., Inoue, S., Shao, W., Miller, W.H., Jr. & Evans, R.M. Role of the histone deacetylase complex in acute promyelocytic leukaemia. (1998). *Nature*, **391,** 811-4.

Lindberg, S.R., Olsson, A., Persson, A.M. & Olsson, I. Interactions between the leukaemia-associated ETO homologues of nuclear repressor proteins. (2003). *Eur J Haematol*, **71,** 439-47.

Lindberg, S.R., Olsson, A., Persson, A.M. & Olsson, I. The Leukemia-associated ETO homologues are differently expressed during hematopoietic differentiation. (2005). *Exp Hematol*, **33,** 189-98.

Linggi, B. & Carpenter, G. ErbB-4 s80 intracellular domain abrogates ETO2-dependent transcriptional repression. (2006). *J Biol Chem*, **281,** 25373-80.

Linggi, B., Cheng, Q.C., Rao, A.R. & Carpenter, G. The ErbB-4 s80 intracellular domain is a constitutively active tyrosine kinase. (2006). *Oncogene*, **25,** 160-3.

Linggi, B., Muller-Tidow, C., van de Locht, L., Hu, M., Nip, J., Serve, H., Berdel, W.E., van der Reijden, B., Quelle, D.E., Rowley, J.D., Cleveland, J., Jansen,

J.H., Pandolfi, P.P. & Hiebert, S.W. The t(8;21) fusion protein, AML1 ETO, specifically represses the transcription of the p14(ARF) tumor suppressor in acute myeloid leukemia. (2002). *Nat Med*, **8,** 743-50.

Lingle, W.L., Barrett, S.L., Negron, V.C., D'Assoro, A.B., Boeneman, K., Liu, W., Whitehead, C.M., Reynolds, C. & Salisbury, J.L. Centrosome amplification drives chromosomal instability in breast tumor development. (2002). *Proc Natl Acad Sci U S A*, **99,** 1978-83.

Liu, Y., Chen, W., Gaudet, J., Cheney, M.D., Roudaia, L., Cierpicki, T., Klet, R.C., Hartman, K., Laue, T.M., Speck, N.A. & Bushweller, J.H. Structural basis for recognition of SMRT/N-CoR by the MYND domain and its contribution to AML1/ETO's activity. (2007). *Cancer Cell*, **11,** 483-97.

Loeb, L.A. A mutator phenotype in cancer. (2001). *Cancer Res*, **61,** 3230-9.

Logarajah, S., Hunter, P., Kraman, M., Steele, D., Lakhani, S., Bobrow, L., Venkitaraman, A. & Wagner, S. BCL-6 is expressed in breast cancer and prevents mammary epithelial differentiation. (2003). *Oncogene*, **22,** 5572-8.

Loo, L.W., Ton, C., Wang, Y.W., Grove, D.I., Bouzek, H., Vartanian, N., Lin, M.G., Yuan, X., Lawton, T.L., Daling, J.R., Malone, K.E., Li, C.I., Hsu, L. & Porter, P.L. Differential patterns of allelic loss in estrogen receptor-positive infiltrating lobular and ductal breast cancer. (2008). *Genes Chromosomes Cancer*, **47,** 1049-66.

Lutterbach, B., Sun, D., Schuetz, J. & Hiebert, S.W. The MYND motif is required for repression of basal transcription from the multidrug resistance 1 promoter by the t(8;21) fusion protein. (1998a). *Mol Cell Biol*, **18,** 3604-11.

Lutterbach, B., Westendorf, J.J., Linggi, B., Patten, A., Moniwa, M., Davie, J.R., Huynh, K.D., Bardwell, V.J., Lavinsky, R.M., Rosenfeld, M.G., Glass, C., Seto, E. & Hiebert, S.W. ETO, a target of t(8;21) in acute leukemia, interacts with the N-CoR and mSin3 corepressors. (1998b). *Mol Cell Biol*, **18,** 7176-84.

Ma, Z., Kanai, M., Kawamura, K., Kaibuchi, K., Ye, K. & Fukasawa, K. Interaction between ROCK II and nucleophosmin/B23 in the regulation of centrosome duplication. (2006). *Mol Cell Biol*, **26,** 9016-34.

Majumder, P.K., Grisanzio, C., O'Connell, F., Barry, M., Brito, J.M., Xu, Q., Guney, I., Berger, R., Herman, P., Bikoff, R., Fedele, G., Baek, W.K., Wang, S., Ellwood-Yen, K., Wu, H., Sawyers, C.L., Signoretti, S., Hahn, W.C., Loda, M. & Sellers, W.R. A prostatic intraepithelial neoplasia-dependent p27 Kip1 checkpoint induces senescence and inhibits cell proliferation and cancer progression. (2008). *Cancer Cell*, **14,** 146-55.

Mantel, C., Braun, S.E., Reid, S., Henegariu, O., Liu, L., Hangoc, G. & Broxmeyer, H.E. p21(cip-1/waf-1) deficiency causes deformed nuclear architecture, centriole overduplication, polyploidy, and relaxed microtubule damage checkpoints in human hematopoietic cells. (1999). *Blood*, **93,** 1390-8.

Margalit, O., Amram, H., Amariglio, N., Simon, A.J., Shaklai, S., Granot, G., Minsky, N., Shimoni, A., Harmelin, A., Givol, D., Shohat, M., Oren, M. & Rechavi, G. BCL6 is regulated by p53 through a response element frequently disrupted in B-cell non-Hodgkin lymphoma. (2006). *Blood*, **107,** 1599-607.

Martinez, N., Drescher, B., Riehle, H., Cullmann, C., Vornlocher, H.P., Ganser, A., Heil, G., Nordheim, A., Krauter, J. & Heidenreich, O. The oncogenic fusion protein RUNX1-CBFA2T1 supports proliferation and inhibits senescence in t(8;21)-positive leukaemic cells. (2004). *BMC Cancer*, **4,** 44.

Mascle, X., Albagli, O. & Lemercier, C. Point mutations in BCL6 DNA-binding domain reveal distinct roles for the six zinc fingers. (2003). *Biochem Biophys Res Commun*, **300,** 391-6.

Matsumoto, Y. & Maller, J.L. A centrosomal localization signal in cyclin E required for Cdk2-independent S phase entry. (2004). *Science*, **306,** 885-8.

Matthews, J.M. & Sunde, M. Zinc fingers--folds for many occasions. (2002). *IUBMB Life*, **54,** 351-5.

McConnell, M.J., Chevallier, N., Berkofsky-Fessler, W., Giltnane, J.M., Malani, R.B., Staudt, L.M. & Licht, J.D. Growth suppression by acute promyelocytic leukemia-associated protein PLZF is mediated by repression of c-myc expression. (2003). *Mol Cell Biol*, **23,** 9375-88.

McGhee, L., Bryan, J., Elliott, L., Grimes, H.L., Kazanjian, A., Davis, J.N. & Meyers, S. Gfi-1 attaches to the nuclear matrix, associates with ETO (MTG8) and histone deacetylase proteins, and represses transcription using a TSA-sensitive mechanism. (2003). *J Cell Biochem*, **89,** 1005-18.

McKinsey, T.A., Zhang, C.L., Lu, J. & Olson, E.N. Signal-dependent nuclear export of a histone deacetylase regulates muscle differentiation. (2000). *Nature*, **408,** 106-11.

Melchor, L., Honrado, E., Huang, J., Alvarez, S., Naylor, T.L., Garcia, M.J., Osorio, A., Blesa, D., Stratton, M.R., Weber, B.L., Cigudosa, J.C., Rahman, N., Nathanson, K.L. & Benitez, J. Estrogen receptor status could modulate the genomic pattern in familial and sporadic breast cancer. (2007). *Clin Cancer Res*, **13,** 7305-13.

Melnick, A., Ahmad, K.F., Arai, S., Polinger, A., Ball, H., Borden, K.L., Carlile, G.W., Prive, G.G. & Licht, J.D. In-depth mutational analysis of the promyelocytic leukemia zinc finger BTB/POZ domain reveals motifs and residues required for biological and transcriptional functions. (2000a). *Mol Cell Biol*, **20,** 6550-67.

Melnick, A., Carlile, G., Ahmad, K.F., Kiang, C.L., Corcoran, C., Bardwell, V., Prive, G.G. & Licht, J.D. Critical residues within the BTB domain of PLZF and Bcl-6 modulate interaction with corepressors. (2002). *Mol Cell Biol*, **22,** 1804-18.

Melnick, A. & Licht, J.D. Deconstructing a disease: RARalpha, its fusion partners, and their roles in the pathogenesis of acute promyelocytic leukemia. (1999). *Blood*, **93,** 3167-215.

Melnick, A.M., Westendorf, J.J., Polinger, A., Carlile, G.W., Arai, S., Ball, H.J., Lutterbach, B., Hiebert, S.W. & Licht, J.D. The ETO protein disrupted in t(8;21)-associated acute myeloid leukemia is a corepressor for the promyelocytic leukemia zinc finger protein. (2000b). *Mol Cell Biol*, **20,** 2075-86.

Minucci, S., Maccarana, M., Cioce, M., De Luca, P., Gelmetti, V., Segalla, S., Di Croce, L., Giavara, S., Matteucci, C., Gobbi, A., Bianchini, A., Colombo, E., Schiavoni, I., Badaracco, G., Hu, X., Lazar, M.A., Landsberger, N., Nervi, C. & Pelicci, P.G. Oligomerization of RAR and AML1 transcription factors as a novel mechanism of oncogenic activation. (2000). *Mol Cell*, **5,** 811-20.

Mistry, A.R., Pedersen, E.W., Solomon, E. & Grimwade, D. The molecular pathogenesis of acute promyelocytic leukaemia: implications for the clinical management of the disease. (2003). *Blood Rev*, **17,** 71-97.

Miyoshi, H., Kozu, T., Shimizu, K., Enomoto, K., Maseki, N., Kaneko, Y., Kamada, N. & Ohki, M. The t(8;21) translocation in acute myeloid leukemia results in production of an AML1-MTG8 fusion transcript. (1993). *Embo J*, **12,** 2715-21.

Moriyama, M., Yamochi, T., Semba, K., Akiyama, T. & Mori, S. BCL-6 is phosphorylated at multiple sites in its serine- and proline-clustered region by mitogen-activated protein kinase (MAPK) in vivo. (1997). *Oncogene*, **14,** 2465-74.

Morohoshi, F., Mitani, S., Mitsuhashi, N., Kitabayashi, I., Takahashi, E., Suzuki, M., Munakata, N. & Ohki, M. Structure and expression pattern of a human MTG8/ETO family gene, MTGR1. (2000). *Gene*, **241,** 287-95.

Morris, L., Allen, K.E. & La Thangue, N.B. Regulation of E2F transcription by cyclin E-Cdk2 kinase mediated through p300/CBP co-activators. (2000). *Nat Cell Biol*, **2,** 232-9.

Mosesson, Y. & Yarden, Y. Oncogenic growth factor receptors: implications for signal transduction therapy. (2004). *Semin Cancer Biol*, **14,** 262-70.

Mouridsen, H., Gershanovich, M., Sun, Y., Perez-Carrion, R., Boni, C., Monnier, A., Apffelstaedt, J., Smith, R., Sleeboom, H.P., Janicke, F., Pluzanska, A., Dank, M., Becquart, D., Bapsy, P.P., Salminen, E., Snyder, R., Lassus, M., Verbeek, J.A., Staffler, B., Chaudri-Ross, H.A. & Dugan, M. Superior efficacy of letrozole versus tamoxifen as first-line therapy for postmenopausal women with advanced breast cancer: results of a phase III study of the International Letrozole Breast Cancer Group. (2001). *J Clin Oncol*, **19,** 2596-606.

Mueller, C.R. & Roskelley, C.D. Regulation of BRCA1 expression and its relationship to sporadic breast cancer. (2003). *Breast Cancer Res*, **5,** 45-52.

Murphy, S.M., Preble, A.M., Patel, U.K., O'Connell, K.L., Dias, D.P., Moritz, M., Agard, D., Stults, J.T. & Stearns, T. GCP5 and GCP6: two new members of the human gamma-tubulin complex. (2001). *Mol Biol Cell*, **12,** 3340-52.

Musgrove, E.A., Lee, C.S., Buckley, M.F. & Sutherland, R.L. Cyclin D1 induction in breast cancer cells shortens G1 and is sufficient for cells arrested in G1 to complete the cell cycle. (1994). *Proc Natl Acad Sci U S A*, **91,** 8022-6.

Nan, X., Ng, H.H., Johnson, C.A., Laherty, C.D., Turner, B.M., Eisenman, R.N. & Bird, A. Transcriptional repression by the methyl-CpG-binding protein MeCP2 involves a histone deacetylase complex. (1998). *Nature*, **393,** 386-9.

Natrajan, R., Lambros, M.B., Geyer, F.C., Marchio, C., Tan, D.S., Vatcheva, R., Shiu, K.K., Hungermann, D., Rodriguez-Pinilla, S.M., Palacios, J., Ashworth, A., Buerger, H. & Reis-Filho, J.S. Loss of 16q in high grade breast cancer is associated with estrogen receptor status: Evidence for progression in tumors with a luminal phenotype? (2009). *Genes Chromosomes Cancer*, **48,** 351-65.

Nielsen, T.O., Hsu, F.D., Jensen, K., Cheang, M., Karaca, G., Hu, Z., Hernandez-Boussard, T., Livasy, C., Cowan, D., Dressler, L., Akslen, L.A., Ragaz, J., Gown, A.M., Gilks, C.B., van de Rijn, M. & Perou, C.M. Immunohistochemical and clinical characterization of the basal-like subtype of invasive breast carcinoma. (2004). *Clin Cancer Res*, **10,** 5367-74.

Nigg, E.A. Centrosome duplication: of rules and licenses. (2007). *Trends Cell Biol*, **17,** 215-21.

Niu, H., Ye, B.H. & Dalla-Favera, R. Antigen receptor signaling induces MAP kinase-mediated phosphorylation and degradation of the BCL-6 transcription factor. (1998). *Genes Dev*, **12,** 1953-61.

Novelli, G., Muchir, A., Sangiuolo, F., Helbling-Leclerc, A., D'Apice, M.R., Massart, C., Capon, F., Sbraccia, P., Federici, M., Lauro, R., Tudisco, C., Pallotta, R., Scarano, G., Dallapiccola, B., Merlini, L. & Bonne, G. Mandibuloacral dysplasia is caused by a mutation in LMNA-encoding lamin A/C. (2002). *Am J Hum Genet*, **71,** 426-31.

Odaka, Y., Mally, A., Elliott, L.T. & Meyers, S. Nuclear import and subnuclear localization of the proto-oncoprotein ETO (MTG8). (2000). *Oncogene*, **19,** 3584-97.

Okuda, M., Horn, H.F., Tarapore, P., Tokuyama, Y., Smulian, A.G., Chan, P.K., Knudsen, E.S., Hofmann, I.A., Snyder, J.D., Bove, K.E. & Fukasawa, K. Nucleophosmin/B23 is a target of CDK2/cyclin E in centrosome duplication. (2000). *Cell*, **103,** 127-40.

Okumura, A.J., Peterson, L.F., Lo, M.C. & Zhang, D.E. Expression of AML/Runx and ETO/MTG family members during hematopoietic differentiation of embryonic stem cells. (2007). *Exp Hematol*, **35,** 978-88.

Okuwaki, M., Tsujimoto, M. & Nagata, K. The RNA binding activity of a ribosome biogenesis factor, nucleophosmin/B23, is modulated by phosphorylation with a cell cycle-dependent kinase and by association with its subtype. (2002). *Mol Biol Cell*, **13,** 2016-30.

Olopade, O.I., Grushko, T.A., Nanda, R. & Huo, D. Advances in breast cancer: pathways to personalized medicine. (2008). *Clin Cancer Res*, **14,** 7988-99.

Ouchi, T., Monteiro, A.N., August, A., Aaronson, S.A. & Hanafusa, H. BRCA1 regulates p53-dependent gene expression. (1998). *Proc Natl Acad Sci U S A*, **95,** 2302-6.

Oyer, J.A., Chu, A., Brar, S. & Turker, M.S. Aberrant epigenetic silencing is triggered by a transient reduction in gene expression. (2009). *PLoS ONE*, **4,** e4832.

Paintrand, M., Moudjou, M., Delacroix, H. & Bornens, M. Centrosome organization and centriole architecture: their sensitivity to divalent cations. (1992). *J Struct Biol*, **108,** 107-28.

Pantano, S., Jarrossay, D., Saccani, S., Bosisio, D. & Natoli, G. Plastic downregulation of the transcriptional repressor BCL6 during maturation of human dendritic cells. (2006). *Exp Cell Res*, **312,** 1312-22.

Pasqualucci, L., Migliazza, A., Fracchiolla, N., William, C., Neri, A., Baldini, L., Chaganti, R.S., Klein, U., Kuppers, R., Rajewsky, K. & Dalla-Favera, R. BCL-6 mutations in normal germinal center B cells: evidence of somatic hypermutation acting outside Ig loci. (1998). *Proc Natl Acad Sci U S A*, **95,** 11816-21.

Pedersen, A.G. & Nielsen, H. Neural network prediction of translation initiation sites in eukaryotes: perspectives for EST and genome analysis. (1997). *Proc Int Conf Intell Syst Mol Biol*, **5,** 226-33.

Perou, C.M., Jeffrey, S.S., van de Rijn, M., Rees, C.A., Eisen, M.B., Ross, D.T., Pergamenschikov, A., Williams, C.F., Zhu, S.X., Lee, J.C., Lashkari, D., Shalon, D., Brown, P.O. & Botstein, D. Distinctive gene expression patterns in human mammary epithelial cells and breast cancers. (1999). *Proc Natl Acad Sci U S A*, **96,** 9212-7.

Perou, C.M., Sorlie, T., Eisen, M.B., van de Rijn, M., Jeffrey, S.S., Rees, C.A., Pollack, J.R., Ross, D.T., Johnsen, H., Akslen, L.A., Fluge, O., Pergamenschikov, A., Williams, C., Zhu, S.X., Lonning, P.E., Borresen-Dale, A.L., Brown, P.O. & Botstein, D. Molecular portraits of human breast tumours. (2000). *Nature*, **406,** 747-52.

Peterson, L.F. & Zhang, D.E. The 8;21 translocation in leukemogenesis. (2004). *Oncogene*, **23,** 4255-62.

Phan, R.T. & Dalla-Favera, R. The BCL6 proto-oncogene suppresses p53 expression in germinal-centre B cells. (2004). *Nature*, **432,** 635-9.

Phan, R.T., Saito, M., Kitagawa, Y., Means, A.R. & Dalla-Favera, R. Genotoxic stress regulates expression of the proto-oncogene Bcl6 in germinal center B cells. (2007). *Nat Immunol*, **8,** 1132-9.

Pihan, G.A., Purohit, A., Wallace, J., Knecht, H., Woda, B., Quesenberry, P. & Doxsey, S.J. Centrosome defects and genetic instability in malignant tumors. (1998). *Cancer Res*, **58,** 3974-85.

Pihan, G.A., Purohit, A., Wallace, J., Malhotra, R., Liotta, L. & Doxsey, S.J. Centrosome defects can account for cellular and genetic changes that characterize prostate cancer progression. (2001). *Cancer Res*, **61,** 2212-9.

Porter, D.C. & Keyomarsi, K. Novel splice variants of cyclin E with altered substrate specificity. (2000). *Nucleic Acids Res*, **28,** E101.

Powell, J.A., Gardner, A.E., Bais, A.J., Hinze, S.J., Baker, E., Whitmore, S., Crawford, J., Kochetkova, M., Spendlove, H.E., Doggett, N.A., Sutherland, G.R., Callen, D.F., Kremmidiotis, G., McKenzie, O.L., Martin, J.M., Secker, G.A., Seshadri, R., O'Callaghan, N.J., Cleton-Jansen, A.M., Cornelisse, C., Whitmore, S.A., Derwas, C., Cornelisse, C.J., Goldup, S., McCallum, B., Settasatian, C., van Beerendonk, H., Moerland, E.W., Smit, V.T., Harris, W.H., Millis, R., Morgan, N.V., Barnes, D. & Mathew, C.G. Sequencing, transcript identification, and quantitative gene expression profiling in the breast cancer loss of heterozygosity region 16q24.3. (2002). *Genomics*, **80,** 303-10.

Qiu, J., Wong, J., Tweardy, D.J. & Dong, S. Decreased intranuclear mobility of acute myeloid leukemia 1-containing fusion proteins is accompanied by reduced mobility and compartmentalization of core binding factor beta. (2006). *Oncogene*, **25,** 3982-93.

Reed, S.I., Bailly, E., Dulic, V., Hengst, L., Resnitzky, D. & Slingerland, J. G1 control in mammalian cells. (1994). *J Cell Sci Suppl*, **18,** 69-73.

Reid, A., Gould, A., Brand, N., Cook, M., Strutt, P., Li, J., Licht, J., Waxman, S., Krumlauf, R. & Zelent, A. Leukemia translocation gene, PLZF, is expressed with a speckled nuclear pattern in early hematopoietic progenitors. (1995). *Blood*, **86,** 4544-52.

Roylance, R., Gorman, P., Harris, W., Liebmann, R., Barnes, D., Hanby, A. & Sheer, D. Comparative genomic hybridization of breast tumors stratified by histological grade reveals new insights into the biological progression of breast cancer. (1999). *Cancer Res*, **59,** 1433-6.

Russo, J., Tait, L. & Russo, I.H. Morphological expression of cell transformation induced by c-Ha-ras oncogene in human breast epithelial cells. (1991). *J Cell Sci*, **99 (Pt 2),** 453-63.

Ryan, K.M. & Birnie, G.D. Myc oncogenes: the enigmatic family. (1996). *Biochem J*, **314 (Pt 3),** 713-21.

Sakai, T., Toguchida, J., Ohtani, N., Yandell, D.W., Rapaport, J.M. & Dryja, T.P. Allele-specific hypermethylation of the retinoblastoma tumor-suppressor gene. (1991). *Am J Hum Genet*, **48,** 880-8.

Sanchez-Beato, M., Sanchez-Aguilera, A. & Piris, M.A. Cell cycle deregulation in B-cell lymphomas. (2003). *Blood*, **101,** 1220-35.

Sankaran, S., Starita, L.M., Simons, A.M. & Parvin, J.D. Identification of domains of BRCA1 critical for the ubiquitin-dependent inhibition of centrosome function. (2006). *Cancer Res*, **66,** 4100-7.

Sato, M., Mori, Y., Sakurada, A., Fukushige, S., Ishikawa, Y., Tsuchiya, E., Saito, Y., Nukiwa, T., Fujimura, S. & Horii, A. Identification of a 910-kb region of common allelic loss in chromosome bands 16q24.1-q24.2 in human lung cancer. (1998). *Genes Chromosomes Cancer*, **22,** 1-8.

Sato, N., Mizumoto, K., Nakamura, M., Maehara, N., Minamishima, Y.A., Nishio, S., Nagai, E. & Tanaka, M. Correlation between centrosome abnormalities and chromosomal instability in human pancreatic cancer cells. (2001). *Cancer Genet Cytogenet*, **126,** 13-9.

Schmidt, M., Fernandez de Mattos, S., van der Horst, A., Klompmaker, R., Kops, G.J., Lam, E.W., Burgering, B.M. & Medema, R.H. Cell cycle inhibition by FoxO forkhead transcription factors involves downregulation of cyclin D. (2002). *Mol Cell Biol*, **22,** 7842-52.

Shaffer, A.L., Yu, X., He, Y., Boldrick, J., Chan, E.P. & Staudt, L.M. BCL-6 represses genes that function in lymphocyte differentiation, inflammation, and cell cycle control. (2000). *Immunity*, **13,** 199-212.

Shaknovich, R., Yeyati, P.L., Ivins, S., Melnick, A., Lempert, C., Waxman, S., Zelent, A. & Licht, J.D. The promyelocytic leukemia zinc finger protein affects myeloid cell growth, differentiation, and apoptosis. (1998). *Mol Cell Biol*, **18,** 5533-45.

Sherr, C.J. G1 phase progression: cycling on cue. (1994). *Cell*, **79,** 551-5.

Sherr, C.J. & Roberts, J.M. CDK inhibitors: positive and negative regulators of G1-phase progression. (1999). *Genes Dev*, **13,** 1501-12.

Shinmura, K., Bennett, R.A., Tarapore, P. & Fukasawa, K. Direct evidence for the role of centrosomally localized p53 in the regulation of centrosome duplication. (2007). *Oncogene*, **26,** 2939-44.

Shinmura, K., Tarapore, P., Tokuyama, Y., George, K.R. & Fukasawa, K. Characterization of centrosomal association of nucleophosmin/B23 linked to Crm1 activity. (2005). *FEBS Lett*, **579,** 6621-34.

Shvarts, A., Brummelkamp, T.R., Scheeren, F., Koh, E., Daley, G.Q., Spits, H. & Bernards, R. A senescence rescue screen identifies BCL6 as an inhibitor of anti-proliferative p19(ARF)-p53 signaling. (2002). *Genes Dev*, **16,** 681-6.

Sluder, G. Two-way traffic: centrosomes and the cell cycle. (2005). *Nat Rev Mol Cell Biol*, **6,** 743-8.

Sorlie, T., Perou, C.M., Tibshirani, R., Aas, T., Geisler, S., Johnsen, H., Hastie, T., Eisen, M.B., van de Rijn, M., Jeffrey, S.S., Thorsen, T., Quist, H., Matese, J.C., Brown, P.O., Botstein, D., Eystein Lonning, P. & Borresen-Dale, A.L. Gene expression patterns of breast carcinomas distinguish tumor subclasses with clinical implications. (2001). *Proc Natl Acad Sci U S A*, **98,** 10869-74.

Sorlie, T., Tibshirani, R., Parker, J., Hastie, T., Marron, J.S., Nobel, A., Deng, S., Johnsen, H., Pesich, R., Geisler, S., Demeter, J., Perou, C.M., Lonning, P.E., Brown, P.O., Borresen-Dale, A.L. & Botstein, D. Repeated observation of breast tumor subtypes in independent gene expression data sets. (2003). *Proc Natl Acad Sci U S A*, **100,** 8418-23.

Stampfer, M.R. & Yaswen, P. Human epithelial cell immortalization as a step in carcinogenesis. (2003). *Cancer Lett*, **194,** 199-208.

Strnad, P., Leidel, S., Vinogradova, T., Euteneuer, U., Khodjakov, A. & Gonczy, P. Regulated HsSAS-6 levels ensure formation of a single procentriole per centriole during the centrosome duplication cycle. (2007). *Dev Cell*, **13,** 203-13.

Strom, D.K., Nip, J., Westendorf, J.J., Linggi, B., Lutterbach, B., Downing, J.R., Lenny, N. & Hiebert, S.W. Expression of the AML-1 oncogene shortens the G(1) phase of the cell cycle. (2000). *J Biol Chem*, **275,** 3438-45.

Sutherland, R.L. & Musgrove, E.A. Cyclins and breast cancer. (2004). *J Mammary Gland Biol Neoplasia*, **9,** 95-104.

Takeda, D.Y., Wohlschlegel, J.A. & Dutta, A. A bipartite substrate recognition motif for cyclin-dependent kinases. (2001). *J Biol Chem*, **276,** 1993-7.

Tamimi, R.M., Baer, H.J., Marotti, J., Galan, M., Galaburda, L., Fu, Y., Deitz, A.C., Connolly, J.L., Schnitt, S.J., Colditz, G.A. & Collins, L.C. Comparison of molecular phenotypes of ductal carcinoma in situ and invasive breast cancer. (2008). *Breast Cancer Res*, **10,** R67.

Tarapore, P., Shinmura, K., Suzuki, H., Tokuyama, Y., Kim, S.H., Mayeda, A. & Fukasawa, K. Thr199 phosphorylation targets nucleophosmin to nuclear speckles and represses pre-mRNA processing. (2006). *FEBS Lett*, **580,** 399-409.

Tassin, A.M., Celati, C., Moudjou, M. & Bornens, M. Characterization of the human homologue of the yeast spc98p and its association with gamma-tubulin. (1998). *J Cell Biol*, **141,** 689-701.

Thompson, J.D., Gibson, T.J., Plewniak, F., Jeanmougin, F. & Higgins, D.G. The CLUSTAL_X windows interface: flexible strategies for multiple sequence alignment aided by quality analysis tools. (1997). *Nucleic Acids Res*, **25,** 4876-82.

Thompson, M.E., Robinson-Benion, C.L. & Holt, J.T. An amino-terminal motif functions as a second nuclear export sequence in BRCA1. (2005). *J Biol Chem*, **280,** 21854-7.

Tirkkonen, M., Tanner, M., Karhu, R., Kallioniemi, A., Isola, J. & Kallioniemi, O.P. Molecular cytogenetics of primary breast cancer by CGH. (1998). *Genes Chromosomes Cancer*, **21,** 177-84.

Tokuyama, Y., Horn, H.F., Kawamura, K., Tarapore, P. & Fukasawa, K. Specific phosphorylation of nucleophosmin on Thr(199) by cyclin-dependent kinase 2-cyclin E and its role in centrosome duplication. (2001). *J Biol Chem*, **276,** 21529-37.

Tsou, M.F. & Stearns, T. Controlling centrosome number: licenses and blocks. (2006a). *Curr Opin Cell Biol*, **18,** 74-8.

Tsou, M.F. & Stearns, T. Mechanism limiting centrosome duplication to once per cell cycle. (2006b). *Nature*, **442,** 947-51.

Tsuda, H., Callen, D.F., Fukutomi, T., Nakamura, Y. & Hirohashi, S. Allele loss on chromosome 16q24.2-qter occurs frequently in breast cancers irrespectively of differences in phenotype and extent of spread. (1994). *Cancer Res*, **54,** 513-7.

Tunyaplin, C., Shaffer, A.L., Angelin-Duclos, C.D., Yu, X., Staudt, L.M. & Calame, K.L. Direct repression of prdm1 by Bcl-6 inhibits plasmacytic differentiation. (2004). *J Immunol*, **173,** 1158-65.

Ukomadu, C. & Dutta, A. Inhibition of cdk2 activating phosphorylation by mevastatin. (2003). *J Biol Chem*, **278,** 4840-6.

van der Groep, P., Bouter, A., van der Zanden, R., Menko, F.H., Buerger, H., Verheijen, R.H., van der Wall, E. & van Diest, P.J. Re: Germline BRCA1 mutations and a basal epithelial phenotype in breast cancer. (2004). *J Natl Cancer Inst*, **96,** 712-3; author reply 714.

van Diest, P.J., Michalides, R.J., Jannink, L., van der Valk, P., Peterse, H.L., de Jong, J.S., Meijer, C.J. & Baak, J.P. Cyclin D1 expression in invasive breast cancer. Correlations and prognostic value. (1997). *Am J Pathol*, **150,** 705-11.

Vasanwala, F.H., Kusam, S., Toney, L.M. & Dent, A.L. Repression of AP-1 function: a mechanism for the regulation of Blimp-1 expression and B lymphocyte differentiation by the B cell lymphoma-6 protooncogene. (2002). *J Immunol*, **169,** 1922-9.

Visvanathan, K., Sukumar, S. & Davidson, N.E. Epigenetic biomarkers and breast cancer: cause for optimism. (2006). *Clin Cancer Res*, **12,** 6591-3.

Vogt, U., Bielawski, K., Schlotter, C.M., Bosse, U., Falkiewicz, B. & Podhajska, A.J. Amplification of erbB-4 oncogene occurs less frequently than that of erbB-2 in primary human breast cancer. (1998). *Gene*, **223,** 375-80.

Vos, C.B., ter Haar, N.T., Rosenberg, C., Peterse, J.L., Cleton-Jansen, A.M., Cornelisse, C.J. & van de Vijver, M.J. Genetic alterations on chromosome 16 and 17 are important features of ductal carcinoma in situ of the breast and are associated with histologic type. (1999). *Br J Cancer*, **81,** 1410-8.

Wade, P.A. Transcriptional control at regulatory checkpoints by histone deacetylases: molecular connections between cancer and chromatin. (2001). *Hum Mol Genet*, **10,** 693-8.

Wang, J., Hoshino, T., Redner, R.L., Kajigaya, S. & Liu, J.M. ETO, fusion partner in t(8;21) acute myeloid leukemia, represses transcription by interaction with the human N-CoR/mSin3/HDAC1 complex. (1998). *Proc Natl Acad Sci U S A*, **95,** 10860-5.

Wang, J., Saunthararajah, Y., Redner, R.L. & Liu, J.M. Inhibitors of histone deacetylase relieve ETO-mediated repression and induce differentiation of AML1-ETO leukemia cells. (1999). *Cancer Res*, **59,** 2766-9.

Wang, J., Wang, M., Liu, J.M., Lasa, A., Carnicer, M.J., Aventin, A., Estivill, C., Brunet, S., Sierra, J., Nomdedeu, J.F., Delaney, C., Bernstein, I.D., Muller-Tidow, C., Steffen, B., Cauvet, T., Tickenbrock, L., Ji, P., Diederichs, S., Sargin, B., Kohler, G., Stelljes, M., Puccetti, E., Ruthardt, M., deVos, S., Hiebert, S.W., Koeffler, H.P., Berdel, W.E., Serve, H., Buonamici, S., Ottaviani, E., Visani, G., Bonifazi, F., Fiacchini, M., Baccarani, M., Martinelli, G., Bernardin-Fried, F., Kummalue, T., Leijen, S., Collector, M.I., Ravid, K., Friedman, A.D., Lindberg, S.R., Olsson, A., Persson, A.M., Olsson, I., Alcalay, M., Meani, N., Gelmetti, V., Fantozzi, A., Fagioli, M., Orleth, A., Riganelli, D., Sebastiani, C., Cappelli, E., Casciari, C., Sciurpi, M.T., Mariano, A.R., Minardi, S.P., Luzi, L., Muller, H., Di Fiore, P.P., Frosina, G., Pelicci, P.G., Chevallier, N., Corcoran, C.M., Lennon, C., Hyjek, E., Chadburn, A., Bardwell, V.J., Licht, J.D., Melnick, A., Fleischman, E.W., Baturina, J.A., Sokova, O.I., Popa, A.V., Kosorukova, I.S., Rowley, J.D., Elsasser, A., Franzen, M., Kohlmann, A., Weisser, M., Schnittger, S., Schoch, C., Reddy, V.A., Burel, S., Zhang, D.E., Ueffing, M., Tenen, D.G., Hiddemann, W., Behre, G., McGhee, L., Bryan, J., Elliott, L., Grimes, H.L., Kazanjian, A., Davis, J.N., Meyers, S., de Guzman, C.G., Johnson, A., Klug, C.A., et al. Domains involved in ETO and human N-CoR interaction and ETO transcription repression. (2004a). *Leuk Res*, **28,** 409-14.

Wang, T.C., Cardiff, R.D., Zukerberg, L., Lees, E., Arnold, A. & Schmidt, E.V. Mammary hyperplasia and carcinoma in MMTV-cyclin D1 transgenic mice. (1994). *Nature*, **369,** 669-71.

Wang, Z.C., Lin, M., Wei, L.J., Li, C., Miron, A., Lodeiro, G., Harris, L., Ramaswamy, S., Tanenbaum, D.M., Meyerson, M., Iglehart, J.D. & Richardson, A. Loss of heterozygosity and its correlation with expression profiles in subclasses of invasive breast cancers. (2004b). *Cancer Res*, **64,** 64-71.

Wei, M., Grushko, T.A., Dignam, J., Hagos, F., Nanda, R., Sveen, L., Xu, J., Fackenthal, J., Tretiakova, M., Das, S. & Olopade, O.I. BRCA1 promoter methylation in sporadic breast cancer is associated with reduced BRCA1 copy number and chromosome 17 aneusomy. (2005). *Cancer Res*, **65,** 10692-9.

Wei, M., Xu, J., Dignam, J., Nanda, R., Sveen, L., Fackenthal, J., Grushko, T.A. & Olopade, O.I. Estrogen receptor alpha, BRCA1, and FANCF promoter methylation occur in distinct subsets of sporadic breast cancers. (2008). *Breast Cancer Res Treat*, **111,** 113-20.

Wingate, H., Zhang, N., McGarhen, M.J., Bedrosian, I., Harper, J.W. & Keyomarsi, K. The tumor-specific hyperactive forms of cyclin E are resistant to inhibition by p21 and p27. (2005). *J Biol Chem*, **280,** 15148-57.

Witton, C.J., Reeves, J.R., Going, J.J., Cooke, T.G. & Bartlett, J.M. Expression of the HER1-4 family of receptor tyrosine kinases in breast cancer. (2003). *J Pathol*, **200,** 290-7.

Wolfe, S.A., Nekludova, L. & Pabo, C.O. DNA recognition by Cys2His2 zinc finger proteins. (2000). *Annu Rev Biophys Biomol Struct*, **29,** 183-212.

Wolford, J.K. & Prochazka, M. Structure and expression of the human MTG8/ETO gene. (1998). *Gene*, **212,** 103-9.

Wooster, R., Neuhausen, S.L., Mangion, J., Quirk, Y., Ford, D., Collins, N., Nguyen, K., Seal, S., Tran, T., Averill, D. & et al. Localization of a breast cancer susceptibility gene, BRCA2, to chromosome 13q12-13. (1994). *Science*, **265,** 2088-90.

Wysocka, J., Reilly, P.T. & Herr, W. Loss of HCF-1-chromatin association precedes temperature-induced growth arrest of tsBN67 cells. (2001). *Mol Cell Biol*, **21,** 3820-9.

Ye, B.H. BCL-6 in the pathogenesis of non-Hodgkin's lymphoma. (2000). *Cancer Invest*, **18,** 356-65.

Ye, B.H., Chaganti, S., Chang, C.C., Niu, H., Corradini, P., Chaganti, R.S. & Dalla-Favera, R. Chromosomal translocations cause deregulated BCL6 expression by promoter substitution in B cell lymphoma. (1995). *Embo J*, **14,** 6209-17.

Zhang, H., Shi, X., Paddon, H., Hampong, M., Dai, W. & Pelech, S. B23/nucleophosmin serine 4 phosphorylation mediates mitotic functions of polo-like kinase 1. (2004). *J Biol Chem*, **279,** 35726-34.

Zhang, J., Hug, B.A., Huang, E.Y., Chen, C.W., Gelmetti, V., Maccarana, M., Minucci, S., Pelicci, P.G. & Lazar, M.A. Oligomerization of ETO is obligatory for corepressor interaction. (2001). *Mol Cell Biol*, **21,** 156-63.

Zhao, L., Wang, L., Jin, F., Ma, W., Ren, J., Wen, X., He, M., Sun, M., Tang, H. & Wei, M. Silencing of estrogen receptor alpha (ERalpha) gene by promoter

hypermethylation is a frequent event in Chinese women with sporadic breast cancer. (2008). *Breast Cancer Res Treat*.

Zhou, Q., Atadja, P. & Davidson, N.E. Histone deacetylase inhibitor LBH589 reactivates silenced estrogen receptor alpha (ER) gene expression without loss of DNA hypermethylation. (2007). *Cancer Biol Ther*, **6,** 64-9.

Zhu, Y., Sullivan, L.L., Nair, S.S., Williams, C.C., Pandey, A.K., Marrero, L., Vadlamudi, R.K. & Jones, F.E. Coregulation of estrogen receptor by ERBB4/HER4 establishes a growth-promoting autocrine signal in breast tumor cells. (2006). *Cancer Res*, **66,** 7991-8.

Zwijsen, R.M., Wientjens, E., Klompmaker, R., van der Sman, J., Bernards, R. & Michalides, R.J. CDK-independent activation of estrogen receptor by cyclin D1. (1997). *Cell*, **88,** 405-15.

Appendices

Appendices for Chapter 4.

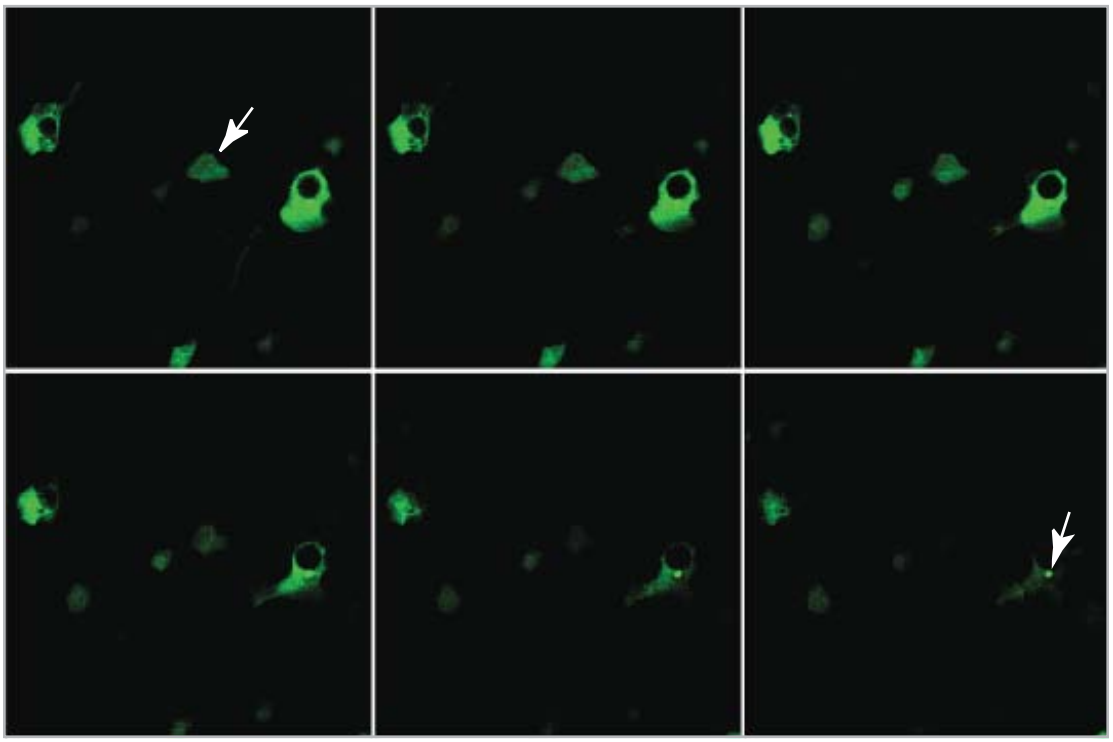

Figure Appendix 1. Serial sections (1-6 from left to right in two rows) taken from myc-LS1-EGFP fusion expressed in MCF7 cells. Arrow indicates the putative centrosomal spots visible in different sections. Images were taken with 20X lense and 2.5X zoom conditions at LSCM.

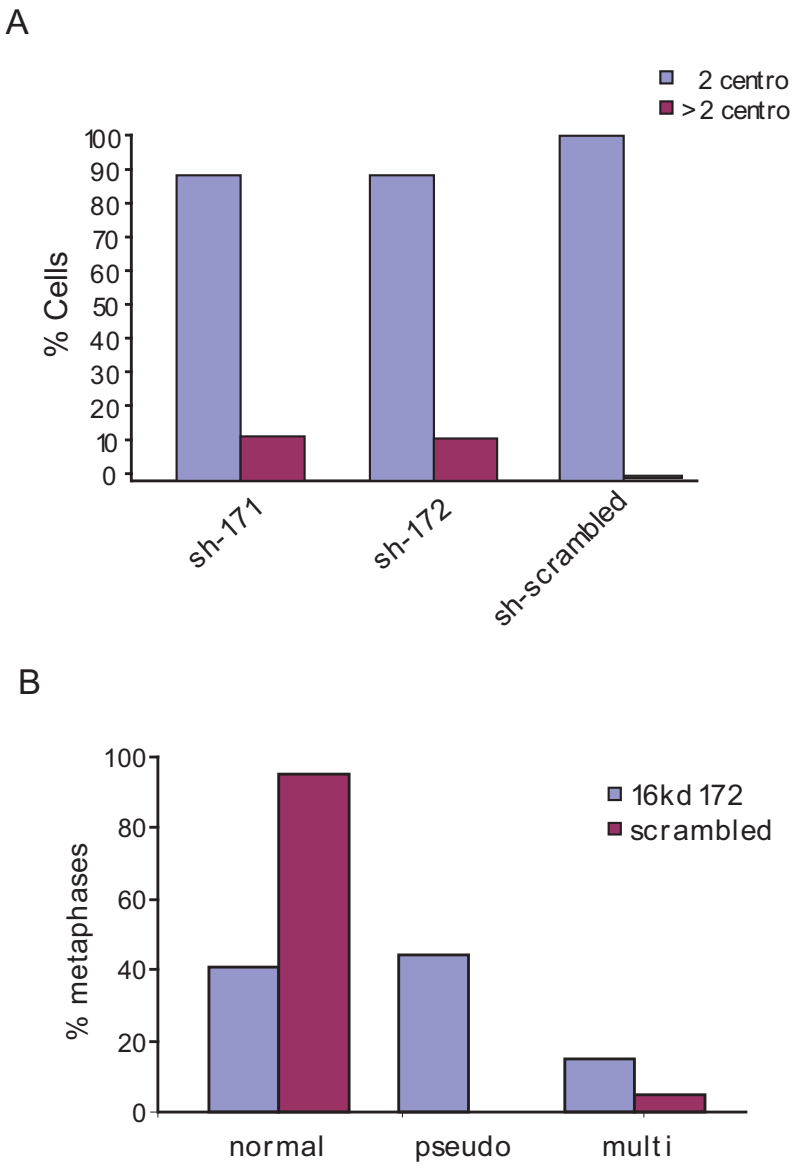

Figure Appendix 2. Effects of sh-171 and sh-172 for CBFA2T3 in HeLa. **A.** sh-171 and sh-172 were transiently expressed in HeLa cells for 24 hours. Centrosomes were stained with α-γ-tubulin antibody. Histogram presents percent cells with different catagories for centrosome numbers per treatment. **B**. Histogram presents percent metaphase types for sh-172 and shscrambled treatment. 150 metaphase spreads were counted for each.

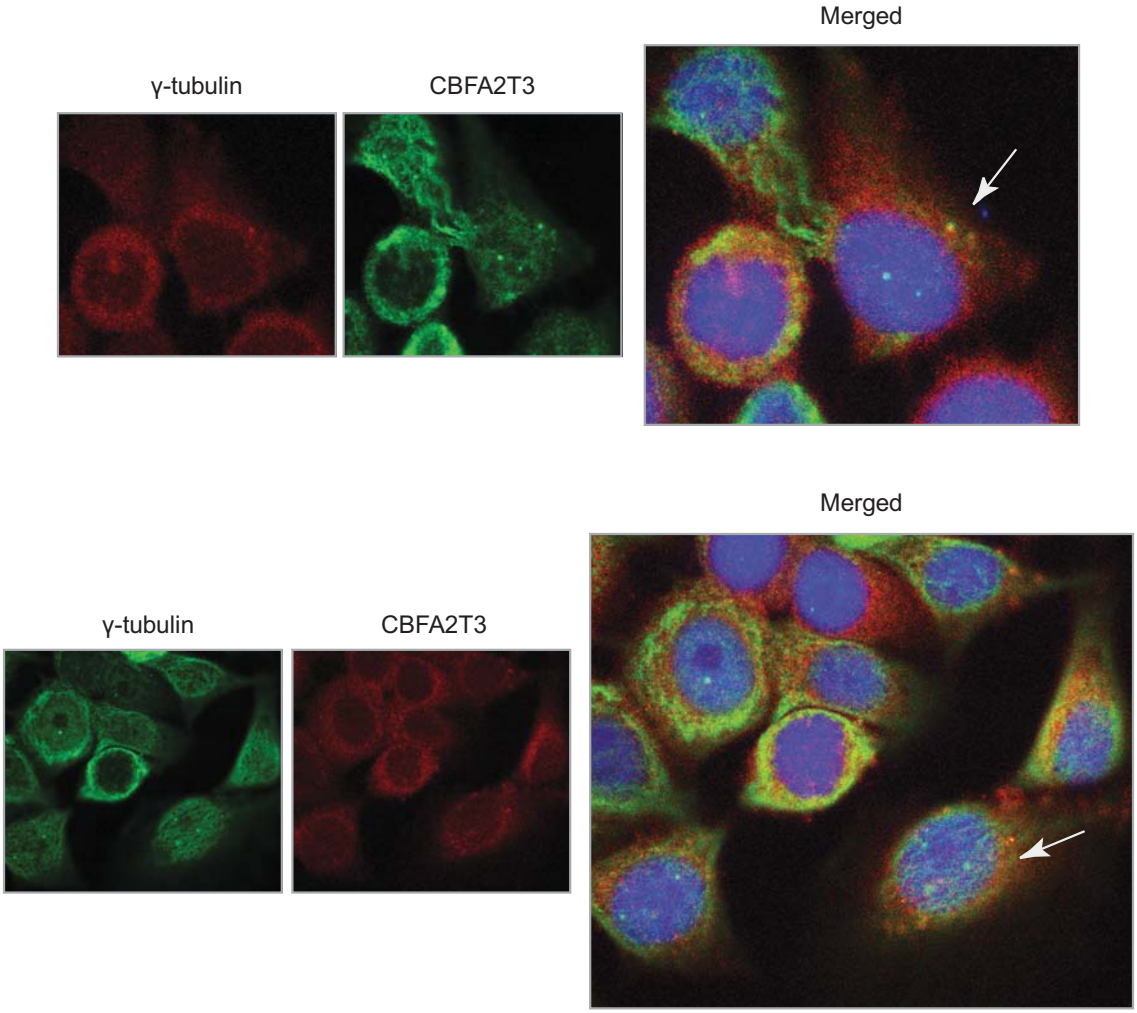

Appendix 3. Co-localization of endogenous CBFA2T3 proteins from MCF7 cell line with γ-tubulin.
This figure is the continuity of Fig 3.11 B lower two panels. MCF7 cells were co-stained with anti-CBFA2T3 (RSH1) and anti-γ-tubulin antibodies. colocalitation to centrosomal spots is marked by arrow.